

**Dissertationes Forestales 215**

**Linking water and carbon cycles: modeling latent heat  
exchange and dissolved organic carbon**

**Ville Kasurinen**

**Department of Forest Sciences  
Faculty of Agriculture and Forestry  
University of Helsinki**

**Academic dissertation**

To be presented, with the permission of the Faculty Agriculture and Forestry of the University of Helsinki, for public criticism in auditorium ls2, Latokartanonkaari 7, on 8th of April, 2016, at 12 o'clock noon.

*Title of dissertation:* Linking water and carbon cycles: modeling latent heat exchange and dissolved organic carbon

*Author:* Ville Kasurinen

*Dissertationes Forestales* 215

<http://dx.doi.org/10.14214/df.215>

*Thesis supervisors:*

University Lecturer, Frank Berninger, Ph.D., Department of Forest Sciences, University of Helsinki.

Professor, Knut Alfredsen, Ph.D., Department of Hydraulic and Environmental Engineering, Norwegian University of Science and Technology.

University Lecturer, Anne Ojala, Ph.D., Department of Environmental Sciences, University of Helsinki.

Professor, Jukka Pumpanen, Ph.D., Department of Environmental Sciences, University of Eastern Finland.

*Pre-examiners:*

Professor, Martin Heimann, Ph.D., Department of Physics, Division of Atmospheric Sciences, University of Helsinki.

Leading researcher, Pirkko Kortelainen, Ph.D., Finnish Environment Institute .

*Opponent:*

Professor of Ecosystem Ecology, Peter A. Raymond, Ph.D., Yale School of Forestry & Environmental Studies.

ISSN 1795-7389 (online)

ISBN 978-951-651-520-8 (pdf)

ISSN 2323-9220 (print)

ISBN 978-951-651-521-5 (paperback)

*Printers:*

Unigrafia, Finland, Helsinki 2016

*Cover photo:*

[www.jonohey.com](http://www.jonohey.com)

*Publishers:*

Finnish Society of Forest Science

Natural Resources Institute Finland

Faculty of Agriculture and Forestry of the University of Helsinki

School of Forest Sciences at the University of Eastern Finland

*Editorial Office:*

Finnish Society of Forest Science P.O. Box 18 FI-01301 Vantaa, Finland

<http://www.metla.fi/dissertationes>

**Kasurinen, V.** 2016. Linking water and carbon cycles: modeling latent heat exchange and dissolved organic carbon. *Dissertationes Forestales* 215. 46 p. Available at <http://dx.doi.org/10.14214/df.215>

Water and carbon cycles of the Earth are tightly linked to each other. One linkage of these cycles is through the water use efficiency of photosynthetic production its interactions with drought, and its possible changes. A second linkage between the water and carbon cycles: the transport of terrestrial carbon as dissolved organic carbon (DOC) to aquatic ecosystems has received much less attention and is, therefore, the subject of this thesis.

The thesis shows that latent heat exchange in boreal and arctic biomes differs, under similar climatic conditions, between different land cover types in the boreal and arctic climatic zones. Furthermore, we found that there are large differences in the way ecosystems are exchanging water in the winter and the summer. Winter time surface resistances were much higher and the transition between the winter and summer phenological stages was slow.

Similarly, stream water DOC concentrations show high temporal and spatial variability between different catchments in boreal landscapes and globally between big river systems. The model, developed here and applied to a boreal catchment simulates stream water DOC concentrations as a function of catchment water storage, soil temperature and runoff. The model is parsimonious, i.e. all parameters could be estimated statistically and it is performed better than previous models for the 18 partially nested sub-catchments of the Kryckland research area.

Finally, the contribution of terrestrial DOC promoting heterotrophic food webs in coastal waters was quantified after receiving a radiation dose corresponding UV-radiation absorbed by Earth's surface in a month. Irradiation removed approximately half from the initial terrestrial chromophoric dissolved organic matter (tCDOM) suggesting that sun-light induced photochemistry is a significant sink of tCDOM in coastal waters. Tropical rainforest covered large basins of Amazon and Congo Rivers contributed the highest production of biologically labile photoproducts (BLPs) and the highest tCDOM fluxes of investigated rivers, which might be linked to large water fluxes and carbon sequestration in their basins.

A strong relationship between photobleaching of tCDOM and bacterial production based on bioavailable labile photoproducts (BLPs) was found and used to estimate BLP production globally. Extrapolation of production revealed that the majority of tDOC will be mineralized to  $CO_2$  either directly or through bacterial respiration in coastal waters. In these research articles, I have investigated biogeochemical cycles of water and carbon focusing to latent heat exchange and DOC dynamics in landscapes, as well as, in coastal waters, describing their variability across space and time.

**Keywords:** Latent heat, evapotranspiration, DOC, hydrology, photochemistry

## Acknowledgements

When I graduated from high school in spring 1999, I was lacking study motivation and decided to work and earn money instead. For a young man, it can take ages to see things more clearly. In this case, it took until the autumn 1999 before I found the motivation again. I continued my studies and signed in to Open University web courses for environmental sciences. When I studied at the Open University, I never dreamed the possibility to become a researcher, but continued to wonder how to get in to the University. During the following years I managed to practice writing in entrance exams four or five times, start a family and work more than I actually had time beside my studies. When I finally received a decision letter from the department of bio- and environmental sciences in the summer 2006 only one thing was certain: I will never become a researcher. I would have never believed a prediction claiming that I will deference my doctoral thesis ten years later.

I started my doctoral studies in April 2012 and changed the topic from limnology to forest sciences without any idea what I am doing. It took some time to get in to a new scientific field and link that to my previous interests. These past four years in my life has been the most challenging in many ways, but one thing turned out to be very clear already in the early phase of this trip. I just love the work I am doing.

I can never start to describe how grateful I am for all the support I have received from my wife, my supervisors and colleagues during the process. Without all this support, I would have never succeeded. I have been privileged and had the opportunity to experience the supportive and creative atmosphere, which is supported by my all colleagues in Finland, Sweden, Norway and all over the world through people that have co-authored my studies included in this doctoral thesis. It is a pleasure to work with people that are passionate about science and are ready to share their knowledge for the greater good. Although, it is not possible to thank everyone personally in this short space, there are some individuals whose impact should be highlighted.

Firstly, I want to thank my wife Jolin for all the unconditional support she has given me during the ups and downs of this process. I also want to thank my daughters Jorunn and Tora for their patience with me when my brain has been overloaded and codes have been crashing. I want to thank Barbro Slotte for providing all needed help and being super nanny for our children during the time I have worked and studied.

Secondly, I want to thank Frank Berninger for the continuous support and positive but critical thinking in science and in life general. Knut Alfredsen was the key person regarding the arrangements during my stay in Trondheim and created the basics for hydrological modeling utilized in my studies. Anne Ojala encouraged me to apply for Ph.D positions from Sweden and Finland and strongly influenced my decision to continue research. Anne together with Jukka Pumpanen provided several inspiring discussions during these four years and I am looking forward to develop new research ideas in the future. I thank Finnish Center of Excellence and Nordic Center of Excellence (CRAICC) for the received funding. Markku Kulmala, Jaana Bäck, Timo Vesala, Michael Boy and Knut Alfredsen arranged together the required financial support for my doctoral studies.

Thirdly, I want to thank my ex-colleagues at Helsinki Deaconess Institute for the support during my administrative career. Ilkka Holopainen, Eija Tuukkanen, Kiikka Sandberg and Timo Mutalahti never stopped to believe in me. Although the environment was turbulent, I managed to stand on my own two feet and continue the work I believed in. Finnish Environment Institute provided the first practical insights to the research field. Matti Verta, Jaakko Mannio, Jukka Mehtonen, Timo Seppälä, Päivi Munne and Taina Nysten encouraged me to continue the work I was good at. The impact of these kind words should not be underestimated.

The decisions I made during the autumn 1999 led finally to my doctoral defense, although it took 17 years, nearly half of my life to see the outcome. This has been a extremely interesting trip, but most likely it is just a start for another journey. Finally, I want to dedicate my public defense and dissertation to my father, Reijo Kasurinen, who never got a chance to witness this moment in my life as he sadly passed away on the 9th of May 2013.

## LIST OF ORIGINAL ARTICLES

This thesis consists of an introductory review, followed by four research articles. In the introductory part, these papers are cited according to their roman numerals. The articles I and IV are reprinted with the kind permission of the publishers, while articles II-III are the authors version of the manuscripts send to the series.

- I Kasurinen V., Alfredsen K., Kolari P., Mammarella I., Alekseychik P., Rinne J., Vesala T., Bernier P., Boike J., Langer M., Belelli Marchesini L., van Huissteden K., Dolman H., Sachs T., Ohta T., Varlagin A., Rocha A., Arain A., Oechel W., Lund M., Grelle A., Lindroth A., Black A., Aurela M., Laurila T., Lohila A. and Berninger F. (2014). Latent heat exchange in the boreal and arctic biomes, *Global Change Biology*, 20(11), 3439-3456,  
<http://dx.doi.org/10.1111/gcb.12640>
- II Alekseychik P., Lindroth A., Mammarella I., Lund M., Rinne J., Kasurinen V., Nilsson M.B., Peichl M., Lohila A., Aurela, M., Laurila, T., Shurpali, N., Tuittila, E.-S., Martikainen, P., Vesala T. (2015). Energy partitioning and evapotranspiration in eight Fennoscandian peatlands. 1-12. Manuscript
- III Kasurinen V., Alfredsen K., Ojala A., Pumpanen J., Weyhenmeyer G.A., Futter M.N., Laudon H. and Berninger F. (2015). Modeling Dissolved Organic Carbon Transport in Boreal Catchments. 1-13. Manuscript
- IV Kasurinen V., Aarnos H. and Vähätalo, A. (2015). Biologically labile photoproducts from riverine non-labile dissolved organic carbon in the coastal waters. *Biogeosciences Discussions*. 12, 8199-8234.  
<http://dx.doi.org/10.5194/bgd-12-8199-2015>

### Author's contribution:

In paper (I) the co-authors provided the data. V. Kasurinen wrote the analytical code and carried out the data analysis. V. Kasurinen took the lead in the writing. All authors contributed to the writing process. In paper (II) V. Kasurinen participated to the writing process of the research. The article will also be included in the doctoral thesis of Pavel Alekseychik. In paper (III) V. Kasurinen wrote the analysis code, developed and parameterized the model. V. Kasurinen wrote the paper with contributions of all co-authors. In paper (IV) V. Kasurinen was responsible for the laboratory work under supervision of Hanna Aarnos and contributed to the writing process under supervision of Anssi Vähätalo.

## TABLE OF CONTENTS

1	INTRODUCTION . . . . .	7
1.1	Energy exchange, latent heat and water cycle . . . . .	7
1.2	Dissolved organic carbon and photochemistry . . . . .	9
1.3	Modeling . . . . .	10
1.4	Aim of the study . . . . .	11
2	MATERIAL AND METHODS . . . . .	13
2.1	Data sources and management . . . . .	13
2.1.1	<i>Eddy covariance data (I, II)</i> . . . . .	13
2.1.2	<i>Stream water dissolved organic carbon data (III)</i> . . . . .	14
2.1.3	<i>Terrestrial chromophoric dissolved organic carbon samples (IV)</i> . . . . .	14
2.2	Analytical methods . . . . .	16
2.2.1	<i>Modeling latent heat (I)</i> . . . . .	16
2.2.2	<i>Comparison of Fennoscandic peatlands (II)</i> . . . . .	17
2.2.3	<i>Modeling stream water dissolved organic carbon concentrations (III)</i> . . . . .	18
2.2.4	<i>Modeling production of biologically labile photoproducts based on chromophoric terrestrial dissolved organic matter (IV)</i> . . . . .	19
3	RESULTS . . . . .	21
3.1	Latent heat exchange in boreal and arctic biomes (I) . . . . .	21
3.1.1	<i>Phenological parameters</i> . . . . .	21
3.1.2	<i>Adaptation to increasing air temperature</i> . . . . .	21
3.1.3	<i>Surface resistance</i> . . . . .	22
3.1.4	<i>Modeling ecosystem scale latent heat exchange</i> . . . . .	22
3.1.5	<i>Latent heat exchange in peatlands (II)</i> . . . . .	22
3.2	Simulating regional hydrology and stream water DOC concentrations in boreal catchments (III) . . . . .	23
3.3	Production of biologically labile photoproducts based on chromophoric terrestrial dissolved organic carbon (IV) . . . . .	25
3.3.1	<i>Bacterial response</i> . . . . .	25
3.3.2	<i>Global estimate for BLPs</i> . . . . .	26
4	DISCUSSION . . . . .	28
4.1	Linking water and carbon cycles . . . . .	28
4.2	Latent heat exchange (I, II) . . . . .	28
4.3	Modeling DOC transport (III) . . . . .	29
4.4	Photochemical transformation of terrestrial chromophoric dissolved organic matter and production of BLPs (IV) . . . . .	30
5	CONCLUSIONS . . . . .	33
	REFERENCES . . . . .	34

## 1 INTRODUCTION

Latent heat exchange (energy used for evapotranspiration) between atmosphere and land surface is one of the ubiquitous biogeochemical processes in which living plants are involved (Collatz et al. 1991; Leuning et al. 1995). In surface energy exchange incoming shortwave solar radiation is converted to latent heat or sensible heat (Kiehl and Trenberth 1997). Latent heat exchange of vegetation is a trade off, where water will be released through a stomata of a plant at the same time when carbon dioxide ( $CO_2$ ) is taken in (Baldocchi et al. 1988).  $CO_2$  is used in photosynthesis and stored to chemical energy, which will be then available for the plant and later also heterotrophic organisms (Farquhar and Sharkey 1982; Farquhar et al. 1989).

Latent heat exchange ( $\lambda E$ ) and carbon cycle are directly linked in biogeochemical processes when organic tissue of a plant senescence (Schlesinger and Melack 1981; Aufdenkampe 2011). After the death of a plant, formerly living tissues will be converted to soil organic matter (SOM) through degradation (Kalbitz et al. 2000; Neff and Asner 2001). SOM constitutes the largest storage of organic carbon that is greater than the atmospheric carbon storage and the carbon storage in living biomass combined (Batjes 1996; Thurner et al. 2014). Therefore, SOM has a significant role in global biogeochemical carbon cycle (Schlesinger and Andrews 2000; Jobbágy and Jackson 2000).

SOM is linked to water cycle through precipitation, snow and discharge (Cole et al. 2007; Tranvik et al. 2009). The water content of soil is regulating the degradation of SOM together with soil temperature (Schlesinger and Andrews 2000; Worrall and Burt 2004). In this continuum, the water content of soil is the source of water for plants and water that cannot be retained in soil, generates discharge (Bergström 1992; Bergström 1995). Limited water availability can limit photosynthetic efficiency and latent heat exchange (Lagergren and Lindroth 2002; Bernier et al. 2006; Wharton et al. 2009; Duursma et al. 2008) leading to decreasing carbon uptake (Clark et al. 2005; Barr et al. 2007). The fraction of SOM, which gets dissolved to water and is transported to rivers, lakes and other water bodies is called dissolved organic carbon. This transport of DOC provides a tight linkage between the water and carbon cycle (Battin et al. 2009; Aufdenkampe 2011; Müller et al. 2013), including responses of DOC exports due to changes in evapotranspiration.

Increasing atmospheric  $CO_2$  concentration might be linked to the water use efficiency of plants (Frank et al. 2015) and the water cycle in land surface (Keenan et al. 2013). On the other hand, increasing mean temperature in boreal biomes are suggested to have an effect to the behavior of the soil organic matter storage (Schlesinger and Andrews 2000) and could increase SOM turnover rates to DOC. Most of the climate scenarios have predicted increasing precipitation for the boreal and arctic region, which would lead to increased transportation of DOC to rivers and ocean (Aufdenkampe 2011; Mann et al. 2012).

Although these biogeochemical processes are suggested to be sensitive to a changing climate (Sheffield et al. 2012; Jasechko et al. 2013), we do not understand well how phenology of the vegetation in the boreal and arctic biomes affect the water balance and its intra-annual variation (Jung et al. 2010; Jasechko et al. 2013).

### 1.1 Energy exchange, latent heat and water cycle

Incoming solar radiation absorbed by the Earth and its atmosphere will be balanced through the release of outgoing long-wave radiation (Figure 1) (Kiehl and Trenberth 1997). Through those processes that reflect, absorb or convert incoming solar energy to water vapor and sensible heat or store the radiation energy into living tissues of plants is called energy exchange

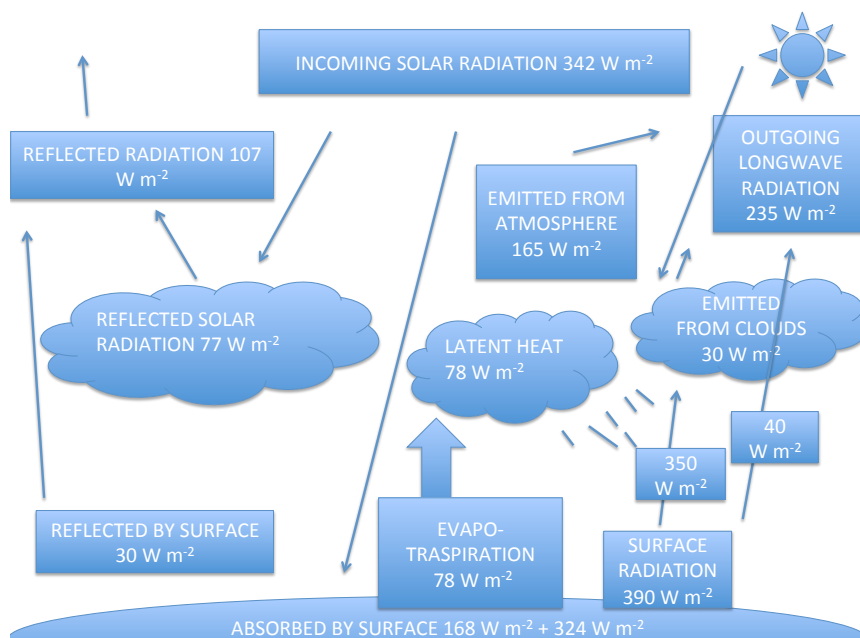


**Figure 1.** Annual and Global Mean Energy Balance of the Earth modified from IPCC 2007. Note that terms are not balanced and figure does not show all terms given in the original.

(Sellers et al. 1997). Approximately half of the incoming extraterrestrial radiation is absorbed by the surface of the earth and about half of the absorbed energy is converted to latent heat through evaporation and transpiration of plants, which are together defined as evapotranspiration (Figure 1) (Kiehl and Trenberth 1997).

Latent heat exchange of the earth surface is the energy used for evapotranspiration, which describes the amount of water evaporated by plants and the soil. The role evapotranspiration is significant in the global water cycle (Figure 2). It will return a part of the precipitation back to atmosphere through plants, which utilize only 1% of the taken water for the formation of products of photosynthesis and release 99% through the transpiration back to atmosphere.

Although transpiration of vegetation dominates the terrestrial ecosystem water fluxes removing up to half of the annual precipitation, it is poorly constrained in earth system models (ESM) (Jasechko et al. 2013). However, global climate predictions seem to be sensitive to changes in latent heat exchange (Sellers et al. 2009). During the past two decades, the interest and need for accurate measurement of energy and gas fluxes between atmosphere and land surface have increased. Due to this development, a global Eddy Covariance (EC) flux tower network (FLUXNET) has been built. In 2015 FLUXNET database reported 775 tower locations of which 520 were active providing tremendous amount of data products regarding the energy exchange between atmosphere land surface ecosystems (Aubinet et al. 2000; Baldocchi et al. 2001)

Most of the previous work based on FLUXNET data products have focused on biosphere-atmosphere carbon exchange (Hollinger et al. 2004; Baldocchi 2008; Jung et al. 2009; Stoy et al. 2009) and on site-specific energy exchange studies (Admiral and Lafleur 2007; Peichl et

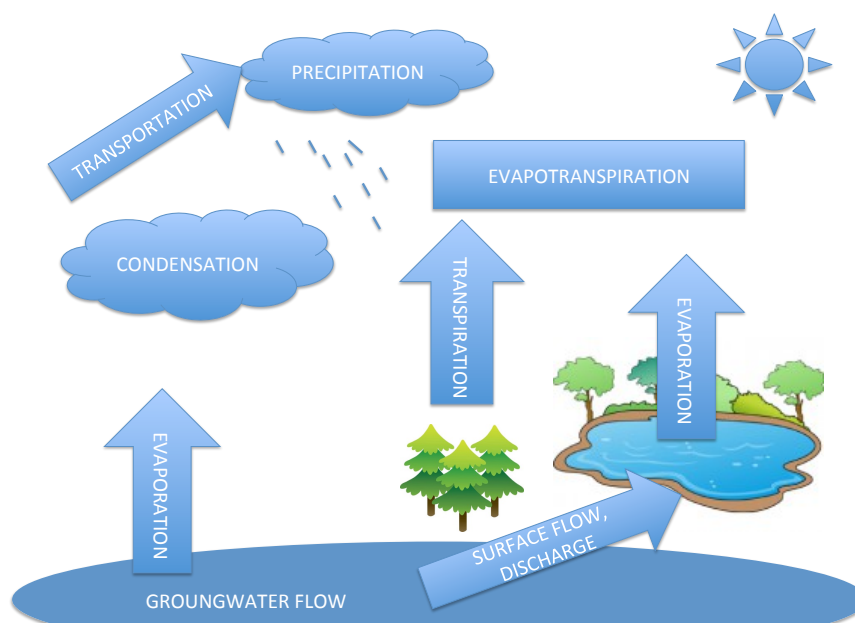


**Figure 2.** Some components of the water cycle of the Earth. Modified from the original from USGS.

al. 2013). At the same time, only a few studies have concentrated on multi-site energy fluxes to describe energy exchange in different biomes (Jung et al. 2010; Wang and Dickinson 2012) and majority of these large scale studies are based on remote sensing data products.

## 1.2 Dissolved organic carbon and photochemistry

Precipitation that is not evaporated is flowing through the soil to streams, lakes and rivers and finally to the ocean. During this transport a substantial proportion of the ecosystems production is transported as dissolved organic matter (Cole et al. 2007; Tranvik et al. 2009; Aufdenkampe 2011; Weyhenmeyer et al. 2012). Furthermore, as shown in this thesis, the export of DOC depends on the water-flow and ultimately also on evapotranspiration.

Dissolved organic carbon (DOC) is the most abundant form of organic carbon in surface waters, largely determining the carbon balance and strongly affecting water quality of freshwater ecosystems (Thackeray 2014). DOC constitutes the majority of organic carbon fluxes from terrestrial ecosystems to streams and rivers (Dai et al. 2012) and soil organic matter(SOM) to carbon cycling and sequestration in aquatic ecosystems (Cole et al. 2007; Tranvik et al. 2009; Weyhenmeyer et al. 2012). The degradation and transport of organic carbon from terrestrial ecosystems to streams is regulated by physical factors such as precipitation and temperature (Köhler et al. 2009; Öquist et al. 2014), but also on evapotranspiration which determines part of the runoff.

The DOC export of any watershed depend on the production and consumption of DOC, as well as, the transport of DOC from the watershed (Wallin et al. 2015). According to the latest estimates, the amount of carbon that rivers receive, process and transport equals the net ecosystem carbon balance in their watersheds thus playing a significant role in global

estimates (Aufdenkampe 2011).

According to its biological availability for heterotrophic organisms DOC can be divided to three categories according to the degradation time of DOC: labile (few hours - two weeks), semi-labile (from few months up to one year) and refractory (several years) (Søndergaard and Middelboe 1995; Davis and Benner 2007; Lønborg and Alvarez-Salgado 2012). The previous studies regarding the biogeochemical processes linked to DOC have concentrated on investigating for example bacterial responses based on labile fractions of DOC, while the studies studying the responses based on semi-labile and refractory DOC, are a minority.

Although, DOC is recognized as an important flow of carbon from a terrestrial reservoir to water bodies, surprisingly few models have concentrated on investigating rapid changes in stream runoff and DOC concentrations in boreal ecosystems (Xu et al. 2012), which are associated to precipitation events or snowmelt. Similarly, excluding few exceptions (Bauer et al. 2013; Fichot and Benner 2014), the fate of riverine non-readily labile DOC in coastal waters is poorly understood, although there are indications that the majority of riverine DOC (80%) cannot be defined as directly bioavailable (Søndergaard and Middelboe 1995; Lønborg and Alvarez-Salgado 2012).

The terrestrial chromophoric dissolved matter (tCDOM) constitutes the fraction of DOC, which contributes the majority of light absorption and thus defining the optical properties of a water column Vähätalo (2009). tCDOM is typically not a readily available substrate for heterotrophic consumers, but can be degraded slowly by the heterotrophic bacteria (Vähätalo et al. 2010; Koehler et al. 2012), although photolytic degradation is several times faster (Vähätalo and Wetzel 2004; Vähätalo and Wetzel 2008). Therefore, the complete sunlight-induced photochemical degradation or transformation of tCDOM to  $CO_2$  and biologically labile photoproducts (BLPs) is the major sink of tCDOM in surface waters (Vähätalo and Wetzel 2008; Spencer et al. 2009; Nelson and Siegel 2013).

Sunlight-induced degradation of tCDOM is an important component in the biogeochemical cycling of terrestrially derived DOC (tDOC) in aquatic ecosystems (Kieber et al. 1989; Mopper et al. 1991; Mopper and Kieber 2002; Zepp et al. 1998). This process produces direct  $CO_2$  emissions and converting non-labile DOC to labile forms providing source of energy for heterotrophic food webs (Vähätalo et al. 2011). For example, the recent study of Cory et al. 2014 suggests that from 70.4% to 94.9% of mineralization of DOC in shallow and optically thin arctic aquatic ecosystems is based on sunlight-induced photochemical degradation. However, similar estimates for riverine terrestrially derived DOC is lacking, although it transports annually about 250 Tg C to coastal waters.

### 1.3 Modeling

Modeling is an umbrella concept that is usually used to describe representation of a process or operational system using theoretical approaches (Wainwright and Mulligan 2004; Lark 2013). Different modeling strategies can be divided to physical, conceptual and empirical approaches. While physical models try to describe the behavior of a system using physically based theories, conceptual models pay a little attention to physics and instead, tries to describe the modeled phenomena using conceptualized model structures like storages and fluxes between storages (Wainwright and Mulligan 2004). Empirical models are based on the observed patterns of the data and cannot typically be extrapolated or used to predict behavior of a system outside of its original range. Models can be based on these represented concepts be a combination of both. Different models typically vary in their complexity. For example, a

simple model can be based on linear regression of measured and predicted variable (I), which can be utilized in the prediction of investigated phenomena within the range of the observed values.

The amount of studies utilizing different modeling approaches is continuously increasing. The simulations of the investigated phenomenon is a cost-efficient method to produce information based on existing measurements, scale them to cover spatially larger regions, as well as, validate or calibrate models. Models can also be the only way to produce information on future changes under warming climate.

The continuously increasing amount of stored data in global, national and research site data bases provide a valuable resource for the development of models, which try to describe the physical behavior of environment. Although several models have been developed for the modeling of latent heat exchange and DOC dynamics, there is ongoing debate regarding the desirable complexity of the used models (Futter et al. 2015).

Previously, several simple (Thorntwaite 1948; Penman 1948; Allen 1998) and more complex methods, as e.g. models based on remote sensing based data products (Mu et al. 2011; Jung et al. 2010), have been developed for the estimation of latent heat exchange (or evapotranspiration). All of these methods are applicable for small or large scale studies and produce reasonable annual and monthly estimates based on mean air temperature, radiation and day length (I) or remote sensing derived data products. However, the effect of seasonal adaptation of plants or the effect of the vegetation cover are rarely taken into account although it seems to have significant effect to latent heat exchange in boreal and arctic ecosystems (I). Further on, ecosystems within the same ecosystem type (e.g. wetlands, peatlands), may vary significantly in their response to environmental forcing (I,II).

In general, physical based biogeochemical models simulating DOC tend to be highly parameterized, because carbon dynamics in soil and water are relatively complex. However, complex presentation may lead to parameter and model uncertainty. On the other hand, a model should be able to describe fairly the behavior of the modeled system and too simple approaches may lead to a coarse representation of a system.

Although, DOC is recognized as a important flow of carbon from a terrestrial reservoir to water bodies, surprisingly few models have concentrated to investigate rapid changes in stream runoff and DOC concentrations in boreal ecosystems (Xu et al. 2012), which are associated to precipitation events or snowmelt (III). Similarly, with a few exceptions (Bauer et al. 2013), the fate of riverine non-readily labile DOC in coastal waters are poorly understood (VI), although there are indications that the majority of riverine DOC (80%) cannot be defined as directly bioavailable (Søndergaard and Middelboe 1995; Lønborg and Alvarez-Salgado 2012).

#### **1.4 Aim of the study**

The aim of this dissertation is to analyze how the water and DOC fluxes are linked in landscapes across space and time. Thus, there are several alternatives to describe the biogeochemical linkages between water and carbon cycles, three major approaches were selected to be covered in this study. The thesis develops firstly a physically as well as biologically based approach to simulate the latent heat fluxes for different ecosystems types in the boreal and arctic regions(I, II). Secondly, I apply thus approach to a model that analyses DOC concentrations in relation to catchment hydrology(III). Thirdly, I investigate to what extend the photochemical transformations of, supposedly terrestrially derived, riverine DOC can be used heterotrophic bacteria (IV). The latter approach provides an estimated flux describing

in which extent the sunlight-induced degradation of tDOC will be converted to BLPs and  $CO_2$  and released to atmosphere. The coupling of photosynthesis with evapotranspiration via stomatal regulation has received a lot attention elsewhere and is, therefore, not part of this thesis.

In these research articles, I have investigated biogeochemical processes related to water and dissolved organic carbon using mainly existing measurements from various data sources and carried out work in laboratory (IV). This multidisciplinary work combines physically and biologically based summary models from the different scientific fields such as micrometeorology, hydrology, microbiology, forest soil and aquatic sciences, as well as, environmental photochemistry. By using these methods, the effect of land cover type on the surface energy exchange (I, II), DOC release from boreal forested catchments (III) and the fate of riverine non-labile terrestrial DOC in coastal waters, were investigated (IV).



**Figure 3.** Location of eddy covariance sites are marked with red star (\*) (I).

## 2 MATERIAL AND METHODS

### 2.1 Data sources and management

#### 2.1.1 Eddy covariance data (I, II)

Sixty-five sites were selected for the latent heat exchange modeling in boreal and arctic biomes from FLUXNET database (<http://fluxnet.ornl.gov>). In these areas, vegetation is expected to experience seasonal adaptation (winter vs. summer) and therefore expressing phenological differences. The selected ecosystems represented natural and the most common ecosystem types in the hemiboreal, boreal or arctic areas (Fig 3). The aim was to select representative EC sites with rather long and continuous measurements providing all data products for the model calibration and reject sites restricted to summer periods or with large gaps during the time  $\lambda E$  are typically high. Agricultural sites were excluded from the analysis, because their seasonal behavior is regulated by the human activity.

The selected sites were grouped based on the dominant plant functional type (PFT) into nine different categories: (i) harvested or burnt areas temporarily void of trees (C), (ii) Douglas-fir forests (D), (iii) pine forests (P), (iv) spruce or fir dominated forests (S), (v) broadleaf deciduous forests (BD), (vi) larch forests (L), (vii) wetlands (W), (viii) tundra (T) and (ix) natural grasslands (G) (I). For the study investigating energy partitioning and evapotranspiration of peat lands, eight sites from Fennoscandia, were selected for the detailed data analysis. The selected peat lands were influenced by anthropogenic impacts in varying degrees and covering pristine open mires, peat lands converted to agricultural and drained peat lands with well developed canopy structure (II). Detailed site descriptions for peatlands are provided in (II).

The data analysis covered in study one comprises more than 400 EC site-years half-hourly of  $\lambda E$  and meteorological data (I). The data were checked and quality controlled for obvious measurement and reporting errors. For the estimation of latent heat exchange, seven meteorological variables were required : air temperature ( $T_a$ ), wind speed ( $u$ ), friction velocity ( $u^*$ ), global radiation ( $R_g$ ), net radiation ( $R_n$ ), air pressure ( $P_a$ ) and relative humidity ( $RH$ ). To avoid conditions when EC technique does not work properly, periods with low turbulent mixing ( $u^*$  less than  $0.1 \text{ m s}^{-1}$ ) were removed (I, II) (Alavi et al. 2006; Papale et al. 2006).

Meteorological variables required for the estimation of  $\lambda E$ , were gap-filled using linear

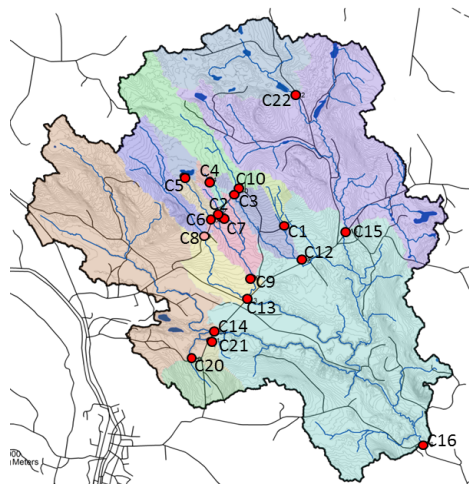


**Figure 4.** Krycklan catchment and measurement stations (III).

interpolation for short measurement gaps up to four hours in duration and longer periods of missing data were filled by using mean diurnal variation (MDV) (Reichstein et al. 2005) in a 14 days moving window (I) and 30 days moving window (II). Flux data were not gap filled and our analysis uses only measured fluxes.

### 2.1.2 Stream water dissolved organic carbon data (III)

The Krycklan catchment (64°23'N, 19°46'E) is located in northern Sweden, approximately 50 km northwest of the Baltic sea (Bothnian bay). At Svartberget field station DOC, hydrological and meteorological data are monitored. The catchment is divided into eighteen partially nested long-term monitored sub-catchments and the size of sub-catchments varies from 0.03 to 68 km<sup>2</sup> (Figure 4). A data set containing approximately 5000 stream water DOC concentration measurements for eighteen sub-catchments from 2003 to 2013, were used for the model calibration predicting stream water DOC concentrations (III).

### 2.1.3 Terrestrial chromophoric dissolved organic carbon samples (IV)

The river water samples (Table 1, Figure 5) used in the study estimating photochemical production of biologically labile photoproducts (BLPs) (III) contributes 28% of the global tDOC flux, and 33% of the freshwater discharge to coastal waters (Carlson 2002; Cauwet 2002; Coynel et al. 2005; Milliman and Farnsworth 2011). These same samples replicates have been used previously for the determination of dissolved black carbon (Jaffé et al. 2013), molecular composition of DOM (Wagner et al. 2015), dissolved iron (Xiao et al. 2013) and the photochemical isotopic fractionation of DOC (Lalonde et al. 2014).

**Table 1.** Locations and dates for sampling. City refers to a location close to the site of sampling given by coordinates. Transport time expresses the days elapsed between the sampling and the arrival of the sample to laboratory (IV).

River	Location			Date		Transport time
	Country	City	Latitude	Longitude	Sampling	
Rio Negro*	Brazil	Manaus	03°07'59"S	59°54'09"W	3 June 2010	82
Rio Solimões*	Brazil	Manaus	03°07'58"S	59°54'04"W	3 June 2010	82
Congo	Congo	Kinshasa	04°18'18"S	15°28'32"E	1 May 2009	25
Danube	Romania	Tulcea	45°13'38"N	28°44'50"E	19 Apr. 2010	21
Ganges-Brah.**	Bangladesh	Dhaka	23°34'12"N	90°10'53"E	1 Oct. 2009	68
Lena	Russia	Tiksi	71°54'14"N	127°15'16"E	16 Aug. 2009	155
Mekong	Kambodza	Phnom Penh	11°33'28"N	104°56'53"E	21 Aug. 2009	34
Mississippi	USA	New Orleans	29°02'20"N	89°19'20"W	22 Apr. 2009	34
Paraná	Argentina	Buenos Aires	34°18'07"S	58°32'47"W	29 Mar. 2009	18
St. Lawrence	Canada	Quebec	46°54'45"N	70°52'32"W	12 Jun. 2009	33
Yangtze	China	Shanghai	31°45'49"N	121°2'22"E	7 Sep. 2009	17

\*Amazon river sample was prepared by mixing samples from Rio Negro (25%) and Rio Solimões (75%) \*\*Ganges-Brahmaputra

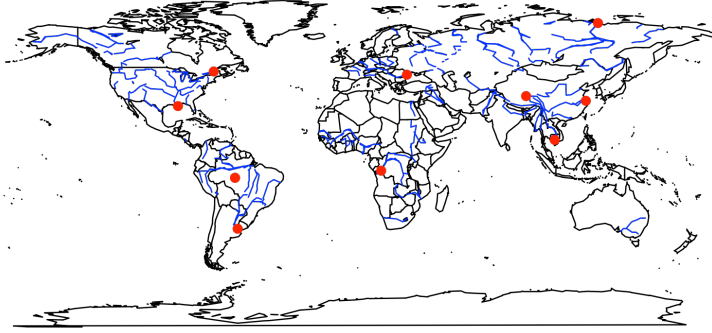


**Figure 5.** Sampling points of riverine DOC samples.

## 2.2 Analytical methods

### 2.2.1 Modeling latent heat (I)

The estimation of  $\lambda E$  was carried out using the Penman-Monteith equation (Penman 1948; Allen 1998) (I) and the surface resistance was estimated using a multiplicative model similar to those originally proposed by Jarvis (1976) and Stewart (1988) yielding:

$$r_s = f(P)f(\delta_e)f(R_g) \quad (1)$$

where  $f(P)$ ,  $f(\delta_e)$  and  $f(R_g)$  are phenological,  $\delta_e$  and  $R_g$  environmental modifiers.

The modifiers accounting the phenology for seasonal resistances (summer vs. winter) are based on the previous work of Mäkelä et al. 2004; Mäkelä et al. 2006; Mäkelä et al. 2008 and Gea-Izquierdo et al. 2010. Phenology modifiers are expressed as follows:

$$f(P) = r_{SMax} - 2 \left( 1 - \frac{1}{1+S(t)} \right) (r_{SMax} - r_{Smin}) \quad (2)$$

where  $r_{SMax}$  and  $r_{Smin}$  are the maximum and minimum stomatal resistances ( $s\ m^{-1}$ ) and  $S(t)$ , a variable describing the phenological state of the plants, yielding:

$$S(t) = \min \left( \frac{\int_{t-\tau}^t T_a(t) dt}{\tau \theta}, 1 \right), \quad (3)$$

where  $T_a$  is air temperature,  $\theta$  ( $^{\circ}C$ ) is a parameter describing the long-term average temperature at which stomatal resistance reaches its minimum value,  $\tau$  is the integration time delay of the response of the stomata (days). The phenological model describes the slow development of a surface resistance to changes in temperature as it occurs during spring. It is a modification of the model of Gea-Izquierdo et al. (2010) that they used for the analysis of Gross Primary Production (GPP). The behavior of  $S(t)$  as a function of  $\tau$  and  $\theta$  and  $T_a$  is shown in Figure 6.

Surface resistance was also assumed to have a hyperbolic dependence on  $R_g$  (Wong et al. 1979; Leuning 1995) as follows:

$$f(R_g) = \frac{k_r + R_g}{(R_g + 5)} \quad (4)$$

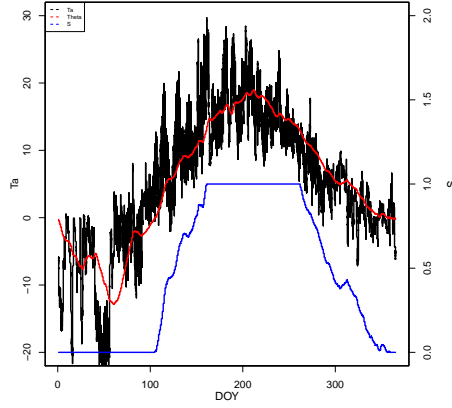


**Figure 6.** Conceptual behavior of  $S$  as a function of  $\theta$  and  $\tau$ . The black line is the measured air temperature. The variable  $S$  (blue line) is calculated based on the running mean (blue line) of the measured air temperature (black line) and with delay (which depends on  $\tau$ ).  $S$  is saturated when it reaches the value 1 (on the right y-axes)

where  $k_R$  is a parameter describing the sensitivity of surface resistance to global radiation. An offset of five  $W m^{-2}$  was added to  $R_g$  (in the denominator) to avoid frequent problems caused by occurrences of negative values of  $R_g$  and to constrain  $r_s$  surface resistance to finite values.

Finally,  $r_s$  was assumed to depend on  $\delta_e$  as follows:

$$f(\delta_e) = \left(1 + \frac{\delta_e}{k_{VPD}}\right) \quad (5)$$

where  $k_{VPD}$  ( $kPa$ ) is an empirically estimated parameter describing the sensitivity of stomatal conductance to  $\delta_e$ . High values of  $k_{VPD}$  indicate low stomatal sensitivity to VPD.

To produce mean model parameters for each ecosystem type, ecosystem specific data from each ecosystem type were concatenated. The average ecosystem type parameters were estimated from this pooled data. Based on the parameters derived from this estimation, the  $\lambda E$  values of different vegetation types were compared by using the ecosystem average model parameters for each vegetation type ( $r_{SMax}, r_{SMin}, k_R$  and  $k_{VPD}$ ) and the meteorological data of the station Hyytiälä (FI-Hyy) for 2011 (I).

## 2.2.2 Comparison of Fennoscandic peatlands (II)

To investigate differences between different peatlands ecosystems, several commonly used micrometeorological analyses were made. These details are provided in (II), but shortly the main focus were in energy partitioning to latent and sensible heat fluxes including short-term storages, contribution of bulk aerodynamic and surface resistances and the behavior of decoupling parameter (Jarvis and McNaughton 1986) and Bowen ratio (Bowen 1926) and their relationship to water table depth.

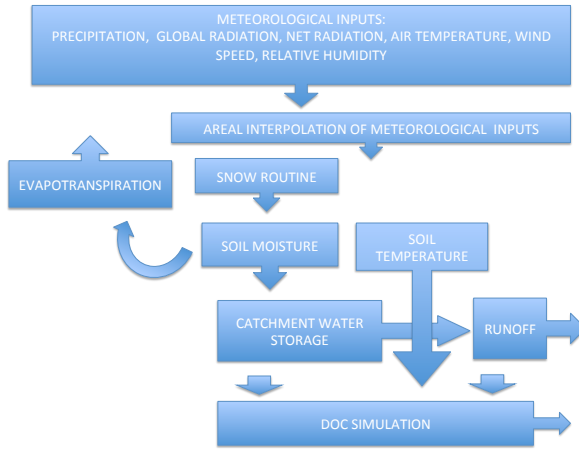


**Figure 7.** Conceptual flow chart of hydrological and DOC simulations

### 2.2.3 Modeling stream water dissolved organic carbon concentrations (III)

The regional discharge required for the simulation of stream water DOC concentrations was produced using distributed hydrological toolbox ENKI (<http://www.opensource-enki.org>) (Kolberg and Bruland 2012; Hailegeorgis and Alfredsen 2014). The hydrological model simulation was executed in  $50 \times 50$  grid cells and responses were aggregated to sub-catchment means (Figure 7). The discharge for all sub-catchments were generated using dynamical rainfall-runoff model (Kirchner 2009), which assumes that discharge can be described using simple equation for conservation-of-mass. In this mass balance the evapotranspiration was estimated using the models from (I).

The method assumes that the discharge ( $Q$ ) is dependent on the catchment water storage ( $S$ ) that can be expressed using a non-linear storage-discharge function (III), which represents the relationship between the change of discharge and discharge (Kirchner 2009).

The model of Xu et al. (2012) and K-DOC requires the estimation of catchment water storage. The relationship of catchment water storage and runoff is non-linear and can be solved by using the method of Kirchner (2009). In this approach, the use of a single storage discharge relationship leads to a fixed relationship between the change of discharge and discharge ( $Q$ ). The differential equation and the relationship between discharge sensitivity ( $g(Q)$ ) and measured discharge were solved yielding:

$$\log(g(Q)) = \log\left(\frac{-dQ/dt}{Q}\right) \approx a_0 + (1 - a_1)\log(Q) + a_2(\log(Q))^2 \quad (6)$$

where,  $a_0$ ,  $a_1$  and  $a_2$  are statistically determined watershed-specific parameters describing the non-linear relationship between  $Q$  and  $S$ .

Stream water DOC concentrations were simulated by using model of Xu et al. (2012). The original model of Xu et al. (2012) was modified to include soil temperature  $T_{soil}$  and catchment water storage  $S$  dependencies of DOC release and consumption. After these modifications, the modified DOC-model, K-DOC, was able to simulate stream water DOC concentrations in boreal catchments that are affected by the thermal winter and snow (III).

The original formulation of Xu et al. (2012) for stream water DOC concentrations is written:

$$\frac{dC_{str}}{dt} = \frac{dC_{Tres}}{dt} = (k_{sr}S - k_{rem}C_{Tres} - QC_{Tres} + [\frac{1}{k'_p} - C_{Tres}]\frac{dS}{dt})/S \quad (7)$$

where,  $C_{str}$  is carbon concentration ( $\text{mg C L}^{-1}$ ) in stream water,  $C_{Tres}$  ( $\text{mg C L}^{-1}$ ) is the carbon concentration in terrestrial reservoir,  $k_{sr}$  ( $\text{mg C L}^{-1}$ ) is the slow release of DOC from soil,  $k_{rem}$  ( $\text{mg C L}^{-1}$ ) is the slow removal of DOC from the soil water.  $k'_p$  ( $\text{L kg}^{-1}$ ) is derived from the relationship of the equilibrium partition coefficient of DOC from SOM ( $k_p$ ) (III).

In the model development the seasonal differences in the slow release rates of the carbon from the soil ( $k_{sr}$ ) and the slow removal rates of carbon from the soil water ( $k_{rem}$ ) were accounted. The process rates were assumed to be dependent on soil temperature ( $T_{soil}$ ) and the catchment water storage ( $S$ ). The slow release of DOC via microbial activity and its consumption are processes that are affected by the microbial biomass, temperature and soil moisture. While the original model of Xu et al. (2012) assumed no environmental sensitivity in DOC release, the relationship of the slow release of DOC on the environment was modified as follows (III):

$$k_{sr} = k_{sr0} e^{(k_{sr1}T_{soil})} S^{k_{sr2}} \quad (8)$$

where  $k_{sr0}$  and  $k_{sr1}$  are empirically estimated parameters determining the dependence on soil temperature and  $k_{sr2}$  is a parameter that describes the dependency of DOC release from the catchment water storage. A similar relationship was assumed for the slow removal process of DOC from the soil water yielding (III):

$$k_{rem} = k_{rem0} e^{(k_{rem1}T_{soil})} S^{k_{rem2}} \quad (9)$$

where  $k_{rem}$ ,  $k_{rem1}$  and  $k_{rem2}$  are calibrated parameters.

The K-DOC model was calibrated separately for two different periods (2003-2013 and 2006-2010) using maximization of NSE as the objective function (III).

#### **2.2.4 Modeling production of biologically labile photoproducts based on chromophoric terrestrial dissolved organic matter (IV)**

To investigate photoproduction of BLPs based on tDOC, the experimental irradiations were designed to degrade approximately half of CDOM to assess a typical (median) photochemical reactivity of tDOC along its transport from estuaries towards open ocean. The quartz flasks were irradiated for 44 h to 46 h with  $765 \text{ W m}^{-2}$  simulated solar radiation (Atlas Suntest CPS+ solar simulator) in a purified water (MQ) bath regulated to  $20^\circ \text{C}$  with a Lauda RE-112 thermostat. The irradiated samples received ultraviolet radiation dose corresponding from 26 to 27 days ultraviolet radiation does absorbed by the surface of Earth, calculated from mean annual energy budget (Kiehl and Trenberth 1997). The apparent quantum yields (AQYs) for the production of biologically labile photoproducts (BLPs) based on photobleached terrestrial derived chromophoric dissolved organic carbon (tDOC, tCDOM) were determined by relating the amount of absorbed photons to the amount of produced or utilized substrates. Detailed descriptions of analytical methods used for the determination of bacterial cell densities, biomass, respiration and calculations of AQYs are described in (IV).

For the global estimates, data were adapted from the previous study of Lalonde et al. (2014), which investigated same river water samples, but photobleached CDOM of the samples completely. Lalonde et al. (2014) reported that direct photomineralization of CDOM

to DIC varied from 16% to 43% (mean 30%) during the 10 days irradiation experiment and the following bioassay was able to degrade from 22% to 38% (mean 30%) of the remaining DOC within 28 days. These results of Lalonde et al. (2014) and determined bacterial growth efficiency (BGE) in (IV) were used in the figure 14 to demonstrate roughly the contribution of photochemical transformation of DOC compared to labile DOC. BGE estimates for labile DOC were taken from the literature and assumed to vary from 3% to 46% (mean 22%) (Giorgio et al. 1997; Giorgio and Davis 2003) and the fraction of labile DOC from total riverine DOC flux was assumed to vary from 3% to 35% (mean 19%), which covers the estimates for labile DOC in coastal waters (Søndergaard and Middelboe 1995; Lønborg et al. 2009; Lønborg and Alvarez-Salgado 2012). In all estimates given in figure 14, the fraction of refractory DOC resisting photochemical and microbial degradation is not taken into account.

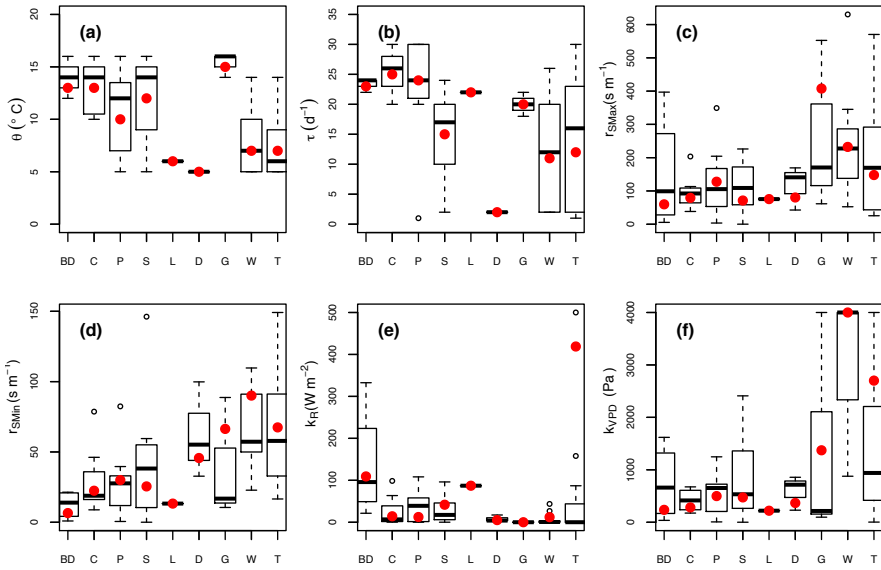


**Figure 8.** Distribution of model parameters  $\theta$  ( $^{\circ}\text{C}$ ) (a),  $\tau$  (days) (b) maximum resistance  $r_{SMmax}$  (c), minimum resistance  $r_{SMmin}$  (d) sensitivity global shortwave radiation  $k_R$  (e) and sensitivity to rapid VPD changes  $k_{VPD}$  (f). Results are presented in all subpanels according to ecosystem types where, BD, broadleaf deciduous forest; C, cut/open/burned f.; P, pine f.; S, spruce f.; L, larch f.; D, Douglas-fir f.; G, grass-land; W, wetland and T, tundra. Red points are model parameters that are calibrated against the all ecosystem type data and represent values estimated for all sites of an ecosystem type. Heavy black line of the box-and-wisker plot shows the arithmetic mean, thin black line 25% and 75% quartiles, and whisker lines (or single points) minimum and maximum values of the data. Red points are model parameters that are calibrated against the all ecosystem type data (I)

### 3 RESULTS

#### 3.1 Latent heat exchange in boreal and arctic biomes (I)

##### 3.1.1 Phenological parameters

The simulated parameters describing the differences in ecosystem behavior in terms of  $\lambda E$  showed clear differences between ecosystem types and also differences between sites within the same ecosystem category (I). Such result indicates that the phenological adaptation even within same ecosystem type (defined based on the dominant tree species and vegetation cover) may vary (Figure 8, 9) (I).

##### 3.1.2 Adaptation to increasing air temperature

The parameters indicating the saturation temperature, where minimum value of  $r_s(\theta)$  and the delay ( $\tau$ ) were reached, was clearly smaller for wetland and tundra land cover types than for forests (Figure 8) (I).

Wetland and tundra ecosystems shifted from the winter state ( $r_{SMmax}$ ) to the summer state

( $r_{SMin}$ ) faster and at lower temperatures (Figure 8) (IV). Among the forested ecosystem category, only larch and Douglas-fir had a similar low temperature requirements, although the latter did not show significant seasonal adaptation (Figure 8).

Typically forests, excluding larch and Douglas-fir, reached phenological state typical for summer resistance when  $\theta$  varied between 10 and 13 °C with  $\tau$  varying from 15 to 25 days (Figure 8a, b). Grassland ecosystems had the longest spring recovery period (defined trough parameters  $\theta$  and  $\tau$ ). For grasslands, the values of  $\theta$  were higher than for other ecosystems and values of  $\tau$  were higher than for tundra and wetland ecosystems (IV).

### 3.1.3 Surface resistance

The modeled maximum surface resistance parameters  $r_{SMax}$  varied between 100 and 250  $s\ m^{-1}$  for all ecosystem types ( $r_{SMax}$  (Figure 8c) (I). The modeled winter values of  $r_s$  were clearly higher than the modeled summer values of  $r_s$  ( $r_{SMin}$  in all ecosystems. The variation in wintertime stomatal resistance ( $r_s$ ) parameters within grassland, broadleaf deciduous forest and wetland ecosystems was large, while the variation for evergreen coniferous forest ecosystems was smaller (Figure. 8c) (I).

The highest modeled mean values of  $r_{SMin}$  were observed for Douglas-fir, grassland, tundra and wetland (Figure 8d). For coniferous forest ecosystems, the values of  $r_{SMin}$  were approximately half of the values for deciduous forests. Broadleaf deciduous forests had the smallest values of summer time  $r_s$  followed by the other forest ecosystems. In general, wetlands and tundra ecosystems had higher values of  $r_s$  than forests (I).

The mean values of  $k_R$  that describes the sensitivity of the surface resistance to  $R_g$  were small for all sites, typically less than 100  $W\ m^{-2}$ . There was no clear relationship of  $k_R$  with vegetation type or climatic characteristics. The largest variation in  $k_R$  was observed for the broadleaf deciduous forest vegetation type (Figure 8e)

High values of  $k_{VPD}$  suggest that  $r_s$  changes slowly with increasing  $e$ , while low values indicate a rapid reduction in  $r_s$  when  $e$  increases. Low values of  $k_{VPD}$  can be interpreted so that stomatal resistance ( $r_s$ ) is sensitive to vapor pressure deficit ( $\delta_e$ ). Values of  $k_{VPD}$  were higher (>500 Pa) for sites where freely evaporating water is present, and low (<500 Pa) for sites where the evaporative flux is governed largely by stomatal regulation. The values were highest for the grass, tundra and wetland-types (Figure 8f).

### 3.1.4 Modeling ecosystem scale latent heat exchange

In order to investigate the differences of  $\lambda E$  between ecosystems, the ecosystem specific  $\lambda E$  flux was generated by using mean ecosystem parameters and meteorological variables from one EC site (Hyytiälä, Finland). These simulations showed clear differences in terms of annual  $\lambda E$  exchange, even when identical levels of meteorological forcing was used in the simulation (I). The proportion of simulated  $\lambda E$  of net radiation varied between ecosystems from 39% in broadleaf deciduous forest to 16% in tundra (Figure 9). This simulation indicates that the vegetation cover type has a crucial role in latent heat exchange in boreal and arctic region and its effect might be larger than the changes in environmental forcing like as in air temperature and radiation (I).

### 3.1.5 Latent heat exchange in peatlands (II)

The comparison of eight Fennoscandinavian peatlands revealed significant variation within same ecosystem type. Although, the mean seasonal course in  $T_a$  was rather similar for all

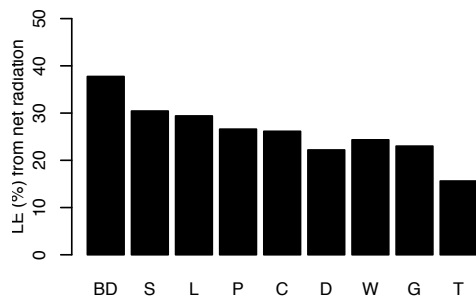


**Figure 9.** Proportion (%) of annual net radiation ( $R_n$ ) used for  $\lambda E$  based on the parameter values estimated for each ecosystem type. Meteorological data from station FI-Hyy were used in the simulations. Results are presented according to ecosystem types where, BD, broadleaf deciduous forest; C, cut/open/ burned forest; P, pine forest; S, spruce forest; L, larch forest; D, Douglas-fir forest; G, grassland; W, wetland and T, tundra.

sites, variation were greater in water table depth (WT), net radiation ( $R_n$ ) and  $VPD$  (Figure 2 in (II)).

Further on, clear differences were observed in seasonal energy partitioning (Figure 10) and showed that peatlands with significant tree density had higher sensible heat fluxes and highest short-term energy storages than naturally open peatlands (II). Surface conductance (inverse surface resistance) defined from the measured  $\lambda E$  was variable between different peatlands (Figure 5 in (II)) and related to changes in water table depth (Figure 6 in (II)). This analysis showed that in some peatlands  $\lambda E$  decreases during the rainless periods, while in some  $\lambda E$  remained nearly similar. The change was the fastest in agriculturally managed peatlands (JOK, LIN) and slowest in peatlands with high WT.

To summarize the interaction and significance of detected ecophysiological parameters ( $\Omega$ ,  $\beta$ ) to measured latent and sensible, a meta-analysis were carried out using WT and above-ground biomass as a proxy describing the measured behavior of peatlands (Figure 11). The analysis clustered peatlands into three groups based on low, intermediate and high WT, which were linked to behavior of decoupling parameter  $\Omega$  and Bowen ratio  $\beta$ . Forested peatlands (ALK, KAL, FAJ) expressed the lowest  $\Omega$  and the highest  $\beta$  indicating these sites are well coupled to atmosphere due the surface roughness and having the highest sensible heat flux. Pristine mires with low surface roughness, high WT expressed low  $\beta$  and high  $\Omega$ . Peatlands, which experienced anthropogenic management had the lowest WT and their  $\Omega$  and  $\beta$  settled between the values of two previous groups (Figure 11, (II)).

### 3.2 Simulating regional hydrology and stream water DOC concentrations in boreal catchments (III)

The parameter set from the regional hydrological model calibrations providing the highest NSE and NSE(log) for stations C7 and C16 was used to generate the discharge for the whole Krycklan catchment area and it was used for subsequent DOC simulations. The best performing parameter set produced NSE values of 0.75 and 0.43 NSE(log) for C7 (from 2003 to 2012) and 0.84 NSE and 0.74 NSE(log) for C16 (from May 2010 to October 2012) (III).

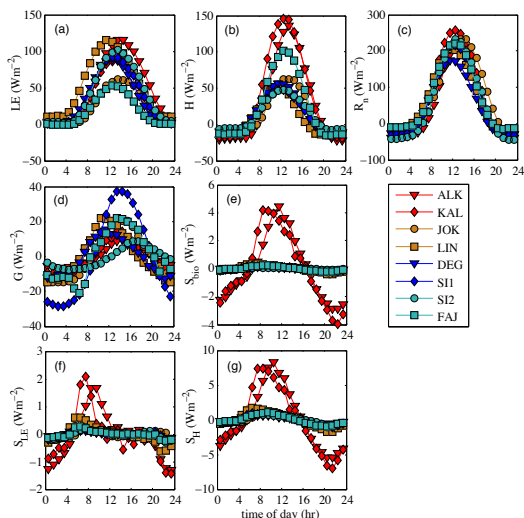


**Figure 10.** Mean snow-free season diurnal curves of (a)  $\lambda E$ , (b)  $H$ , (c)  $R_n$ , (d)  $G$ , (e)  $S_{bio}$ , (f)  $S_{LE}$ , (g)  $SH$ . (II)

This set was assumed to be representative for the whole catchment and able to describe the hydrological response of the remaining 16 ungauged sub-catchments (Figure 4, (III)).

In-stream DOC concentrations were modeled for all 18 sub-catchments using the K-DOC model for 2006-2010 and 2003-2012. The observed DOC values for the shorter simulation period varied for C16 from  $1.9 \text{ mg L}^{-1}$  to  $24.2 \text{ mg L}^{-1}$  and for C3 from  $6.5 \text{ mg L}^{-1}$  to  $80.6 \text{ mg L}^{-1}$  (Fig 12), showing approximately 12-fold difference between the lowest and the highest recorded DOC concentrations.

The NSE for simulated DOC concentrations in different sub-catchments for the years 2006-2010 varied from 0.46 to 0.76 (Figure 12, (III)). When calibration was applied for the longer simulation period, NSE varied from 0.25 to 0.69 (III), being slightly lower than for the simulations spanning 2006-2010. K-DOC was able to successfully simulate DOC concentrations for both forest and wetland dominated sub-catchments (Figure 12). When

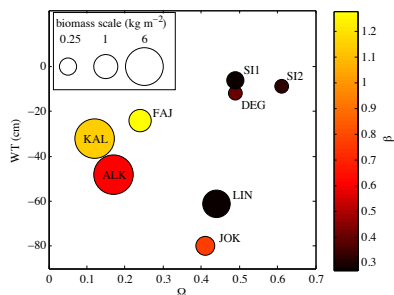


**Figure 11.** Analysis of the mean parameters ( $WT$ ,  $\Omega$ ,  $\beta$  and above-ground biomass) using the data from Tables 1 and 3 in (II)

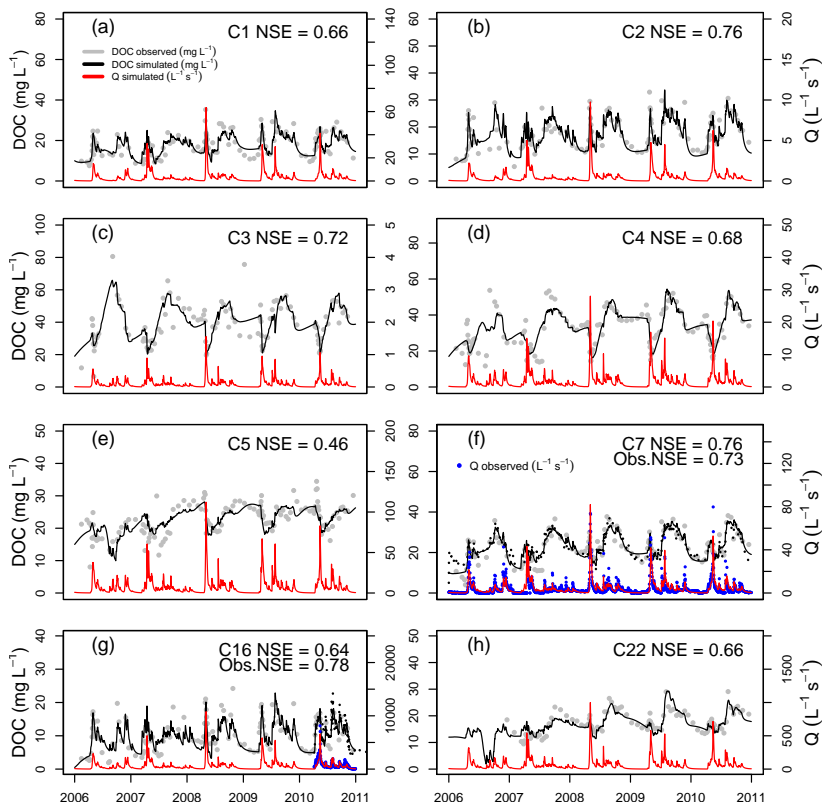


**Figure 12.** Measured and modeled DOC and discharge for selected example stations for the years 2006-2010. Description concerning the land cover types is provided in Figure 3. Grey dots are the measured DOC concentration ( $\text{mg L}^{-1}$ ), black line the simulated DOC by using K-DOC ( $\text{mg L}^{-1}$ ), red line is the simulated  $Q$  ( $\text{L}^{-1} \text{s}^{-1}$ ) and the blue dots observed  $Q$  for C7 and C16 ( $\text{L}^{-1} \text{s}^{-1}$ )

the simulation period was extended to 10 years, NSE were slightly lower than for the short simulation, and decreased most for those sub-catchments with largest proportion of lakes (C5 & C6) varying from 0.25 to 0.29 (III).

### 3.3 Production of biologically labile photoproducts based on chromophoric terrestrial dissolved organic carbon (IV)

#### 3.3.1 Bacterial response

In order to evaluate bacterial production (BP) in irradiated samples and their dark controls, as well as, based on biologically labile photoproducts (BLPs) (the difference of the preceding and the latter), an inoculum of riverine bacterioplankton were introduced to both samples. The initial bacterial cell densities at day 0 were small and increased by one or two orders of magnitude (from five to twelve days) in the irradiated being from 33% to 152% higher than in the dark control samples (IV). After defining bacterial cell densities, BP was evaluated

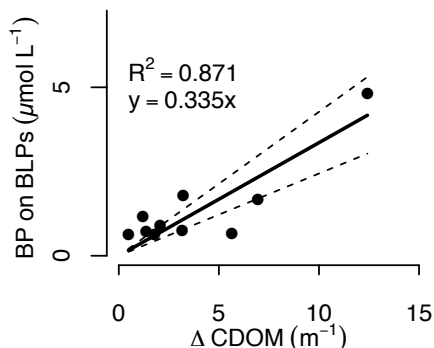


**Figure 13.** The relationship between the bacterial production based on biologically labile photoproducts (BP on BLPs) and the photobleached CDOM at 300 nm.  $\Delta a_{CDOM,300}$  shows individual samples, the solid line linear fit to the individual samples (BP on BLPs = 0.336  $\Delta a_{CDOM,300}$ ;  $R^2 = 0.871$ ,  $F_{1,9} = 68.77$ ,  $df = 1,9$ ,  $p < 0.001$ ) and the dotted lines shows the 95% confidence intervals of linear regression.

based on accumulated bacterial biomass, which were clearly higher in the irradiated than in the dark controls (III). The BP on BLPs was significantly related to the photobleaching by a linear regression coefficient of  $0.336 \text{ mmol C L m}^{-2}$  (Figure 13)

### 3.3.2 Global estimate for BLPs

To estimate quantitatively the photobleaching of (CDOM) and how it is related to BP based on BLPs, the relationship between BP on BLPs and  $\Delta a_{CDOM,300}$  (Figure 13) was multiplied with the annual CDOM fluxes (IV). This estimate describes the photochemical transformation of tDOC in coastal waters in front of each examined river and describes the carbon transfer of non-labile DOC to heterotrophic food webs.

The photobleaching of CDOM fluxes was calculated to promote altogether  $1.1 \pm 0.3 \text{ Mt C yr}^{-1}$  BP on BLPs (mean  $\pm$  95% confidence interval; Table 2). The corresponding amount of BR on BLPs was calculated to be  $9.5 \pm 4.8 \text{ Mt C yr}^{-1}$  when accounting for the 12.0% BGE on BLPs (Table 2). The sum of BP and BR on BLPs was  $10.7 \pm 4.5 \text{ Mt C yr}^{-1}$  representing the total production of BLPs (Table 2). This total production of BLPs corresponds to  $15\% \pm 6.8\%$  of the total DOC flux ( $69 \text{ Mt C yr}^{-1}$ ) of examined rivers (Table 2). Assuming that the rivers examined responsible for 28% of global DOC flux are representative for the remaining 72% DOC flux to ocean, the estimate for the global coastal production of BLPs from tDOC is  $38.0 \pm 15.9 \text{ Mt C yr}^{-1}$  supporting  $4.1 \pm 1.1 \text{ Mt C yr}^{-1}$  BP and  $33.9 \pm 16.9 \text{ Mt C yr}^{-1}$  BR.

**Table 2.** The absorption coefficient of CDOM at 300 nm, water discharge, CDOM and DOC fluxes, bacterial production (BP) and respiration (BR) based on BLPs, the total amount of BLPs and the fraction of BLPs from the DOC flux. (IV)

River	$a_{CDOM,300}^*$ ( $m^{-1}$ )	discharge ( $km^3 yr^{-1}$ )	CDOM flux ( $G m^2 yr^{-1}$ )	DOC flux ( $Mt C yr^{-1}$ )	BP based on BLPs ( $Mt C yr^{-1}$ )	BR based on BLPs ( $Mt C yr^{-1}$ )	BLPs (BP+BR) ( $Mt C yr^{-1}$ )	$\frac{BLPs}{DOC}$ (fraction)
Amazon	26.4	6300	166320	37.5	0.67	5.58	6.25	0.17
Congo	49.4	1300	64220	10.15	0.26	2.16	2.41	0.24
Danube	7.6	210	1596	0.59	0.01	0.05	0.06	0.10
Ganges-Brah**	2.1	1120	2352	3.6	0.01	0.08	0.09	0.02
Lena	21.2	520	27818	3.6	0.11	0.93	1.05	0.29
Mekong	5.1	550	2805	0.87	0.01	0.09	0.11	0.12
Mississippi	11.6	490	8800	3.5	0.04	0.30	0.34	0.09
Parana	8.4	530	4452	5.9	0.02	0.15	0.17	0.03
St. Lawrence	12	340	612	1.55	0.01	0.02	0.03	0.01
Yangtze	5	900	4500	1.8	0.02	0.15	0.17	0.09
Total		12260	283475	69.06	1.4	9.5	10.6	
Average								0.15

<sup>a</sup>  $a_{CDOM,300}$  refers to the measured values from the water samples upon their arrival, water discharge from Milliman and Farnsworth (2011), CDOM fluxes are calculated as the product of  $a_{CDOM,300}$  and water discharges, but for Mississippi, St. Lawrence and Lena published CDOM fluxes were used Stedmon et al. (2011) and Spencer et al. (2013). DOC flux is from Cauwet (2002) but updated for Amazon Coyne et al. (2005) and calculated for Mekong as the product of water discharge and DOC measured ( $1.58 mg L^{-1}$ ) upon arrival of the Mekong sample, BP on BLPs is calculated from CDOM flux using the slope  $0.333 mmol C m^{-2}$  (Figure 13), BR is calculated using BGE of 12.0% on

BLPs.\*\*Ganges-Brahmaputra

## 4 DISCUSSION

### 4.1 Linking water and carbon cycles

Adequate description and linking of water and carbon cycles is important for models trying to simulate ecosystem scale interactions between water and carbon cycles. The explicitly addressed differences in  $\lambda E$  in different ecosystem types led to improved description of  $\lambda E$  taking into account phenological changes in surface resistance (I). The central findings were confirmed also by the comparison of eight Fennoscandian peatlands (II) indicating that significant differences existing also within same ecosystem types. The improved description of  $\lambda E$  was linked to a hydrological model and used to calculate evapotranspiration based on dominant vegetation cover for 18 partially nested sub-catchments (III). The simulated discharge and catchment water storage were linked to biogeochemical model simulating stream water DOC concentrations, which revealed differences in the dynamics controlling DOC release between forested and mire-dominated, as well as, between small and large catchments (III). Based on quantitative estimate regarding the photobleaching of tCDOM and bacterial production based on biologically labile photoproducts, the carbon flux based of terrestrial chromophoric dissolved organic matter after phototransformation in coastal waters is greater than photochemical DIC production in lakes and reservoirs and equal to riverine labile DOC that enters to coastal waters (IV). The estimated conversion of tCDOM to BLPs in coastal waters indicates that the majority of the organic carbon after photochemical transformation will be converted to DIC directly or through bacterial respiration and released back to atmosphere (IV).

### 4.2 Latent heat exchange (I, II)

The latent heat exchange in boreal and arctic biomes was modeled in paper (I). There were clear differences in phenological behavior and the summertime parameter values between the most common ecosystem types, as well as, in measured  $\lambda E$  in peatlands (II). Therefore, the response of the vegetation cover to environmental forcing is not similar and a substantial portion of the land surface energy exchange is controlled by the vegetation type.

However, the range of variation in the  $r_s$  model parameters was large also within ecosystem types. Summer minimum resistance ( $r_{SMin}$ ) parameters and the VPD sensitivity ( $k_{VPD}$ ) for different sites were strongly correlated. Based on the modeled parameters, the surface resistance in peatlands and tundra is fairly constant and does not depend on the environment, indicating that poikilohydric mosses, bare ground and open water dominate the surface resistance, while in forested ecosystem stomatal regulation controls largely  $\lambda E$  (I, II). Nevertheless, the effect of a well developed canopy can be seen also in peatlands, where the forested peatland ecosystems have higher Bowen ratio and lower decoupling coefficient expressing lower  $\lambda E$  than pristine mires or agriculturally managed sites (II). These findings confirms that energy exchange in peatlands and wetland ecosystems (I) is naturally more variable than in forested ecosystem (I, II).

Tundra and wetland ecosystems had also the highest values for  $r_s$ . In these ecosystem types, the vegetation cover is typically dominated by mosses, short shrubs and plants. Feather moss, Sphagnum and lichen, which are typical for wetlands and tundra, are not similar to vascular plants in terms of physiological structures and  $\lambda E$  (Brown et al. 2010), since they have no stomatal control of evapotranspiration. Such differences between forests and wetlands can contribute to differences in  $\lambda E$  of these ecosystems (Kettridge et al. 2013), although this hypothesis cannot be justified only based on the implemented model and the data available in

the Flux databases.

The phenological approach for the modeling of  $\lambda E$  emphasizes a gradual transition from winter to summer states in most common ecosystems typical for boreal and arctic biomes. The model for  $\lambda E$  was able to describe the transition also in other ecosystem types than evergreen coniferous forest (I). The phenological control of photosynthetic capacity has been well documented (Suni et al. 2003; Mäkelä et al. 2004; Mäkelä et al. 2008; Kolari et al. 2007; Gea-Izquierdo et al. 2010) for evergreen coniferous dominated ecosystems, while other ecosystem types have been neglected. Although, phenological models have been used less for  $\lambda E$ ; the stomatal resistance has a tendency to increase during the winter periods (Wieser 2000; Sevanto et al. 2006) as indicated in (I).

The inclusion of phenology improved model estimates for boreal and arctic land cover types. The results showed that differences are large between summer and winter periods even for ever-green conifers. The relatively large differences in  $\lambda E$  between different ecosystem types suggest that an ecosystem type specific approach for the estimation of  $\lambda E$  may improve regional estimates compared simulation of climatic zones using a single ecosystem type and approaches that the phenological behavior and differences in parameter values of different ecosystems (I). Also the comparison of eight Fennoscandinavian peatlands showed that the variation within the same ecosystem type can be large (II).

Previous studies modeling phenological adaptation of photosynthetic capacity and gross primary production have reported shorter adaptation time for recovery of transpiration (Mäkelä et al. 2004; Kolari et al. 2007) than the results for  $\lambda E$ , which varied from 2 to 30 days in different conifer forests. This difference is most likely caused by the development of the ground vegetation, which increases the time interval required for the recovery (indicated by the parameter  $\tau$ ) also the formulation of the lagged temperature effect differed slightly from the approach used in the previous research. For the  $\lambda E$  model saturation temperature ( $\theta$ ) and time interval ( $\tau$ ) was calibrated to implement the transition of the whole ecosystem and its effect on model performance, while in studies dealing with the phenological behavior of photosynthetic capacity the focus has been more onto the adaptation of the dominant tree species (I).

### 4.3 Modeling DOC transport (III)

Ecosystem specific evapotranspiration (ET) was taken into account in the hydrological simulations by using the mean ecosystem specific parameters in the hydrological simulations (I). Actual ET was calculated based on the gridded vegetation maps and dominant tree species composition in different sub-catchments (Laudon et al. 2013). Regionally estimated ET for sub-catchments based on the composition of the different trees (Birch, Spruce, Pine, mires and open water), improved the performance of the hydrological model (data not shown) compared to Priestly-Taylor based approach (Priestley and Taylor 1972) (III).

Adequate description of runoff over different parts of a large watershed is crucial for the modeling of stream water DOC concentrations. Based on the findings in Krycklan catchment, the best performing parameter set for discharge generation was achieved by optimizing the performance for stations C7 & C16 simultaneously (III). When the performance was evaluated using NSE and NSE(log) as optimization criteria, the simulated discharge replicated fairly well observed high flow and low flow conditions.

Based on simulated stream water DOC concentrations, forest and mire dominated land cover types showed differences in terms of DOC release during the hydrological events (III). While in the forest-dominated sub-catchments stream water DOC concentrations increased

during snow melt, in mire dominated sites concentrations decreases indicating dilution of transportable DOC in soil and the highest DOC concentrations were observed and modeled during the low-flow season (I). The K-DOC were able to capture the differences between mire- and forest-dominated catchments that have been reported in several studies (Laudon et al. 2004; Billett et al. 2011)) previously.

K-DOC performed better compared to previous models used in Krycklan catchment. For the period 2006-2010, Oni et al. (2014) reported NSE by using RIM for C2 (forest), C4 (mire) and C7 (mixed) to be 0.62, 0.52 and 0.54, while INCA-C based simulation produced NSE 0.52, 0.49 and 0.50. The corresponding NSE for the same catchments using K-DOC was 0.76, 0.68 and 0.73. For the Krycklan catchment outlet (C16), our results can be compared to RIM and INCA-C simulations that produced  $R^2$  values 0.59 and 0.49 (Oni et al. 2015), while NSE for K-DOC was 0.61.

Although, several DOC models have been published, only four of them have been used in the Krycklan catchment and typically limited to few sub-catchments (Yurova et al. 2008; Winterdahl et al. 2011; Oni et al. 2014; Tiwari et al. 2014; Oni et al. 2015). None of these models has used catchment water storage ( $S$ ) as model input for simulating stream water DOC concentrations. At the same time, most of remaining published DOC models have been used in more southern and partly temperate catchments (Boyer et al. 1995; Michalzik et al. 2003; Jutras et al. 2011; Xu et al. 2012; Dick et al. 2014) (III).

From the hydrological point of view, K-DOC differs compared to other published DOC models (excluding the model of Xu et al. (2012)), because catchment water storage is used to predict stream water concentrations (III). The more common approach in the previous models has been to link soil moisture ( $SM$ ) and DOC production, which describes the DOC production from soil organic matter (SOM). However,  $SM$  is a relatively slowly changing variable that does not respond to rapid hydrological events unlike catchment water storage (Kirchner 2009).

In the K-DOC the simulated discharge is linked with a biogeochemical model that represents the relationship of flow and DOC stream water concentrations using non-linear dependencies (III). This approach combines slowly changing simulated soil temperature and  $S$ , which has instantaneous response to changing discharge. This might be one reason why K-DOC is able to capture stream water DOC concentrations during the hydrological events better than previously tested models in same catchments (III).

The results based on the K-DOC simulations and investigation of model variables, indicates that catchment water storage is important for DOC release, while soil temperature is important for DOC consumption. The simplified approach to divide SOM degradation to DOC release and DOC consumption rates were applicable for 18 partially nested sub-catchment. This finding suggest that a parsimonious conceptual description of interactions between discharge and stream water DOC concentration better and a complex physical model like INCA-C (Futter et al. 2007; Oni et al. 2014) (III).

#### **4.4 Photochemical transformation of terrestrial chromophoric dissolved organic matter and production of BLPs (IV)**

After DOC is released from the soil to stream waters, it is be transported to lakes and rivers and during this time, a part of the DOC will be degraded (Algesten et al. 2004; Weyhenmeyer et al. 2012). However, the retention times in inland waters and rivers are typically short, water columns are optically thick compared to coastal waters. Therefore ultraviolet radiation can penetrate typically less than 0.31 m depth (Salonen and Vähätalo 1994; Amon and

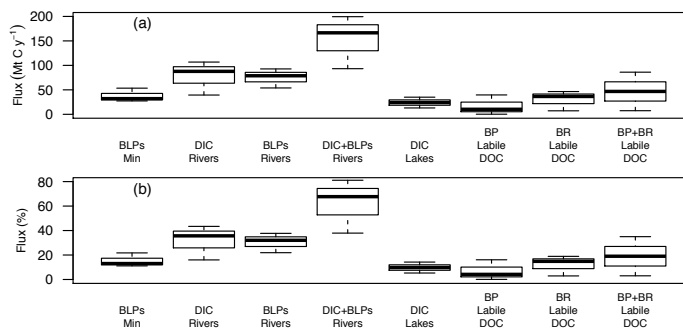


**Figure 14.** BLPs Min is the estimate given in (IV) for assimilation of BLPs, DIC rivers is calculated flux based on the reported DIC production (Lalonde et al. 2014) and BLPs Rivers is reported estimate for BLPs assimilation after 28 day incubation (Lalonde et al. 2014). DIC lakes is the estimate for photochemical production of  $CO_2$  in lakes and reservoirs Koehler et al. 2014. BP Labile DOC and BR labile DOC are bacterial production and bacterial respiration estimated based on the fraction of labile DOC (Søndergaard and Middelboe 1995; Lønborg et al. 2009; Lønborg and Alvarez-Salgado 2012) and BGEs from literature (Giorgio et al. 1997) and BP+BR Labile DOC is the sum or the two latter. Panel a) represents flux estimates in  $Mt C y^{-1}$  and b) proportion from total annual riverine DOC flux  $246 Mt C y^{-1}$  (Cauwet 2002)

Benner 1996; Granéli et al. 1996; Reitner et al. 1997; Vähätalo et al. 2000; Pers et al. 2001; Pullin et al. 2004; Aarnos et al. 2012) (IV). tCDOM is also resistant to microbial degradation Vähätalo and Wetzel 2004; Vähätalo and Wetzel 2008 and is the fraction of tDOC, which is transported to lakes and rivers. Water cycle is important for the biogeochemical cycle of tCDOM, because the effective photochemical degradation require transportation coastal waters (IV) and carbon assimilation in large river basins are associated to latent heat exchange. The most productive tropical basins of Amazon and Congo Rivers receives large amounts of water as precipitation and evapotranspiration can be as high as 1400 mm annually (Jung et al. 2010), while in boreal ecosystems ET is typically less than 350 mm. These large water fluxes are associated to carbon sequestration in their catchments and lead to high DOC fluxes (Aufdenkampe 2011).

The estimate based on photobleaching of tDOC provides the first time a quantitative approximation for the production of BLPs in the coastal waters in front of each river (IV). The estimated production of BLPs from tDOC ( $38.0 \pm 15.9 Mt C yr^{-1}$ ) had only a small contribution compared to estimated earlier ( $206 Mt C yr^{-1}$ ) of Miller et al. (2002). The previous estimate of Miller et al. (2002) corresponds roughly global riverine DOC flux to the ocean ( $246 Mt C yr^{-1}$ ) (Cai 2011) and must be based partly on the autochthonous production in marine waters similarly as in the study of Aarnos et al. (2012), where BLPs originated from marine DOC and tDOC in the Baltic Sea. Therefore, these previous BLP estimates (Miller et al. 2002; Aarnos et al. 2012) do not describe production of BLPs based on tDOC only (IV).

The annual production estimate for BLPs based on tDOC in coastal waters ( $38.0 \pm 15.9 Mt C yr^{-1}$ ) is similar or larger compared to the global photochemical production of dissolved inorganic carbon (DIC) (from 13 to  $35 Mt C yr^{-1}$ ) in inland waters (Koehler et al. 2014) (IV). This comparison suggests that although solar radiation is an effective way to trans-

form a remarkable amount of DOC in lakes and reservoirs (excluding rivers), the majority of sunlight-induced photobleaching of terrestrial and freshwater DOC occurs in coastal waters (IV). These differences between lakes (including reservoirs) and coastal waters are due to differences in optical depth, where photochemical reactions can efficiently degrade tCDOM (Vodacek et al. 1997; Del Vecchio and Subramaniam 2004; Fichot and Benner 2014) (IV).

Assuming that the determined mean BGE on BLPs 12% (IV) is representative for BLPs produced from tDOC, the majority of BLPs will be respired rapidly to DIC contributing  $33.9 \pm 16.9$  Mt C yr<sup>-1</sup> in coastal waters. This estimate is roughly 10% from the DIC transported by the rivers (407 Mt C yr<sup>-1</sup>; Cai 2011). Nevertheless, assimilated BLPs produced based on photobleaching of tDOC produces  $4.1 \pm 1.1$  Mt C yr<sup>-1</sup> bacterial biomass that is an additional carbon source for heterotrophic food webs in coastal waters (IV).

The production of BP based on BLPs was significantly related to the photobleaching of CDOM with an  $R^2$  0.88 (Figure 13). Similar linear relationships have been found for various BLP compounds in earlier studies (Miller and Moran 1997; Obernosterer and Herndl 2000; Brinkmann et al. 2003).  $\Delta a_{CDOM,300}$  explained well ( $R^2 > 96\%$ ) the photoproduction of individual BLP-compounds (formaldehyde, acetaldehyde and glyoxylate (Kieber et al. 1990)), but did not describe the bacterial response to produced BLPs. The estimated  $R^2$ -value (Figure 13) for the production of BP based on BLPs is lower than  $R^2$ -value for BLPs in the study of Kieber et al. (1990). However,  $R^2$ -value is higher than the corresponding one for 38 lake water samples (Bertilsson and Tranvik 2000) indicating that the production of BLPs is quantitatively linked to the photobleaching of CDOM and can be used as a useful proxy for the BLP production based on tDOC.

The results regarding the biological responses based on photobleaching of tDOC complement our understanding regarding the fate of photolabile tDOC in coastal waters, which is the major sink of tDOC (Figure 14). Although, photoproduction rates for single BLPs are previously reported (Kieber et al. 1990; Miller and Moran 1997; Obernosterer and Herndl 2000; Bertilsson and Tranvik 2000), the estimates regarding the relationship of  $\Delta a_{CDOM,300}$  and bacterial responses based on BLPs are scarce. Previous review reported 44 identified BLPs (Vähätalo 2009), but the newest research indicates that the group of compounds that can be considered as BLPs may contain more than 2600 different chemical compounds (Wagner et al. 2015), which can be assimilated by heterotrophic bacteria in coastal waters. For the estimation of global significance of tDOM derived BLPs, the production rates for single compounds cannot be used to estimate the biological significance. Therefore, future research is needed to interpret our first estimate, which suggests that BLP flux is roughly similar to labile DOC flux and in the same scale with the photochemical DIC production in lakes and reservoirs (VI) (Figure 14).

## 5 CONCLUSIONS

The results introduced in these four research articles described linkages between biogeochemical cycles of water and dissolved organic carbon bringing into focus the importance of adequate of description of these processes across time and space. The small and large scale heterogeneity of landscapes is playing a crucial role in the modeling of latent heat exchange and dissolved organic carbon and partly affected by the seasonal behavior of ecosystems. The findings of these studies may help to improve physical and conceptual model descriptions of investigated phenomena in global models simulating these complex interactions between water and carbon cycles.

## REFERENCES

- Aarnos H., Ylöstalo P., and Vähätalo A. V. (2012). Seasonal phototransformation of dissolved organic matter to ammonium, dissolved inorganic carbon, and labile substrates supporting bacterial biomass across the Baltic Sea. *Journal of Geophysical Research* 117(G1):1–14. doi: 10.1029/2010JG001633.
- Admiral S. W. and Lafleur P. M. (2007). Modelling of latent heat partitioning at a bog peatland. *Agricultural and Forest Meteorology* 144(3-4):213–229. doi: 10.1016/j.agrformet.2007.02.005.
- Alavi N., Warland J. S., and Berg A. A. (2006). Filling gaps in evapotranspiration measurements for water budget studies: Evaluation of a Kalman filtering approach. *Agricultural and Forest Meteorology* 141(1):57–66. doi: 10.1016/j.agrformet.2006.09.011.
- Algesten G., Sobek S., Bergström A.-K., Ågren A., Tranvik L. J., and Jansson M. (2004). Role of lakes for organic carbon cycling in the boreal zone. *Global Change Biology* 10(1):141–147. doi: 10.1111/j.1365-2486.2003.00721.x.
- Allen R. G. (1998). Crop Evapotranspiration (guidelines for computing crop water requirements). *FAO Irrigation and Drainage Paper* (56):1–296.
- Amon R. M. W. and Benner R. (1996). Bacterial utilization of different size classes of dissolved organic matter. *Limnology and Oceanography* 41(1):41–51. doi: 10.4319/lo.1996.41.1.0041.
- Aubinet M, Grelle A, Ibrom A, Rannik U, Moncrieff J, Foken T, Kowalski A. S., Martin P. H., Berbigier P, Bernhofer C, Clement R, Elbers J, Granier A, Grunwald T, Morgenstern K, Pilegaard K, Rebmann C, Snijders W, Valentini R, and Vesala T (2000). “Estimates of the annual net carbon and water exchange of forests: The EUROFLUX methodology”. In: *Advances in ecological research*. Vol. 30, 113–175. doi: 10.1016/S0065-2504(08)60018-5.
- Aufdenkampe A. (2011). Riverine coupling of biogeochemical cycles between land, oceans, and atmosphere. *Frontiers in Ecology and the Environment* 9(1):53–60. doi: 10.1890/100014.
- Baldocchi D. D., Hicks B. B., and Meyers T. P. (1988). Measuring biosphere-atmosphere exchanges of biologically related gases with micrometeorological methods. *Ecology* 69(5):1331–1340. doi: 10.2307/1941631.
- Baldocchi D. (2008). Turnet review No. 15. ‘Breathing’ of the terrestrial biosphere: lessons learned from a global network of carbon dioxide flux measurement systems. *Australian Journal of Botany* 56(1):1–26. doi: 10.1071/BT07151.
- Baldocchi D., Falge E., Gu L., Olson R., Hollinger D., Running S., Anthoni P, Bernhofer C., Davis K., Evans R., Fuentes J., Goldstein A., Katul G., Law B., Lee X., Malhi Y.,

- Meyers T., Munger W., Oechel W., Paw K. T. U., Pilegaard K., Schmid H. P., and Valentini R. (2001). FLUXNET: A New Tool to Study the Temporal and Spatial Variability of Ecosystem-Scale Carbon Dioxide, Water Vapor, and Energy Flux Densities. *Bulletin of the American Meteorological Society* 82(11):2415–2434.  
doi: 10.1175/1520-0477(2001)082<2415:FANTTS>2.3.CO;2.
- Barr A. G., Black T. A., Hogg E. H., Griffis T. J., Morgenstern K., Kljun N., Theede A., and Nesic Z. (2007). Climatic controls on the carbon and water balances of a boreal aspen forest, 1994–2003. *Global Change Biology* 13(3):561–576.  
doi: 10.1111/j.1365-2486.2006.01220.x.
- Batjes N. H. (1996). Total carbon and nitrogen in the soils of the world. *European Journal of Soil Science* 47(2):151–163.  
doi: 10.1111/ejss.12120.
- Battin T. J., Luysaert S., Kaplan L. A., Aufdenkampe A. K., Richter A., and Tranvik L. J. (2009). The boundless carbon cycle. *Nature Geoscience* 2(9):598–600.  
doi: 10.1038/ngeo618.
- Bauer J. E., Cai W.-J., Raymond P. A., Bianchi T. S., Hopkinson C. S., and Regnier P. A. G. (2013). The changing carbon cycle of the coastal ocean. *Nature* 504:61–70.  
doi: 10.1038/nature12857.
- Bergström S. (1992). *The HBV model - its structure and applications*. Tech. rep. Norrköping: Swedish Meteorological and Hydrological Institute (SHMI), Hydrology, 1–35.
- (1995). “The HBV Model”. In: *Computer Models of Watershed Hydrology*. Ed. by Singh V. P. Colorado: Water Resources Publications, 443–476.
- Bernier P., Bartlett P., Black T., Barr A., Kljun N., and McCaughey J. (2006). Drought constraints on transpiration and canopy conductance in mature aspen and jack pine stands. *Agricultural and Forest Meteorology* 140(1-4):64–78.  
doi: 10.1016/j.agrformet.2006.03.019.
- Bertilsson S and Tranvik L. (2000). Photochemical transformation of dissolved organic matter in lakes. *Limnology and Oceanography* 45(4):753–762.  
doi: 10.4319/lo.2000.45.4.0753.
- Billett M. F., Garnett M. H., Dinsmore K. J., Dyson K. E., Harvey F., Thomson A. M., Pirainen S., and Kortelainen P. (2011). Age and source of different forms of carbon released from boreal peatland streams during spring snowmelt in E. Finland. *Biogeochemistry* 111(1-3):273–286.  
doi: 10.1007/s10533-011-9645-4.
- Bowen I. S. (1926). The ratio of heat losses by conduction and by evaporation from any water surface. *Physical Review* 27(6):779–787.  
doi: 10.1103/PhysRev.27.779.
- Boyer E. W., Hornberger M, and Bencala K. E. (1995). Overview of a simple model describing variation of dissolved organic carbon in an upland catchment. *Ecological Modelling* 86:183–188.  
doi: DOI:10.1016/0304-3800(95)00049-6.
- Brinkmann T., Hörsch P., Sartorius D., and Frimmel F. H. (2003). Photoformation of low-molecular-weight organic acids from brown water dissolved organic matter. *Environmental science & technology* 37(18):4190–4198.  
doi: 10.1021/es0263339.
- Brown S. M., Petrone R. M., Mendoza C., and Devito K. J. (2010). Surface vegetation controls on evapotranspiration from a sub-humid Western Boreal Plain wetland. *Hydrological*

- Processes 24(8):1072–1085.  
doi: 10.1002/hyp.7569.
- Cai W.-J. (2011). Estuarine and Coastal Ocean Carbon Paradox: CO<sub>2</sub> Sinks or Sites of Terrestrial Carbon Incineration? *Annual Review of Marine Science* 3(1):123–145.  
doi: 10.1146/annurev-marine-120709-142723.
- Carlson C. A. (2002). “Production and Removal Processes”. In: *Biogeochemistry of Marine Dissolved Organic Matter*. Ed. by Hansell D. A. and Carlson C. A. Elsevier. Chap. 4, 91–151.  
doi: 10.1016/B978-012323841-2/50006-3.
- Cauwet G. (2002). “DOM in the Coastal Zone,” in: *Biogeochemistry of Marine Dissolved Organic Matter*. Ed. by Hansell D. A. and Carlson C. A. San Diego: Academic Press. Chap. 12, 579–609.  
doi: 10.1016/B978-012323841-2/50014-2.
- Clark J. M., Chapman P. J., Adamson J. K., and Lane S. N. (2005). Influence of drought-induced acidification on the mobility of dissolved organic carbon in peat soils. *Global Change Biology* 11(5):791–809.  
doi: 10.1111/j.1365-2486.2005.00937.x.
- Cole J. J., Prairie Y. T., Caraco N. F., McDowell W. H., Tranvik L. J., Striegl R. G., Duarte C. M., Kortelainen P., Downing J. A., Middelburg J. J., and Melack J. (2007). Plumbing the Global Carbon Cycle: Integrating Inland Waters into the Terrestrial Carbon Budget. *Ecosystems* 10(1):172–185.  
doi: 10.1007/s10021-006-9013-8.
- Collatz G. J., Ball J. T., Grivet C., and Berry J. A. (1991). Physiological and environmental regulation of stomatal conductance, photosynthesis and transpiration - A model that includes a laminar boundary layer. *Agricultural and Forest Meteorology* 54(2-4):107–136.  
doi: 10.1016/0168-1923(91)90002-8.
- Cory R. M., Ward C. P., Crump B. C., and Kling G. W. (2014). Sunlight controls water column processing of carbon in arctic fresh waters. *Science* 345(6199):925–928.  
doi: 10.1126/science.1253119.
- Coyne A., Seyler P., Etcheber H., Meybeck M., and Orange D. (2005). Spatial and seasonal dynamics of total suspended sediment and organic carbon species in the Congo River. *Global Biogeochemical Cycles* 19(4):1–17.  
doi: 10.1029/2004GB002335.
- Dai M., Yin Z., Meng F., Liu Q., and Cai W.-J. (2012). Spatial distribution of riverine DOC inputs to the ocean: an updated global synthesis supplementary. *Current Opinion in Environmental Sustainability* 4(2):170–178.  
doi: 10.1016/j.cosust.2012.03.003.
- Davis J. and Benner R. (2007). Quantitative estimates of labile and semi-labile dissolved organic carbon in the western Arctic Ocean: A molecular approach. *Limnology and Oceanography* 52(6):2434–2444.  
doi: 10.4319/lo.2007.52.6.2434.
- Del Vecchio R. and Subramaniam A. (2004). Influence of the Amazon River on the surface optical properties of the western tropical North Atlantic Ocean. *Journal of Geophysical Research* 109(C11001):  
doi: 10.1029/2004JC002503.
- Dick J. J., Tetzlaff D., Birkel C., and Soulsby C. (2014). Modelling landscape controls on dissolved organic carbon sources and fluxes to streams. *Biogeochemistry* 122(2-3):361–

374.  
doi: 10.1007/s10533-014-0046-3.
- Duursma R. A., Kolari P., Perämäki M., Nikinmaa E., Hari P., Delzon S., Loustau D., Ilvesniemi H., Pumpanen J., and Mäkelä A (2008). Predicting the decline in daily maximum transpiration rate of two pine stands during drought based on constant minimum leaf water potential and plant hydraulic conductance. *Tree physiology* 28(2):265–76.  
doi: 10.1093/treephys/28.2.265.
- Farquhar G. D. and Sharkey T. D. (1982). Stomatal Conductance and Photosynthesis. *Annual Review of Plant Physiology* 33(1):317–345.  
doi: 10.1146/annurev.pp.33.060182.001533.
- Farquhar G. D., Ehleringer J. R., and Hubick K. T. (1989). Carbon isotope discrimination and photosynthesis. *Annual Review of Plant Physiology* 40:503–537.  
doi: 10.1146/annurev.arplant.40.1.503.
- Ficht C. G. and Benner R. (2014). The fate of terrigenous dissolved organic carbon in a river-influenced ocean margin. *Global Biogeochemical Cycles* 28:300–318.  
doi: 10.1002/2013GB004670.
- Frank D. C., Poulter B., Saurer M., Esper J., Huntingford C., Helle G., Treydte K., Zimmermann N. E., Schleser G. H., Ahlström A., Ciais P., Friedlingstein P., Levis S., Lomas M., Sitch S., Viovy N., Andreu-Hayles L., Bednarz Z., Berninger F., Boettger T., D’Alessandro C. M., Daux V., Filot M., Grabner M., Gutierrez E., Haupt M., Hiltunen E., Jungner H., Kalela-Brundin M., Krapiec M., Leuenberger M., Loader N. J., Marah H., Masson-Delmotte V., Pazdur A., Pawelczyk S., Pierre M., Planells O., Pukiene R., Reynolds-Henne C. E., Rinne K. T., Saracino A., Sonninen E., Stievenard M., Switsur V. R., Szczepanek M., Szychowska-Krapiec E., Todaro L., Waterhouse J. S., and Weigl M. (2015). Water-use efficiency and transpiration across European forests during the Anthropocene. *Nature Climate Change* 5:579–583.  
doi: 10.1038/nclimate2614.
- Futter M. N., Butterfield D., Cosby B. J., Dillon P. J., Wade A. J., and Whitehead P. G. (2007). Modeling the mechanisms that control in-stream dissolved organic carbon dynamics in upland and forested catchments. *Water Resources Research* 43(2):W02424.  
doi: 10.1029/2006WR004960.
- Futter M. N., Whitehead P. G., Sarkar S., Rodda H., and Crossman J. (2015). Rainfall runoff modelling of the Upper Ganga and Brahmaputra basins using PERSiST. *Environmental Science: Processes & Impacts* 17(6):1070–1081.  
doi: 10.1039/C4EM00613E.
- Gea-Izquierdo G., Mäkelä A., Margolis H., Bergeron Y., Black T. A., Dunn A., Hadley J., Kyaw Tha Paw U, Falk M., Wharton S., Monson R., Hollinger D. Y., Laurila T., Aurela M., McCaughey H., Bourque C., Vesala T., and Berninger F. (2010). Modeling acclimation of photosynthesis to temperature in evergreen conifer forests. *The New phytologist* 188(1):175–86.  
doi: 10.1111/j.1469-8137.2010.03367.x.
- Giorgio P. A. del and Davis J (2003). “Patterns in Dissolved Organic Matter Lability and Consumption across Aquatic Ecosystems”. In: *Aquatic Ecosystems*. Ed. by Findlay S. E. G. and Sinsabaugh R. L. *Aquatic Ecology*. Burlington: Academic Press, 399–424.  
doi: 10.1016/B978-012256371-3/50018-4.
- Giorgio P. A. del, Cole J. J., and Cimbleris A (1997). Respiration rates in bacteria exceed phytoplankton production in unproductive aquatic systems. *Nature* 385(9):148–151.  
doi: 10.1038/385148a0.

- Granéli W., Lindell M., and Tranvik L. (1996). Photo-oxidative production of dissolved inorganic carbon in lakes of different humic content and Lars Tranvik. *Limnology and Oceanography* 41(4):698–706.  
doi: 10.4319/lo.1996.41.4.0698.
- Hailegeorgis T. T. and Alfredsen K. (2014). Comparative evaluation of performances of different conceptualisations of distributed HBV runoff response routines for prediction of hourly streamflow in boreal mountainous catchments. *Hydrology Research* 8:1–22.  
doi: 10.2166/nh.2014.051.
- Hollinger D. Y., Aber J., Dail B., Davidson E. A., Goltz S. M., Hughes H., Leclerc M. Y., Lee J. T., Richardson A. D., Rodrigues C., Scott N. A., Achuatavarier D., and Walsh J. (2004). Spatial and temporal variability in forest-atmosphere CO<sub>2</sub> exchange. *Global Change Biology* 10(10):1689–1706.  
doi: 10.1111/j.1365-2486.2004.00847.x.
- Jaffé R., Ding Y., Niggemann J., Vahatalo A. V., Stubbins A., Spencer R. G. M., Campbell J., and Dittmar T. (2013). Global charcoal mobilization from soils via dissolution and riverine transport to the oceans. *Science* 340(6130):345–347.  
doi: 10.1126/science.1231476.
- Jarvis P. G. (1976). The Interpretation of the Variations in Leaf Water Potential and Stomatal Conductance Found in Canopies in the Field. *Philosophical Transactions of the Royal Society of London. B, Biological Sciences* 273(927):593–610.  
doi: 10.1098/rstb.1976.0035.
- Jarvis P. G. and McNaughton K. G. (1986). “Stomatal Control of Transpiration: Scaling Up from Leaf to Region”. In: *Advances in Ecological Research*. Ed. by MacFadyen A and Ford E. D. Vol. 15. *Advances in Ecological Research*. Academic Press, 1–49.  
doi: 10.1016/S0065-2504(08)60119-1.
- Jasechko S., Sharp Z. D., Gibson J. J., Birks S. J., Yi Y., and Fawcett P. J. (2013). Terrestrial water fluxes dominated by transpiration. *Nature* 496(7445):347–50.  
doi: 10.1038/nature11983.
- Jobbágy E. G. and Jackson R. B. (2000). The Vertical Distribution of Soil Organic Carbon and Its Relation to Climate and Vegetation. *Ecological Applications* 10(2):423–436.  
doi: 10.1890/1051-0761(2000)010[0423:TVDOSO]2.0.CO;2.
- Jung M., Reichstein M., and Bondeau A. (2009). Towards global empirical upscaling of FLUXNET eddy covariance observations: validation of a model tree ensemble approach using a biosphere model. *Biogeosciences* 6(10):2001–2013.  
doi: 10.5194/bg-6-2001-2009.
- Jung M., Reichstein M., Ciais P., Seneviratne S. I., Sheffield J., Goulden M. L., Bonan G., Cescatti A., Chen J., Jeu R. de, Dolman A. J., Eugster W., Gerten D., Gianelle D., Gobron N., Heinke J., Kimball J., Law B. E., Montagnani L., Mu Q., Mueller B., Oleson K., Papale D., Richardson A. D., Rouspard O., Running S., Tomelleri E., Viovy N., Weber U., Williams C., Wood E., Zaehle S., and Zhang K. (2010). Recent decline in the global land evapotranspiration trend due to limited moisture supply. *Nature* 467(7318):951–4.  
doi: 10.1038/nature09396.
- Jutras M.-F., Nasr M., Castonguay M., Pit C., Pomeroy J. H., Smith T. P., Zhang C.-f., Ritchie C. D., Meng F.-R., Clair T. A., and Arp P. A. (2011). Dissolved organic carbon concentrations and fluxes in forest catchments and streams: DOC-3 model. *Ecological Modelling* 222(14):2291–2313.  
doi: 10.1016/j.ecolmodel.2011.03.035.

- Kalbitz K., Solinger S., Park J.-H., Michalzik B., and Matzner E. (2000). Controls on the dynamics of dissolved organic matter in soils: A review. *Soil Science* 165(4):277–304.  
doi: 10.1097/00010694-200004000-00001.
- Keenan T. F., Hollinger D. Y., Bohrer G., Dragoni D., Munger J. W., Schmid H. P., and Richardson A. D. (2013). Increase in forest water-use efficiency as atmospheric carbon dioxide concentrations rise. Supplementary material. *Nature* 499(7458):324–7.  
doi: 10.1038/nature12291.
- Kettridge N., Thompson D. K., Bombonato L., Turetsky M. R., Benschoter B. W., and Waddington J. M. (2013). The ecohydrology of forested peatlands: Simulating the effects of tree shading on moss evaporation and species composition. *Journal of Geophysical Research: Biogeosciences* 118(2):422–435.  
doi: 10.1002/jgrg.20043.
- Kieber D. J., McDaniel J., and Mopper K. (1989). Photochemical source of biological substrates in sea water: implications for carbon cycling. *Nature* 341(6243):637–639.  
doi: 10.1038/341637a0.
- Kieber R. J., Zhou X., and Mopper K. (1990). Formation of carbonyl compounds from UV-induced photodegradation of humic substances in natural waters: Fate of riverine carbon in the sea. *Limnology and Oceanography* 35(7):1503–1515.  
doi: 10.4319/lo.1990.35.7.1503.
- Kiehl J. T. and Trenberth K. E. (1997). Earth's Annual Global Mean Energy Budget. *Bulletin of the American Meteorological Society* 78(2):197–208.  
doi: 10.1175/1520-0477(1997)078<0197:EAGMEB>2.0.CO;2.
- Kirchner J. W. (2009). Catchments as simple dynamical systems: Catchment characterization, rainfall-runoff modeling, and doing hydrology backward. *Water Resources Research* 45(2):W02429.  
doi: 10.1029/2008WR006912.
- Koehler B., Wachenfeldt E. von, Kothawala D., and Tranvik L. J. (2012). Reactivity continuum of dissolved organic carbon decomposition in lake water. *Journal of Geophysical Research* 117(G1):G01024.  
doi: 10.1029/2011JG001793.
- Koehler B., Landelius T., Weyhenmeyer G. A., Machida N., and Tranvik L. J. (2014). Sunlight-induced carbon dioxide emissions from inland waters. *Global Biogeochemical Cycles* 28(7):696–711.  
doi: 10.1002/2014GB004850.
- Köhler S., Buffam I., Seibert J., Bishop K., and Laudon H. (2009). Dynamics of stream water TOC concentrations in a boreal headwater catchment: Controlling factors and implications for climate scenarios. *Journal of Hydrology* 373(1-2):44–56.  
doi: 10.1016/j.jhydrol.2009.04.012.
- Kolari P., Lappalainen H. K., Hänninen H., and Hari P. (2007). Relationship between temperature and the seasonal course of photosynthesis in Scots pine at northern timberline and in southern boreal zone. *Tellus B* 59(3):542–552.  
doi: 10.1111/j.1600-0889.2007.00262.x.
- Kolberg S and Bruland O (2012). “ENKI - An Open Source environmental modelling platform”. In: *Geophysical Research Abstracts*. Vol. 14. EGU2012-13630.
- Lagergren F. and Lindroth A. (2002). Transpiration response to soil moisture in pine and spruce trees in Sweden. *Agricultural and Forest Meteorology* 112(2):67–85.  
doi: 10.1016/S0168-1923(02)00060-6.

- Lalonde K., Vähätalo A. V., and Gélinas Y. (2014). Revisiting the disappearance of terrestrial dissolved organic matter in the ocean: a  $\delta^{13}\text{C}$  study. *Biogeosciences* 11(13):3707–3719.  
doi: 10.5194/bg-11-3707-2014.
- Lark R. M. (2013). *Environmental Modelling: Finding Simplicity in Complexity (2nd edition)* - edited by Wainwright, J. & Mulligan, M. Vol. 64. 6. Blackwell Publishing Ltd, 822.  
doi: 10.1111/ejss.12072.
- Laudon H., Köhler S., Buffam I., and Khler S. (2004). Seasonal TOC export from seven boreal catchments in northern Sweden. *Aquatic Sciences - Research Across Boundaries* 66(2):223–230.  
doi: 10.1007/s00027-004-0700-2.
- Laudon H., Taberman I., Ågren A., Futter M., Ottosson-Löfvenius M., and Bishop K. (2013). The Krycklan Catchment Study-A flagship infrastructure for hydrology, biogeochemistry, and climate research in the boreal landscape. *Water Resources Research* 49(10):7154–7158.  
doi: 10.1002/wrcr.20520.
- Leuning R. (1995). A critical appraisal of a combined stomatal-photosynthesis model for C-3 plants. *Plant cell and environment* 18(4):339–355.  
doi: 10.1111/j.1365-3040.1995.tb00370.x.
- Leuning R, Kelliher F. M., Depury D. G. G., and Schulze E. D. (1995). Leaf nitrogen, photosynthesis, conductance and transpiration - scaling from leaves to canopies. *Plant cell and environment* 18(10):1183–1200.  
doi: 10.1111/j.1365-3040.1995.tb00628.x.
- Lønborg C. and Alvarez-Salgado X. A. (2012). Recycling versus export of bioavailable dissolved organic matter in the coastal ocean and efficiency of the continental shelf pump. *Global Biogeochemical Cycles* 26(3):1–12.  
doi: 10.1029/2012GB004353.
- Lønborg C., Davidson K., Alvarez-Salgado X. A., and Miller A. J. (2009). Bioavailability and bacterial degradation rates of dissolved organic matter in a temperate coastal area during an annual cycle. *Marine Chemistry* 113(3-4):219–226.  
doi: 10.1016/j.marchem.2009.02.003.
- Mäkelä A., Hari P., Berninger F., Hänninen H., and Nikinmaa E. (2004). Acclimation of photosynthetic capacity in Scots pine to the annual cycle of temperature. *Tree physiology* 24(4):369–76.  
doi: 10.1093/treephys/24.4.369.
- Mäkelä A., Kolari P., Karimäki J., Nikinmaa E., Perämäki M., and Hari P. (2006). Modelling five years of weather-driven variation of GPP in a boreal forest. *Agricultural and Forest Meteorology* 139(3-4):382–398.  
doi: 10.1016/j.agrformet.2006.08.017.
- Mäkelä A., Pulkkinen M., Kolari P., Lagergren F., Berbigier P., Lindroth A., Loustau D., Nikinmaa E., Vesala T., and Hari P. (2008). Developing an empirical model of stand GPP with the LUE approach: analysis of eddy covariance data at five contrasting conifer sites in Europe. *Global Change Biology* 14:92–108.  
doi: 10.1111/j.1365-2486.2007.01463.x.
- Mann P. J., Davydova a., Zimov N., Spencer R. G. M., Davydov S., Bulygina E., Zimov S., and Holmes R. M. (2012). Controls on the composition and lability of dissolved organic matter in Siberia's Kolyma River basin. *Journal of Geophysical Research* 117(G1):G01028.  
doi: 10.1029/2011JG001798.

- Michalzik B., Tipping E., Mulder J., Lancho J. G., Matzner E., Bryant C., Clarke N., Lofts S., and Esteban M. V. (2003). Modelling the production and transport of dissolved organic carbon in forest soils. *Biogeochemistry* 66(3):241–264.  
doi: 10.1023/B:BIOG.0000005329.68861.27.
- Miller W. L. and Moran M. A. (1997). Interaction of photochemical and microbial processes in the degradation of refractory dissolved organic matter from a coastal marine environment. *Limnology and Oceanography* 42(6):1317–1324.  
doi: 10.4319/lo.1997.42.6.1317.
- Miller W. L., Moran M. A., and Sheldon W. M. (2002). Determination of apparent quantum yield spectra for the formation of biologically labile photoproducts. *Limnology and Oceanography* 47(2):343–352.  
doi: 10.4319/lo.2002.47.2.0343.
- Milliman J. D. and Farnsworth K. L. (2011). *River Discharge to the Coastal Ocean: A Global Synthesis*. Vol. 24. 4. Cambridge University Press, Cambridge, 143–144.  
doi: 10.1017/CBO9780511781247.
- Mopper K. and Kieber D. J. (2002). “Photochemistry and the Cycling of Carbon, Sulfur, Nitrogen and Phosphorus”. In: *Biogeochemistry of Marine Dissolved Organic Matter*. Ed. by Hansell D. A. and Carlson C. A. Elsevier. Chap. Chapter 9, 455–507.  
doi: 10.1016/B978-012323841-2/50011-7.
- Mopper K., Zhou X., Kieber R. J., Kieber D. J., Sikorski R. J., Jones R. D., and Gratzel (1991). Photochemical degradation of dissolved organic carbon and its impact on the oceanic carbon cycle. *Nature* 353(6339):60–62.  
doi: 10.1038/353060a0.
- Mu Q., Zhao M., and Running S. W. (2011). Improvements to a MODIS global terrestrial evapotranspiration algorithm. *Remote Sensing of Environment* 115(8):1781–1800.  
doi: 10.1016/j.rse.2011.02.019.
- Müller R. A., Futter M. N., Sobek S., Nisell J., Bishop K., and Weyhenmeyer G. A. (2013). Water renewal along the aquatic continuum offsets cumulative retention by lakes: implications for the character of organic carbon in boreal lakes. *Aquatic Sciences* 75(4):535–545.  
doi: 10.1007/s00027-013-0298-3.
- Neff J. C. and Asner G. P. (2001). Dissolved Organic Carbon in Terrestrial Ecosystems: Synthesis and a Model. *Ecosystems* 4(1):29–48.  
doi: 10.1007/s100210000058.
- Nelson N. B. and Siegel D. A. (2013). The global distribution and dynamics of chromophoric dissolved organic matter. *Annual Review of Marine Science* 5:447–76.  
doi: 10.1146/annurev-marine-120710-100751.
- Obernosterer I. and Herndl G. (2000). Differences in the optical and biological reactivity of the humic and nonhumic dissolved organic carbon component in two contrasting coastal marine environments. *Limnology and Oceanography* 45(5):1120–1129.  
doi: 10.4319/lo.2000.45.5.1120.
- Oni S. K., Futter M. N., and Laudon H. (2015). Manuscript under preparation. Unpublished x(x):x.
- Oni S. K., Futter M. N., Teutschbein C., and Laudon H. (2014). Cross-scale ensemble projections of dissolved organic carbon dynamics in boreal forest streams. *Climate Dynamics* 42(9-10):2305–2321.  
doi: 10.1007/s00382-014-2124-6.
- Öquist M. G., Bishop K., Grelle A., Klemetsson L., Köhler S. J., Laudon H., Lindroth A., Ottosson Löfvenius M., Wallin M. B., and Nilsson M. B. (2014). The Full Annual Carbon

- Balance of Boreal Forests Is Highly Sensitive to Precipitation. *Environmental Science & Technology Letters* 1(7):315–319.  
doi: 10.1021/ez500169j.
- Papale D., Reichstein M., Aubinet M., Canfora E., Bernhofer C., Kutsch W., Longdoz B., Rambal S., Valentini R., Vesala T., and Yakir D. (2006). Towards a standardized processing of Net Ecosystem Exchange measured with eddy covariance technique: algorithms and uncertainty estimation. *Biogeosciences* 3(4):571–583.  
doi: 10.5194/bg-3-571-2006.
- Peichl M., Sagerfors J., Lindroth A., Buffam I., Grelle A., Klemetsson L., Laudon H., and Nilsson M. B. (2013). Energy exchange and water budget partitioning in a boreal minerogenic mire. *Journal of Geophysical Research: Biogeosciences* 118(1):1–13.  
doi: 10.1029/2012JG002073.
- Penman H. L. (1948). Natural evaporation from open water, bare soil and grass. *Proceedings of the royal society of London series A-mathematical and physical sciences* 193(1032):120–145.  
doi: 10.1098/rspa.1948.0037.
- Pers C., Rahm L., Jonsson A., and Jansson M. (2001). Modelling dissolved organic carbon turnover in humic Lake. *Environmental monitoring and assessment* 6:159–172.  
doi: 10.1023/A:1011953730983.
- Priestley C. H. B. and Taylor R. J. (1972). On the Assessment of Surface Heat Flux and Evaporation Using Large-Scale Parameters. *Monthly Weather Review* 100(2):81–92.  
doi: 10.1175/1520-0493(1972)100<0081:OTAOSH>2.3.CO;2.
- Pullin M. J., Bertilsson S., Goldstone J. V., and Voelker B. M. (2004). Effects of sunlight and hydroxyl radical on dissolved organic matter: Bacterial growth efficiency and production of carboxylic acids and other substrates. *Limnology and Oceanography* 49(6):2011–2022.  
doi: 10.4319/lo.2004.49.6.2011.
- Reichstein M., Falge E., Baldocchi D., Papale D., Aubinet M., Berbigier P., Bernhofer C., Buchmann N., Gilmanov T., Granier A., Grunwald T., Havrankova K., Ilvesniemi H., Janous D., Knohl A., Laurila T., Lohila A., Loustau D., Matteucci G., Meyers T., Miglietta F., Ourcival J.-M., Pumpanen J., Rambal S., Rotenberg E., Sanz M., Tenhunen J., Seufert G., Vaccari F., Vesala T., Yakir D., and Valentini R. (2005). On the separation of net ecosystem exchange into assimilation and ecosystem respiration: review and improved algorithm. *Global Change Biology* 11(9):1424–1439.  
doi: 10.1111/j.1365-2486.2005.001002.x.
- Reitner B., Herndl G. J., and Herzig A. (1997). Role of ultraviolet-B radiation on photochemical and microbial oxygen consumption in a humic-rich shallow lake. *Limnology and Oceanography* 42(5):950–960.  
doi: 10.4319/lo.1997.42.5.0950.
- Salonen K. and Vähätalo A. (1994). Photochemical mineralisation of dissolved organic matter in lake Skjervatjern. *Environment international* 20(3):307–312.  
doi: 10.1016/0160-4120(94)90114-7.
- Schlesinger W. H. and Andrews J. A. (2000). Soil respiration and the global carbon cycle. *Biogeochemistry* (1977):7–20.  
doi: 10.1023/A:1006247623877.
- Schlesinger W. H. and Melack J. M. (1981). Transport of organic carbon in the world's rivers. *Tellus A*:172–187.  
doi: 10.3402/tellusa.v33i2.10706.

- Sellers P. J., Dickinson R. E., Randall D. A., Betts A. K., Hall F. G., Berry J. A., Collatz G. J., Denning A. S., Mooney H. A., Nobre C. A., Sato N., Field C. B., and Henderson-Sellers A. (1997). Modeling the Exchanges of Energy, Water, and Carbon Between Continents and the Atmosphere. *Science* 275(5299):502–509.  
doi: 10.1126/science.275.5299.502.
- Sellers P. J., Bounoua L., Collatz G. J., Randall D. A., Dazlich D. A., Fung I., Tucker C. J., Field C. B., and Jensen T. G. (2009). Comparison of Radiative and Physiological Effects of Doubled Atmospheric CO<sub>2</sub> on Climate. *Science* 271(5254):1402–1406.  
doi: 10.1126/science.271.5254.1402.
- Sevanto S., Suni T., Pumpanen J., Grönholm T., Kolari P., Nikinmaa E., Hari P., and Vesala T. (2006). Wintertime photosynthesis and water uptake in a boreal forest. *Tree physiology* 26(6):749–57.  
doi: 10.1093/treephys/26.6.749.
- Sheffield J., Wood E. F., and Roderick M. L. (2012). Little change in global drought over the past 60 years. *Nature* 491(7424):435–8.  
doi: 10.1038/nature11575.
- Søndergaard M. and Middelboe M. (1995). A cross-system analysis of labile dissolved organic carbon. *Marine Ecology Progress Series* 118:283–294.  
doi: 10.3354/meps118283.
- Spencer R. G. M., Stubbins A., Hernes P. J., Baker A., Mopper K., Aufdenkampe A. K., Dyda R. Y., Mwamba V. L., Mangangu A. M., Wabakanghanzi J. N., and Six J. (2009). Photochemical degradation of dissolved organic matter and dissolved lignin phenols from the Congo River. *Journal of Geophysical Research* 114(G3):G03010.  
doi: 10.1029/2009JG000968.
- Spencer R. G. M., Aiken G. R., Dornblaser M. M., Butler K. D., Holmes R. M., Fiske G., Mann P. J., and Stubbins A. (2013). Chromophoric dissolved organic matter export from U.S. rivers. *Geophysical Research Letters* 40(8):1575–1579.  
doi: 10.1002/grl.50357.
- Stedmon C., Amon R., Rinehart A., and Walker S. (2011). The supply and characteristics of colored dissolved organic matter (CDOM) in the Arctic Ocean: Pan Arctic trends and differences. *Marine Chemistry* 124(1–4):108–118.  
doi: 10.1016/j.marchem.2010.12.007.
- Stewart J. B. (1988). Modelling surface conductance of pine forest. *Agricultural and Forest Meteorology* 43(1):19–35.  
doi: 10.1016/0168-1923(88)90003-2.
- Stoy P. C., Richardson a. D., Baldocchi D. D., Katul G. G., Stanovick J., Mahecha M. D., Reichstein M., Detto M., Law B. E., Wohlfahrt G., Arriga N., Campos J., McCaughey J. H., Montagnani L., Paw U K. T., Sevanto S., and Williams M. (2009). Biosphere-atmosphere exchange of CO<sub>2</sub> in relation to climate: a cross-biome analysis across multiple time scales. *Biogeosciences* 6(10):2297–2312.  
doi: 10.5194/bg-6-2297-2009.
- Suni T, Berninger F, Vesala T, Markkanen T, Hari P, Mäkelä A, Ilvesniemi H, Hänninen H, Nikinmaa E, Huttula T, Laurila T, Aurela M, Grelle A, Lindroth A, Arneth A, Shibistova O, and Lloyd J (2003). Air temperature triggers the recovery of evergreen boreal forest photosynthesis in spring. *Global Change Biology* 9:1410–1426.  
doi: 10.1046/j.1365-2486.2003.00597.x.
- Thackeray S. J. (2014). Freshwater Ecosystems and the Carbon Cycle. In: Excellence in Ecology Series J. J. Cole (2013). Volume 18. International Ecology Institute, Oldendorf,

- Germany. 125 pp. *Freshwater Biology* 59(8):1781.  
doi: 10.1111/fwb.12382.
- Thorntwaite C. W. (1948). An Approach toward a Rational Classification of Climate. *Geographical Review* 38(1):55–94.  
doi: 10.2307/210739.
- Thurner M., Beer C., Santoro M., Carvalhais N., Wutzler T., Schepaschenko D., Shvidenko A., Kompter E., Ahrens B., Levick S. R., and Schmulilius C. (2014). Carbon stock and density of northern boreal and temperate forests. *Global Ecology and Biogeography* 23(3):297–310.  
doi: 10.1111/geb.12125.
- Tiwari T., Laudon H., Beven K., and Ågren A. M. (2014). Downstream changes in DOC: Inferring contributions in the face of model uncertainties. *Water Resources Research* 50(1):514–525.  
doi: 10.1002/2013WR014275.
- Tranvik L. J., Downing J. A., Cotner J. B., Loiselle S. A., Striegl R. G., Ballatore T. J., Dillon P., Finlay K., Fortino K., Knoll L. B., Kortelainen P. L., Kutser T., Larsen S., Laurion I., Leech D. M., McCallister S. L., Mcknight D. M., Melack J. M., Overholt E., Porter J. A., Prairie Y., Renwick W. H., Roland F., Sherman B. S., Schindler D. W., Sobek S., Tremblay A., Vanni M. J., Verschoor A. M., Wachenfeldt E. V., and Weyhenmeyer G. A. (2009). Lakes and reservoirs as regulators of carbon cycling and climate. *Limnology and Oceanography* 54(1):2298–2314.  
doi: 10.4319/lo.2009.54.6{\\_}part{\\_}2.2298.
- Vähätalo A. V. (2009). *Light, Photolytic Reactivity and Chemical Products*. Ed. by Likens G. E. volume 2. Vol. 2. Oxford: Likens, 761–773.
- Vähätalo A. V., Aarnos H., Hoikkala L., and Lignell R. (2011). Photochemical transformation of terrestrial dissolved organic matter supports hetero- and autotrophic production in coastal waters. *Marine Ecology Progress Series* 423:1–14.  
doi: 10.3354/meps09010.
- Vähätalo A., Salkinoja-salonen M., Taalas P., and Salonen K. (2000). Spectrum of the quantum yield for photochemical mineralization of dissolved organic carbon in a humic lake. *Limnology and Oceanography* 45(3):664–676.  
doi: 10.4319/lo.2000.45.3.0664.
- Vähätalo A. V. and Wetzel R. G. (2004). Photochemical and microbial decomposition of chromophoric dissolved organic matter during long (months - years) exposures. *Marine Chemistry* 89(1-4):313–326.  
doi: 10.1016/j.marchem.2004.03.010.
- Vähätalo A. V., Aarnos H., and Mäntyniemi S. (2010). Biodegradability continuum and biodegradation kinetics of natural organic matter described by the beta distribution. *Biogeochemistry* 100(1-3):227–240.  
doi: 10.1007/s10533-010-9419-4.
- Vähätalo A. V. A. and Wetzel R. R. G. (2008). Long-Term Photochemical and Microbial Decomposition of Wetland-Derived Dissolved Organic Matter with Alteration of 13C:12C Mass Ratio. *Limnology and Oceanography* 53(4):1387–1392.  
doi: 10.4319/lo.2008.53.4.1387.
- Vodacek A., Blough N. V., Degrandpre M. D., Peltzer E. T., and Nelson R. K. (1997). Seasonal variation of CDOM and DOC in the Middle Atlantic Bight: Terrestrial inputs and photooxidation. *Limnology and Oceanography* 42(4):674–686.  
doi: 10.4319/lo.1997.42.4.0674.

- Wagner S., Riedel T., Niggemann J., Vähätalo A. V., Dittmar T., and Jaffe R. (2015). Linking the Molecular Signature of Heteroatomic Dissolved Organic Matter To Watershed Characteristics in World Rivers. *Environmental Science & Technology Article AS*: doi: 10.1021/acs.est.5b00525.
- Wainwright J. and Mulligan M., eds. (2004). *Environmental Modelling: Finding Simplicity in Complexity*. West Sussex: John Wiley & Sons Ltd,
- Wallin M. B., Weyhenmeyer G. A., Bastviken D., Chmiel H. E., Peter S., Sobek S., and Klemetsson L. (2015). Temporal control on concentration, character, and export of dissolved organic carbon in two hemiboreal headwater streams draining contrasting catchments. *Journal of Geophysical Research: Biogeosciences* 3:1–15. doi: 10.1002/2014JG002814.
- Wang K. and Dickinson R. E. (2012). A review of global terrestrial evapotranspiration: Observation, modeling, climatology, and climatic variability. *Reviews of Geophysics* 50:1–54. doi: 10.1029/2011RG000373.
- Weyhenmeyer G. A., Fröberg M., Karlton E., Khalili M., Kothawala D., Temnerud J., and Tranvik L. J. (2012). Selective decay of terrestrial organic carbon during transport from land to sea. *Global Change Biology* 18(1):349–355. doi: 10.1111/j.1365-2486.2011.02544.x.
- Wharton S., Schroeder M., Bible K., Falk M., and U K. T. P. (2009). Stand-level gas-exchange responses to seasonal drought in very young versus old Douglas-fir forests of the Pacific Northwest, USA. *Tree physiology* 29:959–974. doi: 10.1093/treephys/tpp039.
- Wieser G. (2000). Seasonal variation of leaf conductance in a subalpine *Pinus cembra* during the winter months. *Phyton-annales rei botanicae* 40(4):185–190.
- Winterdahl M., Futter M., Köhler S., Laudon H., Seibert J., and Bishop K. (2011). Riparian soil temperature modification of the relationship between flow and dissolved organic carbon concentration in a boreal stream. *Water Resources Research* 47(8):W08532. doi: 10.1029/2010WR010235.
- Wong S. C., Cowan I. R., and Farquhar G. D. (1979). Stomatal conductance correlates with photosynthetic capacity. *Nature* 282(5737):424–426. doi: 10.1038/282424a0.
- Worrall F. and Burt T. (2004). Time series analysis of long-term river dissolved organic carbon records. *Hydrological Processes* 18(5):893–911. doi: 10.1002/hyp.1321.
- Xiao Y.-H., Sara-Aho T., Hartikainen H., and Vähätalo A. V. (2013). Contribution of ferric iron to light absorption by chromophoric dissolved organic matter. *Limnology and Oceanography* 58(2):653–662. doi: 10.4319/lo.2013.58.2.0653.
- Xu N., Saiers J. E., Wilson H. F., and Raymond P. A. (2012). Simulating streamflow and dissolved organic matter export from a forested watershed. *Water Resources Research* 48(5):W05519. doi: 10.1029/2011WR011423.
- Yurova A., Sirin A., Buffam I., Bishop K., and Laudon H. (2008). Modeling the dissolved organic carbon output from a boreal mire using the convection-dispersion equation: Importance of representing sorption. *Water Resources Research* 44(7):W07411. doi: 10.1029/2007WR006523.

Zepp R. G., Callaghan T. V., and Erickson D. J. (1998). Effects of enhanced solar ultraviolet radiation on biogeochemical cycles. *Journal of Photochemistry and Photobiology B: Biology* 46(1-3):69–82.  
doi: 10.1016/S1011-1344(98)00186-9.



# Latent heat exchange in the boreal and arctic biomes

VILLE KASURINEN<sup>1,2</sup>, KNUT ALFREDSSEN<sup>2</sup>, PASI KOLARI<sup>1</sup>, IVAN MAMMARELLA<sup>3</sup>, PAVEL ALEKSEYCHIK<sup>3</sup>, JANNE RINNE<sup>3</sup>, TIMO VESALA<sup>3</sup>, PIERRE BERNIER<sup>4</sup>, JULIA BOIKE<sup>5</sup>, MORITZ LANGER<sup>5</sup>, LUCA BELELLI MARCHESINI<sup>6</sup>, KO VAN HUISSTEDEN<sup>6</sup>, HAN DOLMAN<sup>6</sup>, TORSTEN SACHS<sup>7</sup>, TAKESHI OHTA<sup>8</sup>, ANDREJ VARLAGIN<sup>9</sup>, ADRIAN ROCHA<sup>10</sup>, ALTAFA ARAÏN<sup>11</sup>, WALTER OECHEL<sup>12</sup>, MAGNUS LUND<sup>13</sup>, ACHIM GRELLER<sup>14</sup>, ANDERS LINDROTH<sup>15</sup>, ANDY BLACK<sup>16</sup>, MIKA AURELA<sup>17</sup>, TUOMAS LAURILA<sup>17</sup>, ANNALEA LOHILA<sup>17</sup> and FRANK BERNINGER<sup>1</sup>

<sup>1</sup>Department of Forest Sciences, University of Helsinki, POBox 27, Helsinki 00014, Finland, <sup>2</sup>Department of Hydraulic and Environmental Engineering, Norwegian University of Science and Technology, Trondheim, Norway, <sup>3</sup>Department of Physics, University of Helsinki, POBox 48, Helsinki 00014, Finland, <sup>4</sup>Natural Resources Canada, Canadian Forest Service, Stn. Ste-Foy, P.O. Box 10380 Quebec, QC G1V 4C7, Canada, <sup>5</sup>Alfred Wegener Institute, Helmholtz Centre for Polar and Marine Research, Research Unit Potsdam, Telegrafenberg, A 4314473 Potsdam, Germany, <sup>6</sup>Earth and Climate Cluster, Department of Earth Sciences, VU University Amsterdam, De Boelelaan 1085, Amsterdam 1081 HV, The Netherlands, <sup>7</sup>GFZ German Research Centre for Geosciences, Telegrafenberg, Potsdam 14473, Germany, <sup>8</sup>Graduate School of Bioagricultural Sciences, Nogyo University, Furo-cho, Chikusa Ward, Nagoya, Aichi 464-8601, Japan, <sup>9</sup>A.N. Severtsov Institute of Ecology and Evolution, Russian Academy of Sciences, Leninsky pr.33, Moscow 119071, Russia, <sup>10</sup>Department of Biological Sciences and the Environmental Change Initiative, University of Notre Dame, Notre Dame, IN 46556, USA, <sup>11</sup>McMaster Centre for Climate Change and School of Geography and Earth Sciences, McMaster University, Hamilton, Ontario, Canada, <sup>12</sup>Global Change Research Group, San Diego State University, 5500 Campanile Drive, San Diego, CA 92182, USA, <sup>13</sup>Arctic Research Centre, Department of Bioscience, Aarhus University, Frederiksborgvej 399, Roskilde DK-4000, Denmark, <sup>14</sup>Department of Ecology, Swedish University of Agricultural Sciences, Uppsala, Sweden, <sup>15</sup>Department of Earth and Ecosystem Sciences, Lund University, Lund, Sweden, <sup>16</sup>Faculty of Land and Food Systems, University of British Columbia, Vancouver, Canada, <sup>17</sup>Finnish Meteorological Institute, Atmospheric Composition Research, POBox 503, Helsinki Fi-00101, Finland

## Abstract

In this study latent heat flux ( $\lambda E$ ) measurements made at 65 boreal and arctic eddy-covariance (EC) sites were analysed by using the Penman–Monteith equation. Sites were stratified into nine different ecosystem types: harvested and burnt forest areas, pine forests, spruce or fir forests, Douglas-fir forests, broadleaf deciduous forests, larch forests, wetlands, tundra and natural grasslands. The Penman–Monteith equation was calibrated with variable surface resistances against half-hourly eddy-covariance data and clear differences between ecosystem types were observed. Based on the modeled behavior of surface and aerodynamic resistances, surface resistance tightly control  $\lambda E$  in most mature forests, while it had less importance in ecosystems having shorter vegetation like young or recently harvested forests, grasslands, wetlands and tundra. The parameters of the Penman–Monteith equation were clearly different for winter and summer conditions, indicating that phenological effects on surface resistance are important. We also compared the simulated  $\lambda E$  of different ecosystem types under meteorological conditions at one site. Values of  $\lambda E$  varied between 15% and 38% of the net radiation in the simulations with mean ecosystem parameters. In general, the simulations suggest that  $\lambda E$  is higher from forested ecosystems than from grasslands, wetlands or tundra-type ecosystems. Forests showed usually a tighter stomatal control of  $\lambda E$  as indicated by a pronounced sensitivity of surface resistance to atmospheric vapor pressure deficit. Nevertheless, the surface resistance of forests was lower than for open vegetation types including wetlands. Tundra and wetlands had higher surface resistances, which were less sensitive to vapor pressure deficits. The results indicate that the variation in surface resistance within and between different vegetation types might play a significant role in energy exchange between terrestrial ecosystems and atmosphere. These results suggest the need to take into account vegetation type and phenology in energy exchange modeling.

**Keywords:** eddy-covariance, evapotranspiration, latent heat, phenology, stomatal resistance

Received 31 January 2014 and accepted 13 March 2014

Correspondence: Ville Kasurinen, tel. +358-41-5343753, fax +358-9-191-58100, e-mail: ville.kasurinen@helsinki.fi

## Introduction

Boreal and arctic biomes account for 22% of the land surface of the globe (Chapin *et al.*, 2000). Boreal landscapes are often considered to be dominated by evergreen needle leaf conifers, but broadleaf forests, larch forests, open areas also occupy large areas of the boreal and arctic biomes and wetlands occupy large areas of boreal and arctic domain. These boreal and arctic ecosystems play an important role in earth-atmosphere dynamics because of their large extent and their sensitivity to a warming climate (Chapin *et al.*, 2000; Bonan, 2008a).

Transpiration dominates the terrestrial ecosystem water fluxes and is poorly constrained in global modeling (Jasechko *et al.*, 2013). Nevertheless, global climate predictions are sensitive to changes in evapotranspiration (e.g., Sellers *et al.*, 1997, 2009). Over the last two decades, an extensive eddy-covariance (EC) flux tower network (FLUXNET) has been built, which is providing new insights on the energy exchange between the atmosphere and arctic and boreal ecosystems (Aubinet *et al.*, 2000; Baldocchi *et al.*, 2001). However, most of the work has focused on biosphere-atmosphere carbon exchange (Hollinger *et al.*, 2004; Baldocchi, 2008; Jung *et al.*, 2009; Stoy *et al.*, 2009) as well as on site-specific energy exchange studies (Admiral & Lafleur, 2007; Tanaka *et al.*, 2008; Peichl *et al.*, 2013). At the same time, fewer studies have concentrated on multi-site energy fluxes to infer biome wide or regional water and energy fluxes (Jung *et al.*, 2010; Wang & Dickson, 2012) aside from their relationship with CO<sub>2</sub> exchange (Hollinger *et al.*, 1999; Law *et al.*, 2002; Jung *et al.*, 2011).  $\lambda E$  is estimated in eddy flux data from fluxes of water vapor, which are measured by using usually an infra red gas analyser (Foken, 2008). FLUXNET measurements have not been much used to estimate the energy balance of large regions, while micrometeorological problems, like energy balance closure (Wilson *et al.*, 2002; Foken, 2008; Barr *et al.*, 2012; Leuning *et al.*, 2012; Stoy *et al.*, 2013), EC footprint (Göckede *et al.*, 2008) and gap-filling (Falge *et al.*, 2001; Moffat *et al.*, 2007) have received much attention. In spite of these problems, EC technique is one of the best and least biased methods to measure water and energy fluxes at the ecosystem-scale.

The Penman–Monteith (PM) equation is one of the most widely used and accepted approaches to model  $\lambda E$  (Katul *et al.*, 2012; Wang & Dickinson, 2012). The Penman Monteith method models explicitly the energy balance of an ecosystem: Net radiation is partitioned into latent heat flux ( $\lambda E$ ) and sensible heat flux depending on the surface ( $r_s$ ) and aerodynamic resistances ( $r_a$ ). It is widely used as a tool in agricultural related research (Allen, 1998) and has been used to analyze dif-

ferences between boreal and temperate ecosystem (Blanken & Black, 2004; Zha *et al.*, 2010; Brümmner *et al.*, 2012). Recently, the approach has been extended by including various parameterizations to estimating surface resistance ( $r_s$ ) (Grelle *et al.*, 1999; Valiantzas, 2006; Launiainen, 2010). In the simplest modifications, the aerodynamic ( $r_a$ ) and surface resistance ( $r_s$ ) are assumed to be constant on the daily level (Allen, 1998). Models with surface resistances that vary over time give better predictions of latent heat flux during a single day although models with constant canopy resistance give accurate predictions of  $\lambda E$  over longer time spans (as e.g. daily or monthly) (Lecina *et al.*, 2003). However, stomatal regulation could become important, if the climate is changing and might change the values of surface resistance. The PM equation has previously been used successfully to estimate  $r_s$  in remote-sensing algorithms as well as in temperature-based  $\lambda E$  models (Cleugh *et al.*, 2007; Mu *et al.*, 2011).

Lately, the interest concerning the importance and effects of phenology on ecosystem behavior has increased. There have been several studies investigating phenological effects on seasonal and annual carbon balance (Suni *et al.* 2003, Gea-Izquierdo *et al.*, 2010), bud burst (Richardson *et al.*, 2010), feedback mechanisms to the climate system (Richardson *et al.*, 2013) and spring onset (Richardson *et al.*, 2012). Richardson *et al.* (2012) conducted an analysis related to ecosystem-scale CO<sub>2</sub> exchange by using 14 different models in ten forested ecosystems. There are also some studies related to phenology and  $\lambda E$  (e.g. Blanken *et al.*, 1997; Blanken & Black, 2004). However, the effect of delayed stomatal adaptation during the spring recovery to  $\lambda E$  has been rarely estimated (Brümmner *et al.*, 2012).

In this article, flux and climate observations from FLUXNET are used to evaluate simulations of  $\lambda E$  by using the PM equation. Boreal and arctic ecosystem types are investigated to determine how their modeled and measured  $\lambda E$  depends on ecosystem type. Furthermore, a phenological model was used to investigate how the properties of the vegetation type affect  $\lambda E$ . The hypothesis of the study was that different land cover classes differ in their  $\lambda E$  and the way it depends on ecosystem properties and meteorological forcing.

## Materials and methods

### Study sites

Sixty-five sites representing the most common ecosystem types in the subboreal, boreal or arctic areas were selected from FLUXNET database (<http://fluxnet.ornl.gov>) for this study (Fig. 1; Table 1). Agricultural ecosystems were excluded from the analysis, because their annual cycle is mainly con-

trolled by human activity like harvesting and seeding, fertilization or irrigation. Therefore, analysis was limited to natural ecosystems including forests that have been planted with native species after cuts. The selected sites were grouped based on the dominant plant functional type (PFT) into nine different categories. These were: (i) harvested or burnt areas temporarily void of trees (C), (ii) Douglas-fir forests (D), (iii) pine forests (P), (iv) spruce or fir dominated forests (S), (v) broadleaf deciduous forests (BD), (vi) larch forests (L), (vii) wetlands (W), (viii) tundra (T) and (ix) natural grasslands (G).

The attempt was to select available EC sites in the boreal and subboreal region, but to reject sites where measurements are restricted to summer periods with large gaps occur during the periods when  $\lambda E$  are typically high. We acknowledged that the quality requirements were stricter for ecosystem types that are well represented in the database, while we had less stringent requirements for vegetation types that were not often measured. We thought that in these cases it might be important to increase the sample size of 'underrepresented ecosystems'. Exceptions were particularly made for tundra ecosystems, where data from winter months was very scarce. A complete site list with references, land type covers and climatological characteristics are presented in Table 1.

#### Data selection and estimation of missing measurements

For the data analysis, more than 400 EC site-years half-hourly of  $\lambda E$  and meteorological data were checked for obvious measurement errors or reporting errors in units. Rather complete time series of seven meteorological variables were required for the estimation: air temperature ( $T_a$ ), wind speed ( $u$ ), friction velocity ( $u^*$ ), global radiation ( $R_g$ ), net radiation ( $R_n$ ), air pressure ( $P_a$ ) and relative humidity ( $RH$ ). To avoid conditions when EC technique does not work properly, we removed periods with low turbulent mixing ( $u^*$  less than  $0.1 \text{ m s}^{-1}$ ). Similar kind of data filtering criteria has been used previously in other studies (Alavi *et al.*, 2006; Wu *et al.*, 2010), but selected threshold value can be considered low for forests. It was selected mainly to ensure a similar kind of analysis for all ecosystem types (same  $u^*$  and  $\text{KB}^{-1}$ ). Higher filtration criteria would have removed too much data from naturally open ecosystems (tundra, grasslands, wetlands, cut forests) and wintertime measurements from forests. Determination of optimal threshold

value for each site or ecosystem type separately would have been hard and more or less subjective decision.

Thus, the most complete data series of half-hourly data were selected for the analysis and missing values for some of the meteorological data were estimated. First short gaps in  $T_a$  and  $RH$  (up to 4 h) were linearly interpolated (Amiro *et al.*, 2006). Longer gaps of these variables that could not be estimated by using mean diurnal variation (MDV) (Reichstein *et al.*, 2005) in a 14 days moving window, were filled by data recorded at the nearest weather station. This was done only for sites RU-Che, RU-Cok, RU-Ylr, RU-Ypf, RU-Sam, US-Atq, US-Brw, with distances varying from 1 to 50 km from the weather station. Weather station data are reported typically for every third or sixth hour and was interpolated to half-hourly values by using linear regression. Please note that the phenology model requires an air temperature history for the calculations related to delayed response of the vegetation to the increasing temperature during the spring [ $S$  &  $\tau$ ; see Eqn (4)]. It should also be noted that model parameter estimation was always done on nongap filled values of  $\lambda E$ .

Missing periods in  $R_g$  data were estimated by using a linear regression relationships between photosynthetically active radiation (PPFD) as an independent variable. Estimated  $R_g$  was accepted only if the linear correlation coefficient between the estimated values and measured values exceeded 0.95, otherwise data were removed from estimation. Missing periods in  $R_n$  was estimated similarly between  $R_g$  and  $R_n$  and estimated values were accepted, if the linear correlation between estimated and independent variable exceeded 0.8. The theoretical relationship and conversion methods between radiation PPFD and short wave irradiance are reported in many studies (Weiss & Norman, 1985; Papaioannou *et al.*, 1993; Escobedo *et al.*, 2011), and instead of using constant relationships, parameters was estimated for each site separately by using site-specific measurements. Dry-foliage data were not used in the analysis, because all sites did not provided high quality precipitation data.

#### Model of latent heat exchange

The model parameters were estimated using the meteorological variables measured on site. The modeling was implemented using R software (R Core Team, 2013) by applying



Fig. 1 Location of eddy covariance sites are marked with red star (\*).

**Table 1** Eddy covariance sites that were used in the study, coordinates, characteristics and site references

Sites			Coordinates		Characteristics		
Nr	Code	Name	Latitude	Longitude	IGBP	Forest type	Site reference
1	CA-Ca1	BC-Campbell River 1949 Douglas-fir	49.87	-125.33	ENF	Douglas-Fir	Krishnan <i>et al.</i> , 2009;
2	CA-Ca2	BC-Campbell River 2000 Douglas-fir	49.87	-125.29	ENF	Douglas-Fir	Krishnan <i>et al.</i> , 2009;
3	CA-Ca3	BC-Campbell River 1988 Douglas-fir	49.53	-124.9	ENF	Douglas-Fir	Krishnan <i>et al.</i> , 2009;
4	CA-Gro	ON-Groundhog River Mixedwood	48.22	-82.16	MF	Leaf	McCaughey <i>et al.</i> , 2006;
5	CA-Man	MB-Northern Old Black Spruce	55.88	-98.48	ENF	Spruce	Dunn <i>et al.</i> , 2007;
6	CA-Mer	ON-Mer Bleu Eastern Peatland	45.41	-75.52	WET	Wet	Lund <i>et al.</i> , 2009;
7	CA-Na1	NB-Nashwaak Lake 1 1967 Balsam Fir	46.47	-67.1	MF	Spruce	Yuan <i>et al.</i> , 2008;
8	CA-NS1	UCI 1850	55.88	-98.48	ENF	Spruce	Goulden <i>et al.</i> , 2011;
9	CA-NS2	UCI 1930	55.91	-98.52	ENF	Spruce	Goulden <i>et al.</i> , 2011;
10	CA-NS3	UCI-1964	55.91	-98.38	ENF	Spruce	Goulden <i>et al.</i> , 2011;
11	CA-NS4	UCI-1964 wet	55.91	-98.38	ENF	Spruce	Wang <i>et al.</i> , 2003;
12	CA-NS5	UCI 1981	55.86	-98.49	ENF	Spruce	Goulden <i>et al.</i> , 2011;
13	CA-NS6	UCI 1989	55.92	-98.96	ENF	Cut	Goulden <i>et al.</i> , 2011;
14	CA-NS7	UCI 1998	56.64	-99.95	ENF	Cut	Goulden <i>et al.</i> , 2011;
15	CA-Oas	SK-Old Aspen	53.63	-106.2	MF	Leaf	Black <i>et al.</i> , 1996;
16	CA-Obs	SK-Southern Old Black Spruce	53.99	-105.12	ENF	Spruce	Jarvis <i>et al.</i> , 1997;
17	CA-Ojp	SK-Old Jack Pine	53.92	-104.69	ENF	Pine	Griffis <i>et al.</i> , 2003; Zha <i>et al.</i> , 2010
18	CA-Qc2	QC-1975 Harvested Black Spruce	49.76	-74.57	MF	Cut	-
19	CA-Qcu	QC-2000 Harvested Black Spruce	-49.27	-74.04	ENF	Cut	Bergeron <i>et al.</i> , 2008;
20	CA-Qfo	QC-Eastern Old Black Spruce	49.69	-74.34	ENF	Spruce	Bergeron <i>et al.</i> , 2008;
21	CA-Sf1	SK-1977 Fire	54.49	-105.82	ENF	Pine	Mkhabela <i>et al.</i> , 2009;
22	CA-Sf2	SK-1997 Fire	54.25	-105.88	MF	Cut	Mkhabela <i>et al.</i> , 2009;
23	CA-Sf3	SK-1998 Fire	54.09	-106.01	ENF	Cut	Mkhabela <i>et al.</i> , 2009;
24	CA-Sj2	SK-2002 Jack Pine	53.94	-104.65	ENF	Cut	Coursolle <i>et al.</i> , 2006;
25	CA-Sj3	SK-1975 (Young) Jack Pine	53.88	-104.65	ENF	Pine	Margolis & Ryan, 1997;
26	CA-TPW	ON-Turkey Point 1974 White Pine	42.71	-80.35	MF	Pine	Peichl <i>et al.</i> , 2010;
27	CA-Tp4	ON-Turkey Point 1939 White Pine	42.71	-80.36	MF	Pine	Peichl <i>et al.</i> , 2010;
28	CA-Wp1	AB-Western Peatland	54.95	-112.47	MF	Wet	Flanagan & Syed, 2011;
29	CA-Wp2	AB-Western Peatland Poor Fen	55.54	-112.33	ENF	Wet	Adkinson <i>et al.</i> , 2011;
30	CA-Wp3	AB-Western Peatland Rich Fen	54.47	-113.32	MF	Wet	Adkinson <i>et al.</i> , 2011;
31	DK-Sor	Soroe- Lille Bogeskov	55.49	11.64	DBF	Leaf	Pilegaard <i>et al.</i> , 2001, 2003;
32	FI-Hyy	Hyytiälä	61.85	24.3	ENF	Pine	Launiainen, 2010;
33	FI-Kaa	Kaamanen wetland	69.14	27.3	WET	Wet	Aurela <i>et al.</i> , 2004; Lund <i>et al.</i> , 2009;
34	FI-Lom	Lompolojänkää	68	24.21	WET	Wet	Aurela <i>et al.</i> , 2009; Lohila <i>et al.</i> , 2010;
35	FI-Sii	Siikaneva	61.83	24.19	WET	Wet	Lund <i>et al.</i> , 2009;
36	FI-Sod	Sodankylä	67.36	26.64	ENF	Pine	Thum <i>et al.</i> , 2007;
37	RU-Che	Cherskii	68.61	161.34	OSH	Tundra	Corradi <i>et al.</i> , 2005; Merbold <i>et al.</i> , 2009;
38	RU-Cok	Chokurdakh/Kytalyk	70.83	147.49	OSH	Tundra	van Huissteden <i>et al.</i> , 2005;
39	RU-Fyo	Fedorovskoye wet spruce stand	56.46	32.92	ENF	Spruce	Kurbatova <i>et al.</i> , 2008;
40	RU-Ha1	Ubs Nur-Hakasija-grassland	54.73	90	GRA	Grass	Belelli-Marchesini <i>et al.</i> , 2007a;
41	RU-Ha2	Ubs Nur-Hakasija-recovering grassland	54.77	89.96	GRA	Grass	Belelli-Marchesini, 2007b;
42	RU-Ha3	Ubs Nur-Hakasija-Site 3	54.7	89.08	GRA	Grass	Belelli-Marchesini, 2007b;
43	RU-Sam	Samoylov Island Lena Delta	72.37	126.5	OSH	Tundra	Boike <i>et al.</i> , 2013;

Table 1 (continued)

Sites			Coordinates		Characteristics		
Nr	Code	Name	Latitude	Longitude	IGBP	Forest type	Site reference
44	RU-Ylr	Yakutsk-Larch	62.26	129.62	DNF	Larch	Ohta <i>et al.</i> , 2008;
45	RU-Ypf	Yakutsk-Pine	62.24	129.65	DNF	Pine	Hamada <i>et al.</i> , 2004;
46	RU-Zot	Zotino	60.8	89.35	ENF	Pine	Tchebakova <i>et al.</i> , 2002;
47	SE-Deg	Degero Stormyr	64.18	19.56	GRA	Wet	Lund <i>et al.</i> , 2009;
48	SE-Faj	Fajemyr	56.27	13.55	WET	Wet	Lund <i>et al.</i> , 2007;
49	SE-Fla	Flakaliden	64.11	19.46	ENF	Spruce	Lindroth <i>et al.</i> , 2008;
50	SE-Nor	Norunda	60.09	17.48	ENF	Spruce	Lindroth <i>et al.</i> , 1998;
51	SE-Sk1	Skyttorp young	60.13	17.92	ENF	Pine	-
52	SE-Sk2	Skyttorp	60.13	17.84	ENF	Pine	Gioli <i>et al.</i> , 2004;
53	US-An1	Anaktuvuk River Severe Burn	68.99	-150.28	OSH	Tundra	Rocha & Shaver, 2011;
54	US-An2	Anaktuvuk River Moderate Burn	68.95	-150.21	OSH	Tundra	Rocha & Shaver, 2011;
55	US-An3	Anaktuvuk River Unburned	68.93	-150.27	OSH	Tundra	Rocha & Shaver, 2011;
56	US-Atq	Atqasuk	70.47	-157.41	GRA	Tundra	Lund <i>et al.</i> , 2009;
57	US-Bn1	Delta Junction 1920 Control site	63.92	-145.38	ENF	Spruce	Liu <i>et al.</i> , 2005;
58	US-Brw	Barrow	71.32	-156.63	SNO,BSV	Tundra	Walker <i>et al.</i> , 2003;
59	US-Ha1	Harvard Forest EMS Tower (HFR1)	42.54	-72.17	MF	Leaf	Urbanski <i>et al.</i> , 2007;
60	US-Ho1	Howland Forest (Main Tower)	45.2	-68.74	MF	Spruce	Hollinger <i>et al.</i> , 2004;
61	US-Ich	Imnavait Creek Watershed	68.61	-149.3	OSH	Tundra	Euskirchen <i>et al.</i> , 2012;
62	US-ICs	Imnavait Creek Watershed Heath Tundra	68.61	-149.31	OSH	Tundra	Euskirchen <i>et al.</i> , 2012;
63	US-Ict	Imnavait Creek Watershed Wet Sedge Tundra	68.61	-149.3	OSH	Tundra	Euskirchen <i>et al.</i> , 2012;
64	US-Ivo	Tussock Tundra	68.61	-149.3	OSH	Tundra	Euskirchen <i>et al.</i> , 2012;
64	US-Ivo	Ivotuk	68.49	-155.75	OSH	Tundra	Epstein <i>et al.</i> , 2004;
65	US-NR1	Niwot Ridge (LTER NWT1)	40.03	-105.55	ENF	Spruce	Hu <i>et al.</i> , 2010;

nonlinear least squares regressions (using the nls-function of the statistics package with the nl2sol algorithm).

We estimated  $\lambda E$  using the PM equation written as follows (Penman, 1948; Allen, 1998):

$$\lambda E = \frac{\Delta R_n + \rho_a c_p \delta_e r_a^{-1}}{\Delta + \gamma(r_s + r_a)r_a^{-1}} \quad (1)$$

where  $\rho_a$  is the air density ( $\text{kg m}^{-3}$ ),  $c_p$  is the specific heat of air ( $\text{J kg}^{-1} \text{K}^{-1}$ ),  $\Delta$  is the rate of change of saturation vapor pressure with air temperature ( $\text{Pa K}^{-1}$ ) and  $\gamma$  is the psychrometric constant ( $66 \text{ Pa K}^{-1}$ ),  $r_s$  the surface resistance ( $\text{s m}^{-1}$ ) and  $r_a$  the aerodynamic resistance ( $\text{s m}^{-1}$ ). The latter was calculated from the EC data following the method used by Launiainen (2010):

$$r_a = \frac{u}{u_*^2} + \frac{\text{kB}^{-1}}{u_*} \quad (2)$$

where  $\text{kB}^{-1}$  is the Stanton number (dimensionless). The excess resistance parameter  $\text{kB}^{-1}$  was set to the value of two (dimensionless) to estimate  $r_a$  in a similar way for all sites. This value is suggested to be representative for a wide range of vegetation types (Garratt, 1978), and has been found to be representative for forests (Verma, 1989; Launiainen, 2010). Among different studies various values for  $\text{kB}^{-1}$  has been used and its optimal value can vary between vegetation types as well as seasonally (Kustas *et al.*, 1989; Wu *et al.*, 2000; Barr *et al.*, 2001; Zha *et al.*, 2010). Although we used the same value of  $\text{kB}^{-1}$  for

all sites, it has been reported to range from 1 to 12 (Shuttleworth & Wallace, 1985; Kustas *et al.*, 1991; Troufleur *et al.*, 1995).

Normally the PM equation includes the available energy flux ( $R_n - G - \Delta S$ , where  $G$  is the soil heat flux and  $\Delta S$  is the rate of heat storage in the canopy volume), whereas we have chosen to neglect  $G$  and  $\Delta S$  since they are usually small compared to  $R_n$  particularly when using the equation on a daily basis (the two terms become small on a 24-h cycle). Based on the results of those studies that has been investigating EC energy balance closure problems, measurement errors of  $G$  and  $\Delta S$  varies from 20 to 50% and the absolute flux gradient from 20 to  $50 \text{ W m}^{-2}$  (Foken, 2008). These components are small compared to  $R_n$ ,  $\lambda E$  and sensible heat flux ( $H$ ) and their vertical and horizontal scales are limited to near ground level. Because these components were not widely reported for all ecosystem types present in the study, these terms were neglected from the estimation procedure and the decision to prioritize the wider coverage of different ecosystem types were made.

The surface resistance was estimated using a multiplicative model (Jarvis, 1976; Stewart, 1988) as follows:

$$r_s = f(P)f(\delta_e)f(R_g) \quad (3)$$

where  $f(P)$ ,  $f(\delta_e)$  and  $f(R_g)$  are phenology,  $\delta_e$  and  $R_g$  modifiers, respectively. The values of the modifiers vary between 0 and 1.

**Table 2** Ecosystem specific calibrated model parameters

Vegetation types	Model parameters					
	$\theta$ (°C)	$\tau$ (d)	$r_{SMax}$ (s m <sup>-1</sup> )	$r_{SMin}$ (s m <sup>-1</sup> )	$k_R$ (W m <sup>-2</sup> )	$k_{VPD}$ (Pa)
Cut	13	25	79.2	22.4	14.3	282.8
Douglas-Fir	5	2	80.4	45.7	5.2	367.8
Grass	15	20	407.7	66.4	0.1	1372.1
Larch	6	22	75.5	13.2	87.1	220.0
Broadleaf deciduous	13	23	59.8	6.6	109.3	236.4
Pine	10	24	127.8	30.0	12.5	498.9
Spruce	12	15	71.3	25.5	41.8	473.8
Tundra	7	12	147.8	80.3	418.9	2700.7
Wet	7	11	232.3	90.1	12.2	4000.0

The phenology modifier which accounted for seasonal (i.e. summer and winter) are based on the work of Mäkelä *et al.* (2004) and Gea-Izquierdo *et al.* (2010) and is expressed as follows:

$$f(P) = r_{SMax} - 2 \left( 1 - \frac{1}{1 + S(t)} \right) (r_{SMax} - r_{SMin}) \quad (4)$$

where  $r_{SMax}$  and  $r_{SMin}$  are the maximum and minimum stomatal resistances (s m<sup>-1</sup>) and  $S(t)$ , a variable describing the phenological state of the plants, is calculated as follows:

$$S(t) = \min \left( \frac{\int_{t-\tau}^t T_a(t) dt}{\tau \theta}, 1 \right), \quad (5)$$

where  $T_a$  is air temperature,  $\theta$  (°C) is a parameter describing the long-term average temperature at which stomatal resistance reaches its minimum value,  $\tau$  is the integration time delay of stomatal response in days. The phenological model describes the slow development of surface resistance to changes in temperature as it occurs during spring. It is a modification of the model of Gea-Izquierdo *et al.* (2010) that they used for the analysis of Gross Primary Production (GPP). The behavior of  $S(t)$  as a function of  $\tau$  and  $\theta$  and  $T_a$  is shown in Fig. 2.

Surface resistance was also assumed to have a hyperbolic dependence on  $R_g$  (Wong *et al.*, 1979; Leuning, 1995) as follows:

$$f(R_g) = \frac{k_R + R_g}{(R_g + 5)} \quad (6)$$

where  $k_R$  is a parameter describing the sensitivity of surface resistance to global radiation. An offset of five W m<sup>-2</sup> was added to  $R_g$  (in the denominator) to avoid frequent problems caused by occurrences of negative values of  $R_g$  and to constrain  $r_s$  surface resistance to finite values.

Finally,  $r_s$  was assumed to depend on  $\delta_e$  as follows:

$$f(\delta_e) = \left( 1 + \frac{\delta_e}{k_{VPD}} \right) \quad (7)$$

where  $k_{VPD}$  (kPa) is an empirically estimated parameter describing the sensitivity of stomatal conductance to  $\delta_e$ .

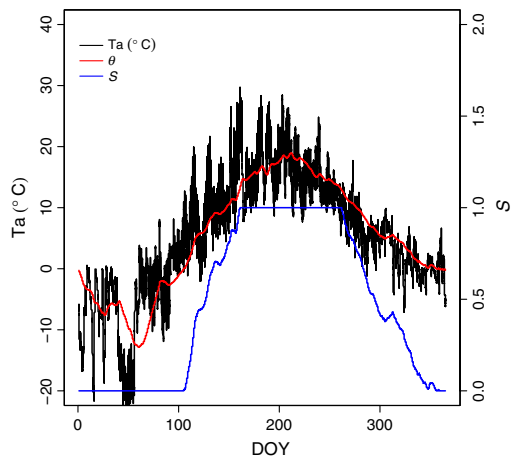


**Fig. 2** Conceptual behavior of  $S$  as a function of  $\theta$  and  $\tau$ . The black line is the measured air temperature. The variable  $S$  (blue line) is calculated based on the running mean (blue line) of the measured air temperature (black line) and with delay (which depends on  $\tau$ ).  $S$  is saturated when it reaches the value 1 (on the right  $y$ -axes).

High values of  $k_{VPD}$  indicate a low stomatal sensitivity to VPD.

### Statistical analysis

Parameter estimation was done using half-hourly values of  $r_s$  calculated by inverting Eqn (1) using nongapped  $\lambda E$ ,  $R_{ir}$ ,  $T_a$ ,  $\delta_e$ ,  $u$  and  $u_s$  data. The values of the parameters  $k_R$ ,  $k_{VPD}$ ,  $r_{SMin}$ ,  $r_{SMax}$ ,  $\theta$  and  $\tau$  were estimated to maximize the fit of the model to measured  $\lambda E$  data using ordinary least squares. Over all, two different parameter sets are estimated. Firstly, estimated parameter values for each site is provided separately and secondly, the estimated average parameters are provided for each vegetation type.

The values of the parameters  $k_R$ ,  $k_{VPD}$ ,  $r_{SMin}$  and  $r_{SMax}$  were estimated simultaneously. The parameters  $\theta$  and  $\tau$ , linked to the phenology of latent heat exchange, were estimated, iteratively. The values of  $\theta$  and  $\tau$  were first fixed and then the other parameters were estimated by using the nonlinear regression. The reported values are the combination of all parameters (including  $\theta$  and  $\tau$ ), which minimizes the residual sum of squares. This was done for a grid with a density of 1 day ( $\tau$ ) and 1 °C ( $\theta$ ). The grid ranged from 1 to 30 days for  $\tau$  and for 5–20 °C for  $\theta$ . In rare cases where the use of the phenology model improved the fit of the model by less than 2%,  $\theta$  and  $\tau$  were set to 5 °C and 2 days, respectively.

To produce mean model parameters for each ecosystem type, all ecosystem specific data were concatenated and average ecosystem type parameters were estimated from this pooled data. Based on the parameters derived from this estimation, the  $\lambda E$  values of different vegetation types were compared by using the ecosystem average model parameters for each vegetation type ( $r_{SMax}$ ,  $r_{SMin}$ ,  $k_R$  and  $k_{VPD}$ ) and the meteorological data of the station Hyytiälä (FI-Hyy) for 2011. Hyytiälä was selected it represents somehow an ‘average climate’ in the dataset [mean annual air temperature 1961–1990 + 2.9 °C and precipitation 709 mm (Sevanto *et al.*, 2006)]. To compare the annual mean behavior of measured and modeled  $\lambda E$ , site-specific data were aggregated (measured and modeled) over the whole data range as daily means (Table 3).

The goodness of the model fit was estimated by using the proportion of explained variance (PR<sup>2</sup>), defined as:

$$PR^2 = 1 - \frac{\sum(y - \hat{y})^2}{\sum(y - \bar{y})^2}, \tag{8}$$

where  $y$  is the measured value of the variable in question,  $\hat{y}$  is its predicted value and  $\bar{y}$  its mean measured value. For a linear regression, this gives the same values as the traditional  $R^2$ .

*Climatological and land cover data*

To characterize the relations of vegetation characteristics to climate, long-term averages of climate variables were used. These were extracted from the Climatic Research Unit (CRU) gridded climatology (New *et al.*, 2002). This data have a spa-

tial resolution of 10 min and the climate variables were gridded averages1960–2000. Averaged annual mean temperatures were in a good agreement with temperatures calculated from the available EC site data. Recorded  $T_a$  data from the EC sites could not directly be used, because from some sites data were available only for the summer time and some time series were quite short.

Leaf Area Index (LAI) and Normalized Difference Vegetation Index (NDVI) data are derived from the Moderate Resolution Imaging Spectroradiometer (MODIS) products [MOD13Q1 (18 days) & MOD15A2 (8 day)]. Grid size for LAI was 1 × 1 km and for NDVI 0.25 × 0.25 km from the center coordinates of the flux tower site. LAI and NDVI data are reported for July, which were assumed to be the time of maximum leaf area index at most sites.

**Results**

*Site characteristics*

Annual average  $T_a$  (as calculated from the climatological data) ranged between –10 to +8 °C, being lowest for tundra and highest for the Douglas-fir sites. Some of the most continental sites, Yakutsk-larch and pine sites (RU-Ylr and RU-Ypf) also had very low annual mean temperatures (–10 °C) (Fig. 3a). The mean annual precipitation was highest for the Douglas-fir sites (1600 mm a<sup>-1</sup> CA-Ca1, CA-Ca2, CA-Ca3) and lowest for tundra sites (200 mm a<sup>-1</sup> RU-Che, RU-Cok, US-Atq, US-An1, US-An2, US-An3, US-Brw, US-Ich, US-ICs, US-Ict, US-Ivo), while the mean precipitation for other vegetation types ranged between 500 and 600 mm a<sup>-1</sup> (Fig. 3b). Mean annual  $T_a$  and precipitation were highly correlated ( $\log(y) = 6.31e^{(0.0134x)}$  PR<sup>2</sup>: 0.77 where  $y$  is mean annual precipitation and  $x$  is mean air temperature Fig. 3c).

Moderate Resolution Imaging Spectroradiometer derived mean summer LAI (using projected LAI) for most vegetation types in July, were around two and lowest summer time means were observed for grass, tundra and wetland sites (Fig. 3d). The highest LAI

**Table 3** Statistical summary for the modeled ecosystem specific fit. RMSE is root-mean-square deviation, MM is measured mean

Ecosystem	Half an hour				Daily				Monthly			
	Bias	RMSE	MM	PR <sup>2</sup>	Bias	RMSE	MM	PR <sup>2</sup>	Bias	RMSE	MM	PR <sup>2</sup>
Cut	-0.82	23.61	51.72	0.6	0.93	11.3	46.11	0.84	1.19	6.79	46.05	0.94
Douglas-fir	0.28	27.74	64.34	0.48	0.54	15.1	57.92	0.71	1.18	7.28	58.61	0.9
Grass	2.67	26.08	87.89	0.71	2.64	14.11	79.56	0.86	5.41	8.58	73.76	0.93
Broadleaf deciduous	-3.59	30.88	68.24	0.67	-0.38	15.44	65.64	0.85	-0.08	10.58	66.29	0.93
Pine	0.73	22.7	48.94	0.62	3.09	10.27	45.86	0.87	3.2	6.22	44.21	0.95
Spruce	-0.12	25.86	54.54	0.59	3.68	11.47	52.26	0.84	3.57	7.88	51.93	0.93
Tundra	6.19	24.96	53.75	0.52	5.81	14.21	36.82	0.61	4.69	8.28	27.24	0.83
Wet	1.51	23.09	67.1	0.76	3.22	11.94	60.22	0.88	3.76	8.39	61.08	0.95

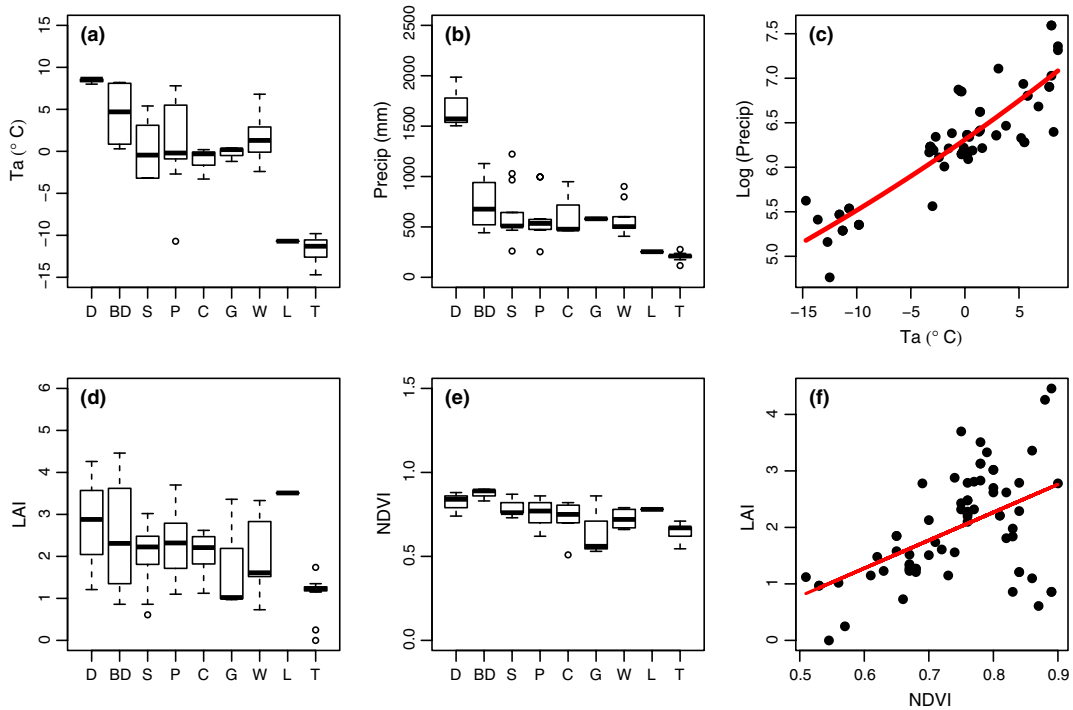


**Fig. 3** Characteristic of the different vegetation types. (a) the variation in the mean annual air temperature ( $^{\circ}\text{C}$ ) (b) mean annual precipitation (mm) (c) logarithmic relationship of mean annual precipitation and air temperature  $\log(y) = 6.31e^{(0.0134x)}$   $\text{PR}^2: 0.77$ , (d) mean summer time LAI-index (e) Mean summer time NDVI, (f) regression between mean summer time LAI and NDVI index  $y = 4.9504x - 1.6940$   $\text{PR}^2: 0.26$ . Results are presented in subpanels a, b, c and e by ecosystem type where, D, Douglas-fir forest; BD, broadleaf deciduous f.; S, spruce f.; P, pine f.; C, cut/open/ burned f.; G, grassland; W, wetland; L, larch forest and T, tundra.

was observed in deciduous broadleaf, larch and Douglas-fir forests. The variation in NDVI and LAI was quite similar between ecosystem types (Fig. 3e). However, MODIS-derived NDVI as well as the LAI, were only weakly correlated with mean annual  $T_a$  ( $y = 0.0081x + 0.7509$   $R^2 = 0.29$ , where  $y$  is NDVI and  $x$  is  $T_a$ ;  $y = 0.0485x + 2.0669$   $R^2 = 0.10$ , where  $y$  is LAI and  $x$  is air temperature). Also the correlation between NDVI and LAI was not strong ( $y = 5.6x - 2.71$ ;  $R^2 = 0.31$  where  $y$  is LAI and  $x$  is NDVI) (Fig. 3f). The larch forest was the exception because, despite the low annual mean  $T_a$  and precipitation, summer time mean LAI and NDVI were almost as high as for the broadleaf-type forests (Fig. 3d and e).

#### Phenological model parameters

For the wetland- and tundra land cover types, the parameters indicating the saturation temperature to reach minimum value of  $r_s$  ( $\theta$ ) and the delay ( $\tau$ ) were smaller than for the forested sites. In other words, these

ecosystems shifted from the winter to the summer state more rapidly and at lower temperatures. Among the forest sites, only the larch forest had a similar low temperature requirement. Usually forests reached summer resistance when  $\theta$  varied between 10 and  $13^{\circ}\text{C}$  with  $\tau$  varying from 15 to 25 days (Table 2; Fig. 4a, b). The longest spring recovery period (as measured by  $\tau$  and  $\theta$ ), were observed for grassland ecosystems. For these ecosystems, the values of  $\theta$  were higher than for other ecosystems and values of  $\tau$  were higher than for tundra and wetland ecosystems. Douglas-fir did not show any seasonal pattern for  $r_s$ , and the parameter values for the phenology model are not reliable since the difference between parameters describing wintertime resistance ( $r_{SMax}$ ), and summertime resistance ( $r_{SMin}$ ) was small (Table 2).

$r_{SMax}$ . The calculated maximum canopy resistance parameters  $r_{SMax}$  varied between 100 and  $250 \text{ s m}^{-1}$  for all vegetation types ( $r_{SMax}$  in Fig. 4c). Winter values of  $r_s$  values were clearly higher than the summer values in

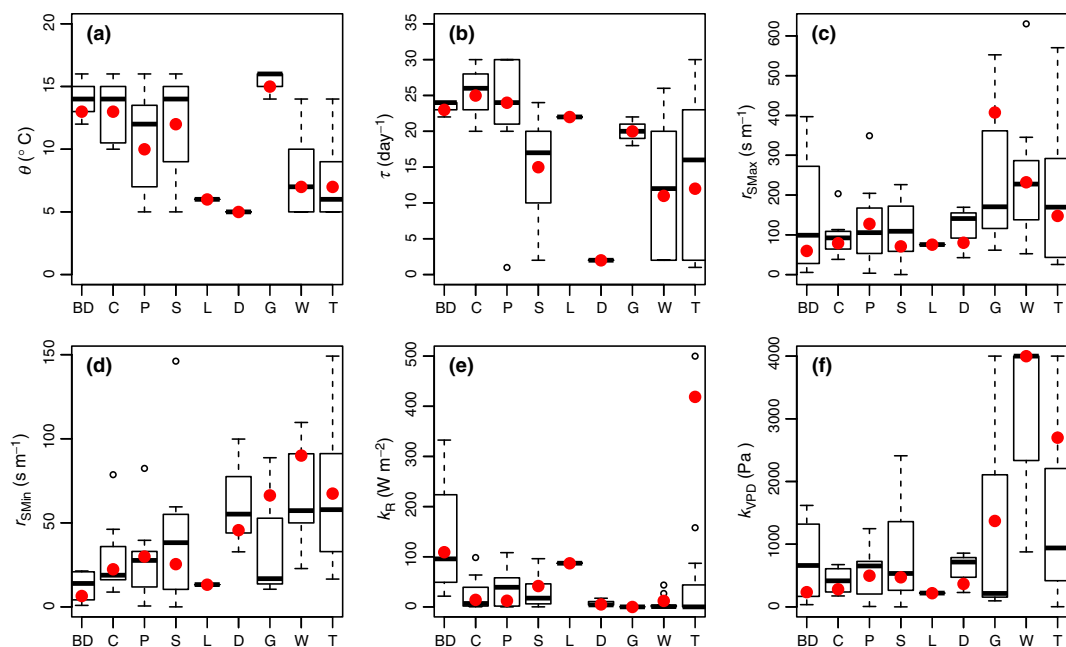


**Fig. 4** Distribution of model parameters  $\theta$  ( $^{\circ}\text{C}$ ) (a),  $\tau$  (days) (b) maximum resistance  $r_{s\text{Max}}$  (c), minimum resistance  $r_{s\text{Min}}$  (d) sensitivity global shortwave radiation  $k_R$  (e) and sensitivity to rapid VPD changes  $k_{\text{VPD}}$  (f). Results are presented in all subpanels according to ecosystem types where, BD, broadleaf deciduous forest; C, cut/open/burned f.; P, pine f.; S, spruce f.; L, larch f.; D, Douglas-fir f.; G, grassland; W, wetland and T, tundra. Red points are model parameters that are calibrated against the all ecosystem type data and represent values estimated for all sites of an ecosystem type. Heavy black line of the box-and-whisker plot shows the arithmetic mean, thin black line 25% and 75% quartiles, and whisker lines (or single points) minimum and maximum values of the data. Red points are model parameters that are calibrated against the all ecosystem type data.

all ecosystems excluding Douglas-fir. The variation in wintertime  $r_s$  parameters within grassland, broadleaf deciduous forest and wetland ecosystems was large, while the variation for evergreen coniferous forest ecosystems was smaller (Fig. 4c).

$r_{s\text{Min}}$ . The highest mean values of  $r_{s\text{Min}}$  were observed for Douglas-fir, grassland, tundra and wetland (Fig. 4d). For coniferous forests, the values of  $r_{s\text{Min}}$  were about half of the values for deciduous forests. Broadleaf deciduous forests had the smallest values of summer time  $r_s$  followed by the other forest ecosystems with exception of Douglas-fir. Douglas-fir had high values of  $r_s$ . In general, wetlands and tundra ecosystems had higher values of  $r_s$  than forests.

$k_R$ . The mean values of  $k_R$ , which describes the sensitivity of the surface resistance to  $R_g$  were small for all sites, typically less than  $100 \text{ W m}^{-2}$ . There was no clear relationship of  $k_R$  with vegetation type or climatic char-

acteristics. The largest variation in  $k_R$  was observed for the broadleaved deciduous forest vegetation type (Fig. 4e).

$k_{\text{VPD}}$ . High values of  $k_{\text{VPD}}$  indicate that  $r_s$  changes slowly with increasing  $e_a$  while low values indicate a rapid reduction in  $r_s$  when  $e_a$  increases. Low values of  $k_{\text{VPD}}$  can be interpreted that stomatal resistance ( $r_s$ ) is sensitive to vapor pressure deficit ( $\delta_e$ ). Values of  $k_{\text{VPD}}$  were higher ( $>500 \text{ Pa}$ ) for sites where freely evaporating water is present, and low ( $<500 \text{ Pa}$ ) for sites where the evaporative flux is governed by largely by stomatal regulation. The values were highest for the grass, tundra and wetland-types (Fig. 4f).

#### Mean parameters for ecosystem types

Modeled mean parameters (red dots in Fig. 4; Table 2) for different ecosystem types were mainly within the variation range and close to arithmetic means from the site-specific estimation (black lines in Fig. 4).  $r_{s\text{Max}}$

was slightly lower for all ecosystem types than the calculated mean, grassland and pine excluded.  $r_{SMin}$  was higher than the mean for grassland, tundra and wetland, while values for Douglas-fir, broadleaf deciduous and spruce were slightly lower. For all ecosystems types,  $k_R$  values were similar to the mean values and only for tundra-type the parameter was clearly higher. The modeled  $k_{VPD}$  parameter was similar to the mean or slightly lower for all other sites, but higher for grassland and tundra.

#### Aerodynamic resistance ( $r_a$ )

Aerodynamic resistance was calculated from the recorded EC data based on Eqn (2). Typically  $r_a$  was smaller for forests than for open ecosystems (Fig. 5a). In most forest ecosystems, median values of  $r_a$  from half-hourly data were less than  $50 \text{ s m}^{-1}$ , Douglas-fir excluded. For grassland, tundra and wetlands that are usually more open ecosystems than forests,  $r_a$  varied typically from 50 to  $150 \text{ (s m}^{-1}\text{)}$  (Fig. 5a).  $r_a$  values derived from estimation where ecosystem specific data were pooled, (red dots) were quite similar to calculated averages for ecosystems (black horizontal lines in Fig. 5a).

#### Surface resistance ( $r_s$ )

Surface resistance was calculated according to Eqns (3-7) and the overall pattern of ecosystem median values was opposite to  $r_a$ . Usually, those systems that had low  $r_a$  had higher  $r_s$ , and those with high  $r_a$  had low  $r_s$  (Fig. 5b). The highest median values of  $r_s$ , calculated from half-hourly data, were found for broadleaf decid-

uous and larch, followed by evergreen needle leaf and cut forests. For wetlands, grasslands and tundra  $r_s$  was typically lower than for forest ecosystems.  $r_s$  from pooled ecosystem calibration were quite similar to calculated means (red dots in Fig. 5b), but lower for broadleaf deciduous forests. For wetlands and tundra, estimated values from pooled data were higher than the calculated means (Fig. 5b).

#### Partitioning total resistance between $r_s$ and $r_a$

Total resistance was calculated as the sum of  $r_a$  and  $r_s$ . Forests have typically higher  $r_s$  than ecosystems with short vegetation, where aerodynamic resistance controls the total resistance (Fig. 5c). This can be seen from Fig. 5c where  $r_s$  in all forest ecosystems contributes clearly more than 50% of the total resistance ( $r_s + r_a$ ), while for other ecosystems this proportion is typically less. The range in of the ratio of  $r_s$  to  $r_s + r_a$  varies mostly in cut forests, wetland and tundra. This indicates the heterogeneity of these ecosystem types. For example, the length of the roughness elements (height of the vegetation) is not similar in different kind of cut forests, wetlands or tundra, while in mature forests and grasslands the variation is smaller. The importance of  $r_s$  calculated based on pooled data is within the range of the ecosystem specific variation. However, in the pooled data the importance of  $r_s$  was larger for wetlands and tundra (Fig. 5c).

#### Fit of the model

The proportion of explained variance ( $PR^2$ ) between measured and predicted  $\lambda E$  for half-hourly values var-

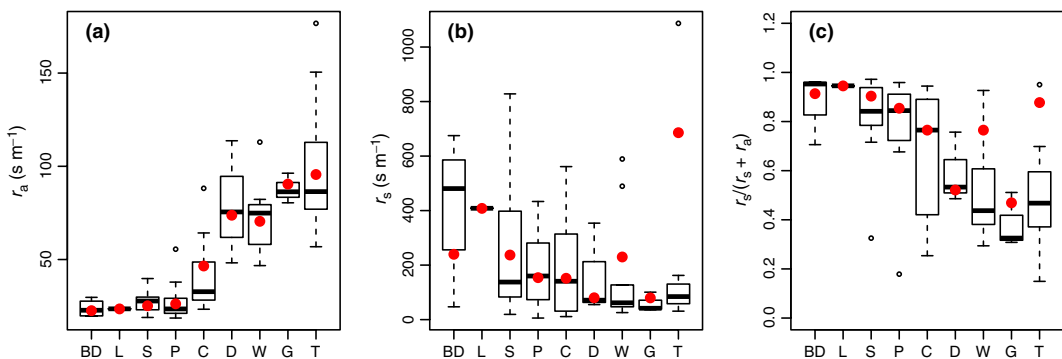


**Fig. 5** Distribution of calculated median aerodynamic resistance ( $r_a$ ) from half an hour data (a), distribution of calculated median surface resistance ( $r_s$ ) from half an hour data (b) and proportion of total resistance accounted for  $r_s$  (i.e., the ratio of  $r_s$  to  $r_s + r_a$ ) (c) based on the data presented in panels a and b. Results are presented in all subpanels according to ecosystem types where, BD, broadleaf deciduous forest, C, cut/open/burned forest; P, pine forest; S, spruce forest; L, larch forest; D, Douglas-fir forest; G, grassland; W, wetland and T, tundra.

ied from 0.4 to 0.84 among sites. The mean  $PR^2$  value was  $0.65 \pm 0.11$  (mean  $\pm$  SD). When we compared daily mean  $\lambda E$  values to daily averages of the modeled data the  $PR^2$  varied from 0.33 (CA-Man) to 0.92 (CAN55) with a mean of  $0.76 \pm 0.11$ , and for monthly aggregation from 0.58 (RU-Cok) to 0.99 (RU-Ha1) with a mean  $0.90 \pm 0.07$  (Table 3; Fig. 6). All model and statistical parameters for sites, as well as, ecosystem types are reported in S1.

Fits of the model based on the ecosystem type specific estimation, were slightly lower than the arithmetic mean from the site-specific calibration (red dots in Fig. 6a). However, for daily and monthly time steps, the fit was generally better than the arithmetic mean from the site-specific estimation (red dots in Fig. 6b and c). This was due to the increase in variance of the data when all the data for an ecosystem is pooled, and not actually due to a better fit of the model.

The aggregated daily mean values over the whole data range showed that the yearly patterns of measured and modeled  $\lambda E$  in all ecosystem types were similar and indicate a good fit over all of the year (examples provided in Fig. 7).

#### Vegetation differences in $\lambda E$

There was a strong relationship [ $92.16e^{(0.0418x)}$ ,  $P < 0.05$ ,  $R^2 = 0.99$ ] between ecosystem type specific model parameters  $r_{SMin}$  and  $k_{VPD}$  calibrated against the pooled data (Fig. 8). In this regression, the small  $r_{SMin}$  indicates low summer time resistance that typically leads to higher  $\lambda E$  flux. Like it can be seen from the Fig. 5c,  $r_s$  mainly controls  $\lambda E$  in forest ecosystems. Forests seem also to be more sensitive to VPD changes (Fig. 8). Ecosystems that have values of  $r_{SMin}$  greater than  $500 \text{ s m}^{-1}$  (grasslands, wetlands and tundra), are not

sensitive to VPD changes, but have lower value of  $r_s$  than most forests.

To compare the differences between ecosystems, the ecosystem specific  $\lambda E$  flux was simulated by using mean ecosystem parameters and meteorological variables from site FI-Hyy. Even with identical levels of meteorological forcing differences between ecosystems were observed. The proportion of simulated  $\lambda E$  of net radiation varied between ecosystems from 39% in broadleaf deciduous forest to 16% in tundra (Fig. 9).

#### Discussion

This study presents a comprehensive analysis of  $\lambda E$  for different vegetation types of the northern temperate, boreal and arctic vegetation zones. The boreal and arctic zones are, by no means homogenous, but a mixture of different land cover types that are determined by the proportion of wetlands and frequency of disturbances (Bonan, 2008a,b). This study presents a new quantification of energy exchange of different land cover types based on the data of 65 FLUXNET stations. It is demonstrated that these land cover types differ in their energy exchange and their response of surface resistance to the environment. The PM equation gave an adequate description of the  $\lambda E$  for all vegetation types, however, the  $r_s$  parameters and the response of  $r_s$  to the environment differed between sites. Furthermore, phenological effects were important since wintertime and summer time resistances were different for all sites, except Douglas-fir.

The resistances,  $r_a$  and  $r_s$ , govern  $\lambda E$  between vegetated surface and atmosphere. The resistances estimated for different ecosystem types are within the range of the reported variation in boreal ecosystems (Baldocchi *et al.*, 2000; Eugster *et al.*, 2000). Baldocchi *et al.* (2000) and Eugster *et al.* (2000) reported that total

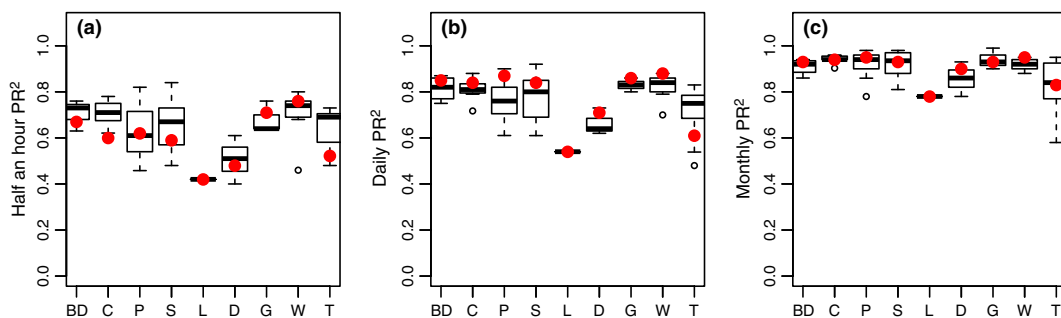


**Fig. 6** Proportion of explained variance ( $PR^2$ ) for 0.5 h (a), daily (b) and monthly (c) time span. Results are presented in all subpanels according to ecosystem types where, BD, broadleaf deciduous forest; C, cut/open/burned f.; P, pine f.; S, spruce f.; L, larch f.; D, Douglas-fir f.; G, grassland; W, wetland and T, tundra. Red points are  $PR^2$  values from pooled estimation based on the ecosystem specific model parameters presented in Fig. 4.

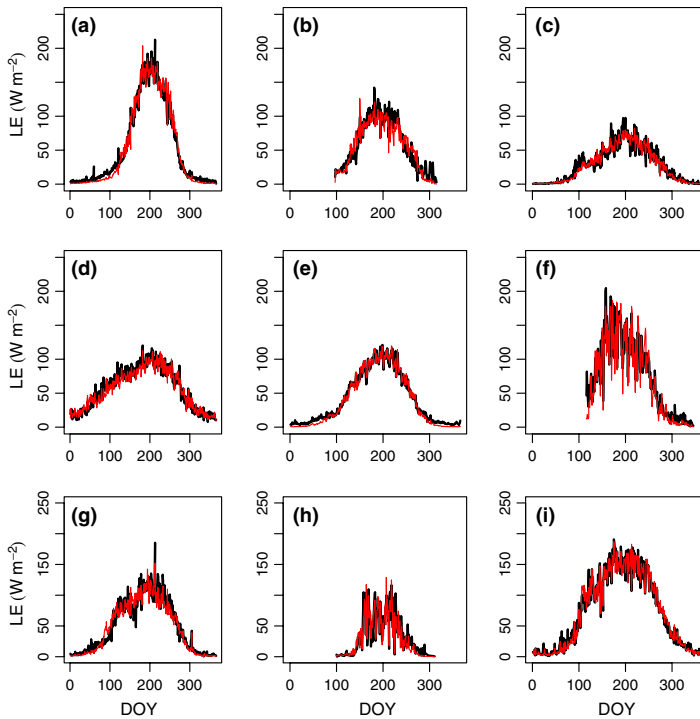


**Fig. 7** Aggregated annual measured and predicted  $\lambda E$  for different vegetation types over the data range used in the estimation. The black line is the mean daily  $\lambda E$  and the red line represents modeled daily values. Subpanels represent data and fit of the model for following sites a: CA-Oas PR<sup>2</sup> 0.98, b: RU-Ylr PR<sup>2</sup> 0.85, c: CA-Sj2 PR<sup>2</sup> 0.92, d: CA-Ca1 PR<sup>2</sup> 0.93, e: FI-Hyy PR<sup>2</sup> 0.98, f: RU-Ha1 PR<sup>2</sup> 0.91, g: RU-Fyo PR<sup>2</sup> 0.94, h: RU-Che PR<sup>2</sup> 0.83, i: CA-Mer PR<sup>2</sup> 0.98. Ecosystem types that sites are represented are (a) broadleaf deciduous forest, (b) larch forest, (c) cut forest, (d) Douglas-fir forest, (e) pine forest, (f) grassland, (g) spruce forest, (h) tundra, (i) wetland.

resistance in boreal ecosystems varies between 20 and 1500 s m<sup>-1</sup>. In this study, we found that when the calculated median  $r_s$  exceeds 500 s m<sup>-1</sup> in half-hourly data, the ratio of  $r_s$  to the total resistance is typically greater than 0.7. This suggests that in all these ecosystems  $r_s$  is the most important vegetation characteristics controlling  $\lambda E$ . The range of the variation in the  $r_s$  model parameters was large also within the ecosystem types. Summer minimum resistance values ( $r_{SMin}$ ) and the VPD sensitivity of the stomata ( $k_{VPD}$ ) for different sites were strongly correlated (see Fig. 8). In this regression, broadleaf deciduous forest has the smallest  $r_{SMin}$ , followed by the other young and mature forest types, while grassland, tundra and wetland-type ecosystems have significantly higher  $r_{SMin}$  and seem not to be sensitive to changes in VPD. The observation of this study is consistent with previous findings (Kelliher *et al.*, 1995; Baldocchi & Vogel, 1997) and suggest that evergreen needle leaf forests have higher values of  $r_s$  than deciduous broadleaf stands.

Based on the findings of this study,  $\lambda E$  in wetlands and tundra ecosystems occurs often from open water surface or the ground, while stomata largely control the  $\lambda E$  of forests. The highest values for  $r_s$  were observed in tundra and wetland ecosystems. In both ecosystems types, mosses are very common or in some cases, the dominant vegetation cover.  $\lambda E$  from feather moss, *Sphagnum* species and lichen are not similar to vascular plants due to the difference in physiological structure. Brown *et al.* (2010) reported that feather moss has higher resistance to  $\lambda E$  than *Sphagnum* species, and Kettridge *et al.* (2013) showed that a higher tree density in wetlands affects  $\lambda E$ .

The fit of the model was fair for half-hourly time periods (PR<sup>2</sup> around 0.6 for most ecosystem types) and the model was able to capture variation in all ecosystem types. Used radiation and flux data in the estimation was not corrected for the energy balance closure or other potential errors. Energy balance closure calculations were also not possible for some of the tundra sites

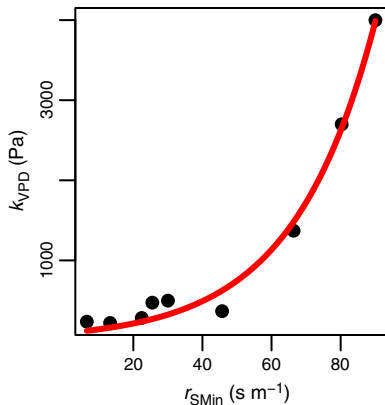


**Fig. 8** Relationship between modeled ecosystem type specific parameters  $r_{SMin}$  and  $k_{VPD}$   $y = 92.16e^{(0.0418x)}$   $PR^2 0.98$ . The order of dots from right to left with increasing  $r_{SMin}$  and  $k_{VPD}$  is broadleaf deciduous forest, larch forest, cut/open/burned forest, spruce forest, pine forest, Douglas-fir forest, grassland, tundra and wetland.

where ground heat flux was not measured and eddy flux data for the whole year was not available. The mean  $PR^2$  values of this study, were similar to values usually reported for carbon fluxes in similar ecosystems (Gea-Izquierdo *et al.*, 2010). It is notable that the model performance was less than average for the Douglas-fir stands in both studies (this study and Gea-Izquierdo *et al.*, 2010). While the explanatory power of the models was quite high, parameter values varied within and between vegetation types. Some of the variation in the parameters within a vegetation type can be explained by differences in the functioning of ecosystems on different sites, but some can be attributed to cross-correlation of parameters that increase the errors of the estimated parameter values (e.g. Gea-Izquierdo *et al.*, 2010). Aside from the Douglas-fir sites the fit was also poor for some tundra sites.

The reasons for the lack of fit to Douglas-fir is ignored, because this ecosystem have not responded well either to earlier attempt to use phenological models. However, it can be considered that in tundra ecosystems some of the assumptions of the PM equation are not realized. Tundra ecosystems have a sparse vegetation cover and the melting of the active layer may induce a large heat sink (Rouse, 1984). Therefore, it is likely that the plant canopy is not warming as expected by the PM equation and the assumptions are violated in tundra ecosystems where the difference between  $R_n$  and soil heat flux might be necessary in estimating the available energy flux. For some sites, it is estimated that soil heat flux might account up to 30% of  $R_n$  (Rouse,

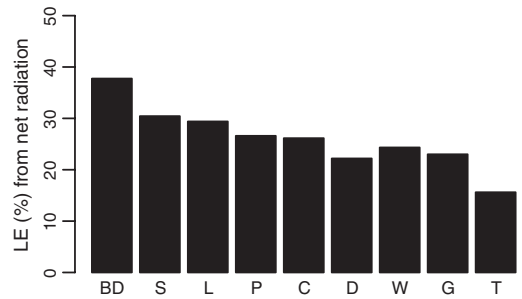


**Fig. 9** Proportion (%) of annual net radiation ( $R_n$ ) accounted for by of  $\lambda E$  based on the parameter values estimated for each ecosystem type. Meteorological data from station FI-Hyy were used in the simulations. Results are presented according to ecosystem types where, BD, broadleaf deciduous forest; C, cut/open/burned forest; P, pine forest; S, spruce forest; L, larch forest; D, Douglas-fir forest; G, grassland; W, wetland and T, tundra.

1984; Boike *et al.*, 2008). This is particularly true since in some of our tundra sites a thin layer that overlays permafrost and heats up is used primarily to melt ice (Boike *et al.*, 2008; Langer *et al.*, 2011). Also, the evaporation in some tundra ecosystems seems to depend on precipitation since it changes the area covered by open water surfaces in these wet ecosystems (Boike *et al.*, 2008).

Comparison of the simulated  $\lambda E$  rates for different land cover types using climate data of the FI-Hyy site shows that  $\lambda E$  and its sensitivity to environmental factors differs between land cover types. At identical values of  $R_n$ ,  $u^*$  and  $u$ ,  $\lambda E$  was usually higher for forested sites than for the other sites, including wetlands. This is probably due to their larger transpiring leaf area. The highest values of  $\lambda E$  were found for deciduous forests, followed by larch forests and fir or spruce forests. This is in agreement with the previous case studies that suggest that  $\lambda E$  from deciduous leaf forest can be from 50 to 90% of the annual precipitation (Baldochi *et al.*, 2000; Chapin *et al.*, 2000; Blanken *et al.*, 2001) and  $r_s$  of evergreen conifers can be twice as large as that of deciduous broadleaf forests (Eugster *et al.*, 2000). The simulated  $\lambda E$  of short vegetation sites, grassland and tundra was less than for forests. The real difference is probably even larger since  $r_a$  tends to be larger for short vegetation sites. For example Nordbo *et al.* (2011) found that  $\lambda E$  from the Hyytiälä pine forest exceeded the  $\lambda E$  of a nearby lake, because the forest was better coupled to the atmosphere, i.e. the forest had a lower  $r_a$ .

The selected model for this study may also be criticized since it does not include drought in the soil. Although, several studies have shown the connection between soil moisture, LAI and  $\lambda E$  (Barr *et al.*, 2007;

Granier *et al.*, 2007), their relationship can be inconsistent and complex in different ecosystems (Eugster *et al.*, 2000). Typically conifers are less sensitive to drought than deciduous broadleaf trees (Lagergren & Lindroth, 2002; Bernier *et al.*, 2006; Kljun *et al.*, 2006). Because all sites did not provide both soil moisture and precipitation data, the effect of drought to  $\lambda E$  is neglected from this study. Previous studies have shown that the effect of drought can be hard to capture even with detailed models (Duursma *et al.*, 2008). Based on the analysis of the selected sites and data in this study, a special need to estimate model parameters separately was not found. The fit of our model is good without taking into account the possible drought effect throughout the season, which may indicate that drought in the northern ecosystems is not very important in boreal and arctic ecosystem.

There is also a large difference in parameters of the  $\lambda E$  model between summer and winter periods for all ecosystem types except coastal Douglas-fir. The approach of this study to explain the seasonal variation in  $r_s$  is phenomenological and that the model describes different processes, like physiological changes of evergreens, snow melt and leaf growth for different land cover types. A similar approach has been used previously to predict GPP and explains well the differences between different seasons in the  $r_s$  model parameters (Berninger *et al.*, 1996; Mäkelä *et al.*, 2004; Mäkelä *et al.*, 2006).

The  $\lambda E$  of deciduous broad leaf forests should depend largely on the expansion of leaf area (Blanken *et al.*, 1997). A shift from winter to summer values of  $r_s$  is expected when the forest starts to leaf out and GPP starts to increase. Leafing out of trees has traditionally been predicted using accumulated temperature models (Raulier & Bernier, 2000) and the temperature sum required partially depends on the genetic origin of the trees, but is mostly driven by the accumulation of cold days prior to warming. Baldocchi *et al.* (2005) used successfully an approach based on running averages of temperatures to predict the date when NEE equals 0 in northern deciduous broadleaf forests. We did not use the same approach as Baldocchi *et al.* (2005), since we have focused mainly on evergreen forests, where the approach does not apply. Instead, our approach emphasizes a gradual transition from winter to summer states in most common ecosystem types in boreal and arctic regions.

For evergreen conifers, it can be argued that the pronounced seasonal cycle we usually observe is caused by stomatal closure in the winter (Wieser, 2000) and to some extent by higher energy requirements when energy is used to melt snow rather than to evaporate water. Differences between winter and summer gas

exchange are relatively well documented for photosynthetic capacity and attributed to photosynthetic down regulation (Suni *et al.*, 2003; Mäkelä *et al.*, 2004, 2008; Kolari *et al.*, 2007; Gea-Izquierdo *et al.*, 2010). Although, this approach has been used less for  $\lambda E$ ; there is evidence that stomatal resistance increase during the winter periods (Wieser, 2000; Sevanto *et al.*, 2006). The values of the time interval required for the recovery of transpiration (indicated by the parameter  $\tau$ ) were slightly higher than previously reported values related to the delayed photosynthesis using a large part of this data set (Gea-Izquierdo *et al.*, 2010). In this study, we observed values of the delay ( $\tau$ ) ranging from 2 to 30 days in different conifer forests. We think that the development of the LAI of the understory or other factors may play a role in determining the value of  $\tau$ . Also Brümmer *et al.* (2012) reported clearly longer values for the delays in  $\lambda E$  than for the photosynthesis thus the approach was more statistical than in this study and was done by using normalized cross-correlation coefficients (NCCC) to evaluate the lag of evapotranspiration behind  $R_n$ . The results of Brümmer *et al.* (2012) support the findings of this study that the delay on average is smaller in wetland and tundra ecosystems while from some ecosystems (Douglas-fir) or some sites it cannot be detected. However, without a comprehensive analysis of the links in the recovery of photosynthesis and evapotranspiration the linkages of down regulation recovery of GPP and of evapotranspiration after the winter remain speculative even if previous studies have indicated their potential relevance (Running, 1980; Grace, 1990).

At cut forest sites, the ecosystem is to some degree disturbed and consists of a natural mosaic of young trees, grass, shrubs and mosses. After a clear-cut,  $\lambda E$  from the tree canopy ceases and  $\lambda E$  from the ground vegetation increases. However, the disturbance does not necessarily decrease  $\lambda E$  significantly (Vesala *et al.*, 2005; Jassal *et al.*, 2009). Increased light intensity in undergrowth increases photosynthesis and through that  $\lambda E$  from vegetation and undergrowth and shrubs might be mainly accountable to  $\lambda E$  (Baldocchi *et al.*, 2000; Rouse, 2000). Kelliher *et al.* (1998) reported that the understory might contribute between 30% and 92% (mean 54%) of the daily  $\lambda E$  even in a mature pine forest and Blanken *et al.* (1997) that hazelnut understory transpiration exceeded 25% of total stand evapotranspiration in a mature aspen forest during the summer months.

Vesala *et al.* (2005) reported that thinning of a pine forest in the southern part of Finland did not change fluxes of water or carbon within the detection limits, but affected the physical properties of the canopy like wind speed normalized by the friction velocity. Alto-

gether, it is not clear how leaf area,  $u^*$  and water use of trees interact. Intermediate disturbances of ecosystems do therefore not necessarily decrease fluxes of  $\lambda E$  while the effect has been reported to be significant for the carbon balance in a boreal forest (Bergeron *et al.*, 2008). Indeed studies of water fluxes after thinning or other intermediate-severity disturbances show inconsistently either increases (Lagergren *et al.*, 2008) no changes (Veisala *et al.*, 2005) or small decreases in  $\lambda E$  (Dore *et al.*, 2012).

For tundra and wetlands the interpretation of our temperature-based model for phenology is not very clear because mosses are typically the dominant plant functional type in these ecosystems. Therefore, the concept of surface resistance can be disputed and it is not as clear as in forests, where it is controlled by the stomata. In these systems, high  $r_{sMax}$  values are partly artificial, because stomatal resistance should not be important while the site is mainly snow covered, although evapotranspiration is still occurring through evaporation from the snow surface and sublimation.

Altogether, the temperature-based approach was useful, although for some ecosystems like tundra, it might be necessary to take into account also the soil heat flux. It seems that the approaches for GPP modeling by Gea-Izquierdo *et al.* (2010) for conifers and the approach of Baldocchi *et al.* (2005) for deciduous vegetation indicate that there are different environmental factors governing the recovery of the canopy. These phenological aspects should be explored in future modeling exercises at a more detailed scale. However, the phenomenological scheme worked quite well for large areas.

The relatively large variation in both site and ecosystem type specific  $k_R$  and  $k_{VPD}$  parameters suggests that the sensitivity of stomatal resistance to irradiance and VPD varies between ecosystem types but also between different sites covered by the same ecosystem type. The estimated  $k_R$  were smaller than we would have expected from physiological measurements of stomatal responses to irradiance (e.g. Gea-Izquierdo *et al.*, 2010). The estimated  $k_R$  values were usually small for deciduous forests ecosystems and tundra. The larger variation in  $k_{VPD}$  suggests that within grassland, tundra and wetland land cover types different ecosystems can have different sensitivities of  $r_s$  to  $\delta_e$  (Fig. 4). Sites that have high  $k_{VPD}$ , usually suffer less from water stress and their stomatal resistance is not sensitive to VPD. In the ecosystem type pooled estimation, the mean  $k_{VPD}$  values for tundra and wetlands were much higher than for forests where the  $r_s$  is expected to be the dominant term governing the water vapor flux. For some tundra- and wetland-type sites the summer resistance and sensitivity to VPD was higher than for other ecosystems.

The analysis suggests that there are large differences in the surface and aerodynamic resistances between different vegetation types in the boreal and arctic biomes (Fig. 5, Fig. 9). Surface resistance seems to regulate  $\lambda E$  over the year in larch, most deciduous, pine and spruce forest, while the role of aerodynamic resistance is significant in clear-cut and burnt sites, tundra and wetland ecosystems.

Boreal landscapes are, from a standpoint of energy exchange, by no means homogenous and there are large differences in  $\lambda E$  between different ecosystem types. The used approach led to relatively good estimates of latent heat exchange for these land cover types. Differences in surface resistance between the summer and winter periods are large, also for evergreen conifers, and might be important for the estimation of winter- and spring time latent heat exchange. The results suggest that the accuracy of regional energy exchange estimates will be vastly improved if the significance of stomatal regulation and phenology in different vegetation types is explicitly addressed.

#### Acknowledgements

This research was funded by the Nordic Center of Excellence CRAICC (Cryosphere-atmosphere interactions in a changing Arctic climate), Center of Excellence (project numbers 1118615, ICOS 271878 and ICOS-Finland 281255, ICOS-ERIC 281250 and EU through projects GHG-Europe and InGOS).

We are grateful from the possibility to utilized resources and data that are funded by Fluxnet-Canada, AmeriFlux and US National Science Foundation. The Fluxnet-Canada Research network was funded by the Canadian Foundation for Climate and Atmospheric Sciences (CFCAS), the Natural Sciences and Engineering Research Council (NSERC) of Canada, BIOCAP Canada, Natural Resources Canada and Environment Canada. The Canadian Carbon Program (CCP) was funded by CFCAS, BIOCAP Canada, Natural Resources Canada and Environment Canada. Additional support for both networks was provided by various provincial agencies and industry collaborators: Ministry of Environment (Ontario), Forestry Research Partnership (Canada) and Forestry Canada. The NOBS-MB site also received support from NASA (NAG5-11154 and NASA NNG05GA76G). We also thank TCOS-Siberia that enabled data collection in some Russian flux-towers as well as Helmholtz Association (Helmholtz Young Investigators Group, grant VH-NG-821) that funded the work of Torsten Sachs. We also thank FLUX-Asia for providing data for this study.

We also thank personally the following site PI's: Alan Barr, Allison Dunn, Brian Amiro, Charles Bourque, David Hollinger, Corinna Rebmann, Eugenie Euskirchen, Gaius Shaver, Hank Margolis, Harry McCaughey, J. William Munger, James Randonson, Lawrence Flanagan, Lise Soerensen, M. Martin Heimann, Mats Nilsson, Mike Goulden, Nigel Roulet, Peter Blanken and Riccardo Valentini and as well as all other persons who are not mentioned here, but has helped to produce data utilized in this study.

## References

- Adkinson AC, Syed KH, Flanagan LB (2011) Contrasting responses of growing season ecosystem CO<sub>2</sub> exchange to variation in temperature and water table depth in two peatlands in northern Alberta, Canada. *Journal of Geophysical Research*, **116**, 1–17.
- Admiral SW, Lafluer PM (2007) Modelling of latent heat partitioning at a bog peatland. *Agricultural and Forest Meteorology*, **144**, 213–229.
- Alavi N, Warland JS, Berg AA (2006) Filling gaps in evapotranspiration measurements for water budget studies: evaluation of a Kalman filtering approach. *Agricultural and Forest Meteorology*, **141**, 57–66.
- Allen RG (1998) Crop Evapotranspiration (guidelines for computing crop water requirements). *FAO Irrigation and Drainage Paper*, **56**, 1–296.
- Amiro B, Barr A, Black T *et al.* (2006) Carbon, energy and water fluxes at mature and disturbed forest sites, Saskatchewan, Canada. *Agricultural and Forest Meteorology*, **136**, 237–251.
- Aubinet M, Grelle A, Ibrom A *et al.* (2000) Estimates of the annual net carbon and water exchange of forests: the EUROFLUX methodology. *Advances in Ecological Research*, **30**, 113–175.
- Aurela M, Laurila T, Tuovinen JP (2004) The timing of snow melt controls the annual CO<sub>2</sub> balance in a subarctic fen. *Geophysical Research Letters*, **31**, L16119.
- Aurela M, Lohila A, Tuovinen J, Hatakka J, Riutta T, Laurila T (2009) Carbon dioxide exchange on a northern boreal fen. *Boreal Environment Research*, **6095**, 699–710.
- Baldocchi D (2008) Breathing of the terrestrial biosphere: lessons learned from a global network of carbon dioxide flux measurement systems. *Australian Journal of Botany*, **56**, 1.
- Baldocchi DD, Vogel CA (1997) Seasonal variation of energy and water vapor exchange rates above and below a boreal jack pine forest canopy. *Journal of Geophysical Research*, **102**, 28939–28951.
- Baldocchi D, Kelliher FM, Black TA, Jarvis P (2000) Climate and vegetation controls on boreal zone energy exchange. *Global Change Biology*, **6**, 69–83.
- Baldocchi D, Falge E, Gu L *et al.* (2001) FLUXNET: a new tool to study the temporal and spatial variability of ecosystem-scale carbon dioxide, water vapor, and energy flux densities. *Bulletin of the American Meteorological Society*, **82**, 2415–2434.
- Baldocchi DD, Black TA, Curtis PS *et al.* (2005) Predicting the onset of net carbon uptake by deciduous forests with soil temperature and climate data: a synthesis of FLUXNET data. *International Journal of Biometeorology*, **49**, 377–387.
- Barr G, Betts AK, Black TA, McCaughey JH, Smith CD (2001) Intercomparison of BOREAS northern and southern study area. *Journal of Geophysical Research*, **106**, 543–550.
- Barr AG, Black AT, Hogg EH *et al.* (2007) Climatic controls on the carbon and water balances of a boreal aspen forest, 1994–2003. *Global Change Biology*, **13**, 561–576.
- Barr AG, van der Kamp G, Black TA, McCaughey JH, Nesic Z (2012) Energy balance closure at the BERMS flux towers in relation to the water balance of the White Gull Creek watershed 1999–2009. *Agricultural and Forest Meteorology*, **153**, 3–13.
- Belelli-Marchesini L (2007b) Analysis of the carbon cycle of steppe and old field ecosystems of central Asia. Ph.D. thesis, 209 pp, University of Tuscia, Viterbo, Italy Available at: <http://dspace.univ.it/handle/2067/540> (accessed 15 May 2013).
- Belelli-Marchesini L, Papale D, Reichstein M *et al.* (2007a) Carbon balance assessment of a natural steppe of southern Siberia by multiple constraint approach. *Biogeosciences*, **4**, 581–595.
- Bergeron O, Margolis HA, Coursolle C, Giasson MA (2008) How does forest harvest influence carbon dioxide fluxes of black spruce ecosystems in eastern North America? *Agricultural and Forest Meteorology*, **148**, 537–548.
- Bernier PY, Bartlett P, Black TA, Barr A, Kljun N, McCaughey JH (2006) Drought constraints on transpiration and canopy conductance in mature aspen and jack pine stands. *Agricultural and Forest Meteorology*, **140**, 64–78.
- Berninger F, Mäkelä A, Hari P (1996) Optimal control of gas exchange during drought: empirical evidence. *Annals of Botany*, **77**, 469–476.
- Black TA, den Hartog G, Neumann HH *et al.* (1996) Annual cycles of water vapor and carbon dioxide fluxes in and above a boreal aspen forest. *Global Change Biology*, **2**, 219–229.
- Blanken PD, Black TA (2004) The canopy conductance of a boreal aspen forest, Prince Albert National Park, Canada. *Hydrological Processes*, **18**, 1561–1578.
- Blanken PD, Black TA, Neumann HH, den Hartog G, Yang PC, Nesic Z, Lee X (2001) The seasonal water and energy exchange above and within a boreal aspen forest. *Journal of Hydrology*, **245**, 118–136.
- Blanken PD, Black TA, Yang PC *et al.* (1997) Energy balance and canopy conductance of a boreal aspen forest: partitioning overstory and understory components. *Journal of Geophysical Research*, **102**, 28915–28927.
- Boike J, Wille C, Abnizova A (2008) Climatology and summer energy and water balance of polygonal tundra in the Lena River Delta, Siberia. *Journal of Geophysical Research*, **113**, G03025.
- Boike J, Kattenstroth B, Abramova K *et al.* (2013) Baseline characteristics of climate, permafrost and land cover from a new permafrost observatory in the Lena River Delta, Siberia (1998–2011). *Biogeosciences*, **10**, 2105–2128.
- Bonan GB (2008a) Forests and climate change: forcings, feedbacks, and the climate benefits of forests. *Science*, (New York, N.Y.), **320**, 1444–1449.
- Bonan GB (2008b) *Ecological climatology - Concepts and applications*. 2nd edn. Cambridge University Press, New York.
- Brown SM, Petrone RM, Mendoza C, Devito KJ (2010) Surface vegetation controls on evapotranspiration from a sub-humid Western Boreal Plain wetland. *Hydrological Processes*, **24**, 1072–1085.
- Brümmer C, Black TA, Jassal RS *et al.* (2012) How climate and vegetation type influence evapotranspiration and water use efficiency in Canadian forest, peat land and grassland ecosystems. *Agricultural and Forest Meteorology*, **153**, 14–30.
- Chapin FS, McGuire AD, Randerson J *et al.* (2000) Arctic and boreal ecosystems of western North America as components of the climate system. *Global Change Biology*, **6**, 211–223.
- Cleugh HA, Leuning R, Mu Q, Running SW (2007) Regional evaporation estimates from flux tower and MODIS satellite data. *Remote Sensing of Environment*, **106**, 285–304.
- Corradi C, Kolle O, Walter K, Zimov SA, Schulze E-D (2005) Carbon dioxide and methane exchange of a north-east Siberian tussock tundra. *Global Change Biology*, **11**, 1910–1925.
- Coursolle C, Margolis HA, Barr AG *et al.* (2006) Late-summer carbon fluxes from Canadian forests and peatlands along an east–west continental transect. *Canadian Journal of Forest Research*, **36**, 783–800.
- Dore S, Montes-Helu M, Hart SC *et al.* (2012) Recovery of ponderosa pine ecosystem carbon and water fluxes from thinning and stand-replacing fire. *Global Change Biology*, **18**, 3171–3185.
- Dunn AL, Barford CC, Wofsy SC, Goulden ML, Daube BC (2007) A long-term record of carbon exchange in a boreal black spruce forest: means, responses to interannual variability, and decadal trends. *Global Change Biology*, **13**, 577–590.
- Duursma RA, Kolari P, Perämäki M *et al.* (2008) Predicting the decline in daily maximum transpiration rate of two pine stands during drought based on constant minimum leaf water potential and plant hydraulic conductance. *Tree Physiology*, **28**, 265–276.
- Epstein HE, Calef MP, Walker MD, Chapin ST III, Starfield AM (2004) Detecting changes in arctic tundra plant communities in response to warming over decadal time scales. *Global Change Biology*, **10**, 1325–1334.
- Escobedo JF, Gomes EN, Oliveira AP, Soares J (2011) Ratios of UV, PAR and NIR components to global solar radiation measured at Botucatu site in Brazil. *Renewable Energy*, **36**, 169–178.
- Eugster W, Rouse WR, Pielke RA *et al.* (2000) Land-atmosphere energy exchange in Arctic tundra and boreal forest: available data and feedbacks to climate. *Global Change Biology*, **6**, 84–115.
- Euskirchen ES, Bret-Harte MS, Cott GJ, Edgar C, Shaver GR (2012) Seasonal patterns of carbon dioxide and water fluxes in three representative tundra ecosystems in northern Alaska. *Ecosphere*, **3**, Article 4 1–19.
- Falge E, Baldocchi D, Olson R *et al.* (2001) Gap filling strategies for long term energy flux data sets. *Agricultural and Forest Meteorology*, **107**, 71–77.
- Flanagan LB, Syed KH (2011) Stimulation of both photosynthesis and respiration in response to warmer and drier conditions in a boreal peatland ecosystem. *Global Change Biology*, **17**, 2271–2287.
- Foken T (2008) The energy balance closure problem: an overview. *Ecological Applications*, **18**, 1351–1367.
- Garraff JR (1978) Transfer characteristics for a heterogeneous surface of large aerodynamic roughness. *Quarterly Journal of the Royal Meteorological Society*, **104**, 491–502.
- Gea-Izquierdo G, Mäkelä A, Margolis H *et al.* (2010) Modeling acclimation of photosynthesis to temperature in evergreen conifer forests. *The New Phytologist*, **188**, 175–186.
- Gioli B, Miglietta F, De Martino B *et al.* (2004) Comparison between tower and aircraft-based eddy covariance fluxes in five European regions. *Agricultural and Forest Meteorology*, **127**, 1–16.
- Göckede M, Foken T, Aubinet M *et al.* (2008) Quality control of CarboEurope flux data – Part 1: coupling footprint analyses with flux data quality assessment to evaluate sites in forest ecosystems. *Biogeosciences*, **5**, 433–450.
- Goulden ML, McMillan AMS, Winston GC, Rocha AV, Manies KL, Harden JW, Bond-Lamberty BP (2011) Patterns of NPP, GPP, respiration, and NEP during boreal forest succession. *Global Change Biology*, **17**, 855–871.
- Grace J (1990) Cuticular water loss unlikely to explain tree-line in Scotland. *Oecologia*, **84**, 64–68.

- Granier A, Reichstein M, Bréda N *et al.* (2007) Evidence for soil water control on carbon and water dynamics in European forests during the extremely dry year: 2003. *Agricultural and Forest Meteorology*, **143**, 123–145.
- Grelle A, Lindroth A, Mölder M (1999) Seasonal variation of boreal forest surface conductance and evaporation. *Agricultural and Forest Meteorology*, **99**, 563–578.
- Griffis TJ, Black TA, Morgenstern K *et al.* (2003) Ecophysiological controls on the carbon balances of three southern boreal forests. *Agricultural and Forest Meteorology*, **117**, 53–71.
- Hamada S, Ohta T, Hiyama T, Kuwada T, Takahashi A, Maximov TC (2004) Hydro-meteorological behaviour of pine and larch forests in eastern Siberia. *Hydrological Processes*, **18**, 23–39.
- Hollinger DY, Goltz SM, Davidson EA, Lee JT, Tu K, Valentine HT (1999) Seasonal patterns and environmental control of carbon dioxide and water vapour exchange in an ecotonal boreal forest. *Global Change Biology*, **5**, 891–902.
- Hollinger DY, Aber J, Dail B *et al.* (2004) Spatial and temporal variability in forest-atmosphere CO<sub>2</sub> exchange. *Global Change Biology*, **10**, 1689–1706.
- Hu J, Moore DJP, Riveros-Iregui DA, Burns SP, Monson RK (2010) Modeling whole-tree carbon assimilation rate using observed transpiration rates and needle sugar carbon isotope ratios. *The New Phytologist*, **185**, 1000–1015.
- van Huissteden J, Maximov TC, Dolman A (2005) High methane flux from an arctic floodplain (Indigirka lowlands, eastern Siberia). *Journal of Geophysical Research*, **110**, G02002.
- Jarvis PG (1976) The interpretation of the variations in leaf water potential and stomatal conductance found in canopies in the field. *Philosophical Transactions of the Royal Society of London B, Biological Sciences*, **273**, 593–610.
- Jarvis PG, Massheder JM, Hale SE, Moncrieff JB, Rayment M, Scott SL (1997) Seasonal variation in carbon dioxide, water vapor, and energy exchanges of a boreal black spruce forest. *Journal of Geophysical Research*, **102**, 28953–28966.
- Jasechko S, Sharp ZD, Gibson JJ, Birks SJ, Yi Y, Fawcett PJ (2013) Terrestrial water fluxes dominated by transpiration. *Nature*, **496**, 347–350.
- Jassal RS, Black TA, Spittlehouse DL, Brümmer C, Nesic Z (2009) Evapotranspiration and water use efficiency in different-aged Pacific Northwest Douglas-fir stands. *Agricultural and Forest Meteorology*, **149**, 1168–1178.
- Jung M, Reichstein M, Bondeau A (2009) Towards global empirical upscaling of FLUXNET eddy covariance observations: validation of a model tree ensemble approach using a biosphere model. *Biogeosciences*, **6**, 2001–2013.
- Jung M, Reichstein M, Ciais P *et al.* (2010) Recent decline in the global land evapotranspiration trend due to limited moisture supply. *Nature*, **467**, 951–954.
- Jung M, Reichstein M, Margolis HA *et al.* (2011) Global patterns of land-atmosphere fluxes of carbon dioxide, latent heat, and sensible heat derived from eddy covariance, satellite, and meteorological observations. *Journal of Geophysical Research*, **116**, G00J07.
- Katul GG, Oren R, Manzoni S, Higgins C, Parlange MB (2012) Evapotranspiration: a process driving mass transport and energy exchange in the soil-plant-atmosphere-climate system. *Reviews of Geophysics*, **50**, RG3002.
- Kelliher FM, Leuning R, Raupach MR, Schulze E (1995) Maximum conductances for evaporation vegetation types from global. *Agricultural and Forest Meteorology*, **1923**, 1–16.
- Kelliher FM, Lloyd J, Arneith A *et al.* (1998) Evaporation from a central Siberian pine forest. *Journal of Hydrology*, **205**, 279–296.
- Kettridge N, Thompson DK, Bombonato L, Turetsky MR, Benscoter BW, Waddington JM (2013) The ecohydrology of forested peatlands: simulating the effects of tree shading on moss evaporation and species composition. *Journal of Geophysical Research: Biogeosciences*, **118**, 422–435.
- Kljun AN, Black TA, Griffis TJ *et al.* (2006) Response productivity stands of net of three to ecosystem boreal forest. *Ecosystems*, **9**, 1128–1144.
- Kolari P, Lappalainen HK, Hänninen H, Hari P (2007) Relationship between temperature and the seasonal course of photosynthesis in Scots pine at northern timberline and in southern boreal zone. *Tellus B*, **59**, 542–552.
- Krishnan P, Black TA, Jassal RS, Chen B, Nesic Z (2009) Interannual variability of the carbon balance of three different-aged Douglas-fir stands in the Pacific Northwest. *Journal of Geophysical Research*, **114**, G04011.
- Kurbatova J, Li C, Varlagin A, Xiao X, Vygodskaya N (2008) Modeling carbon dynamics in two adjacent spruce forests with different soil conditions in Russia. *Biogeosciences*, **5**, 969–980.
- Kustas WP, Choudhury BJ, Moran MS, Reginato RJ, Jackson RD, Gay LW, Weaver HL (1989) Determination of sensible heat flux over sparse canopy using thermal infrared data. *Agricultural and Forest Meteorology*, **44**, 197–216.
- Kustas WP, Goodrich DC, Moran MS *et al.* (1991) An Interdisciplinary Field Study of the Energy and Water Fluxes in the Atmosphere-Biosphere System over Semi-arid Rangelands: Description and Some Preliminary Results. *Bulletin of the American Meteorological Society*, **72**, 1683–1705.
- Lagergren F, Lindroth A (2002) Transpiration response to soil moisture in pine and spruce trees in Sweden. *Agricultural and Forest Meteorology*, **112**, 67–85.
- Lagergren F, Lankreier H, Kučera J, Cienciala E, Mölder M, Lindroth A (2008) Thinning effects on pine-spruce forest transpiration in central Sweden. *Forest Ecology and Management*, **255**, 2312–2323.
- Langer M, Westermann S, Muster S, Piel K, Boike J (2011) The surface energy balance of a polygonal tundra site in northern Siberia – Part 2: winter. *The Cryosphere*, **5**, 509–524.
- Launiainen S (2010) Seasonal and inter-annual variability of energy exchange above a boreal Scots pine forest. *Biogeosciences*, **7**, 3921–3940.
- Law BE, Falge E, Gu L *et al.* (2002) Environmental controls over carbon dioxide and water vapor exchange of terrestrial vegetation. *Agricultural and Forest Meteorology*, **113**, 97–120.
- Lecina S, Martínez-Cob A, Pérez PJ, Villalobos FJ, Baselga JJ (2003) Fixed versus variable bulk canopy resistance for reference evapotranspiration estimation using the Penman–Monteith equation under semiarid conditions. *Agricultural Water Management*, **60**, 181–198.
- Leuning R (1995) A critical appraisal of a coupled stomatal–photosynthesis model for C<sub>3</sub> plants. *Plant, Cell and Environment*, **18**, 339–357.
- Leuning R, van Gorsel E, Massman WJ, Isaac PR (2012) Reflections on the surface energy imbalance problem. *Agricultural and Forest Meteorology*, **156**, 65–74.
- Lindroth A, Grelle A, More A (1998) Long-term measurements of boreal forest carbon balance. *Global Change Biology*, **4**, 443–450.
- Lindroth A, Lagergren F, Aurela M *et al.* (2008) Leaf area index is the principal scaling parameter for both gross photosynthesis and ecosystem respiration of Northern deciduous and coniferous forests. *Tellus B*, **60**, 129–142.
- Liu H, Randerson JT, Lindfors J, Chapin FS III (2005) Changes in the surface energy budget after fire in boreal ecosystems of interior Alaska: an annual perspective. *Journal of Geophysical Research*, **110**, D13101.
- Lohila A, Aurela M, Hatakka J, Pihlatie M, Minkkinen K, Penttilä T, Laurila T (2010) Responses of N<sub>2</sub>O fluxes to temperature, water table and N deposition in a northern boreal fen. *European Journal of Soil Science*, **61**, 651–661.
- Lund M, Lindroth A, Christensen TR, Ström L (2007) Annual CO<sub>2</sub> balance of a temperate bog. *Tellus B*, **59**, 804–811.
- Lund M, Lafleur PM, Roulet NT *et al.* (2009) Variability in exchange of CO<sub>2</sub> across 12 northern peatland and tundra sites. *Global Change Biology*, **16**, 2436–2488.
- Mäkelä A, Hari P, Berninger F, Hänninen H, Nikinmaa E (2004) Acclimation of photosynthetic capacity in Scots pine to the annual cycle of temperature. *Tree Physiology*, **24**, 369–376.
- Mäkelä A, Kolari P, Karimäki J, Nikinmaa E, Perämäki M, Hari P (2006) Modelling five years of weather-driven variation of GPP in a boreal forest. *Agricultural and Forest Meteorology*, **139**, 382–398.
- Mäkelä A, Pulkkinen M, Kolari P *et al.* (2008) Developing an empirical model of stand GPP with the LUE approach: analysis of eddy covariance data at five contrasting conifer sites in Europe. *Global Change Biology*, **14**, 92–108.
- Margolis HA, Ryan MG (1997) A physiological basis for biosphere-atmosphere interactions in the boreal forest: an overview. *Tree physiology*, **17**, 491–499.
- McCaughey JH, Pejam MR, Arain MA, Cameron DA (2006) Carbon dioxide and energy fluxes from a boreal mixedwood forest ecosystem in Ontario, Canada. *Agricultural and Forest Meteorology*, **140**, 79–96.
- Merbold L, Kutsch WL, Corradi C *et al.* (2009) Artificial drainage and associated (CO<sub>2</sub>/CH<sub>4</sub>) in a tundra ecosystem. *Global Change Biology*, **15**, 2599–2614.
- Mkhabela MS, Amiro BD, Barr AG *et al.* (2009) Comparison of carbon dynamics and water use efficiency following fire and harvesting in Canadian boreal forests. *Agricultural and Forest Meteorology*, **149**, 783–794.
- Moffat AM, Papale D, Reichstein M *et al.* (2007) Comprehensive comparison of gap-filling techniques for eddy covariance net carbon fluxes. *Agricultural and Forest Meteorology*, **147**, 209–232.
- Mu Q, Zhao M, Running SW (2011) Improvements to a MODIS global terrestrial evapotranspiration algorithm. *Remote Sensing of Environment*, **115**, 1781–1800.
- New M, Lister D, Hulme M, Makin I (2002) A high-resolution data set of surface climate over global land areas. *Climate research*, **21**, 1–25.
- Nordbo A, Launiainen S, Mammarella I, Leppäranta M, Huotari J, Ojala A, Vesala T (2011) Long-term energy flux measurements and energy balance over a small boreal lake using eddy covariance technique. *Journal of Geophysical Research*, **116**, 1–17.
- Ohta T, Maximov TC, Dolman AJ *et al.* (2008) Interannual variation of water balance and summer evapotranspiration in an eastern Siberian larch-forest over a 7-year period (1998–2006). *Agricultural and Forest Meteorology*, **148**, 1941–1953.

- Papaioannou G, Papanikolaou N, Retalis D (1993) Relationships of photosynthetically active radiation and shortwave irradiance. *Theoretical and Applied Climatology*, **48**, 23–27.
- Peichl M, Brodeur JJ, Khomik M, Arain MA (2010) Biometric and eddy-covariance based estimates of carbon fluxes in an age-sequence of temperate pine forests. *Agricultural and Forest Meteorology*, **150**, 952–965.
- Peichl M, Sagerfors J, Lindroth A *et al.* (2013) Energy exchange and water budget partitioning in a boreal minerogenic mire. *Journal of Geophysical Research: Biogeosciences*, **118**, 1–13.
- Penman HL (1948) Natural evaporation from open water, bare soil and grass. *Proceedings of the Royal Society London Academy*, **193**, 120–146.
- Pilegaard K, Hummelshøj P, Jensen N, Chen Z (2001) Two years of continuous CO<sub>2</sub> eddy-flux measurements over a Danish beech forest. *Agricultural and Forest Meteorology*, **107**, 29–41.
- Pilegaard K, Mikkelsen TN, Beier C, Jensen NO, Abmus P, Ro-Poulsen H (2003) Field measurements of atmosphere – biosphere interactions in a Danish beech forest. *Boreal Environment Research*, **8**, 315–333.
- R Core Team (2013) R: A language and environment for statistical computing. R Foundation for Statistical Computing, Vienna, Austria. ISBN 3-900051-07-0. Available at: <http://www.R-project.org/> (accessed 3 January 2013)
- Raulier F, Bernier PY (2000) Predicting the date of leaf emergence for sugar maple across its native range. *Canadian Journal of Forest Research*, **30**, 1429–1435.
- Reichstein M, Falge E, Baldocchi D *et al.* (2005) On the separation of net ecosystem exchange into assimilation and ecosystem respiration: review and improved algorithm. *Global Change Biology*, **11**, 1424–1439.
- Richardson AD, Black TA, Ciais P *et al.* (2010) Influence of spring and autumn phenological transitions on forest ecosystem productivity. *Philosophical Transactions of the Royal Society of London. Series B, Biological Sciences*, **365**, 3227–3246.
- Richardson AD, Anderson RS, Arain MA *et al.* (2012) Terrestrial biosphere models need better representation of vegetation phenology: results from the North American Carbon Program Site Synthesis. *Global Change Biology*, **18**, 566–584.
- Richardson AD, Keenan TE, Migliavacca M, Ryu Y, Sonnentag O, Toomey M (2013) Climate change, phenology, and phenological control of vegetation feedbacks to the climate system. *Agricultural and Forest Meteorology*, **169**, 156–173.
- Rocha AV, Shaver GR (2011) Burn severity influences postfire CO<sub>2</sub> exchange in arctic tundra. *Ecological applications: a publication of the Ecological Society of America*, **21**, 477–489.
- Rouse WR (1984) Microclimate of arctic tree line 2. soil microclimate of tundra and forest. *Water Resources Research*, **20**, 67–73.
- Rouse WR (2000) The energy and water balance of high-latitude wetlands: controls and extrapolation. *Global Change Biology*, **6**, 59–68.
- Running SW (1980) Relating plant capacitance to the water relations of *Pinus contorta*. *Forest Ecology and Management*, **24**, 237–252.
- Sellers PJ, Dickinson RE, Randall DA *et al.* (1997) Modeling the exchanges of energy, water, and carbon between continents and the atmosphere. *Science*, **275**, 502–509.
- Sellers APJ, Bououna L, Collatz GJ *et al.* (2009) Comparison of radiative and physiological effects of doubled atmospheric CO<sub>2</sub> on climate. *Science*, **271**, 1402–1406.
- Sevanto S, Suni T, Pumpanen J *et al.* (2006) Wintertime photosynthesis and water uptake in a boreal forest. *Tree Physiology*, **26**, 749–757.
- Shuttleworth W, Wallace J (1985) Evaporation from sparse crops—an energy combination theory. *Quarterly Journal of the Royal Meteorological Society*, **111**, 839–855.
- Stewart JB (1988) Modelling surface conductance of pine forest. *Agricultural and Forest Meteorology*, **43**, 19–35.
- Stoy PC, Richardson AD, Baldocchi DD *et al.* (2009) Biosphere-atmosphere exchange of CO<sub>2</sub> in relation to climate: a cross-biome analysis across multiple time scales. *Biogeosciences*, **6**, 2297–2312.
- Stoy PC, Mauder M, Foken T *et al.* (2013) A data-driven analysis of energy balance closure across FLUXNET research sites: the role of landscape scale heterogeneity. *Agricultural and Forest Meteorology*, **171–172**, 137–152.
- Suni T, Berninger F, Vesala T *et al.* (2003) Air temperature triggers the recovery of evergreen boreal forest photosynthesis in spring. *Global Change Biology*, **9**, 1410–1426.
- Tanaka H, Hiayama T, Kobayashi N *et al.* (2008) Energy balance and its closure over a young larch forest in eastern Siberia. *Agricultural and Forest Meteorology*, **148**, 1954–1967.
- Tchebakova NM, Kollé O, Zolotoukhine D *et al.* (2002) Inter-annual and seasonal variations of energy and water vapour fluxes above a *Pinus sylvestris* forest in the Siberian middle taiga. *Tellus B*, **54**, 537–551.
- Thum T, Aalto T, Laurila T, Aurela M, Kolari P, Hari P (2007) Parametrization of two photosynthesis models at the canopy scale in a northern boreal Scots pine forest. *Tellus B*, **59**, 874–890.
- Troufleau D, Lhomme JP, Monteny B, Vidal A, Moran MS (1995) Using thermal infrared temperature over sparse semi-arid vegetation for sensible heat flux estimation. In: *Geoscience and Remote Sensing Symposium*, 1995. IGARSS 95. “Quantitative Remote Sensing for Science and Applications”, International, Firenze, Italy (ed. Stein TL), pp. 2227–2229. Institute of Electrical and Electronics Engineers, New York. Available at: <http://ieeexplore.ieee.org/stamp/stamp.jsp?tp=&arnumber=524155&number=11411> (accessed 1 June 2013).
- Urbanski S, Barford C, Wofsy S *et al.* (2007) Factors controlling CO<sub>2</sub> exchange on timescales from hourly to decadal at Harvard Forest. *Journal of Geophysical Research*, **112**, G02020.
- Valiantzas JD (2006) Simplified versions for the Penman evaporation equation using routine weather data. *Journal of Hydrology*, **331**, 690–702.
- Verma SB (1989) Aerodynamic resistances for transfer of mass, heat and momentum. In: *Estimation of Aerial Evapotranspiration* (Proceedings of a workshop held at Vancouver, B.C. Canada, August 1987), IAHS Publication no. 177, 1989 (ed. Black TA), pp. 13–20. IAHS Press, Wallingford.
- Vesala T, Suni T, Rannik U *et al.* (2005) Effect of thinning on surface fluxes in a boreal forest. *Global Biogeochemical Cycles*, **19**, 1–12.
- Walker DA, Jia GJ, Epstein HE *et al.* (2003) Vegetation-soil-thaw-depth relationships along a low-arctic bioclimate gradient, Alaska: synthesis of information from the ATLAS studies. *Permafrost and Periglacial Processes*, **14**, 103–123.
- Wang C, Bond-Lamberty B, Gover ST (2003) Carbon distribution of a well- and poorly-drained black spruce fire chronosequence. *Global Change Biology*, **9**, 1066–1079.
- Wang K, Dickinson RE (2012) A review of global terrestrial evapotranspiration: observation, modeling, climatology, and climatic variability. *Reviews of Geophysics*, **50**, 1–54.
- Weiss A, Norman JM (1985) Partitioning solar radiation into direct and diffuse, visible and near-infrared components. *Agricultural and Forest Meteorology*, **34**, 205–213.
- Wieser G (2000) Seasonal variation of leaf conductance in a subalpine *Pinus cembra* during the winter months. *Phyton - Annales Rei Botanicae*, **40**, 185–190.
- Wilson K, Goldstein A, Falge E *et al.* (2002) Energy balance closure at FLUXNET sites. *Agricultural and Forest Meteorology*, **113**, 223–243.
- Wong SC, Cowan IR, Farquhar GD (1979) Stomatal conductance correlates with photosynthetic capacity. *Nature*, **282**, 424–426.
- Wu A, Black TA, Verseghy DL, Blanken PD, Novak MD, Chen W, Yang PC (2000) A comparison of parameterizations of canopy conductance of aspen and Douglas-fir forests for CLASS. *Atmosphere-Ocean*, **38**, 81–112.
- Wu J, Kutzbach L, Jager D, Wille C, Wilmking M (2010) Evapotranspiration dynamics in a boreal peatland and its impact on the water and energy balance. *Journal of Geophysical Research*, **115**, G04038.
- Yuan F, Arain MA, Barr AG *et al.* (2008) Modeling analysis of primary controls on net ecosystem productivity of seven boreal and temperate coniferous forests across a continental transect. *Global Change Biology*, **14**, 1765–1784.
- Zha T, Barr AG, van der Kamp G, Black TA, McCaughey JH, Flanagan LB (2010) Interannual variation of evapotranspiration from forest and grassland ecosystems in western Canada in relation to drought. *Agricultural and Forest Meteorology*, **150**, 1476–1484.

## Supporting Information

Additional Supporting Information may be found in the online version of this article:

**Appendix S1.** The calibrated best-fit model parameters for the sites used in the study and proportion of explained variance (PR<sup>2</sup>), bias, root-mean-square-error (RMSE) and measured mean (MM) of the model in half hour, daily and monthly time scale. Calibrated model and statistical parameters for different vegetation types are presented in the end of the table (C, cutter/open/burned forest; D, Douglas-Fir; G, grass; L, larch, BD, broadleaf deciduous forest; P, pine; S, spruce; T, tundra; W, wetland/mire/bog). The amount of 30 min data points for the site or ecosystem is reported in the column Rows.



# Surface energy exchange in natural and managed Fennoscandian peatlands

P. Alekseychik<sup>1</sup>, A. Lindroth<sup>3</sup>, I. Mammarella<sup>1</sup>, M. Lund<sup>3,8</sup>, J. Rinne<sup>2</sup>, V. Kasurinen<sup>9</sup>, M. B. Nilsson<sup>4</sup>, M. Pechl<sup>4</sup>, A. Lohila<sup>5</sup>, M. Aurela<sup>5</sup>, T. Laurila<sup>5</sup>, N. Shurpali<sup>6</sup>, E.-S. Tuittila<sup>7</sup>, P. Martikainen<sup>6</sup> and T. Vesala<sup>1</sup>

**Abstract.** The surface energy fluxes were examined at eight northern peatland sites in Finland and Sweden (56°12'–62°11' N, 13°103'–30°05' E) subjected to a varying degree of anthropogenic impact through management. Four sites represent pristine open mires (Siikaneva-1, Siikaneva-2, Degerö Stormyr and Fajemyr), two are peatlands converted to agricultural land or bioenergy crop plantation (Jokioinen and Linnansuo), while Alkka and Kalevansuo are essentially forests growing on drained peat soil. Their energy balances thus possess certain characteristic features, such as specific energy partitioning, different resistance to moisture exchange and response to drying after rain. A clear variation in the energy exchange patterns between peatlands was observed, which correlated with the peatland type and land use at the site. A wide range of site-mean snow-free season values of Bowen ratio (0.27 to 1.28), Priestley-Taylor alpha (0.75 to 1.35), bulk surface conductance (9.9 to 38.7 mm<sup>-1</sup>) and Jarvis-McNaughton decoupling coefficient (0.12 to 0.61) was found. Response to vapor pressure deficit and the seasonality of the energy fluxes and energy partitioning also differed, in correspondence with the site hydrology and the seasonal cycle of vegetation development. Variations in water table level and precipitation played a role in modulating the energy exchange and partitioning. On the basis of the results, three groups of peatland sites possessing unique energy balance characteristics were identified: tree-covered, cropland and treeless pristine. Determining the climatic significance of the energy budgets across this range of peatland classes is a problem demanding further study.

## 1. Introduction

Peatlands occupy a significant fraction of the boreal land area and are susceptible to climate change, to a degree which is still debated [Gorham *et al.*, 1991; Friberg, 2003; Charman *et al.*, 2013]. Prior to management, peatlands represent a variety of ecosystems which is traditionally systematized using the concept of fen-bog gradient [Bridgham *et al.*, 1996]. In addition to the climatic forcing, boreal peatlands experience direct anthropogenic influences including drainage and

peat extraction [Maljanen *et al.*, 2010], with the subsequent establishment of forests [Lohila *et al.*, 2007] or crop plantations [Lohila *et al.*, 2004; Shurpali *et al.*, 2009]. Finland and Sweden together have 45% of the world's forestry-drained peatlands [Minkkinen *et al.*, 2008]. Peatland conversion to agriculture is important as well, affecting about 2% of the combined Finnish and Swedish peatland area [Maljanen *et al.*, 2010].

Upon management/land use change, all biogeochemical functions of peatlands are affected: vegetation, hydrology and peat layer structure become altered, often irreversibly, causing a cascade of derivative effects. One of them, the modification of C-balance, has been thoroughly studied based on both the chamber and eddy-covariance (EC) measurements [Desjardins *et al.*, 2007; Shurpali *et al.*, 2009; Maljanen *et al.*, 2010; Ojanen *et al.*, 2012, 2013; Lohila *et al.*, 2007, 2011; Petrescu *et al.*, 2015]. In studies addressing the peatland CO<sub>2</sub> exchange employing EC technique, the energy balance data in terms of latent and sensible heat fluxes (LE) and (H), net radiation (R<sub>n</sub>) and soil surface heat flux (G) are routinely collected. Despite the availability of such data, the number of studies focused on boreal peatland energy balance is limited [Bridgham *et al.*, 1999; Kurbatova *et al.*, 2002; Lafleur *et al.*, 2005; Pechl *et al.*, 2013; Runkle *et al.*, 2014]. Therefore, one of the aims of this paper is to synthesize the peatland energy balance data measured at several study locations across Fennoscandia.

The scarcity of peatland energy balance studies is regrettable, since the modification in the surface energy balance occurring upon management constitutes another class of climate feedbacks related to energy partitioning and albedo [Eugster *et al.*, 2000], independent of greenhouse gas fluxes. The energy balance is directly related to tree/plant phenology and ecophysiology through transpiration, and to soil hydrology through water table level (WT) affecting both evaporation and transpiration [Kasurinen *et al.*, 2014]. By modifying these crucial processes, management/land use change

<sup>1</sup>Department of Physics, University of Helsinki, PO Box 48, FI-00014 Helsinki, Finland

<sup>2</sup>Department of Geosciences and Geography, University of Helsinki, PO Box 48, FI-00014 Helsinki, Finland

<sup>3</sup>Department of Physical Geography and Ecosystems Science, Lund University, P.O. Box 117, 22100 Lund, Sweden

<sup>4</sup>Department of Forest Ecology and Management, Swedish University of Agricultural Sciences, 901 83 Ume, Sweden

<sup>5</sup>Finnish Meteorological Institute, Atmospheric Composition Research, PO Box 503, 00101 Helsinki, Finland

<sup>6</sup>Department of Environmental Science, University of Eastern Finland, Yliopistonranta 1 E,D, FI-70211 Kuopio, Finland

<sup>7</sup>School of Forest Sciences, University of Eastern Finland, P.O. Box 111, FIN-80101 Joensuu, Finland

<sup>8</sup>Department of Bioscience, Arctic Research Centre, Aarhus University, C.F. Millers All 8, bldg. 1110, DK-8000 Aarhus, Denmark

<sup>9</sup>Department of Forest Sciences, University of Helsinki, P.O. Box 27, FI-00014 Helsinki, Finland

introduces a degree of uncertainty into the future of the ecosystem-climate system. To our knowledge, the energy balances of a range of peatlands, natural and managed, have never been summarized in this context before.

In order to encompass the variation typical of Fennoscandian region, we examined 43 site-years of snow-free period EC and auxiliary data from eight sites representing a gradient from pristine to developed forestry and agricultural and. In the following, as a first approximation, we employ the formal classification of the pristine sites into bogs and fens, and the managed sites into agricultural (cropland) and forestry lands. In understanding the energy balance of a range of these peatlands, we formulated the following hypotheses:

i) Knowledge of management category and fen-bog status can be used to predict the energy balance features of a peatland site. In many peatlands, the management activities have caused them to diverge greatly from the original, natural state. However, since the management is usually limited to either forestry or agricultural uses, it is reasonable to expect close grouping of peatland ecosystems according to the energy exchange rates and partitioning. This would imply that the post-management changes in the energy balance are a direct function of a management/land-use option. For the pristine peatlands, the fen-bog classification has to be accounted for.

ii) Significant differences in the seasonality of energy exchange exist between the peatlands of different management categories and fen-bog classes. Peatland-atmosphere exchange processes are sensitive to temperature [Dorrepaal *et al.*, 2009] and temporal patterns in solar radiation [Loisel and Yu, 2013]. Native vegetation shows a discernible effect on energy exchange in peatlands [Peichl *et al.*, 2013] and in the sites with higher vegetation density, the phenological state of the dominant plants was found to control energy partitioning [Burba *et al.*, 1999; Shurpali *et al.*, 2009]. These drivers, having a clear trend over the growing season, in turn cause a well-pronounced trend in the energy exchange characteristics.

iii) Peatlands of different classes respond differently to water availability (atmospheric vapor pressure deficit (VPD), WT and precipitation). The link between the soil water content and surface conductance [Kurbatova *et al.*, 2002; Raddatz *et al.*, 2009; Sottocornola and Kiely, 2010] makes WT and precipitation important modifiers of evapotranspiration. Being largely waterlogged, pristine peatlands receive an ample supply of water at the surface, which enhances evaporation and thus establishes a close link between the water and energy cycles [Bridgman *et al.*, 1999]. High WT enables evaporation via capillary action [Rouse, 2000; Lafleur *et al.*, 2005]. The ecosystem-atmosphere moisture exchange is therefore less restricted as compared with the boreal conifer forests. The natural, largely treeless peatlands normally demonstrate LE greater or equal than H [Bay, 1961; Kurbatova *et al.*, 2002; Sottocornola and Kiely, 2010; Peichl *et al.*, 2013; Runkle *et al.*, 2014]. However, the phenological behavior and LE has been reported to vary widely in nine boreal biomes including peatlands [Kasurinen *et al.*, 2014]. Temporal variation in ecophysiological response is strongly controlled by VPD fluctuations [Peichl *et al.*, 2013]. WT may act as a strong controller of the energy balance through the supply of water to the surface layers, where it can contribute to LE [Bridgman *et al.*, 1999]. When the vascular vegetation cover is continuous, the WT control might be largely manifested via its effect on bulk surface conductance, as suggested for wetlands of different types by e.g. Acreman *et al.* [2003] and Peichl *et al.* [2013]. However, it should be noted that some studies do not find strong WT effects Sonntag *et al.* [2010]; Sottocornola and Kiely [2010]; Wu *et al.* [2010]; Brümmer *et al.* [2012]; Moore *et al.* [2013]; Runkle *et al.* [2014].

## 2. Material and Methods

### 2.1. Site description

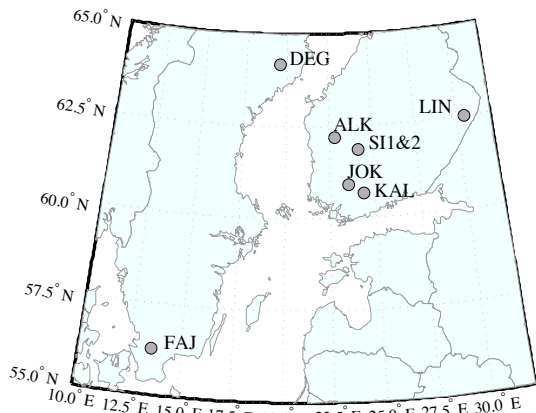


**Figure 1.** Study site locations in Finland and Sweden. The blue and red solid lines show the borders between the mid-boreal, south boreal and hemi-boreal zones

Eight measurement sites in Finland and Sweden were selected (Fig 1). The characteristics of the sites vary, with four being pristine and the other four drained for forestry or crop plantation (see Table 1 for details). The sites are classified as southern boreal, except for Degerö, which is mid-boreal, and hemiboreal Fajemyr. Brief site descriptions are given below.

#### Alkkia (ALK):

In Alkkia, a natural Sphagnum bog was drained in 1936-1938. The site remained in agricultural use until 1969, which involved regular fertilization and soil preparation by introducing mineral soil admixture. In 1971 and 1991, the site was fertilized with phosphorus (P) and potassium (K). Pine forest was then established in 1971 with 3 m to 8 m row spacing, and by the early 2000s the mean tree height had reached 12 m. The site was again fertilized with P and K in 1971 and 1991. Natural growth of birch fills the openings between the pine rows. The measurement station is located on the border between the managed and natural areas. The undisturbed peatland soils lie in the sector 135°-S-270° [Lohila *et al.*, 2007], so, only the data from the managed area sector (°-N°, 20 ha) were accepted for the analyses.

#### bfKalevansuo (KAL):

Originally a dwarf pine-shrub bog, this site was drained in 1969, which enabled tree encroachment. The fetch of the eddy-covariance system was at least 200m in all directions [Lohila *et al.*, 2011]. During the measurements in 2005-2008, the site (65 ha) was covered with a predominantly Scots pine stand averaging 15 m in height. The site is laid out with drainage ditches at approximately 40 m intervals. The forest floor vegetation is dominated by characteristic vascular plants and Sphagnum mosses.

#### Jokioinen (JOK):

This site with peat soil has experienced about a century of

agricultural exploitation. The management history includes the installation of subsurface drainage pipes in 1954 and their maintenance in 1992, when the pipes were re-buried at a greater depth of 0.8-1 m following the peat subsidence in the past years. The water table subsequently fell to about the depth of the drainage pipes. During the measurement period (2000-2003), alternatively barley or forage grass were cultivated at the site [Lohila *et al.*, 2004].

#### Linnansuo (LIN):

After the initial drainage, peat extraction for fuel was carried out at Linnansuo peatland (Eastern Finland) between 1976 and 2001. By the time the peat harvesting ceased, the remaining peat layer was only 20-85 cm deep. Later on, the site was fertilized with nitrogen (N), P and K and used as an experimental plantation of Palaton reed canary grass (RCG). The site was also tilled once, at the beginning of RCG cultivation. Later on, the site was fertilized every year at the rates recommended for regional farming (about 60 Kg N ha<sup>-1</sup>). After the third year of planting, RCG was harvested every year. The mean peak height of the bioenergy crop was 1.7 m in the years 2004-2010 [Shurpali *et al.*, 2009].

#### Degerö Stormyr (DEG):

Degerö Stormyr is an acidic mire system covering 6.5 km<sup>2</sup>, located in the county of Västerbotten, Northern Sweden. The mire complex is comprised of multiple smaller mires separated by ridges and glacial tills. However, the mire surface within about 100 m around the measurement setup is homogeneous and completely devoid of any microtopographical features. The vegetation consists of various sedge, shrub and moss species characteristic of carpet and lawn communities [Yurova *et al.*, 2007; Sagerfors *et al.*, 2008; Peichl *et al.*, 2013].

#### Siikaneva-1 (SI1):

Siikaneva is the largest natural peatland in Southern Finland. Its structure is complex and areas of various trophic levels are represented, but the first measurement site was established in the fen area of the peatland in 2004 [Aurela, Mika, Laurila, Tuomas, Tuovinen, 2004; Rinne *et al.*, 2007]. The distribution of microforms is rather uniform within at least 200m around the station location; microtopographic features, such as strings/hollows, are sparse in the vicinity of the measurement location. The vegetation is dominated by typical peatland mosses and sedges [Riutta *et al.*, 2007; Rinne *et al.*, 2007].

#### Siikaneva-2 (SI2):

A new station was established in 2011 just 1.2 km NW of Siikaneva-1. Over this relatively short distance, a complete transition from fen- to bog-type mire occurs. Typical bog features, such as a higher amplitude of the hollow-hummock microtopographical variation, a denser cover of shrubs, and a frequent occurrence of degrading mud-bottom microsites set Siikaneva-2 apart from Siikaneva-1. Small, isolated Scots pine trees populate the strings.

#### Fajemyr (FAJ):

Southern Swedish peatland Fjemyr is a natural, well-developed eccentric bog, therefore, water level is relatively low compared with the other natural peatlands in this study. So far, the only external influence in the area has been the N deposition of anthropogenic origin. The site features a well-developed microtopography of hummocks, carpets and lawns, while hollows are less common [Lund *et al.*, 2007]. The site is vegetated with a mixture of dwarf shrubs, Sphagnum mosses and sedges, with a sparse tree cover formed by dwarf pine (which is notably more dense, than in Siikaneva-2).

## 2.2. Measurements

All the sites in this study were equipped with Rn sensors and EC setups to measure LE and SH. The auxiliary

**Table 1.** Tab2

Site	EC height (m)	Accepted WD (°)	u* threshold (ms <sup>-1</sup> )	Data coverage (%)
ALK	18	270-N-135	0.2a	30
KAL	17.5/21.5	all	0.1b	69
LIN	3.7	140-S-310	0.1c	30
JOK	3	all	0.1d	56
DEG	1.8	all	0.1e	80
FAJ	3.4	all	0.1f	82
SI1	2.5	50-S-280	0.1g	65
SI2	2.5	100-S-340	0.085h	36

measurements included air temperature and relative humidity (Ta, RH), peat temperature (Tp) profiles at 3-8 depths, precipitation intensity, WT and the wind parameters (wind speed U wind direction WD and friction velocity u\*). All measured data have a 30 min resolution. The micrometeorological characteristics of the sites are given in Table 2. The measurements made during the periods of low turbulence were removed from the analyses using the u\* filtering method. The u\* threshold values were adopted from the earlier studies or (for SI2) derived as the u\* value at which nocturnal respiration reaches saturation [Papale *et al.*, 2006], assuming that at low mixing, both the measured fluxes of matter and energy are not representative of the surface exchange. Furthermore, in four sites the EC fluxes and derived quantities were only accepted from within certain wind sectors in order to avoid the effects of flow distortion due to the presence of the mast or unrepresentative areas of the EC footprint (Table 2). Only the snow-free season data were selected for the analyses, which typically lasts from late April until October in most of the study sites except for FAJ, where the winter snow-cover is discontinuous and only occasional between November and February. Ultimately, the coverage of the quality-controlled data available for the analyses was 30-82%. Local winter time is used for each site. For the details on instrumentation setups and raw data treatment, refer to the publications listed in Table 1.

## 2.3. Energy flux gap-filling

The daytime LE and H were gapfilled with the model values estimated from linear regressions against Rn constructed in a moving time-window of 30 days. The Rn range available within a time window was divided into 4 equal-sized bins, which proved to yield reliable linear regressions, and the linear fitting was performed to the corresponding bin-averages. The nighttime fluxes were gap-filled with the mean good-quality nocturnal flux value in the moving window, as it proved difficult to formulate more detailed statistical models for the nocturnal fluxes. When Rn was not available for a particular 30min period and/or fitting was not feasible due to the lack of data, the lookup table method was used. Rn was itself gapfilled using the mean diurnal variation method and/or lookup tables, depending on data availability [Falge *et al.*, 2001]. The gap-filled energy fluxes were used only for the derivation of the cumulative fluxes and the other long-term mean parameter values (see section 3.5 and Table 3 therein); for the other purposes, the filtered and quality-controlled original data were used.

## 2.4. Storage change fluxes

The change in Ta and water vapor content of the air column were used to compute the sensible (SH) and latent (SLE) heat storage change fluxes [Haverd *et al.*, 2007]:

$$S_H = \int_o^{z_{EC}} \rho C_p \frac{dT_a}{dt} dz \approx \sum_{i=1}^n \left( \rho C_p \frac{\Delta T_a}{\Delta t} \Delta z_i \right) \quad (1)$$

**Table 2.** Measurement site characteristics

Site Code	Latitude	Longitude	Period	Management	Peat depth (m)	Water level	Biomass	LAI	Ref.
ALK	62.2 N	22.8 E	2002-2004	drained for agriculture	1.56	-48	6.40 <sup>a</sup>	1.6/2.0 <sup>b</sup>	<sup>n</sup>
KAL	60.6 N	24.3 E	2005-2008	drained for forestry	1.3-3, 2.2 mean	-32	6.60 <sup>a</sup>	5.0/0.6 <sup>c</sup>	<sup>o</sup>
JOK	60.9 N	23.5 E	2000-2003	agricultural field	0.5-0.6	-80 <sup>d</sup>	0.34-0.45 <sup>e</sup>	0.5-5.0 <sup>f</sup>	<sup>p</sup>
LIN	62.5 N	30.5 E	2004-2010	peat extraction, plantation	0.2-0.85	-61	1.49 <sup>g</sup>	2.5	<sup>q</sup>
DEG	64.2 N	19.5 E	2001-2010	pristine fen	3-4	-12	0.14;	0.8 <sup>h</sup>	<sup>r</sup>
SI1	61.8 N	24.2 E	2005-2012	pristine fen	4 <sup>i</sup>	-6	0.25;	0.4 <sup>j</sup>	<sup>s</sup>
SI2	61.8 N	24.2 E	2011-2013	pristine bog	5-6i	-9	0.11 <sup>k</sup>	0.188 <sup>k</sup>	
FAJ	56.2 N	13.5 E	2006-2009	pristine eccentric bog	4-5	-24 <sup>l</sup>	0.70 <sup>m</sup>		<sup>t</sup>

<sup>a</sup> LAI: leaf area index. All the given values are snow-free season averages.

<sup>b</sup> Scots pine stand LAI/ forest floor LAI [Lohila et al., 2007]

<sup>c</sup> all-sided for Scots pine/ one-sided for moss layer [Lohila et al., 2011].

<sup>d</sup> an estimate based on the depth of the drainage pipes, A. Lohila, personal communication

<sup>e</sup> mean values for forage grass and barley, respectively

<sup>f</sup> typical range in summer; rapid crop growth and varying harvest times create a lot of variation [Lohila et al., 2004]

<sup>g</sup> mean value of the intermediate-wetness plots [Shurpali et al., 2009]

<sup>h</sup> summer peak total LAI, M. Peichl, personal communication and Peichl et al., 2015.

<sup>i</sup> P. Mathijssen, personal communication

<sup>j</sup> one-sided LAI [Riutta et al., 2007]

<sup>k</sup> A. Korrensalo, personal communication.

<sup>l</sup> May-September mean value. The original WT values were corrected by adding -20cm to be more representative of the mean WT within the EC footprint M. Lund, personal communication

<sup>m</sup> approximate value [M. Lund, personal communication].

<sup>n</sup> Lohila et al. [2007]

<sup>o</sup> Lohila et al. [2011]

<sup>p</sup> Lohila et al. [2004]

<sup>q</sup> Shurpali et al. [2009, 2013]

<sup>r</sup> Sagerfors et al. [2008]; Peichl et al. [2013]

<sup>s</sup> Rinne et al. [2007]; Aurela et al. [2007]; Riutta et al. [2007]

<sup>t</sup> Lund et al. [2007, 2009]

$$S_{LE} = \int_0^{z_{EC}} \rho \Lambda \frac{dT_a}{dt} dz \approx \sum_{i=1}^n \left( \rho \Lambda \frac{\Delta \chi H_2O}{\Delta t} \Delta z_i \right) \quad (2)$$

where  $z_{EC}$  is the EC sensor mounting height (m) and  $\chi H_2O$  the atmospheric mixing ratio of water vapor, derived from RH. However, since  $T_a$  and RH were measured at only one level in each site, they had to be adopted as column averages between the ground and  $z_{EC}$ . The biomass heat storage  $S_{bio}$  was calculated using the biomass temperature  $T_{bio}$  following Launiainen [2010]:

$$S_{bio} \approx M_b C_{p,bio} \frac{\Delta T_{bio}}{\Delta t} \quad (3)$$

where  $M_b$  is the mean biomass at the site and  $C_{p,bio}$  the biomass specific heat capacity.  $T_{bio}$  was obtained for the more densely forested sites (ALK, KAL) as  $T_a$  with a phase shift (2 hours) and 1.54 times smaller amplitude (obtained by Launiainen [2010] for the comparable SMEAR-II site, see also Hari et al. [2005]). For the rest of the sites,  $T_{bio} = T_a$  due to the smallness of the vegetation canopy heat capacity. A biomass heat capacity value used by Lindroth et al. [2010],  $C_{p,bio} = 2800 \text{ J kg}^{-1} \text{ K}^{-1}$ , was adopted.

The soil heat storage change flux was calculated from the soil temperature profiles following e.g. [Ochsner et al., 2007] with the parameterization for peat moisture profile from [Yurova et al., 2007]. The flux calculated this way closely approached the storage-corrected heat plate flux (not shown). For consistency, in the following we will use the soil heat flux derived from the peat temperature profile at each site, denoted with  $G$ .

The overall surface energy balance can be expressed as:

$$R_n - G - S = LE + H \quad (4)$$

where  $S$  is the total heat storage change term.

## 2.5. Environmental and ecophysiological parameters

Penman-Monteith potential evapotranspiration was calculated in the form cited by Peichl et al. [2013]:

$$PET = \frac{AE\zeta + (\rho C_p VPD r_a^{-1})}{(\zeta \gamma) \Lambda} \quad (5)$$

where the available energy (AE) equals  $R_n - G$ ,  $\rho$  is the air density ( $\text{kgm}^{-3}$ ),  $C_p$  the air heat capacity at constant pressure ( $\text{Jkg}^{-1}\text{K}^{-1}$ ),  $r_a$  the aerodynamic resistance ( $\text{sm}^{-1}$ ),  $\gamma$  the psychrometric constant ( $\text{kPaK}^{-1}$ ),  $\zeta$  the slope of saturation vapor pressure curve ( $\text{kPaK}^{-1}$ ) and  $\Lambda$  the latent heat of vaporization ( $\text{Jkg}^{-1}$ ).

Aerodynamic resistance was calculated after Verma [1989] as:

$$r_a = \frac{U}{u_*^2} + \frac{kB^{-1}}{ku_*} \quad (6)$$

where  $B^{-1}$  is the dimensionless sublayer Stanton number [Owen and Thomson, 1963]. The second summand on the right-hand side, the excess resistance to water vapor transport, was adopted as equal to 2 in ALK and KAL (assuming they have sufficiently closed canopies, after Garratt and Hicks [1973]), or, otherwise, 3.23 (the value representative of pristine open peatlands, Mölder and Kellner [2002]).

Bulk surface resistance was expressed from the Penman-Monteith equation [Thom, 1975]:

$$r_s = r_a \left( \frac{\zeta}{\gamma \beta} - 1 \right) + \left( \frac{\rho C_p VPD}{\gamma AE} \right) (1 + \beta) \quad (7)$$

where  $\beta$  is the Bowen ratio. Aerodynamic and bulk surface conductances ( $g_a$  and  $g_s$ , correspondingly) are the reciprocals of resistance:  $g_a = r_a^{-1}$ . Only the daytime conductance and resistance values were accepted (9AM-3PM); the periods with  $R_n < 100 \text{ W m}^{-2}$  were rejected to ensure that the challenging twilight conditions are excluded.

Modified Lohammar's function was employed to formalize the dependency of  $g_s$  on VPD [Oren *et al.*, 1999; Launiainen, 2010]:

$$g_{s,mod} = g_1 - m \ln(VPD) \quad (8)$$

where  $g_1$  is the reference conductance at  $VPD = 1 \text{ kPa}$  and  $m$  the sensitivity of  $g_s$  to VPD. The decoupling parameter  $\Omega$  originally proposed by Jarvis and McNaughton [1986] shows the relative role of aerodynamic and surface resistances, which is often interpreted as the degree of ecosystem-atmosphere coupling. [Jarvis and McNaughton, 1986] define it as:

$$\Omega = \frac{\zeta/\gamma + 1}{\zeta/\gamma + 1 + g_a/g_s} \quad (9)$$

In a fully-coupled state,  $g_s < g_a$  and  $\Omega = 0$ ; conversely, in a maximally decoupled state,  $g_s > g_a$  and  $\Omega = 1$ . In the former case, transpiration is constrained and stomatal control is the limiting factor; in the latter case, evaporation is constrained so that available energy becomes the limiting factor.

The  $\alpha_{PT}$  parameter was originally introduced to compensate for the absence of the aerodynamic term in the Priestley-Taylor equation. It was noted that, in general,  $\alpha_{PT}$  is inversely related to bulk surface resistance Pereira [2004]. According to the original definition by Priestley and Taylor [1972],  $\alpha_{PT}$  was derived as:

$$\alpha_{PT} = \frac{LE}{LE + H} \frac{\zeta + \gamma}{\zeta} \quad (10)$$

$\Omega$  and  $\alpha_{PT}$  are only accepted from the daytime period, in order to avoid the complications in their definition arising in twilight and night time.

The evaporative fraction was estimated as the ratio of latent heat flux to available energy:

$$EF = \frac{LE}{AE} \quad (11)$$

### 3. Results

Here, we present the parameters related to the energy balance and ecophysiology that have a common link to the changes in land use and management strategies. We begin with the description of the daily and seasonal cycle in the energy balance components, aiming to elucidate the patterns in energy partitioning. This is followed by the discussion of the controls on evapotranspiration, including VPD, WT and precipitation. The summary of various ecophysiological parameters, presented as averages for each site, concludes the section.

#### 3.1. Environmental conditions

Mean seasonal variation in the main environmental drivers ( $T_{air}$ , WT,  $R_n$  and VPD) is presented in Figure 2.  $T_{air}$  and  $R_n$  values range according to the latitude of the site, as the lower and upper curves are represented by the

DEG and FAJ sites, correspondingly. The seasonal maximum  $T_{air}$  is reached between the days 180-220 (July-August), while most intense sunshine falls between the days 130-200 (May-July). VPD peaks in June-July, too, the level of the mean summertime maxima being from 0.4 kPa to 0.6 kPa. WT varies widely between the pristine and drained peatlands. In the pristine peatlands WT varies between the peat surface and -30cm depth, while in the forested peatlands the variation is typically between -20 to -50 cm, and in the peatland crop plantations at -60 to -80 cm. One common feature, however, is the summertime drawdown of WT in virtually all sites, which starts after snowmelt and continues until the day 230-260 (late August-September).

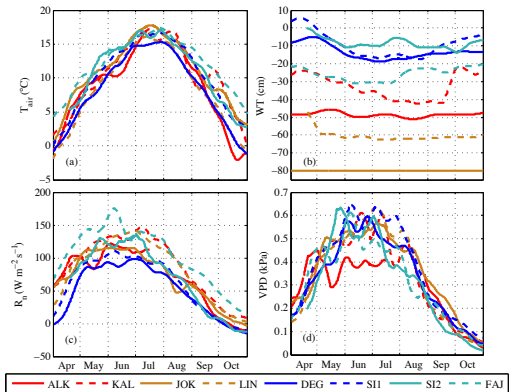


**Figure 2.** Mean seasonal courses of the main driving parameters; (a) air temperature, (b) water table level, (c) net radiation and (d) vapor pressure deficit. The curves have been smoothed with a 7-day moving average filter. Constant WT is shown for JOK, where no systematic WT observations were made; the ALK WT is an interpolant of monthly measurements. Color-coding corresponds to the four peatland site classes (treed in red, croplands in brown, pristine fens in blue and pristine bogs in cyan)

#### 3.2. Diurnal course of the energy balance components

The maximum daily levels of LE were clearly different between the sites (Fig.3a). Note that the site diurnal curves are not in phase due to the slight deviation of the solar noon from midday according to the site local time.

The maximum midday LE varied from  $52 \text{ Wm}^{-2}$  (FAJ) to  $114\text{-}115 \text{ Wm}^{-2}$  (LIN, ALK). The mean diurnal variation of the remaining sites fit well between these lower and upper envelopes. Nocturnal LE was generally close to zero. The highest mean diurnal maximum of H was observed at KAL ( $146 \text{ Wm}^{-2}$ ) and the lowest at SI2 ( $47 \text{ Wm}^{-2}$ ; Fig.3b). In three sites (ALK, KAL, FAJ), H was clearly higher than in the rest of the studied peatlands. H was typically negative during the night, with the nocturnal means averaging  $-5 \text{ Wm}^{-2}$  (SI2) to  $-20 \text{ Wm}^{-2}$  (ALK). The hourly mean maxima of  $R_n$  reached  $171 \text{ Wm}^{-2}$  at the site with the lowest  $R_n$  (DEG) and  $257 \text{ Wm}^{-2}$  at the site with highest  $R_n$  (KAL); the mean nocturnal minima of  $R_n$  ranged from  $-11$  to  $-43 \text{ Wm}^{-2}$  (FAJ and SI2, correspondingly, Fig.3c).

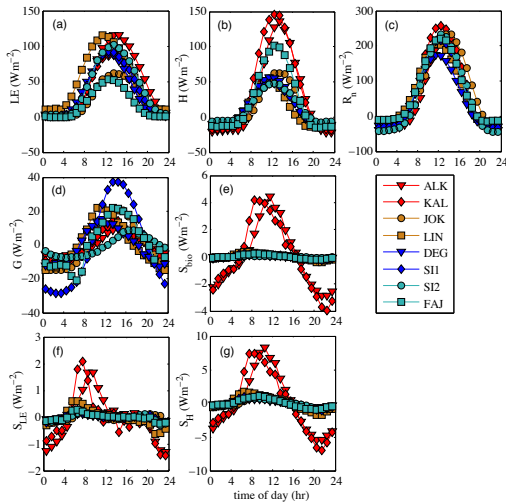


**Figure 3.** Mean snow-free season diurnal curves of (a) LE, (b) H, (c)  $R_n$ , (d) G, (e)  $S_{bio}$ , (f)  $S_{LE}$ , (g)  $S_H$ . See the explanation of symbols in the Nomenclature section.

G follows  $R_n$  (Fig. 3c,d) with a lag from 1 to 3 hours that resulted mainly from the absence of the temperature sensors in the first 2-5cm of soil. In SI1 the amplitude of G was the largest, ranging between  $-12$  and  $17.6 \text{ W m}^{-2}$ ; the smallest amplitude was observed in DEG, where the variation was between  $-3$  and  $3.5 \text{ W m}^{-2}$ . The mean atmospheric storage change fluxes of sensible and latent heat and the biomass heat were small at all sites in comparison with the major energy fluxes. The maximal daily mean of  $S_{bio}$ ,  $S_{LE}$  and  $S_H$  equaled approximately 4, 2 and  $8 \text{ W m}^{-2}$ , correspondingly, and were observed in the forested sites ALK and KAL. In comparison, the storage change fluxes in the sites lacking a tall forest canopy were one order of magnitude smaller (Fig.3e,f,g).

### 3.3. Seasonality of energy partitioning

Three open mires (DEG, SI1, SI2) showed nearly constant summertime  $\beta$  (Fig.4a), indicating even partitioning of  $R_n$  into LE and H (Fig.4b,c). On the contrary, the hemiboreal bog FAJ and the four managed sites displayed a wider seasonal amplitude of  $\beta$ . The sites KAL and FAJ might be called the driest for simplicity, as their monthly  $\beta$  start at 4-5 in early spring and then fall off rapidly, reaching the minima of about 1-1.5 by mid-summer. In comparison,  $\beta$  in the wetter open mires of DEG, SI1 and SI2 remained constant at about 0.5 between May and September. These variations in energy partitioning are augmented, in part, by the specific seasonal course of  $R_n$ . In the majority of sites it is in the month of May that  $R_n$  reaches its annual peak; however, insolation remains high until August (Fig.2c). Note also that the H curves form very consistent groups, which include: (1)

ALK, KAL and FAJ; (2) JOK and LIN; (3) SI1, DEG and SI2. LE seasonal curves do not demonstrate such grouping.

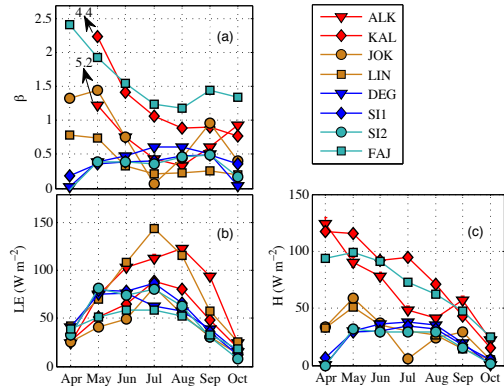


**Figure 4.** Growing season cumulative  $\beta$  (a) and monthly averages of H (b) and LE (c).  $\beta$  was calculated as a ratio of H and LE sums for the respective months. The bars showing standard deviation of the mean are mostly invisible behind the markers.

### 3.4. Evapotranspiration as a function of environmental drivers and management status

$g_s$  as a function of VPD is presented in Fig.5 using both the 30 min average data and the bin-averages across the VPD range. The absolute majority of the  $g_s$  data are under  $60 \text{ mm s}^{-1}$ , although the  $g_s$  range is very site-dependent. The entire range of VPD occurring in the data (up to 3 kPa) is shown, which is typical of Fennoscandian climate. A logarithmic relation between VPD and  $g_s$ , characterized by rapid reduction in  $g_s$  at VPD increasing from 0 to 1 and an asymptotic behavior at higher VPD, was observed at all sites, as elsewhere [Lange *et al.*, 1971; Humphreys *et al.*, 2006; Admiral *et al.*, 2006; Peichl *et al.*, 2013]. The slope of this relation is obviously variable, which is clear from the inter-site range of the m parameter (2.89-16.30). In all cases, the model (Eq.7) fit to the bin-averages describes the observations well (RMSE ranging between 0.3 to 1.8  $\text{mm s}^{-1}$ ) except in JOK, where the observed  $g_s$  exhibited a too steep change with VPD to be reliably captured by the model (RMSE = 3.9  $\text{mm s}^{-1}$ ).

Another mechanism that affects ET in a natural ecosystem is the change in WT. We present this control through the relation between WT and  $\alpha_{PT}$ ,  $\Omega$ ,  $r_a$  and  $r_s$  Fig.6a,b (see Eqs. 5, 6, 8 and 9). For ALK and JOK, the overall means are shown, as those sites lacked continuous high-frequency WT measurements (monthly in ALK). In all sites, the relative importance of surface resistance generally increases as WT falls, which is independently suggested by both  $\alpha_{PT}$  and  $\Omega$ . The slopes are not constant;  $\alpha_{PT}$  and  $\Omega$  show more rapid falloff at initial reduction in WT down to about -20 cm and reach saturation at further WT lowering. FAJ and SI2 curves clearly form a common trend, implying that although their WT ranges almost do not overlap, the ecosystem responses are rather similar in these two bogs. Everywhere except in LIN,  $r_s$  falls off in a logarithmic manner as WT approaches the soil surface (Fig.6c). Certain WT dependency of  $r_a$  can also be seen in SI1, DEG and SI2 (Fig.6d).

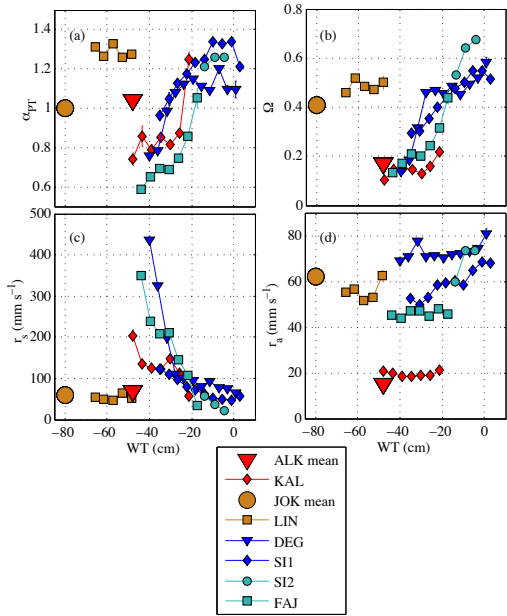


**Figure 6.** WT shown as a driver of (a)  $\alpha_{PT}$ ; (b)  $\Omega$ ; (c)  $r_s$ ; (d)  $r_g$ . The snow-free season data are averaged over WT bins. For ALK and JOK, the overall averages are shown

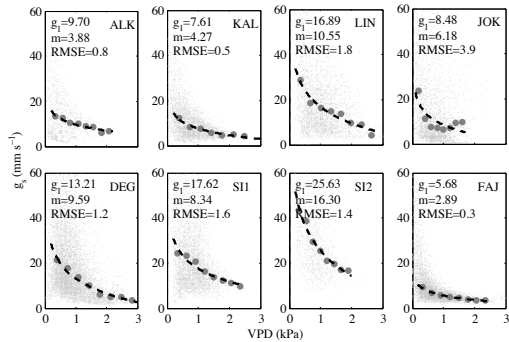


**Figure 5.** Trend in  $g_s$  against VPD, with small dots for the original half-hourly data and big dots for the bin-medians. The thick dash line is the model (Eq.7) fitted to the bin-medians; model parameters and RMSE are shown inside the plots.

Finally, the effect of drying during the rainless periods was considered. We chose to show it as the change in ET/PET,  $\Omega$  and  $\beta$  as a function of time elapsed after the last rain (Fig.7 a-f). The temporal change in the above parameters is ubiquitous, but the rate of this change is very unequal between the sites. The general trend is towards growing surface constraints hence, lower ET, ET/PET and  $\Omega$  mostly decrease with time, while  $\beta$  increases. However,

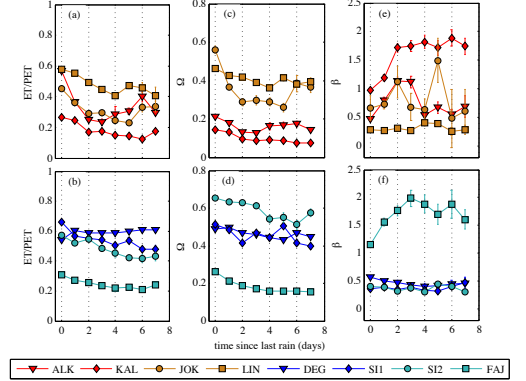


**Figure 7.** Ecophysiological parameters versus time since last rain: ET/PET (a,b),  $\Omega$  (c,d) and  $\beta$  (e,f). The managed and natural sites are shown in separate panels. The datapoints are bin-medians over 1-day intervals. The value at  $x=0$  is the median value during the rain and up to 0.5 days after the rain.

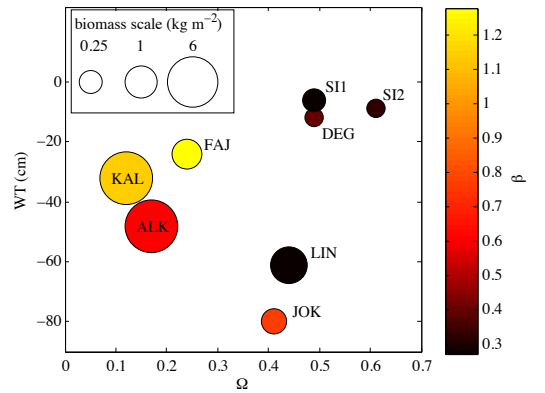


**Figure 8.** Meta-analysis of the mean parameters (WT,  $\Omega$ ,  $\beta$  and aboveground biomass) using the data from Tables 1 and 3

this pertains more to the four managed sites and FAJ, and less to the wetter, open peatland sites SI1, DEG and SI2. The manner of the temporal change differed as well: while SI1, DEG and SI2 exhibited a slow and steady change, in the rest of the sites a saturating trend was present. Indeed, the ecophysiological parameters of ALK, KAL, JOK, LIN and FAJ were changing rapidly until the second, third or fourth day after rain, after which the change slowed down. This dynamics is most readily seen in Fig.7a,c,e,f (except for the ALK and JOK graphs in (e), where the trend remains significant only until day 3).

**Table 3.** Summary of the mean ecophysiological parameters of the examined sites. The range of the mean annual values is given in parentheses

Site	$\beta$	VPD (kPa)	EF	ET (mm day <sup>-1</sup> )	ET/PET	$\alpha_{PT}$	$\Omega$	$g_s$ (mm s <sup>-1</sup> )	$g_a$ (mm s <sup>-1</sup> )
ALK	0.61 (0.46-0.71)	0.32 (0.30-0.33)	0.46 (0.40-0.50)	2.6 (1.5-3.0)	0.48 (0.38-0.52)	1.04 (0.93-1.08)	0.17 (0.14-0.19)	14.3 (11.7-15.6)	66.2 (55.3-69.0)
KAL	1.15 (0.78-1.41)	0.36 (0.20-0.51)	0.34 (0.29-0.44)	1.9 (1.5-2.7)	0.21 (0.13-0.27)	0.75 (0.52-0.89)	0.12 (0.09-0.15)	10.2 (6.3-12.4)	71 (66.3-75.3)
JOK	0.76 (0.46-1.46)	0.46 (0.37-0.59)	0.3 (0.19-0.35)	1.6 (0.8-2.1)	0.36 (0.22-0.41)	1 (0.75-1.10)	0.41 (0.31-0.44)	16.8 (8.2-22.9)	16 (14.5-18.8)
LIN	0.27 (0.06-0.35)	0.52 (0.41-0.73)	0.49 (0.44-0.58)	3.5 (2.8-4.2)	0.72 (0.56-1.04)	1.35 (1.29-1.51)	0.44 (0.38-0.52)	23.6 (16.9-35.8)	23.7 (21.8-25.6)
DEG	0.4 (0.26-0.58)	0.4 (0.27-0.56)	0.47 (0.41-0.55)	2.2 (1.5-2.9)	0.6 (0.42-0.77)	1.16 (0.97-1.34)	0.49 (0.38-0.59)	20.7 (10.4-31.8)	16.6 (16.2-17.3)
SI1	0.28 (0.22-0.31)	0.36 (0.30-0.48)	0.46 (0.42-0.49)	2.1 (1.7-2.9)	0.6 (0.56-0.66)	1.34 (1.23-1.43)	0.49 (0.43-0.60)	25.1 (19.0-34.5)	22.1 (17.1-25.3)
SI2	0.33 (0.32-0.34)	0.37 (0.32-0.49)	0.45 (0.43-0.49)	2.4 (2.1-2.9)	0.59 (0.58-0.6)	1.28 (1.27-1.28)	0.61 (0.56-0.65)	38.7 (29.3-46.2)	19.9 (19.1-20.9)
FAJ	1.28 (1.14-1.37)	0.27 (0.22-0.49)	0.25 (0.23-0.28)	1.1 (1.0-1.2)	0.26 (0.25-0.3)	0.75 (0.73-0.77)	0.24 (0.23-0.26)	9.9 (9.3-10.6)	26.7 (26.1-28.1)

### 3.5. Comparison of the mean ecophysiological parameters

The summary of the various physical and ecophysiological parameters is given in Table 3. The sites differed widely in terms of vegetation canopy height and structure, which is reflected in the range of mean  $g_a$  values. The open natural mires of SI1, SI2 and DEG are tightly clustered together with regard to each parameter. These three sites are characterized by low  $\beta$  and high ET, which correlates with their high surface and aerodynamic conductances. In comparison, tree-covered FAJ is much drier, with its low moisture availability and low conductance resulting in limited ET and, consequently, high  $\beta$ . LIN is at the opposite end of the spectrum; by virtue of its dense graminoid vegetation, LIN supports high ET, and thus low  $\beta$ . In relation to FAJ, all sites except LIN evapotranspire, on average, 50-100% more, and LIN 200% more. The evaporative fraction (EF) values are arranged in the same order, albeit with lower inter-site variability.

ALK, KAL and JOK are not far from the open mires in terms of ET, but impose a tighter control on evapotranspiration in terms of both  $g_s$  and ET/PET. ALK and KAL demonstrate close values, having  $g_s$  of 10.2-14.3  $\text{mm s}^{-1}$ ,  $\Omega$  of 0.12-0.17, ET of 1.9-2.6,  $\beta$  of 0.61-1.15,  $\alpha_{PT}$  of 1.04-0.75. Due to different crop biomass and canopy structure, JOK and LIN are disparate in terms of  $g_s$  (16.8 and 23.6  $\text{mm s}^{-1}$ ), evapotranspiration (1.6 and 3.5  $\text{mm d}^{-1}$ ),  $\alpha_{PT}$  (1.00 and 1.35), and, ultimately,  $\beta$  (0.76 and 0.27), respectively. However, LIN is also much rougher than JOK by virtue of having taller crops, so that their mean  $\Omega$  values are about equal (0.44 and 0.41, correspondingly). According to the mean VPD levels, the air is typically moister in FAJ and drier in JOK and LIN, with the rest of the sites showing intermediate values.

The data presented in Tables 1 and 3 was used to demonstrate the clustering of the sites according to their mean parameters. Fig. 8 shows the relation between a pair of controlling factors (WT and aboveground biomass) and the resulting energy balance features ( $\Omega$  and  $\beta$ ). The sites form 3 clusters: (i) ALK, KAL and FAJ; (ii) LIN and JOK; (iii) SI1, DEG and SI2. The first group unifies the sites having moderate to significant tree biomass, intermediate water level, low  $\Omega$  and high  $\beta$ . The second group has a high graminoid biomass, the lowest water levels, intermediate  $\Omega$ , and low to intermediate  $\beta$ . The last group contains the wettest open mires with small biomass, highest  $\Omega$  and the lowest  $\beta$ .

## 4. Discussion

Management and natural development are the two main reasons that have determined the current ecosystem proper-

ties of the eight examined peatlands. Vegetation, hydrology and soil structure shifts that followed these changes have become reflected in energy partitioning, seasonality of energy fluxes and sensitivity of ET and derivative parameters ( $\Omega$ , ET/PET,  $g_s$ , EF,  $\beta$ ,  $\alpha_{PT}$ ) to environmental forcing. Based on the results, three new ecosystem groups can be introduced that are characterized by notable energy exchange traits: pristine mires (SI1, DEG and SI2), treed peatlands (ALK, KAL and FAJ), and croplands (JOK and LIN).

### 4.1. Pristine open mires: SI1, DEG and SI2

The three pristine mires in this study were characterized by high average water level, continuous, well humidified moss cover and almost complete absence of tree cover. Somewhat surprisingly, although SI2 is formally classified as bog, it clusters closely with the two fen sites in all regards. The two fens, SI1 and DEG and the bog, SI2, fit well in a wide range of values observed elsewhere for pristine mires. The 20.7-38.7  $\text{mm s}^{-1}$  range of  $g_s$  in the open natural mires DEG, SI1 and SI2 falls close to the values from a Danish riparian wetland (32  $\text{mm s}^{-1}$ , *Andersen et al.* [2005]) and a Russian boreal bog (18.6-28  $\text{mm s}^{-1}$ , *Runkle et al.* [2014]). In this study,  $\Omega$  was about 0.5-0.6 at the open mires (DEG, SI1 and SI2); compare with  $\Omega = 0.65-0.73$  obtained by *Runkle et al.* [2014] at a site similar to SI2. *Kurbatova et al.* [2002] obtained an  $\Omega$  of 0.4 at two oligotrophic bogs, and *Brümmer et al.* [2012] estimated  $\Omega \approx 0.29-0.34$  in the bog of Mer Bleu.

High water availability for evapotranspiration grants the natural mires a number of special features. The effects of ET promotion by rain or constraint in the absence of rain might be significant, but remains poorly understood [*Nijp et al.*, 2015]. In this study, resilience, or, at least, a very gradual response to drying after the rain was observed. The absence of rapid change in the evapotranspiration dynamics after the rain in the wet mires DEG, SI1 and SI2 is an illustration of weak initial effect of WT drawdown in the beginning of a rainless period. Moss surfaces may experience high water stress due to Sphagnum intolerance to even partial desiccation [*Gerdol et al.*, 1996], which causes an increase in total resistance to water vapor transport [*Kettridge and Waddington*, 2014]. However, the water is kept in sufficient supply at the surface until WT falls below a certain critical depth [*Humphreys et al.*, 2006], therefore the smooth  $\Omega$  reduction in DEG, SI1 and SI2 is maybe due to the vascular plant stress rather than moss desiccation.

Homeostatic qualities of the wet open mires are also seen on a seasonal scale as the stability of  $\beta$  (Fig. 4); the May-September mean monthly  $\beta$  are close to 0.4-0.6, with a slight

upward trend towards autumn. Similar stable  $\beta$  dynamics were reported for a Southern Finnish fen *Wu et al.* [2010] and a central Siberian bog [*Kurbatova et al.*, 2002], although a much more pronounced increase in  $\beta$  in late growing season was also observed at Mer Bleu bog [*Admiral et al.*, 2006] and in a bog in North-Western Russia [*Runkle et al.*, 2014]. The slight  $\beta$  offset in DEG relative to the similar SI1 and SI2 seems to actually be driven by a reduction of LE in DEG, which becomes apparent in July (Fig.4b).

Apparently, the natural tolerance to drought can be broken when the water table is too low, which can be manifested as a step change in ET. For example, in one drought event of 2006,  $\Omega$  went down steeply in DEG, reflecting a significant increase in  $r_s$  at WT falling below -30 cm (Fig.6). The other sites, having data coverage for that year, did not exhibit a similar step-change. It was shown that WT drawdown to critical depths may cause rapid drying of the peat surface and the eventual formation of crust non-conductive for water transport, with the examples from a blanket bog [*Sottocornola and Kiely*, 2010] and SI2 site (visual observation by the authors). This might be another example of high sensitivity of DEG evapotranspiration to the summertime drawdown of WT, as in the aforementioned extreme example of the 2006 drought.

Similarly, the high water levels might reduce the ecosystem-atmosphere coupling as well, as the dependency of  $r_a$  on WT suggests. The effect was seen in DEG, SI1 and SI2 data (Fig.6d). Aerodynamic resistance increasing together with WT implies diminishing roughness, therefore, it may be the consequence of partial inundation at high water table (i.e. the reduction in roughness due to the appearance and/or area increase of open water pools).

#### 4.2. Tree-covered peatlands: ALK, KAL and FAJ

In ALK and KAL, the tall tree stands are the dominant feature, with a significant biomass contained within the 12-15 m tall pine canopies. The 20-40 cm lowering of WT by drainage has created the conditions suitable for trees. FAJ has reached a state similar to that of KAL, except that its low WT is a natural feature of a raised bog. Tree canopies shelter the ground and so create a specific microclimate, which explains the large differences in the LE, H and biomass heat storage change fluxes compared with the open sites.

The tree-covered peatlands, first of all ALK but also KAL, share the major features ( $\beta$ , ET,  $\alpha_{PT}$ ,  $\Omega$  and a response of  $g_s$  to VPD) with a Finnish boreal Scots pine forest growing on mineral soil [*Launiainen*, 2010]. In turn, FAJ resembles the forested sites. Low  $\Omega$  (0.24) in FAJ approached that of KAL and ALK (0.17 and 0.12, correspondingly). A similar value was observed by Brummer et al. [2012] in a tree-covered fen ( $\Omega = 0.16$  on average). FAJ bulk surface conductance was only 9.9 in the snow-free season, however it is still higher than 6.25  $\text{mms}^{-1}$  reported for the Stormossen bog [*Kellner*, 2001], 4-14  $\text{mms}^{-1}$  in Salmisuo fen [*Wu et al.*, 2010], or even 2.81-4.32 in a Canadian tree-covered fen and the Mer Bleu bog [*Brummer et al.*, 2012]. Generally, ALK, KAL and FAJ occupy the lower end of the mean  $g_s$  range in this study.

In the tree-covered sites, the ET dynamics is largely the product of vegetation response to WT and precipitation. A rapid reduction in actual and relative ET occurs in the first 2-3 days after the rain. On this short time scale, the dominating factor is the physiological reaction of trees increasing VPD, because the corresponding WT drawdown is not yet significant enough to cause water stress for the trees [*Launiainen*, 2010]. Besides, at poor capillary water supply combined with intense water loss at the surface, it is possible that the topsoil dries up within 2 or 3 days. The subsequent stabilization in the environmental parameters implies that

the water supply has been broken, i.e. became decoupled from the surface, and WT does not control the moisture exchange at the surface any more [*Price et al.*, 2003].

More evidence of the water supply breakdown comes from the WT relations in FAJ and KAL, where  $\alpha_{PT}$  is sensitive to the WT deviation from its highest levels, but reach saturation at the low end of the WT range. As in the case of pristine mires, an independent parameter,  $\alpha_{PT}$ , confirms this trend, since higher  $\alpha_{PT}$  is typically accompanied by lower bulk surface resistance (and vice versa; e.g. *Pereira* [2004]). The limit when the ecophysiological state becomes invariant of WT seems to be at -25 to -30cm in KAL and FAJ, correspondingly (Fig.6). Similarly, a laboratory study by *Kettridge and Waddington* [2014] found soil moisture being sustained at -10cm; WT; 0cm, but falling steeply when WT went below that level in vascular plant-free peat cores. Thus, the threshold WT is about the same as in the above group of the open mires, but the frequency of decoupling events is higher owing to the lower mean WT. Besides, the FAJ tree cover might be sparse enough to reduce the overall ET, instead of increasing it - by causing an additional water level drawdown [*Fay and Lavoie*, 2009; *Limpens et al.*, 2014].

$\beta$  in treed peatlands generally exceeded 0.5 and had a strong seasonal cycle, as in the Stormossen bog, where  $\beta$  was found to peak already in May-June and then decrease towards later summer [*Kellner*, 2001]. This seasonal dynamics in energy partitioning goes hand in hand with the stomatal control: reduced to resist the spring stress, then progressively more relaxed during the growing season. Nevertheless, in terms of mean values,  $\beta$  in ALK with LAI=1.6 is about 0.5-1 units lower than that in KAL, which has a LAI of 5.0. The mode of management, i.e. intentional afforestation in ALK versus natural drainage succession in KAL, must be the main source of these differences. In fact, here KAL again bears more similarity with FAJ. This may be interpreted as convergence of management and natural succession: originating as dwarf-shrub bogs, the former had developed a pronounced raised bog topography and a natural pine cover, while the latter acquired a denser pine forest as a result of drainage succession. Both pathways have eventually led to a relatively dry top peat layer and an increased vegetative control on surface conductance, which contribute to higher H at the expense of lower LE. As a side note, lower LE is also supported in FAJ by comparatively low atmospheric demand typical of its moist hemi-boreal/maritime climate.

#### 4.3. Peat croplands: JOK and LIN

The sites of JOK and LIN acquired their ecophysiological features due to the agricultural exploitation. This mode of land use implies a low water level (20-40 cm lower than in the forested sites), and the presence of a homogeneous crop canopy. These common features allow segregation of JOK and LIN from the rest of the study sites based on their mean WT, and the seasonal trend of  $\beta$  (e.g. Fig.8).

However, the similarity is limited due to the very different crop biomass and phenological development; LIN is also the only site in this study where the top peat layer has been removed. Reed canary grass at LIN has a higher biomass, grows rapidly (typically up to 1.7m at the peak), using up more water (in consistency with higher evapotranspiration). Biomass differences and leaf area differences between JOK and LIN are best demonstrated by the mean ET (1.6 and 3.5 mm/d, correspondingly).

The topsoil in LIN may be permanently decoupled from the saturated zone [*Gong et al.*, 2013], which could explain the absence of identifiable trends related to WT. Thus, topsoil wetness in LIN and JOK (also FAJ) might depend on precipitation, which is consistent with rapid surface conductance reduction after the rain (Fig.7). In fact, JOK shows a lower resilience to the rainless conditions than LIN probably

due to the more open crop canopy allowing a more intense drying of the soil.

The agricultural fields develop a dense vegetation cover that reduces  $\beta$  to very low levels, at least from June to August when the crop biomass is at its peak. The intense growth of barley/forage grass in JOK makes up for the lowest monthly  $\beta$  in July, when LAI reaching 5–6 m<sup>2</sup>/m<sup>2</sup> [Lohila *et al.*, 2004] creates the conditions for complete domination of LE and, correspondingly, very low H. This  $\beta$  plunge is followed by a steep increase after the crops are harvested (typically between August–September, occasionally in June). Interannual variations in  $\beta$  demonstrated at this site correlate with the sowing/harvesting times, which varied from year to year. In contrast, LIN retains  $\beta$  of 0.25 also later in the season as canary reed grass is only harvested in the spring of the following year.

## 5. Conclusions

The variety of management/land use strategies practiced at the boreal peatlands has greatly diversified the previously more homogeneous pristine peatlands: vegetation cover, soil and hydrology were affected. While sharing common origins as natural mires, the eight examined ecosystems have diverged into a variety of states following the management and environmental drivers. The sites in this study are representative of the complex mosaic found in contemporary Fennoscandia, featuring natural mires and drained forestry/agricultural peatlands.

It is important to note the wide inter-site variation in the quantities that establish links to climate, such as  $\Omega$  and  $\beta$ . In general, values close to 0.5 at JOK, LIN DEG, SI1 and SI2 indicate intermediate levels of ecosystem-atmosphere coupling, whereas in ALK, KAL and FAJ the domination of stomatal control and low WT support a higher degree of coupling. The mean growing season  $\beta$  was between 0.26 (LIN) and 1.28 (FAJ). This range fits well in the large-scale picture of energy partitioning presented by Wilson *et al.* [2002], where the agriculture-conifer forest continuum had the same typical  $\beta$  values, although that study did not include peatland data. The share of sensible heat, i.e. the dryness of the sites increases along the continuum: (a) pristine open mires (DEG, SI1 and SI2) (b) peat croplands (JOK and LIN) (c) tree-covered peatlands (ALK, KAL and FAJ) Ultimately,  $\Omega$  and  $\beta$  are directly controlled by WT and the dominant vegetation phenology, both subject to drastic changes after land-use changes and management activities. Therefore, the hypothesis (i) proposing the existence of discrete site groups is supported by the results, although in a slightly different form.

Seasonality of the energy balance components and derivative parameters such as  $\beta$  was widely different between the site classes, which confirms the second hypothesis. Responses to the environmental drivers (water level, precipitation, VPD) were very site-specific. High sensitivity to WT changes and the effects of topsoil drying was universal everywhere, except in the sites with low mean WT. The reaction to soil moisture changes was manifested in increasing controls on ET with falling WT and increasing VPD; temporal dynamics were illustrated by the increasingly limited ET and bulk surface conductance over the course of a few days after rain. Effectively, this observation confirms the third hypothesis about significant and diverse ecosystem reactions to the water availability.

Thus, despite the perceived diversity of the peatland types, three distinct groups could be identified. Within those groups, the responses to environmental drivers, seasonality, as well as the mean energy balance characteristics were similar. The group of pristine bogs, proposed in the

beginning of this study and supposed to include SI2 and FAJ was disbanded, as those sites appeared to rather belong to the groups (a) and (b), correspondingly. In the view of these findings, we may conclude that the energy balance modification through anthropogenic impacts on mires is significant, and the innate ecological diversity of mires only adds to the complexity of the picture. The range of climatic feedbacks emerging from the diversity of the peatland energy balances remains to be explored in more detail.

**Acknowledgments.** The authors gratefully acknowledge: the Academy of Finland Centre of Excellence (project No. 272041 and 118780) and Academy Professor projects (No. 1284701 and 1282842), ICOS (project No. 271878), ICOS-Finland (project No. 281255) and ICOS-ERIC (project No. 281250), Nordic Centre of Excellence DEFROST, Faculty of Science and Forestry, University of Eastern Finland, Norwegian University of Technology (NTNU), and the Centre for Studies of Carbon Cycle and Climate Interactions (LUCCI) financed by a Linnaeus grant (Swedish research council). The studies at Deger were financed by Swedish Research Council for Environment, Agricultural Sciences and Spatial Planning (grant no. 2007-666), the Kempe Foundation and Swedish University of Agricultural Sciences through the Long Term Environmental Monitoring program. The measurement data used in this study is available on request from the authors.

## References

- Acreman, M. C., R. J. Harding, C. R. Lloyd, and D. D. McNeil (2003), Evaporation characteristics of wetlands: experience from a wetgrassland and a reedbed using eddy correlation measurements, *Hydrology and Earth System Sciences*, 7(1), 11–21, doi:10.5194/hess-7-11-2003.
- Admiral, S. W., P. M. Lafleur, and N. T. Roulet (2006), Controls on latent heat flux and energy partitioning at a peat bog in eastern Canada, *Agricultural and Forest Meteorology*, 140(1–4), 308–321, doi:10.1016/j.agrformet.2006.03.017.
- Andersen, H. E., S. Hansen, and H. E. Jensen (2005), Evapotranspiration from a riparian fen wetland, *Hydrology Research*, 36(2), 121–135.
- Aurela, M., T. Riutta, T. Laurila, J. P. Tuovinen, T. Vesala, E. S. Tuittila, J. Rinne, S. Haapanala, and J. Laine (2007), CO<sub>2</sub> exchange of a sedge fen in southern Finland - The impact of a drought period, *Tellus, Series B: Chemical and Physical Meteorology*, 59(5), 826–837, doi:10.1111/j.1600-0889.2007.00309.x.
- Aurela, Mika, Laurila, Tuomas, Tuovinen, J.-P. (2004), The timing of snow melt controls the annual CO<sub>2</sub> balance in a sub-arctic fen, *Geophysical Research Letters*, 31(16), L16,119, doi: 10.1029/2004GL020315.
- Bay, R. R. (1961), The Hydrology of Several Peat Deposits in Northern Minnesota, U. S. A., in *Proceedings of the third international peat congress. Quebec, Canada*, pp. 212–218, Natural Resources Council Canada.
- Bridgman, S. D., J. Pastor, J. A. Janssens, C. Chapin, and T. J. Malterer (1996), Multiple limiting gradients in peatlands: A call for a new paradigm, *Wetlands*, 16(1), 45–65, doi:10.1007/BF03160645.
- Bridgman, S. D., J. Pastor, K. Updegraff, T. J. Malterer, N. Nov, C. A. L. Harth, and J. Chen (1999), Ecosystem Control over Temperature and Energy Flux in Northern Peatlands, *Ecological Applications*, 9(4), 1345–1358.
- Brümmer, C., et al. (2012), How climate and vegetation type influence evapotranspiration and water use efficiency in Canadian forest, peatland and grassland ecosystems, *Agricultural and Forest Meteorology*, 153, 14–30, doi: 10.1016/j.agrformet.2011.04.008.
- Burba, G. G., S. B. S. Verma, and J. Kim (1999), A comparative study of surface energy fluxes of three communities (Phragmites australis, Scirpus acutus, and open water) in a prairie wetland ecosystem, *Wetlands*, 19(2), 451–457, doi: 10.1007/BF03161776.
- Charman, D. J., et al. (2013), Climate-related changes in peatland carbon accumulation during the last millennium, *Biogeosciences*, 10(2), 929–944, doi:10.5194/bg-10-929-2013.

- Desjardins, R. L., M. V. K. Sivakumar, and C. de Kimpe (2007), The contribution of agriculture to the state of climate: Workshop summary and recommendations, *Agricultural and Forest Meteorology*, 142(24), 314–324, doi: <http://dx.doi.org/10.1016/j.agrformet.2006.07.011>.
- Dorrepaal, E., et al. (2009), Carbon respiration from subsurface peat accelerated by climate warming in the subarctic, *Nature*, 460(7255), 616–619, doi:10.1038/nature08216.
- Eugster, W., W. R. Rouse, R. A. P. Sr, J. P. Mcfadden, D. D. Baldocchi, T. G. F. Kittel, F. S. I. Chapin, G. E. Liston, and P. L. Vidale (2000), Land-atmosphere energy exchange in Arctic tundra and boreal forest : available data and feedbacks to climate, *Global Change Biology*, 6, 84–115, doi:10.1046/j.1365-2486.2000.06015.x.
- Falge, E., et al. (2001), Gap filling strategies for long term energy flux data sets, *Agricultural and Forest Meteorology*, 107, 71–77.
- Fay, E., and C. Lavoie (2009), The impact of birch seedlings on evapotranspiration from a mined peatland: an experimental study in southern Quebec, Canada, *Mires and Peat*, 5, 1–7.
- Friborg, T. (2003), Siberian wetlands: Where a sink is a source, *Geophysical Research Letters*, 30(21), 1999–2002, doi:10.1029/2003GL017797.
- Garratt, J. R., and B. B. Hicks (1973), Momentum, heat and water vapour transfer to and from natural and artificial surfaces, *Quarterly Journal of the Royal Meteorological Society*, 99(422), 680–687, doi:10.1002/qj.49709942209.
- Gerdol, R., A. Bonora, R. Gualandri, and S. Pancaldi (1996), CO<sub>2</sub> exchange, photosynthetic pigment composition, and cell ultrastructure of Sphagnum mosses during dehydration and subsequent rehydration, *Canadian Journal of Botany*, 74(5), 726–734, doi:10.1139/b96-091.
- Gong, J., N. J. Shurpali, S. Kellomäki, K. Wang, C. Zhang, M. M. A. Salam, and P. J. Martikainen (2013), High sensitivity of peat moisture content to seasonal climate in a cutaway peatland cultivated with a perennial crop (*Phalaris arundinacea*, L.): A modelling study, *Agricultural and Forest Meteorology*, 180, 225–235, doi:10.1016/j.agrformet.2013.06.012.
- Gorham, E., S. E. Applications, and N. May (1991), Northern Peatlands: Role in the Carbon Cycle and Probable Responses to Climatic Warming, *Ecological Applications*, 1(2), 182–195.
- Hari, P., E. Nikinmaa, T. Pohja, E. Siivola, J. Bäck, T. Vesala, and M. Kulmala (2005), Station for measuring ecosystem-atmosphere relations: SMEAR, *Physical and Physiological Forest Ecology*, 9789400756(October), 471–487, doi:10.1007/978-94-007-5603-8\_9.
- Haverd, V., M. Cuntz, R. Leuning, and H. Keith (2007), Air and biomass heat storage fluxes in a forest canopy: Calculation within a soil vegetation atmosphere transfer model, *Agricultural and Forest Meteorology*, 147(34), 125–139, doi: <http://dx.doi.org/10.1016/j.agrformet.2007.07.006>.
- Humphreys, E. R., P. M. Laffeur, L. B. Flanagan, N. Hedstrom, K. H. Syed, A. J. Glenn, and R. Granger (2006), Summer carbon dioxide and water vapor fluxes across a range of northern peatlands, *Journal of Geophysical Research: Biogeosciences*, 111(4), doi:10.1029/2005JG000111.
- Jarvis, P. G., and K. G. McNaughton (1986), Stomatal Control of Transpiration: Scaling Up from Leaf to Region, in *Advances in Ecological Research, Advances in Ecological Research*, vol. 15, edited by A. MacFadyen and E. D. Ford, pp. 1–49, Academic Press, doi:[http://dx.doi.org/10.1016/S0065-2504\(08\)60119-1](http://dx.doi.org/10.1016/S0065-2504(08)60119-1).
- Kasurinen, V., et al. (2014), Latent heat exchange in the boreal and arctic biomes, *Global Change Biology*, 20(11), 3439–3456, doi:10.1111/gcb.12640.
- Kellner, E. (2001), Surface Energy Exchange and Hydrology of a Poor Sphagnum Mire, Ph.D. thesis.
- Kettridge, N., and J. M. Waddington (2014), Towards quantifying the negative feedback regulation of peatland evaporation to drought, *Hydrological Processes*, 28(11), 3728–3740, doi:10.1002/hyp.9898.
- Kurbatova, J., A. Arneht, N. N. Vygodskaya, O. Kolle, A. V. Varlargin, I. M. Milyukova, N. M. Tchebakova, and E.-D. Schulze (2002), Comparative ecosystem atmosphere exchange of energy and mass in a European Russian and a central Siberian bog I. Interseasonal and interannual variability of energy and latent heat fluxes during the snowfree period, *Tellus*, pp. 497–513, doi:10.1034/j.1600-0889.2002.01354.x.
- Lafleur, P. M., R. A. Hember, S. W. Admiral, and N. T. Roulet (2005), Annual and seasonal variability in evapotranspiration and water table at a shrub-covered bog in southern Ontario, Canada, *Hydrological Processes*, 19(18), 3533–3550, doi:10.1002/hyp.5842.
- Lange, O. L., R. Lösch, E. D. Schulze, and L. Kappen (1971), Responses of stomata to changes in humidity, *Planta*, 100(1), 76–86, doi:10.1007/BF00386887.
- Launiainen, S. (2010), Seasonal and inter annual variability of energy exchange above a boreal Scots pine forest, *Biogeosciences*, 7(4), 6441–6494, doi:10.5194/bg-7-6441-2010.
- Limpens, J., M. Holmgren, C. M. J. Jacobs, S. E. A. T. M. Van Der Zee, E. Karofeld, and F. Berendse (2014), How does tree density affect water loss of peatlands? A mesocosm experiment, *PLoS ONE*, 9(3), doi:10.1371/journal.pone.0091748.
- Lindroth, a., M. Mölder, and F. Lagergren (2010), Heat storage in forest biomass improves energy balance closure, *Biogeosciences*, 7(1), 301–313, doi:10.5194/bg-7-301-2010.
- Lohila, A., M. Aurela, J. P. Tuovinen, and T. Laurila (2004), Annual CO<sub>2</sub> exchange of a peat field growing spring barley or perennial forage grass, *Journal of Geophysical Research Atmospheres*, 109(18), 1–13, doi:10.1029/2004JD004715.
- Lohila, A., M. Aurela, K. Regina, J. P. Tuovinen, and T. Laurila (2007), Wintertime CO<sub>2</sub> exchange in a boreal agricultural peat soil, *Tellus, Series B: Chemical and Physical Meteorology*, 59(5), 860–873, doi:10.1111/j.1600-0889.2007.00314.x.
- Lohila, A., K. Minkkinen, M. Aurela, J. P. Tuovinen, T. Penttilä, P. Ojanen, and T. Laurila (2011), Greenhouse gas flux measurements in a forestry-drained peatland indicate a large carbon sink, *Biogeosciences*, 8(11), 3203–3218, doi:10.5194/bg-8-3203-2011.
- Loisel, J., and Z. Yu (2013), Recent acceleration of carbon accumulation in a boreal peatland, south central Alaska, *Journal of Geophysical Research: Biogeosciences*, 118(1), 41–53, doi:10.1029/2012JG001978.
- Lund, M., A. Lindroth, T. R. Christensen, and L. Ström (2007), Annual CO<sub>2</sub> balance of a temperate bog, *Tellus B*, 59(5), 804–811, doi:10.1111/j.1600-0889.2007.00303.x.
- Lund, M., T. R. Christensen, M. Mastepanov, a. Lindroth, and L. Ström (2009), Effects of N and P fertilization on the greenhouse gas exchange in two northern peatlands with contrasting N deposition rates, *Biogeosciences*, 6(10), 2135–2144, doi:10.5194/bg-6-2135-2009.
- Maljanen, M., B. D. Sigurdsson, J. Guömundsson, H. Öskarsson, J. T. Huttunen, and P. J. Martikainen (2010), Greenhouse gas balances of managed peatlands in the Nordic countries present knowledge and gaps, *Biogeosciences*, 7(9), 2711–2738, doi:10.5194/bg-7-2711-2010.
- Minkkinen, K., K. A. Byrne, and C. C. Trettin (2008), *Climate Impacts of Peatland Forestry*, 98–122 pp., International Peat Society, Jyväskylä.
- Mölder, M., and E. Kellner (2002), Excess resistance of bog surfaces in central Sweden, *Agricultural and Forest Meteorology*, 112(1), 23–30, doi:10.1016/S0168-1923(02)00043-6.
- Moore, P. A., T. G. Pypker, and J. M. Waddington (2013), Effect of long-term water table manipulation on peatland evapotranspiration, *Agricultural and Forest Meteorology*, 178–179, 106–119, doi:10.1016/j.agrformet.2013.04.013.
- Nijp, J. J., J. Limpens, K. Metselaar, M. Peichl, M. B. Nilsson, S. E. A. T. M. van der Zee, and F. Berendse (2015), Rain events decrease boreal peatland net CO<sub>2</sub> uptake through reduced light availability, *Global Change Biology*, 21(6), 2309–2320, doi:10.1111/gcb.12864.
- Ochsner, T. E., T. J. Sauer, and R. Horton (2007), Soil Heat Storage Measurements in Energy Balance Studies Supported in part by the Iowa State Univ. Agronomy Dep. Endowment Funds. Mention of trade names or commercial products in this article is solely for the purpose of providing specific information and does not imply recommendation or endorsement by the USDA. , *Agronomy Journal*, 99, doi:10.2134/agronj2005.0103S.
- Ojanen, P., K. Minkkinen, A. Lohila, T. Badorek, and T. Penttilä (2012), Chamber measured soil respiration: A useful tool for estimating the carbon balance of peatland forest soils?, *Forest Ecology and Management*, 277, 132–140, doi:10.1016/j.foreco.2012.04.027.
- Ojanen, P., K. Minkkinen, and T. Penttilä (2013), The current greenhouse gas impact of forestry-drained boreal peatlands, *Forest Ecology and Management*, 289, 201–208, doi:10.1016/j.foreco.2012.10.008.

- Oren, R., J. Sperry, G. Katul, D. Pataki, B. Ewers, N. Phillips, and K. Schäfer (1999), Survey and synthesis of intra- and interspecific variation in stomatal sensitivity to vapour pressure deficit, *Plant, Cell & Environment*, 22(12), 1515–1526, doi:10.1046/j.1365-3040.1999.00513.x.
- Owen, P. R., and W. R. Thomson (1963), Heat transfer across rough surfaces, *Journal of Fluid Mechanics*, 15(03), 321–334, doi:10.1017/S0022112063000288.
- Papale, D., et al. (2006), Towards a standardized processing of Net Ecosystem Exchange measured with eddy covariance technique: algorithms and uncertainty estimation, *Biogeosciences*, 3(4), 571–583, doi:10.5194/bg-3-571-2006.
- Peichl, M., J. Sagerfors, A. Lindroth, I. Buffam, A. Grelle, L. Klemedtsson, H. Laudon, and M. B. Nilsson (2013), Energy exchange and water budget partitioning in a boreal minerogenic mire, *Journal of Geophysical Research: Biogeosciences*, 118(1), 1–13, doi:10.1029/2012JG002073.
- Pereira, A. R. (2004), The Priestley-Taylor parameter and the decoupling factor for estimating reference evapotranspiration, *Agricultural and Forest Meteorology*, 125(3-4), 305–313, doi:10.1016/j.agrformet.2004.04.002.
- Petrescu, A. M. R., et al. (2015), The uncertain climate footprint of wetlands under human pressure., *Proceedings of the National Academy of Sciences of the United States of America*, 112(15), 4594–9, doi:10.1073/pnas.1416267112.
- Price, J. S., A. L. Heathwaite, and A. J. Baird (2003), Hydrological processes in abandoned and restored peatlands: An overview of management approaches, *Wetlands Ecology and Management*, 11(1), 65–83, doi:10.1023/A:1022046409485.
- Priestley, C. H. B., and R. J. Taylor (1972), On the Assessment of Surface Heat Flux and Evaporation Using Large-Scale Parameters, *Monthly Weather Review*, 100(2), 81–92, doi:10.1175/1520-0493(1972)100<0081:OTAOSH>2.3.CO;2.
- Raddatz, R. L., T. N. Papakyriakou, K. A. Swystun, and M. Tenuta (2009), Evapotranspiration from a wetland tundra sedge fen: Surface resistance of peat for land-surface schemes, *Agricultural and Forest Meteorology*, 149(5), 851–861, doi:10.1016/j.agrformet.2008.11.003.
- Rinne, J., T. Riutta, M. Pihlatie, M. Aurela, S. Haapanala, J. P. Tuovinen, E. S. Tuittila, and T. Vesala (2007), Annual cycle of methane emission from a boreal fen measured by the eddy covariance technique, *Tellus, Series B: Chemical and Physical Meteorology*, 59(3), 449–457, doi:10.1111/j.1600-0889.2007.00261.x.
- Riutta, T., J. Laine, M. Aurela, J. Rinne, T. Vesala, T. Laurila, S. Haapanala, M. Pihlatie, and E. S. Tuittila (2007), Spatial variation in plant community functions regulates carbon gas dynamics in a boreal fen ecosystem, *Tellus, Series B: Chemical and Physical Meteorology*, 59(5), 838–852, doi:10.1111/j.1600-0889.2007.00302.x.
- Rouse, W. R. (2000), The energy and water balance of high-latitude wetlands: controls and extrapolation, *Global Change Biology*, 6(S1), 59–68, doi:10.1046/j.1365-2486.2000.06013.x.
- Runkle, B. R. K., C. Wille, M. Gazovic, M. Wilmking, and L. Kutzbach (2014), The surface energy balance and its drivers in a boreal peatland fen of northwestern Russia, *Journal of Hydrology*, 511, 359–373, doi:10.1016/j.jhydrol.2014.01.056.
- Sagerfors, J., A. Lindroth, A. Grelle, L. Klemedtsson, P. Weslien, and M. B. Nilsson (2008), Annual CO<sub>2</sub> exchange between a nutrient-poor, minerotrophic, boreal mire and the atmosphere, *Journal of Geophysical Research: Biogeosciences*, 113(1), 1–15, doi:10.1029/2006JD000306.
- Shurpali, N. J., N. P. Hyvönen, J. T. Huttunen, R. J. Clement, M. Reichstein, H. Nykänen, C. Biasi, and P. J. Martikainen (2009), Cultivation of a perennial grass for bioenergy on a boreal organic soil - carbon sink or source?, *GCB Bioenergy*, 1(2009), 35–50, doi:10.1111/j.1757-1707.2009.01003.x.
- Shurpali, N. J., C. Biasi, S. Jokinen, N. Hyvönen, and P. J. Martikainen (2013), Linking water vapor and CO<sub>2</sub> exchange from a perennial bioenergy crop on a drained organic soil in eastern Finland, *Agricultural and Forest Meteorology*, 168, 47–58, doi:10.1016/j.agrformet.2012.08.006.
- Sonnentag, O., G. van der Kamp, A. G. Barr, and J. M. Chen (2010), On the relationship between water table depth and water vapor and carbon dioxide fluxes in a minerotrophic fen, *Global Change Biology*, 16(6), 1762–1776, doi:10.1111/j.1365-2486.2009.02032.x.
- Sottocornola, M., and G. Kiely (2010), Energy fluxes and evaporation mechanisms in an Atlantic blanket bog in southwestern Ireland, *Water Resources Research*, 46(11), 1–13, doi:10.1029/2010WR009078.
- Thom, A. (1975), Momentum; Mass and heat exchange of plant communities, *Vegetation and the Atmosphere*, 1, 57–109, doi:10.1017/S0014479700008607.
- Verma, S. (1989), *Aerodynamic resistances to transfers of heat, mass and momentum in estimation of areal evaporation*, vol. 177.
- Wilson, K. B., et al. (2002), Energy partitioning between latent and sensible heat flux during the warm season at FLUXNET sites, *Water Resources Research*, 38(12), 1–11, doi:10.1029/2001WR000989.
- Wu, J., L. Kutzbach, D. Jager, C. Wille, and M. Wilmking (2010), Evapotranspiration dynamics in a boreal peatland and its impact on the water and energy balance, *Journal of Geophysical Research*, 115(G4), G04,038, doi:10.1029/2009JG001075.
- Yurova, A., A. Wolf, J. Sagerfors, and M. Nilsson (2007), Variations in net ecosystem exchange of carbon dioxide in a boreal mire: Modeling mechanisms linked to water table position, *Journal of Geophysical Research*, 112(2), 1–13, doi:10.1029/2006JG000342.



# MODELING DISSOLVED ORGANIC CARBON TRANSPORT IN BOREAL CATCHMENTS

Ville Kasurinen,<sup>1,2</sup> Knut Alfredsen,<sup>2</sup> Anne Ojala,<sup>1,3</sup> Jukka Pumpanen<sup>1</sup>, Gesa A. Weyhenmeyer<sup>4</sup>, Martyn N. Futter<sup>5</sup>, Hjalmar Laudon<sup>6</sup> and Frank Berninger<sup>1</sup>

**Abstract.** Stream water dissolved organic carbon (DOC) concentrations display high spatial and temporal variation in boreal catchments. Understanding and predicting these patterns is a scientific challenge with great implications for our ability to make water quality projections and carbon balance estimates. Although several biogeochemical models have been used to estimate stream water DOC dynamics, under- or over-predictions are common during both rain and snow melt driven events. Here, we present a parsimonious distributed model, which is capable of predicting stream water DOC concentrations also during these events. The developed model, K-DOC, accounts for catchment water storage and soil temperature dependencies of DOC release and consumption. We used the K-DOC to estimate the stream water DOC concentrations over five years, for eighteen nested boreal catchments. The model successfully simulated DOC concentrations during base flow conditions, as well as, hydrological events in catchments dominated by organic and mineral soils. Our semi-mechanistic model was parsimonious enough to have all parameters estimated using statistical methods. We did not find any clear differences between forest and mire dominated catchments that could be explained by soil type or tree species composition. However, parameters controlling slow release and consumption of DOC from soil water behaved differently for small headwater catchments (less than 2 km<sup>2</sup>) than for those that integrate larger areas of different ecosystem types (10-68 km<sup>2</sup>). Our results emphasize that it is important to account for non-linear dependencies of both, soil temperature and catchment water storage, when simulating DOC dynamics of boreal catchments.

## 1. Introduction

Dissolved organic carbon (DOC) is the most abundant form of organic carbon in boreal surface waters, largely determining the carbon balance and strongly affecting the water quality of freshwater ecosystems [Thackeray, 2014]. DOC constitutes the majority of organic carbon fluxes from terrestrial ecosystems to streams and rivers [Dai et al., 2012] and connects soil organic matter sources (SOM) to carbon cycling and sequestration in aquatic ecosystems [Tranvik et al., 2009; Weyhenmeyer et al., 2012]. The production and transport of DOC from terrestrial ecosystems to streams is largely regulated by physical factors such as precipitation, temperature [Köhler et al., 2009; Öquist et al., 2014] and the characteristics of the terrestrial environment [Moody et al., 2013; Mengistu et al., 2014].

DOC export from ecosystem depend on its production, its consumption and its transport from the watershed [Laudon et al., 2012]. According to recent estimates, the amount of carbon that streams and rivers receive, process and transport is of the same size as the net biome productivity (NBP) suggesting aquatic processes play a significant role in global carbon balance [Aufdenkampe, 2011]. However, the processes regulating the export of DOC are difficult to parametrize, because several concurrent processes control its production and consumption. For example, DOC is often immobilized by iron and aluminum in mineral soils [Clark et al., 2008; Kerr and Eimers, 2012; Pumpanen et al., 2014], which solubilities in turn are regulated by pH [Evans et al., 2008; Worrall et al., 2008], oxygen and water availability [Clark et al., 2005; Hribljan et al., 2014].

Together with microbial activity in soils, these biogeochemical reactions largely determine the behavior of SOM storage and reactions controlling conversion of the stored organic carbon pool in the soil into dissolved fractions. Heterogeneity in land cover causes spatial variability in stream DOC concentrations while rainfall and snow melt events are typically associated with much of the temporal dynamics [Laudon et al., 2011]. Developing parsimonious models capable of capturing this spatial and temporal variability remains one of the greatest challenges in the understanding of DOC in the boreal region.

Stream flow and DOC concentrations have been described in mathematical models that differ conceptually from each other [Boyer et al., 1996; Neff and Asner, 2001; Michalzik et al., 2003; Futter et al., 2007]. Several models have been developed to understand and predict the dynamics of DOC concentrations and export from forest- and mire-dominated landscapes [Futter et al., 2007; Yurova et al., 2008; Jutras et al., 2011; Winterdahl et al., 2011a; Wu et al., 2013; Zhang

<sup>1</sup>University of Helsinki, Department of Forest Sciences, P.O. Box 27, Helsinki, Finland

<sup>2</sup>Norwegian University of Science and Technology, 7491 Trondheim, Norway

<sup>3</sup>University of Helsinki, Department of Environmental Sciences, P.O. Box 65, 00014 Helsinki, Finland

<sup>4</sup>Uppsala University, Department of Ecology and Genetics/Limnology, Norbyvägen 18D, 75236 Uppsala, Sweden

<sup>5</sup>Swedish University of Agricultural Sciences, Department of Aquatic Sciences and Assessment

<sup>6</sup>Swedish University of Agricultural Sciences, Department of Forest Ecology and Management

et al., 2013]. These models differ in their underlying theoretical concepts, their modeling approach, as well as, their predictive power. Typically, previous models have been developed for either a single land cover type [Yurova et al., 2008; Winterdahl et al., 2011b; Zhang et al., 2013] or are using a semi-distributed approach [Futter et al., 2007; Juras et al., 2011]. In a distributed approach, different land cover types in a heterogenic landscape can be parametrized separately.

Usually the hydrological part of the models is using lumped catchment models as HBV [Bergström, 1976, 1992; Killington and Sæthun, 1995] or ForHyM [Balland et al., 2006]. Although, it has been suggested that biogeochemical models tend to be highly parametrized, only few studies have used simplified runoff generation routines for discharge generation [Kirchner, 2009; Xu et al., 2012; Dick et al., 2014]. In a complex model structure, parameter values can be unidentifiable and uncertain since they are based on too few empirical measurements to allow a statistical estimation of parameters. In order to build more robust parsimonious models, there is a need to investigate DOC dynamics on a catchment scale by using physically based, but simplified process models [Dick et al., 2014]. A parsimonious model structure allow parametrization of simple environmental variables that control the DOC release from the soil to stream water [Birkel et al., 2014]. The model of Xu et al. [2012] is an example of such simple parsimonious model of DOC concentrations.

The model of Xu et al. [2012] is based on the simple rainfall-runoff model of Kirchner [2009] to describe discharge and catchment water storage. The hydrological responses are linked to a simple presentation of SOM dynamics that describes equilibrium partitioning of SOM to DOC, slow release of DOC from SOM and consumption of DOC in soil water. The majority of previous models have used soil moisture to predict stream water DOC concentration assuming that it controls conversion of SOM to DOC [Naden et al., 2010]. However, this approach does not take into account that DOC production and DOC release from soil to stream water are not necessarily synchronous. While soil moisture probably governs DOC production from SOM, rapid changes in catchment water storage are more closely related to changes in stream water DOC concentrations.

The original Xu et al. [2012] model was tested only for one temperate forested headwater catchment and applied over short time periods varying from 30 to 60 days. Furthermore, Xu et al. [2012] assumed that SOM conversion to DOC is in an equilibrium with stream water DOC concentrations and does not vary temporally. However, this assumption may not be valid for boreal catchments, where the seasonally varying temperature and snow cover have a fundamental role in controlling stream water DOC concentrations [Futter et al., 2007; Futter and de Wit, 2008; Laudon et al., 2012].

In this study, we modified the model of Xu et al. [2012] so that the slow release of DOC from SOM and consumption of DOC in soil water was dependent on modeled soil temperature and catchment water storage. The new modified model, K-DOC, was tested on eighteen nested boreal streams ranging in size from 0.03 to 68 km<sup>2</sup> over a five- and a ten-year-long simulation period, including approximately 5000 stream samples (for 10-year period). K-DOC was able to predict stream water DOC concentrations better than the models that have previously been used to simulate DOC concentrations for the same catchments. We discuss how our modeling concepts differ from previous work and what are the requirements for parsimonious DOC models.

## 2. Material and Methods

### 2.1. Site description

The Krycklan catchment (64°23N, 19°46E) is located at Svartberget, approximately 50 km northwest of the Baltic sea in northern Sweden (Umeå). Several water quality

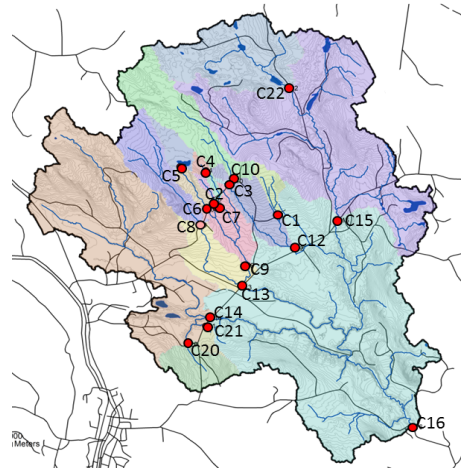


**Figure 1.** Krycklan catchment and measurement stations.

variables, including DOC, as well as, hydrological and meteorological data are monitored at the research catchment as part of the national field research infrastructure (www.fieldsites.se). The Krycklan Catchment Study (KCS) is an interdisciplinary field research site and probably one of the most intensively monitored catchments in the boreal region [Laudon et al., 2013]. The catchment is divided into eighteen partially nested long-term monitored sub-catchments, abbreviated as C1 to C22 (Table 1, Figure 1). Long-term (1981-2010) mean annual precipitation and temperature are 623 mm and +1.7°C respectively [Oni et al., 2014]. Approximately half of the annual precipitation falls as snow, and the catchment is usually snow covered from between October to May [Laudon et al., 2011].

The upper parts of the catchment are dominated by forests that consist mainly of Norway spruce (*Picea abies* (L.) Karst.), Scots pine (*Pinus sylvestris* L.), deciduous species (*Alnus glutinosa* (L.) Gaertn.), (*Betula pendula* Roth) and shrubs [Laudon et al., 2013]. Coniferous trees dominate in the catchment, but deciduous species become more common in the areas close to the stream channels, especially along the larger rivers. The average overall proportion of mires in the catchment is 8% but can reach up to 40% in some small first-order sub-catchments (Table 1). A full description at DOC sampling frequency and analysis are provided by Laudon et al. [2011, 2013] and Oni et al. [2013]. In short, DOC samples were collected from all monitoring stations with up to daily sampling during snow melt in the spring, fortnightly sampling during the snow-free period and monthly during winter base flow.

In this study, DOC-concentrations and hydrology were simulated for all 18 sub-catchments. To simplify the presentation of our results (as done by Laudon et al. [2011]) we selected the catchments C2 representative for fully forested (forest cover 99.9%), C4 as mire dominated (mire cover 44.1%) and C7 (forest cover 82%) and C16 (forest cover 87.2%) as mixed sub-catchments that integrates forest and mire dominated ecosystems for most of our figures (Table 1). We refer to these selected catchments throughout the text. A presentation of all catchments and simulation results for these can be found in the supplementary material.

### 2.2. Hydrological and soil temperature modeling

To generate runoff for all sub-catchments, a daily discharge was modeled by using the fully distributed hydro-

**Table 1.** Catchment characteristics for 18 sub-catchments in Krycklan.

Site code	Station name	Cum. area (km <sup>2</sup> )	Ind. area (km <sup>2</sup> )	Forest (%)	Mire (%)	Lake (%)	Till (%)	Sorted sediments (%)	Tree vol. (m <sup>3</sup> ha <sup>-1</sup> )	Birch (%)	Spruce (%)	Pine (%)	Stand Age (years)
C1	Risbäcken	0.48	0.48	98	2	0	92.1	0	187	2	63	35	87
C2	Västrabäcken	0.12	0.12	99.9	0	0	84.2	0	212	0	36	64	103
C3	Lillmyrbäcken	0.04	0.04	59	40.4	0	43.2	3.7	133	1	5	93	77
C4	Kalkällsmyren	0.18	0.18	55	44.1	0	22	0	83	0	45	55	57
C5	Stortjärnen outlet	0.65	0.65	54	39.5	6.4	40.4	0	64	12	26	62	50
C6	Stortjärnbäcken	1.10	0.44	71.4	24.8	3.8	53.7	0	117	4	26	70	69
C7	Kalkällsbäcken	0.47	0.17	82	18	0	65.2	0	167	1	35	64	86
C8	Fullbäcken	2.30	2.30	88	11.9	0	62.8	0	118	12	20	68	71
C9	Nyängesbäcken	2.88	1.32	84.4	14.1	1.5	69.1	4.1	150	6	29	65	78
C10	Stormyrbäcken	3.36	3.36	73.8	26.1	0	59.9	0.5	93	12	21	68	60
C12	Nymyrbäcken	5.44	1.57	82.6	17.3	0	66.6	5.9	129	8	34	57	72
C13	Långbacken	7.00	1.82	88.2	10.3	0.7	60.9	15.9	145	8	25	68	78
C14	Åhedbacken	14.10	12.39	90.1	5.4	0.7	44.9	38.1	106	10	23	67	62
C15	Övre Krycklan	19.13	14.21	81.6	14.5	2.4	64.8	9.5	85	10	26	64	54
C16	Krycklan	67.90	22.28	87.2	8.7	1	50.8	30.2	106	10	26	63	62
C20	Stormullkälsmyran	1.45	1.45	87.7	9.6	0	45	21.4	59	16	16	68	42
C21	Mullkälen	0.26	0.26	98.9	1	0	52.8	43.8	138	8	10	82	74
C22	Bergtjärn outlet	4.91	4.91	68.3	29	2.6	61.2	0	78	10	22	67	54

logical model ENKI (<http://www.opensource-enki.org>, *Kolberg and Bruland* [2012]; *Hailegeorgis and Alfredsen* [2014]). ENKI is a toolbox that contains several different routines, which allow users to combine various process models to simulate catchment hydrology. The ENKI framework provides tools for distributed calibration and extraction of runoff from any point in a gridded catchment model.

The hydrological model was set up at a  $50 \times 50$  meter grid. Precipitation and temperature were distributed over the grid using the inverse distance method implemented in ENKI utilizing calibrated adiabatic gradients for temperature ( $^{\circ}\text{C}$ ) (from  $-0.6$  to  $-1$ ) and a gradient for precipitation (from  $0$  to  $0.4\%$ ) to take the elevation differences into consideration. For each grid cell, a hydrological process model and all sub-models were executed, and outputs from each grid cell were accumulated and aggregated for sub-catchments. For each cell precipitation as snow or rain was handled using a transition temperature, and snowmelt was computed using a degree-day model [*Bergström*, 1976, 1992, 1995; *Killingtveit and Sæthun*, 1995]. Soil moisture was computed using the method of the HBV model [*Killingtveit and Sæthun*, 1995] and runoff was computed using the runoff model as described by *Kirchner* [2009], both implemented in ENKI.

Evapotranspiration was computed using a Penman-Monteith model calibrated for different boreal vegetation types [*Kasurinen et al.*, 2014], utilizing gridded vegetation maps for Krycklan to define the vegetation in each grid cell. We used separate parameters for evapotranspiration of spruce, pine and broadleaf forests as well as for peat lands in our simulations. Details of the used vegetation maps and distribution of tree species in different sub-catchments are given in [*Laudon et al.*, 2013].

The dynamical rainfall-runoff model assumes that the discharge can be simulated by using a single-valued function that is dependent on catchment water storage as described by *Kirchner* [2009]. Therefore, discharge can be described with the simple conservation-of-mass equation yielding [*Kirchner*, 2009]:

$$\frac{dS}{dt} = P - ET - Q \quad (1)$$

where,  $dS$  (mm day<sup>-1</sup>) denotes the change of the water volume stored in the catchment and,  $P$ ,  $ET$ , and  $Q$  describe the rates of precipitation (mm d<sup>-1</sup>), evapotranspiration (mm d<sup>-1</sup>) and discharge (mm d<sup>-1</sup>) respectively. These values are considered to be sub-catchment averages in this

study. The method of *Kirchner* [2009] assumes that the discharge ( $Q$ ) is dependent on the amount of water in the catchment ( $S$ ), and this relationship can be described by a simple storage-discharge function:

$$Q = f(S) \quad (2)$$

Equations (1) and (2) form a first-order dynamical system, where variables  $Q$ ,  $P$ ,  $ET$  and  $S$  vary of time. The simplest possible linear relationship for storage-discharge function in equation (2) is not always valid, and  $Q$  tends to be a non-linear function of  $S$  [*Kirchner*, 2009] as follows:

$$S = f^{-1}(Q) \quad (3)$$

Generally, the non-linear rainfall-runoff method is considered to be suitable for most catchments. The assumptions are violated, if large lakes control the discharge or most of the precipitation falls onto surfaces that generate direct flow (lake surface area that are large compared to catchment size or impermeable or saturated surfaces) [*Kirchner*, 2009]. The method by *Kirchner* [2009] is suitable for Krycklan, because the proportion of lakes in the whole catchment is only 1% [*Laudon et al.*, 2013].

A differentiation of equation (2) and substitution of equation (1) with time yields the differential equation for the rate change of discharge through time:

$$\frac{dQ}{dt} = \frac{dQ}{dS} \frac{dS}{dt} = \frac{dQ}{dS} (P - ET - Q) \quad (4)$$

The function that describes the dependence of discharge on changes in the catchment water storage is called the sensitivity function.

$$\frac{dQ}{dS} = f'(S) = f'(f^{-1}(Q)) = g(Q) \quad (5)$$

In Kirchners analysis, the use of a single storage discharge relationship leads to a fixed relationship between the change of discharge and discharge. Finally, the differential equation and the relationship between discharge sensitivity and measured discharge were solved yielding:

$$\log(g(Q)) = \log\left(\frac{-dQ/dt}{Q}\right) \approx a_0 + (1 - a_1)\log(Q) + a_2(\log(Q))^{k_p}$$

where,  $a_0$ ,  $a_1$  and  $a_2$  are statistically determined watershed specific parameters describing the non-linear relationship between  $Q$  and  $S$ .

### 2.2.1. Soil temperature model

Soil temperature ( $T_{soil}$ ) was estimated by using the soil temperature model of Rankinen *et al.* [2004] as in a previous study in the Krycklan catchment [Oni *et al.*, 2014]. The model of Rankinen *et al.* [2004] is a simple approach, where soil temperature is calculated based on air temperature and snow depth. The model has seven parameters that must be estimated empirically. Model parameters were calibrated against measured soil temperature at 10 cm depth at the Riparian zone observatory in Krycklan.  $T_{soil}$  was then modeled for each sub-catchment separately using optimized parameters, but distributed air temperature and snow cover depth as an input for the soil temperature model. This approach allows the same resolution for simulated  $T_{soil}$  than the used hydrological model.

## 2.3. DOC modeling

### 2.3.1. Combined Kirchner and DOC transport (K-DOC)

In the original DOC-model by Xu *et al.* [2012] the DOC transport is described as a function of the total rate of change in catchment water storage ( $S$ ) and the run-off ( $Q$ ). DOC is produced via solution from the SOM and removed by other soil processes from the soil water.

The concentration of DOC in the discharge is written as:

$$\frac{dC_{str}}{dt} = \frac{dC_{Tres}}{dt} = (k_{sr}S - k_{rem}C_{Tres} - QC_{Tres} + \left[\frac{1}{k_p}' - C_{Tres}\right]\frac{dS}{dt})/S \quad (7)$$

where,  $C_{str}$  is carbon concentration ( $\text{mg C L}^{-1} \text{d}^{-1}$ ) in stream water,  $C_{Tres}$  ( $\text{mg C L}^{-1} \text{d}^{-1}$ ) is the carbon concentration in terrestrial reservoir,  $k_{sr}$  ( $\text{mg C L}^{-1} \text{d}^{-1}$ ) is the slow release of DOC from soil,  $k_{rem}$  ( $\text{d}^{-1}$ ) is the slow removal of DOC from the soil water.  $k_p$  ( $\text{L mg C}^{-1}$ ) is derived from the relationship of the equilibrium partition coefficient of DOC from SOM ( $k_p$ ) ( $\text{L kg}^{-1}$ ) yielding:

$$k_p' = \frac{k_p}{O_{rs}} \quad (8)$$

where, the amount of readily soluble organic carbon content in the soil is described by parameter  $O_{rs}$  ( $\text{mg C kg}^{-1}$ ) and can be assumed constant describing the potential amount of transportable carbon in the soil reservoir.  $O_{rs}$  was set to constant ( $120 \text{ mg C kg}^{-1}$ ) because there were no available measurements throughout the catchment on the soil water DOC concentrations that would cover the whole simulation time of this study. However, previous studies have reported similar concentrations for soluble DOC than used in this study [Xu and Saiers, 2010; Haei *et al.*, 2010; Grabs *et al.*, 2012].

The rate of the DOC release by dissolution from the soil is controlled by the equilibrium partitioning coefficient  $k_p$  ( $\text{L kg}^{-1}$ ) and it defines the equilibrium between terrestrial carbon reservoir  $C_{Tres}$  and stream carbon concentration as follows:

$$C_{Tres} = \frac{O_{rs}}{k_p} \quad (9)$$

Since, both organic carbon content in soil ( $O_{rs}$ ) and equilibrium partitioning ( $k_p$ ) are unknown, the model is not identifiable, if we do not fix the value of either parameter. Even though ( $O_{rs}$ ) was assumed constant for all sub-catchments, the catchment specific release rates of DOC were estimated indirectly when values of the parameter  $k_p$  were estimated separately for each sub-catchment. In the original model description of Xu *et al.* [2012] parameters for slow release of DOC, removal of DOC from soil water and equilibrium partitioning ( $k_{sr}$ ,  $k_{rem}$  and  $k_p$ ) were assumed to be constant and independent of climate and soil water content. The original implementation of the model is operational only under snow free conditions.

In our model development we accounted for the seasonal differences in slow release rates of the carbon from the soil ( $k_{sr}$ ) and slow removal rates of carbon from the soil water ( $k_{rem}$ ). The process rates were assumed to be dependent on soil temperature ( $T_{soil}$ ) and the catchment water storage ( $S$ ). The slow release of DOC via microbial activity and its consumption are processes affected by the microbial biomass, temperature and soil moisture. We modified the original model of Xu *et al.* [2012] and modeled the relationship of the slow release of DOC on the environment as follows:

$$k_{sr} = k_{sr0} \exp(k_{sr1}T_{soil})S^{k_{sr2}} \quad (10)$$

where  $k_{sr0}$  is a parameter,  $k_{sr1}$  is empirically estimated parameters determining the dependence on soil temperature and  $k_{sr2}$  is a parameter that describes the dependency of DOC release from the catchment water storage. A similar relationship was assumed for the slow removal process of DOC from the soil water yielding:

$$k_{rem} = k_{rem0} \exp(k_{rem1}T_{soil})S^{k_{rem2}} \quad (11)$$

where  $k_{rem}$ ,  $k_{rem1}$   $k_{rem2}$  are calibrated parameters.

## 2.4. Model calibration and statistical analysis

The hydrological and DOC models were calibrated separately. Simulated runoff of the hydrological model were used as an input for the DOC model to estimate stream water DOC concentrations. The hydrological model was simultaneously calibrated by using two discharge time series from stations C7 (2003-2012) and C16 (May 2010 to October 2012) (Figure 1). The latter station is also the outlet of the  $68 \text{ km}^2$  catchment area. The calibration period was set to cover the season from 1 September 2003 to 1 September 2012 and simulated hydrological data were used to model DOC concentrations from 2003 to 2012. Calibration of runoff was performed using a shuffled complex evolution (SCE) algorithm [Duan *et al.*, 1992].

The aim of the regional hydrological calibration was to find a parameter set that describes the properties of the whole catchment and could be used to generate flow simulations for all sub-catchments where measured discharge data were not available. We used the Nash Sutcliffe Efficiency criteria (NSE; Nash and Sutcliffe [1970]) criteria (also called proportion of explained variance or pseudo-R2 to evaluate model fit). We applied the criteria to both the original data and the log-transformed data. The hydrological model was calibrated using the average of NSE and the NSE of the log-transformed flow values (called thereafter NSE & NSE(log) criteria), where NSE(log) was used to ensure good fit for the low flow periods. A combination of the two gauged catchments and the calibration criteria were tested using the best

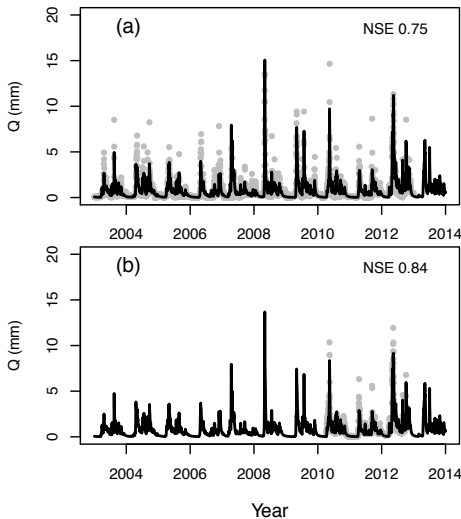


**Figure 2.** Hydrological simulations and model performance for C7 (a) and C16 (b) for the years 2003-2013. Black line describes the simulated  $Q$  and gray dots the measured values

performing NSE & NSE(log) criteria as the objective function. For the DOC model only NSEs were used as calibration criteria for each station.

The K-DOC model was calibrated separately for two different periods using maximization NSE as the objective function. Firstly, we simulated the time from 2006 to 2010 that is comparable to previous studies [Tiwari et al., 2014; Oni et al., 2014]. Secondly, the calibration was also carried out for from the ten-year period ranging from 2003 to 2013 to test the long-term model performance. In order to investigate the effect of our simulated hydrology to DOC model performance, two calibrations were carried out for C7 and C6 by using the measured runoff together with the reconstructed  $S$ . The  $S$  for measured  $Q$  was estimated from Eq. (6).

The K-DOC model was programmed in the R language [R Core Team, 2014] and the model parameters were estimated using a non-linear least squares regression (using a modification of Levenberg-Marquardt algorithm from the package minpack.lm) [Elzhov et al., 2013]. In order to increase the stability of the ordinary differential equation solver (ODE) and to avoid 0-values for  $S$  in exponential and power functions (Eq (10),(11)), a 30 mm minimal water storage was added on top of the simulated  $S$ . This minimal water storage was assumed to be equal for all stations. The K-DOC model equations were solved using a fourth order Runge-Kutta method (package deSolve Version 1.10-9) [Soetaert et al., 2014].

### 3. Results

#### 3.1. Hydrological and DOC simulations

The best performing parameter set for the hydrological simulations produced a good fit to the measured runoff data (NSE values of 0.75 and 0.43 NSE(log) for C7 (from 2003 to 2012) and 0.84 NSE and 0.74 NSE(log) for C16 (from May 2010 to October 2012) (Figure 2). NSE and NSE(log) criteria were used simultaneously to confirm that calibrated

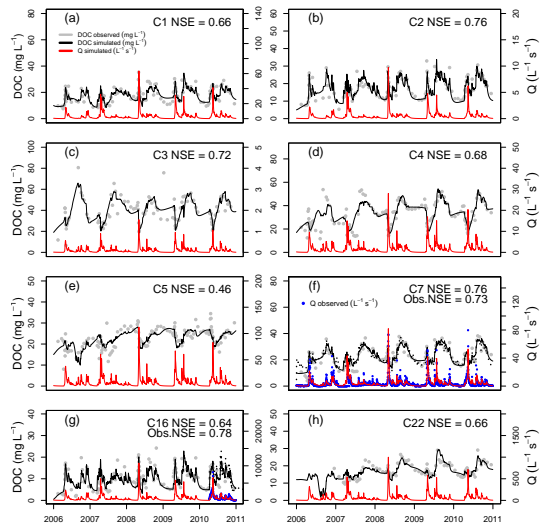


**Figure 3.** Measured and modeled DOC and discharge for selected example stations for the years 2006-2010. Description concerning the land cover types is provided in Table 4. Grey dots are the measured DOC concentration ( $\text{mg L}^{-1}$ ), black line the simulated DOC by using K-DOC ( $\text{mg L}^{-1}$ ), red line is the simulated  $Q$  ( $\text{L}^{-1} \text{s}^{-1}$ ) and the blue dots observed  $Q$  for C7 and C16 ( $\text{L}^{-1} \text{s}^{-1}$ )

model have good peak performance (NSE) and it is able to simulate well also during the low-flow conditions (NSE(log)).

The observed DOC values for the shorter simulation period (2006-2010) varied for C16 from  $1.9 \text{ mg L}^{-1}$  to  $24.2 \text{ mg L}^{-1}$  and for C3 from  $6.5 \text{ mg L}^{-1}$  to  $80.6 \text{ mg L}^{-1}$  (Figure 3), Table 1), showing approximately 12-fold difference between the lowest and the highest recorded DOC concentrations. K-DOC captures these variation ranges well during the base flow and high-flow periods and was able to predict also pulse-like variation in stream water DOC concentrations (Figures 3, S1).

The K-DOC model reproduced contrasting annual patterns of in-stream DOC concentration in the forest-dominated (C1 & C2) and mire-dominated (C3, C4 & C22) sub-catchments. The NSE for simulated DOC concentrations in different sub-catchments for the years 2006-2010 varied from 0.46 to 0.76 (Figure 3, Table 2, Figure S1). For the longer simulation period, NSE varied from 0.25 to 0.69 (Figure S2, Table S1), being slightly lower than for the simulations spanning over 2006-2010. For the longer simulation period the largest decreases in the model fit were observed for the sub-catchments with the largest proportion of lakes (C5 & C6) with NSE varying from 0.25 to 0.29 (Table S1, Figures S1, S2).

The hydrological model was not able to capture all short, high discharge peaks in C7 and C16. This underestimation of flow did not influence significantly the performance of the model to simulate DOC concentrations of C7. The use of the observed runoff (instead of simulated ones) slightly increased the performance in C16 (Figure 3). For the catchment C7 the NSE based on simulated  $Q$  was 0.76, and the NSE based on measured  $Q$  was 0.73. Measured  $Q$  for C16 was available for only 2.5 years between 6 April 2010 and 24 October 2012, and the use of measured  $Q$  improved NSE slightly from 0.73 to 0.78.

**Table 2.** Fitted parameters and NSE for K-DOC model for the simulation period 2006-2010

Station	$C_{Tres}$	$k_{sr0}$	$k_{rem0}$	$k_p$	$k_{sr1}$	$k_{sr2}$	$k_{rem1}$	$k_{rem2}$	NSE	Bias	RMSE	MM
C01	18.3	5.22e-03	2.79e-01	2.4	0.27939	1.471	0.2622	-0.347	0.57	0.0107	3.1	18.3
C02	17.4	2.49e-10	2.91e-09	1.2	-0.05836	6.316	-0.1164	4.914	0.68	0.0117	2.5	17.4
C03	60.0	4.47e-26	9.79e-33	1.6	0.09456	16.600	0.0463	19.936	0.69	0.0238	4.6	36.6
C04	55.0	5.04e-05	1.16e-04	4.7	0.15602	2.466	0.1645	1.166	0.62	0.1156	4.7	31.3
C05	15.0	1.06e-06	5.14e+05	4.7	0.03351	3.342	0.1881	-5.253	0.25	-0.0303	3.2	21.7
C06	17.5	1.66e-05	1.46e+03	4.1	0.03347	2.450	0.1270	-3.341	0.29	-0.0358	3.0	17.5
C07	42.0	5.75e-05	6.57e-05	3.4	0.11246	2.195	0.1208	1.250	0.58	0.0759	3.4	22.6
C08	20.0	8.08e-03	3.60e+02	1.9	0.00089	1.186	-0.0538	-2.488	0.62	-0.0042	3.1	20.0
C09	16.1	2.16e-04	8.82e-04	4.6	0.05145	1.668	0.0748	0.527	0.49	0.0107	2.5	16.1
C10	18.7	3.22e-03	5.77e-02	2.9	0.28137	1.433	0.2692	-0.108	0.54	0.0105	3.6	18.7
C12	17.6	3.09e-02	2.17e-01	3.3	0.18606	0.874	0.1756	-0.303	0.45	0.0230	3.2	17.6
C13	17.9	1.79e-02	1.61e-02	4.7	0.17509	0.932	0.1723	0.321	0.41	0.0273	3.1	17.9
C14	12.5	1.27e-03	4.40e-03	4.1	0.13549	1.444	0.1355	0.528	0.54	0.0114	2.3	12.5
C15	11.7	1.11e-04	4.59e-02	5.4	0.10303	2.004	0.1491	-0.250	0.50	0.0107	1.9	11.7
C16	10.9	2.67e-04	3.93e-01	3.3	0.24681	1.973	0.2544	-0.576	0.61	0.0073	2.1	10.9
C20	10.7	2.09e-08	3.24e-09	1.5	-0.07404	4.715	-0.1418	4.593	0.58	0.0149	2.6	10.7
C21	16.7	3.37e-07	1.44e-07	1.7	-0.08066	3.990	-0.1470	3.523	0.55	-0.0062	3.5	16.7
C22	17.6	1.17e-06	4.66e-01	5.4	0.09433	3.187	0.1887	-1.316	0.61	0.0452	2.0	17.6
C7*	5.0	1.29e-03	7.12e-01	3.0	0.0752	1.702	0.04575	-0.8325	0.73	-0.02	2.86	22.69
C16**	5.0	3.36e-02	5.70e+01	3.1	0.2589	0.943	0.24739	-1.6217	0.78	0.07	1.60	12.55

\* Simulation based on measured  $Q$  for C7 for the years 2006-2010

\*\* Simulation based on measured  $Q$  for C16 for the years 2010-2012

## 3.2. Annual and seasonal patterns of modeled K-DOC parameters

### 3.2.1. The modeled slow release of DOC from soil

Simulated annual and seasonal variation of the simulated values of the slow release of DOC ( $k_{sr}$  in the model) followed largely the modeled soil temperature. The values of  $k_{sr}$  varied from close to 0 to 70 ( $\text{mg C L}^{-1} \text{d}^{-1}$ ) in sub-catchments (Figures 4, S3). The ranges of  $k_{sr}$  were also variable in different sub-catchments. While modeled  $k_{sr}$  values for C4 and C16 (Figures 4a,d, S3), were typically less than 10, for C2 and C7 the range of variation was clearly higher (Figure 4a,c, S3).

Despite differences in values of  $k_{sr}$  between sites, simulated values were low during winter and had the highest values either during spring thaw (April-May) or during summer (June-August) (Figures 4, S3). In sub-catchments C2, C7 and C16, which are forest-dominated and the C4 mire-dominated, the pattern of  $k_{sr}$  for C2 and C7 were similar. The signal for C16 was similar to that observed in C4 (Figure 4). However, there were no such differences in  $k_{sr}$  for forest or mire dominated sub-catchments that would be linked to dominant vegetation or soil type (Figure S3).

### 3.2.2. The modeled removal of DOC from soil water

The annual and seasonal behavior of simulated removal of DOC from soil water (modeled as  $k_{rem} \text{ d}^{-1}$ ) was similar to modeled  $k_{sr}$ , but values were clearly lower, typically smaller than five, at all sites (Figures 6, S6). The highest values occurred during spring thaw or during the periods with highest soil temperatures (Figures 6, S6). While the  $k_{rem}$  signal for C2 and C7, seems to peak mainly in May and July having otherwise low values, the seasonal development and variation of  $k_{rem}$  seems to follow strictly the variation of  $T_{soil}$  in C4 and C16 (Figures 6, S6). As observed with  $k_{sr}$ , the behavior of calculated  $k_{rem}$  values was similar for forest and mire dominated sub-catchments.

## 3.3. Seasonal model parameter dependency on soil temperature and catchment water storage

The seasonal variability in simulated slow release of DOC ( $k_{sr} \text{ mg C L}^{-1} \text{ d}^{-1}$ ) behavior showed mixed responses against  $T_{soil}$  and  $S$  (Figures 5, S4, S5).  $k_{sr}$  values were higher during spring thaw when soil temperature is typically close to 0 °C and on the other hand during the summer, when soil temperature reaches its annual maximum (Figures 5, S4). A similar variation was observed between

the simulated  $S$  and  $k_{sr}$  (Figures 5, S5) showing differences between seasons. The relationship between  $k_{sr}$  and  $S$  was clearly non-linear in C2 and C7, while in C4 and C16 the slope was nearly linear (Figure 5, S5). Additionally, the relationship between  $k_{sr}$  and  $S$  showed a clear seasonal shift in parameter values in C4 and C16, where the values during spring thaw (April and May) were lower than those in the summer (Figures 5, S5).

The behavior of simulated DOC removal from soil water ( $k_{rem}$ ) also showed a clear response to modeled  $T_{soil}$  and  $S$  (Figure 7, S7, S8). The response was typically similar to that of  $k_{sr}$  to modeled  $T_{soil}$ . Sub-catchments C2 and C7 had higher  $k_{rem}$  values during May and during periods with high  $T_{soil}$ , while in C4 and C16 the between simulated  $T_{soil}$  and  $k_{rem}$  was clearly non-linear. The relationship between  $S$  and  $k_{rem}$  was smooth, but non-linear for C2 and C7, while for other sub-catchments the relationship was nearly linear with clear seasonal shifts in both shape and magnitude of the modeled  $k_{rem}$  values (Figures S7, S8).

Catchment size seems to have a significant effect on the slow release ( $k_{sr}$ ) and consumption parameters ( $k_{rem}$ ). The influence of catchment size to variables ( $k_{sr}$  and  $k_{rem}$ ) was tested in a simulation using a constant soil temperature (12 °C) and simulated  $S$  for each sub-catchment. We chose this values to fix  $T_{soil}$  during this simulation because used  $T_{soil}$  is representative for summer time conditions. Additionally, the fixing of  $T_{soil}$  eliminates the fluctuation of DOC release caused by the varying air temperature while it maintains the responses of DOC production to varying  $S$ . In these simulations, the average simulated values of  $k_{sr}$  and  $k_{rem}$  for small catchments (less than 2 km<sup>2</sup>) were higher than those for large catchments (Figure 8).

## 4. Discussion

### 4.1. Regional hydrological simulations

Modeling of stream water DOC concentrations depends to a large extent on an adequate simulation of the runoff from the watershed. Based on our distributed hydrological model, we found that in order to simulate DOC concentrations in stream water, the best performing parameter set for hydrological simulation was achieved by optimizing the performance for multiple hydrological stations (C7&C16) and by using both the NSE and NSE(log) as optimization criteria simultaneously. The selected approach simulated well

runoff during high and low flow conditions and resulted in a better fit (measured by NSE and  $\log(\text{NSE})$ ) for the simulated discharge.

Our findings agree the previous studies on distributed hydrological models, where the optimized parameter set for a single hydrological unit does not describe the hydrology of nearby catchments [Seibert *et al.*, 2000; Merz and Blöschl, 2004]. Models using regionally calibrated parameters have typically slightly lower performance [Wrede *et al.*, 2013; Kumar *et al.*, 2013] compared to single catchment calibration. However, regional calibrations make it possible to simulate discharge and other hydrological responses for the whole Krycklan catchment by using a single parameter set to drive the hydrology. The approach takes into account differences in the sub-catchments in snow accumulation, precipitation and air temperature, while most previous studies have used scaled discharge for all sub-catchments assuming that the discharge at C7 is proportional to the discharge of the other sub catchments [Ågren *et al.*, 2007, 2014].

To our knowledge, this is the first distributed simulation of flow and DOC at multiple sites in a boreal catchment. The maximization of NSE(log) was, for our application, more adequate than the maximization of NSE as calibration objective. The implemented calibration strategy improved the performance of the hydrological model during low-flow conditions and during recession limbs of the hydrograph as observed recently by Hailegeorgis *et al.* [2015]. While it would have been possible to gain slightly higher

performance of the models (as measured by NSE) by calibrating for C7 or C16 independently, the parametrization would not describe the runoff for the remaining stations well. Furthermore, the use of the NSE(log) criteria resulted in a better model performance for our application since it produced an improved timing for falling recession limb and a better balance between  $Q$  and  $S$ . An adequate modeling of the relationship between  $Q$  and  $S$  is central in our DOC model and therefore over- or underestimation of low-flow conditions of the used hydrological model would directly reduce the performance of the DOC model.

#### 4.2. The K-DOC model performance

In forest-dominated sub-catchments, the DOC concentration increases during snow melt, while the mire-dominated sub-catchments experience a reduction of DOC concentrations during this period [Laudon *et al.*, 2011]. In mire-dominated sites, high DOC concentrations tended to be more common during the base flow season, whereas the opposite was true for the forested sub-catchments (Figure 3, Fig S1, S2). Our DOC simulations were able to reproduce these variable patterns that have been observed in several previous studies [Laudon *et al.*, 2004; Billett *et al.*, 2011]. However, it has been challenging to avoid under- or overestimation of DOC-concentrations for this wide spectrum of responses to hydrological events [Winterdahl *et al.*, 2011a; Xu *et al.*, 2012; Oni *et al.*, 2014]. The performance of K-DOC was better compared to previous studies using different models [Winterdahl *et al.*, 2011a; Oni *et al.*, 2014]. For the period 2006–2010, Oni *et al.* [2014] reported NSE by using RIM for C2 (forest), C4 (mire) and C7 (mixed) to be 0.62, 0.52 and 0.54, while INCA-C based simulation produced NSE 0.52, 0.49 and 0.50. The corresponding NSE for the same catchments using K-DOC was 0.76, 0.68 and 0.73. For the Krycklan catchment outlet (C16), our results can be compared to RIM and INCA-C simulations that produced  $R^2$  values 0.59 and 0.49 [Oni, 2015], while NSE for

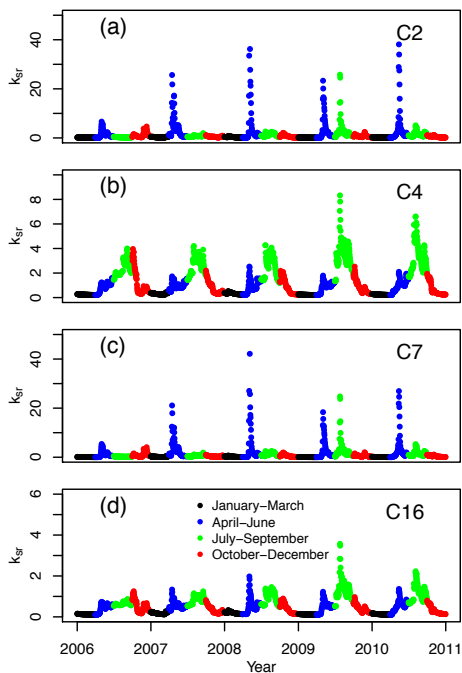


**Figure 4.** The annual and seasonal variation of the parameter  $k_{sr}$ , calculated according to equation (10) controlling the slow release of DOC from the soil for the selected example stations. Data is presented for the years 2006–2010. Sub-catchments C2 and C7 are forest (99.9% and 82% of the total cover) while C4 is wetland dominated. In C16 forests cover 87.2% from the total catchment area being also the outlet of the Krycklan catchment.

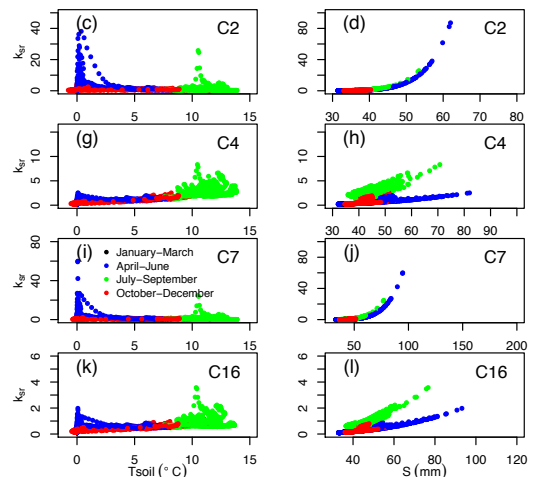


**Figure 5.** Variation of the variable controlling the slow release of DOC from the soil ( $k_{sr}$  as a function of modeled soil temperature and S-storage. Values are based on the simulations covering the years 2006–2010. Further details concerning the land cover types of the catchments are provided in Figure 4

K-DOC was 0.61. The performance of K-DOC was fair also for the other remaining 14 sub-catchments, although we cannot compare our result to any other previous studies (Fig S1, S2).

When the simulation period was extended to cover the years 2003-2013 (Fig S2), NSE for C2, C4, and C7 were 0.68, 0.62 and 0.60, being slightly lower than for the period 2006-2010. One reason for the less good fit for longer simulation periods was a slow increase in the DOC concentrations, especially during low flow conditions. These changes in the DOC concentrations were not captured by K-DOC and are probably linked to climatic warming [Oni *et al.*, 2014] or the recovery from acidification [Futter *et al.*, 2011], but also slow change in forest structure and soil carbon might affect the DOC concentrations at that time scale. Our results for C2 can be compared to RIM simulations of Winterdahl *et al.* [2011a] that reported adjusted NSE 0.69 for the period 1993-2006. The previous study by Oni *et al.* [2014] used simulation period that was shorter than 10 years. Although K-DOC performed well also for period 2003-2012 in most sub-catchments, the performance decreased significantly for catchments containing lakes (C5 & C6). For C5 and C6, DOC concentrations were particularly lower for the years 2003-2006 than in 2007-2013 (Fig S1, S2). A similar, but less pronounced, trend is also visible in C4, C7 and C16 (Figure 3, S1, S2).

The poorer K-DOC performance for lake-dominated catchments could be caused by a violation of assumptions in

K-DOC. Terrestrially derived DOC remaining for prolonged periods in lakes, is subject to in-lake processing. This is not modeled in K-DOC and consequently, relations of DOC-concentrations with soil temperature and soil water storage break down. Furthermore, K-DOC does not contain components describing photochemical or microbiological DOC decomposition or production processes in lake water columns [Vähätalo *et al.*, 2000; Pers *et al.*, 2001; Weyhenmeyer *et al.*, 2012] that are implemented for example in INCA-C [Futter

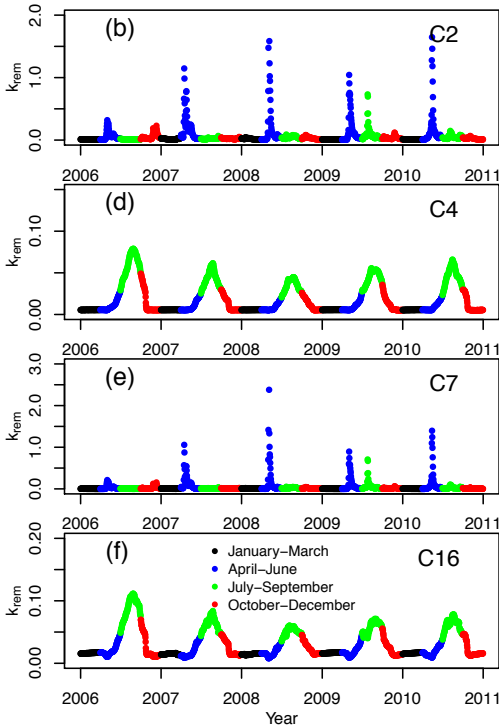


**Figure 6.** The annual and seasonal variation of the variable  $k_{rem}$  controlling the consumption of DOC in soil water for the selected example stations. Values are given for the years 2006-2010.

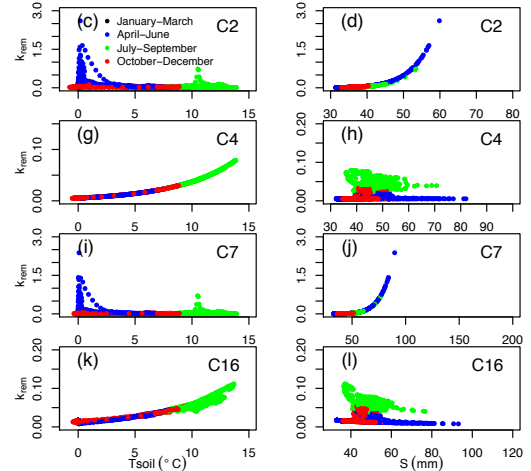


**Figure 7.** Variation of the variable  $k_{rem}$  controlling the consumption of DOC in soil water as a function of modeled soil temperature and S-storage.

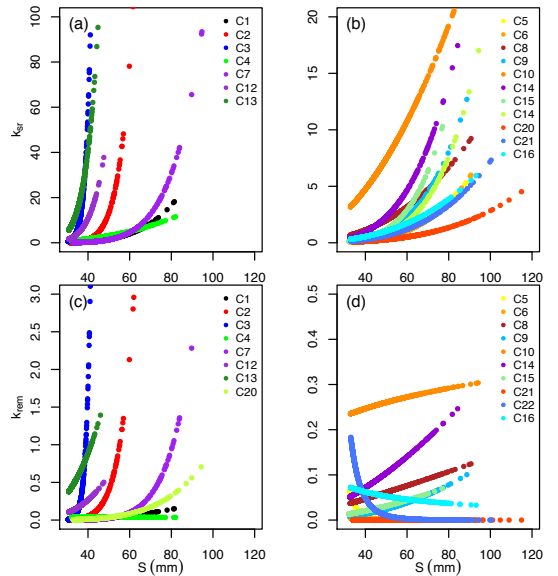


**Figure 8.** Simulated  $k_{sr}$  and  $k_{rem}$  for all sub-catchments by using a constant  $T_{soil}$ .

*et al.*, 2007]. However, in-stream photochemical and microbial processes have been shown to be negligible in previous Krycklan studies, since during periods of the largest DOC export the residence time is less than 10 hours [Ågren *et al.*, 2007; Tiwari *et al.*, 2014]. As a summary, the simulation for the short simulation period (2006-2010) succeeded fairly well also for catchments with lakes indicating that the effect of lakes attenuate rapidly in a stream network as also suggested in a recent study of Lepistö *et al.* [2014]. Therefore, K-DOC is suitable also for catchments, where the lake proportion is small (e.g. less than 4%), like in most sub-catchments in Krycklan.

#### 4.3. Conceptual comparison of different DOC models

Although there are several published DOC models, only four of them have been used in the Krycklan catchment. All these previous models have been limited to cover only few catchments from the Krycklan catchment [Yurova *et al.*, 2008; Winterdahl *et al.*, 2011a; Oni *et al.*, 2014; Tiwari *et al.*, 2014; Oni, 2015] and are different in their complexity. The INCA-C is a result of long-term development of integrated catchment modeling tools that calculates substance transport and reaction rates between SOM, DIC and DOC based on the simulated lateral flow conditions [Futter *et al.*, 2007], where reaction rates depend on soil temperature and soil moisture. The landscape-mixing model of Tiwari *et al.* [2014] calculates DOC concentrations based on empirically determined concentrations from peat, till and sorted sediments dominated sub-catchments taking into account ground water inputs diluting the in-stream DOC concentration, as well as, bulk in-stream bacterial degradation and photochemical degradation. The Riparian Integration Model (RIM) [Seibert *et al.*, 2009; Winterdahl *et al.*, 2011a] is a model that contains soil temperature control on DOC release and can simulate DOC concentrations using directly measured discharge. The parameters of RIM are statistically estimated. Yurova *et al.* [2008] developed a sophisticated process model to one mire dominated sub-catchment, which have a good performance for a single sub-catchment, but cannot be utilized in forest dominated sites.

Neither of these previous biogeochemical approaches described above has used catchment water storage ( $S$ ) to model stream water DOC concentrations. These models are also the most used in studies that have simulated stream water DOC concentration in boreal catchments in Sweden, Norway and Finland with significant influence of snow, while the majority of other published DOC models have been developed in more southern and partly temperate catchments [Boyer *et al.*, 1996; Michalzik *et al.*, 2003; Jutras *et al.*, 2011; Xu *et al.*, 2012; Dick *et al.*, 2014].

K-DOC is less parametrized than INCA-C and does not require separate equations or process descriptions for different land cover types. However, K-DOC is parametrized and optimized on a sub-catchment basis. K-DOC is more complex than RIM, because the fitting of slow release of DOC and consumption of DOC in soil water ( $k_{sr}$  and  $k_{rem}$ ) depends on soil temperature and catchment water storage ( $T_{soil}$  and  $S$ ) at the same time. In RIM-model stream water DOC concentrations are driven by the discharge directly, while K-DOC integrates the total catchment water storage change and the runoff. The relationship of  $Q$  and  $S$  is represented as non-linear relationship, which is controlled by the discharge sensitivity function [Kirchner, 2009].

In hydrological terms, a clear difference in K-DOC compared to RIM is that stream water DOC concentrations depend on  $S$  and not only discharge. In INCA-C stream water DOC concentrations depends on discharge and soil moisture ( $SM$ ), which is distinct from the catchment water storage ( $S$ ) described by Kirchner [2009].  $SM$  is a common variable

in HBV type hydrological models [Bergström, 1992; Futter *et al.*, 2007; Jutras *et al.*, 2011] and simulates the partitioning of water between soil retention and runoff generation. Compared to  $S$ , which respond rapidly to hydrological events,  $SM$  is relatively slowly varying.

In biogeochemical models,  $SM$  is used to describe how DOC production from SOM is dependent on  $SM$  in different soil horizons. However, this process is fundamentally different to the process of K-DOC that describes the affinity of DOC to be transported from soil to stream through rapid changes of  $S$ . It should be noticed that pulse-like hydrological events increase stream water DOC concentrations and affect catchment water storage ( $S$ ), but K-DOC does not assume that these rapid changes would be connected to changes in DOC production in soil. Therefore, K-DOC is a less parametrized and probably more parsimonious description of how DOC is transported to stream water from the soil than how DOC is produced from SOM in the soil.

In K-DOC runoff generation is coupled with a biogeochemical model where all responses are described by using non-linear dependencies. The approach combines slowly changing  $T_{soil}$  and rapidly changing  $S$ . Therefore, the use of  $S$  may perform better than  $SM$  especially regarding the rapid hydrological events (precipitation or snow melt) that quickly flushes leachable DOC from soil to stream [Xu *et al.*, 2012]. The use of soil temperature in our modified version of K-DOC leads to a differentiation of the snowmelt-driven hydrological events that do not transport high DOC concentrations from the high flow conditions during the snow-free season that frequently lead to high stream water DOC concentrations.

Although several DOC models have been developed, no DOC model has been used to compare the catchment response to the environmental forcing that regulates stream water DOC concentrations. Through this approach, we were able to analyze the seasonal patterns of the used parameter modifiers and a sub-catchment specific response of the model to  $T_{soil}$  and  $S$ . While most of the previously used DOC models have concentrated to evaluate model performance from two up to four catchments [Futter *et al.*, 2007; Jutras *et al.*, 2011; Winterdahl *et al.*, 2011b; Oni *et al.*, 2014; Birkel *et al.*, 2014], we analyzed the model performance for eighteen sub-catchment using the distributed hydrological responses. Based on our findings, we believe that K-DOC is suitable for the most boreal catchments and potentially for temperate catchments that are influenced by snow.

#### 4.4. The control of the non-linear responses

Although we used a non-linear function to fit the release and consumption processes of DOC ( $k_{sr}$  and  $k_{rem}$ ), the relationship of these variables with  $T_{soil}$  and  $S$  is almost linear for shorter time periods. This suggests that in boreal catchments, both water storage and soil temperature, are important factors regulating the stream water DOC concentrations and the control may differ between seasons. The simulated values of  $k_{sr}$  and  $k_{rem}$  displayed a distinct seasonal variation and generally non-linear response with the environmental drivers. The simulated responses were variable in different sub-catchments indicating that the response is catchment dependent and varies within a small geographical area.

The simulated annual patterns of in-stream DOC concentrations for mire- and forest-dominated catchments were opposite (Figure 3). For the forest dominated small catchments C2 and C7 (99% & 82% of forest cover) the release of DOC from SOM (as measured by  $k_{sr}$ ), was similar. The seasonal variation of  $k_{sr}$  was different for the mire-dominated (44%) catchment C4 nearby. While  $k_{sr}$  values in the mire ecosystems peaked in the late summer in the forest ecosystems the values were at the maximum in the later spring or early summer. As C4 drains to the C7 catchment, the

variability of the simulated  $k_{sr}$  over time was reduced. An annual pattern of DOC concentration similar to C4 was as a consequence not observable at the C7 measurement point, even though the distance between these stations is only a few hundred meters. The reason could be that the quantitative contribution of C4 to DOC concentrations observed in C7 was small and the largest part of the  $k_{sr}$  signal originated from the forested areas. On the other hand, when DOC concentration in C4 was at its highest values, the discharge was low and the contribution of C4 to the DOC concentrations at C7 was small. When the catchment area increased as can be seen from the  $k_{sr}$  pattern for C16, at the outlet of the Krycklan catchment, the responses were more similar to C4 than to C7. We think that the simulated pattern of  $k_{sr}$  can be attributed to the fact that C16 integrates all land cover types of the catchment and that therefore the response of DOC concentration to precipitation events or changes in temperature are much slower than for the smaller catchments.

The average values for our variables  $k_{sr}$  and  $k_{rem}$  for small catchments, typically less than  $2 \text{ km}^2$ , were higher than those for larger catchments (Figure 8). The differences associated to catchment size might be caused by the differences in runoff generation. While in a small catchment, the response is naturally much faster after precipitation events or snow thaw, in larger catchments the role of groundwater inputs to in-stream DOC concentrations becomes more important [Laudon et al., 2007; Tiwari et al., 2014; Peralta-tapia et al., 2015] and responses become slower.

#### 4.5. The importance of seasonal and annual variation of environmental forcing for in-stream DOC concentrations

We investigated the seasonal differences in in-stream DOC concentrations by using the relationship between environmental forcing and fitted parameters and modeled in-stream DOC concentrations in 18 sub-catchments. The estimated high values of the variables  $k_{sr}$  and  $k_{rem}$  during the spring thaw were associated with high discharge, while the high values during the summer time were connected to heavy rainfall events. Furthermore, the distribution of the values of the variables  $k_{sr}$  and  $k_{rem}$  showed a seasonal variation that was connected to hydrological events such as intense precipitation events and snow melt of the catchments. However, there were no clear patterns in the variation of  $k_{sr}$  or  $k_{rem}$  in mire dominated and forested catchments. While in most sub-catchments the slow release of DOC ( $k_{sr}$ ) had a clearer relationship with simulated  $S$ , the slow removal of DOC from soil water ( $k_{rem}$ ) showed a more pronounced non-linear relationship with the modeled  $T_{soil}$ .

These findings are in accordance with previous studies suggesting stream water DOC concentrations might be sensitive to discharge or temperature [Weyhenmeyer and Karlsson, 2009; Futter et al., 2011; Winterdahl et al., 2014]. For example Futter et al. [2011] reported on the basis of INCA-C simulations carried out in four Swedish integrated monitoring sites that all the investigated catchments were sensitive to soil temperature. However, in one of the investigated sites with pronounced seasonality caused by the snowmelt, stream water DOC concentrations were governed mainly by the discharge, not  $T_{soil}$ . In our simulations, most sub-catchments showed a non-linear response between the slow release of DOC ( $k_{sr}$ ) and the catchment water storage ( $S$ ), while the removal of DOC from soil water ( $k_{rem}$ ) was associated with  $T_{soil}$ . Our findings suggest that catchment water storage is more important for DOC release, while soil temperature is more important for DOC consumption. This indicates that the release and consumption rates may vary in different catchments. Furthermore, our simplified approach to divide SOM degradation to DOC release and DOC consumption rates were applicable for 18 partially nested sub-catchment of this study covering wider selection of different ecosystems than previous studies.

Previous studies have suggested that the length of winter and thawing season [Ågren et al., 2010a], spring floods

[Ågren et al., 2010b] together with discharge have an effect on DOC export. The soil processes of the antecedent season (summer or autumn) might affect DOC export of the following spring in forest and mire dominated catchments [Yurova et al., 2008; Ågren et al., 2010a]. However, based on statistical analyses, Ågren et al. [2010a] suggested that winter climate has a larger effect on stream water DOC concentration than the DOC export during the previous summer or autumn. The approach of the K-DOC, where stream water DOC concentrations are calculated as a series of differential equation that take into account the history of  $S$  and catchment DOC storage. We did not see strong carryover effects from one season to another (except the increase in low flow DOC concentrations discussed above), but future research has to show to what extend a dynamic simulation of  $S$ ,  $T_{soil}$  and the DOC storage in the soil are sufficient to explain inter-annual variation in DOC. It is also possible that long-term variations are driven by variations in litter input and productivity as suggested by Pumpanen et al. [2014]. Such model structure should be able to take into account the inter-annual and annual variability of the in-stream DOC concentrations better than purely statistical models like RIM that is dependent solely on environmental conditions.

While there is evidence that terrestrial ecosystems have a memory that is affected by the preceding environmental conditions, it highlights the need of simplified process based modeling tools that could be used to investigate these delayed responses to environmental conditions, which are typical for boreal ecosystems. We believe that taking into account catchment water storage, helped to gain good response to pulse-like stream water DOC concentrations and differentiate dry and wet years. K-DOC was able to perform better for same simulation period than previously used models that have more complex structure. This indicates that our parsimonious model has a small number of uniquely identifiable parameters, which facilitate global maximization of goodness of fit criteria.

## 5. Summary and Conclusions

Our simulations carried out for 18 sub-catchments suggests that in individual catchments stream water DOC concentrations are regulated by DOC release and consumption processes. Although the seasonal pattern for forest and mire dominated catchments seems to be roughly similar, the timing of the release of DOC from SOM (as measured by  $k_{sr}$ ) is different. In forest dominated catchments simulated  $k_{sr}$  values are at their maximum during the time when soil temperature is low, while in mire-dominated sub-catchments the highest simulated  $k_{sr}$  was observed the season with high soil temperature. Our results suggests that both, soil water storage and soil temperature, are important factors controlling DOC release from forest and mire dominated catchments, but their contribution from stream water DOC concentrations varies between different seasons.

**Acknowledgments.** This research was funded by the Nordic Center of Excellence CRAICC (Cryosphere-atmosphere interactions in a changing Arctic climate), Center of Excellence (project numbers 1118615, Norwegian University of Science and Technology (NTNU), ICOS 271878 and ICOS-Finland 281255, ICOS-ERIC 281250 and EU through projects GHG-Europe and InGOS. Martyn N. Futter was funded by the MISTRA Future Forests program and the NordForsk DomQua project. The Krycklan Catchment Study is funded by the Swedish Science Foundation (VR) SITES, ForWater (Formas), Future Forest, Kempe Foundation, FOMA and SKB.

## References

Ågren, A., I. Buffam, M. Jansson, and H. Laudon (2007), Importance of seasonality and small streams for the landscape regulation of dissolved organic carbon export, *Journal of Geophysical Research*, 112(G3), G03,003, doi:10.1029/2006JG000381.

- Ågren, A., M. Haei, S. J. Köhler, K. Bishop, and H. Laudon (2010a), Regulation of stream water dissolved organic carbon (DOC) concentrations during snowmelt; the role of discharge, winter climate and memory effects, *Biogeosciences*, 7(9), 2901–2913, doi:10.5194/bg-7-2901-2010.
- Ågren, A., I. Buffam, K. Bishop, and H. Laudon (2010b), Modeling stream dissolved organic carbon concentrations during spring flood in the boreal forest: A simple empirical approach for regional predictions, *Journal of Geophysical Research*, 115(G1), G01,012, doi:10.1029/2009JG001013.
- Ågren, A. M., I. Buffam, D. M. Cooper, T. Tiwari, C. D. Evans, and H. Laudon (2014), Can the heterogeneity in stream dissolved organic carbon be explained by contributing landscape elements?, *Biogeosciences*, 11(4), 1199–1213, doi:10.5194/bg-11-1199-2014.
- Aufdenkampe, A. (2011), Riverine coupling of biogeochemical cycles between land, oceans, and atmosphere, *Frontiers in Ecology and the Environment*, 9(1), 53–60.
- Balland, V., J. Bhatti, R. Errington, M. Castonguay, and P. A. Arp (2006), Modeling snowpack and soil temperature and moisture conditions in a jack pine, black spruce and aspen forest stand in central Saskatchewan (BOREAS SSA), *Canadian Journal of Soil Science*, 86(Special Issue), 203–217, doi:10.4141/S05-088.
- Bergström, S. (1976), Development and application of a conceptual runoff model for Scandinavian catchments, *Tech. Rep. NO 7*, SMHI Reports RHO, Norrköping.
- Bergström, S. (1992), The HBV model - its structure and applications, *Tech. rep.*, Swedish Meteorological and Hydrological Institute (SMHI), Hydrology, Norrköping.
- Bergström, S. (1995), The HBV Model, in *Computer Models of Watershed Hydrology*, edited by V. P. Singh, pp. 443–476, Water Resources Publications, Colorado.
- Billett, M. F., M. H. Garnett, K. J. Dinsmore, K. E. Dyson, F. Harvey, A. M. Thomson, S. Piirainen, and P. Kortelainen (2011), Age and source of different forms of carbon released from boreal peatland streams during spring snowmelt in E. Finland, *Biogeochemistry*, 111(1-3), 273–286, doi:10.1007/s10533-011-9645-4.
- Birkel, C., C. Soulsby, and D. Tetzlaff (2014), Developing a consistent process-based conceptualization of catchment functioning using measurements of internal state variables, *Water Resources Research*, 50(5), 2108–2123, doi:10.1002/2012WR013085.
- Boyer, E. W., M. Hornberger, and K. E. Bencala (1996), Overview of a simple model describing variation of dissolved organic carbon in an upland catchment, *Ecological Modelling*, 86, 183–188.
- Clark, J. M., P. J. Chapman, J. K. Adamson, and S. N. Lane (2005), Influence of drought-induced acidification on the mobility of dissolved organic carbon in peat soils, *Global Change Biology*, 11(5), 791–809, doi:10.1111/j.1365-2486.2005.00937.x.
- Clark, J. M., S. N. Lane, P. J. Chapman, and J. K. Adamson (2008), Link between DOC in near surface peat and stream water in an upland catchment, *Science of The Total Environment*, 404(23), 308–315, doi: http://dx.doi.org/10.1016/j.scitotenv.2007.11.002.
- Dai, M., Z. Yin, F. Meng, Q. Liu, and W.-J. Cai (2012), Spatial distribution of riverine DOC inputs to the ocean: an updated global synthesis, *Current Opinion in Environmental Sustainability*, 4(2), 170–178, doi:10.1016/j.cosust.2012.03.003.
- Dick, J. J., D. Tetzlaff, C. Birkel, and C. Soulsby (2014), Modelling landscape controls on dissolved organic carbon sources and fluxes to streams, *Biogeochemistry*, 122(2-3), 361–374, doi:10.1007/s10533-014-0046-3.
- Duan, Q., S. Sorooshian, and V. Gupta (1992), Effective and Efficient Global Optimization for Conceptual Rainfall-Runoff Models, *Water Resources Research*, 28(4), 1015–1031.
- Elzhov, T. V., K. M. Mullen, A.-n. Spiess, B. Bolker, and M. K. Mullen (2013), minpack.lm: R interface to the Levenberg-Marquardt nonlinear least-squares algorithm found in MINPACK, plus support for bounds.
- Evans, C. D., D. T. Monteith, B. Reynolds, and J. M. Clark (2008), Buffering of recovery from acidification by organic acids., *The Science of the total environment*, 404(2-3), 316–25, doi:10.1016/j.scitotenv.2007.11.003.
- Futter, M. N., and H. A. de Wit (2008), Testing seasonal and long-term controls of streamwater DOC using empirical and process-based models., *The Science of the total environment*, 407(1), 698–707, doi:10.1016/j.scitotenv.2008.10.002.
- Futter, M. N., D. Butterfield, B. J. Cosby, P. J. Dillon, A. J. Wade, and P. G. Whitehead (2007), Modeling the mechanisms that control in-stream dissolved organic carbon dynamics in upland and forested catchments, *Water Resources Research*, 43(2), W02,424, doi:10.1029/2006WR004960.
- Futter, M. N., S. Löfgren, S. J. Köhler, L. Lundin, F. Moldan, and L. Bringmark (2011), Simulating dissolved organic carbon dynamics at the swedish integrated monitoring sites with the integrated catchments model for carbon, INCA-C., *Ambio*, 40(8), 906–19, doi:10.1007/s13280-011-0203-z.
- Grabs, T., K. Bishop, H. Laudon, S. W. Lyon, and J. Seibert (2012), Riparian zone hydrology and soil water total organic carbon (TOC): implications for spatial variability and upscaling of lateral riparian TOC exports, *Biogeosciences*, 9(10), 3901–3916, doi:10.5194/bg-9-3901-2012.
- Haei, M., M. G. Öquist, I. Buffam, A. Ågren, P. Blomkvist, K. Bishop, M. Ottosson Löfvenius, and H. Laudon (2010), Cold winter soils enhance dissolved organic carbon concentrations in soil and stream water, *Geophysical Research Letters*, 37(8), L08,501, doi:10.1029/2010GL042821.
- Hailegeorgis, T. T., and K. Alfredsen (2014), Comparative evaluation of performances of different conceptualizations of distributed HBV runoff response routines for prediction of hourly streamflow in boreal mountainous catchments, *Hydrology Research*, 08, 1–22, doi:10.2166/hh.2014.051.
- Hailegeorgis, T. T., K. Alfredsen, Y. S. Abdella, and S. Kolberg (2015), Evaluation of different parameterizations of the spatial heterogeneity of subsurface storage capacity for hourly runoff simulation in boreal mountainous watershed, *Journal of Hydrology*, 522, 522–533, doi:10.1016/j.jhydrol.2014.12.061.
- Hribljan, J. A., E. S. Kane, G. Pyker, Thomas, and R. A. Chimner (2014), Journal of Geophysical Research: Biogeosciences, *Journal of Geophysical Research: Biogeosciences*, 119, 577–595, doi:10.1002/2013JG002527.
- Jutras, M.-F., et al. (2011), Dissolved organic carbon concentrations and fluxes in forest catchments and streams: DOC-3 model, *Ecological Modelling*, 222(14), 2291–2313, doi:10.1016/j.ecolmodel.2011.03.035.
- Kasurinen, V., et al. (2014), Latent heat exchange in the boreal and arctic biomes, *Global Change Biology*, 20(11), 3439–3456, doi:10.1111/gcb.12640.
- Kerr, J. G., and M. C. Eimers (2012), Decreasing soil water Ca<sup>2+</sup> reduces DOC adsorption in mineral soils: implications for long-term DOC trends in an upland forested catchment in southern Ontario, Canada., *The Science of the total environment*, 427-428, 298–307, doi:10.1016/j.scitotenv.2012.04.016.
- Killingtveit, Å., and N. R. Sælthun (1995), Hydrology. Hydropower Development, pp. 1–213.
- Kirchner, J. W. (2009), Catchments as simple dynamical systems: Catchment characterization, rainfall-runoff modeling, and doing hydrology backward, *Water Resources Research*, 45(2), n/a–n/a, doi:10.1029/2008WR006912.
- Köhler, S., I. Buffam, J. Seibert, K. Bishop, and H. Laudon (2009), Dynamics of stream water TOC concentrations in a boreal headwater catchment: Controlling factors and implications for climate scenarios, *Journal of Hydrology*, 373(1-2), 44–56, doi:10.1016/j.jhydrol.2009.04.012.
- Kolberg, S., and O. Bruland (2012), ENKI - An Open Source environmental modelling platform, in *Geophysical Research Abstracts*, vol. 14, EGU2012-13630.
- Kumar, R., L. Samaniego, and S. Attinger (2013), Implications of distributed hydrologic model parameterization on water fluxes at multiple scales and locations, *Water Resources Research*, 49(1), 360–379, doi:10.1029/2012WR012195.
- Laudon, H., S. Köhler, I. Buffam, and S. Köhler (2004), Seasonal TOC export from seven boreal catchments in northern Sweden, *Aquatic Sciences - Research Across Boundaries*, 66(2), 223–230, doi:10.1007/s00027-004-0700-2.
- Laudon, H., V. Sjöblom, I. Buffam, J. Seibert, and M. Mörth (2007), The role of catchment scale and landscape characteristics for runoff generation of boreal streams, *Journal of Hydrology*, 344(3-4), 198–209, doi:10.1016/j.jhydrol.2007.07.010.
- Laudon, H., M. Berggren, A. Ågren, I. Buffam, K. Bishop, T. Grabs, M. Jansson, and S. Köhler (2011), Patterns and Dynamics of Dissolved Organic Carbon (DOC) in Boreal Streams: The Role of Processes, Connectivity, and Scaling, *Ecosystems*, 14(6), 880–893, doi:10.1007/s10021-011-9452-8.

- Laudon, H., J. Buttle, S. K. Carey, J. McDonnell, K. McGuire, J. Seibert, J. Shanley, C. Soulsby, and D. Tetzlaff (2012), Cross-regional prediction of long-term trajectory of stream water DOC response to climate change, *Geophysical Research Letters*, *39*(18), L18,404, doi:10.1029/2012GL053033.
- Laudon, H., I. Taberman, A. Ågren, M. Futter, M. Ottosson-Löfvenius, and K. Bishop (2013), The Krycklan Catchment Study-A flagship infrastructure for hydrology, biogeochemistry, and climate research in the boreal landscape, *Water Resources Research*, *49*(10), 7154–7158, doi:10.1002/wrcr.20520.
- Lepistö, A., M. N. Futter, and P. Kortelainen (2014), Almost 50 years of monitoring shows that climate, not forestry, controls long-term organic carbon fluxes in a large boreal watershed., *Global change biology*, *20*(4), 1225–37, doi:10.1111/gcb.12491.
- Mengistu, S. G., I. F. Creed, K. L. Webster, E. Enanga, and F. D. Beall (2014), Searching for similarity in topographic controls on carbon, nitrogen and phosphorus export from forested headwater catchments, *Hydrological Processes*, *28*(8), 3201–3216, doi:10.1002/hyp.9862.
- Merz, R., and G. Blöschl (2004), Regionalisation of catchment model parameters, *Journal of Hydrology*, *287*(1-4), 95–123, doi:10.1016/j.jhydrol.2003.09.028.
- Michalzik, B., E. Tipping, J. Mulder, J. G. Lancho, E. Matzner, C. Bryant, N. Clarke, S. Lofts, and M. V. Esteban (2003), Modelling the production and transport of dissolved organic carbon in forest soils, *Biogeochemistry*, *66*(3), 241–264, doi:10.1023/B:BIOG.0000005329.68861.27.
- Moody, C., F. Worrall, C. Evans, and T. Jones (2013), The rate of loss of dissolved organic carbon (DOC) through a catchment, *Journal of Hydrology*, *492*, 139–150, doi:10.1016/j.jhydrol.2013.03.016.
- Naden, P. S., N. Allott, L. Arvola, M. Järvinen, K. Moore, C. N. Aonghusa, D. Pierson, and E. Schneiderman (2010), Modelling the Impacts of Climate Change on Dissolved Organic Carbon, in *The Impact of Climate Change on European Lakes, Aquatic Ecology Series*, vol. 4, edited by G. George, pp. 221–252, Springer Netherlands, Dordrecht, doi:10.1007/978-90-481-2945-4.1.
- Nash, J. E., and J. V. Sutcliffe (1970), River flow forecasting through conceptual models part I: A discussion of principles, *Journal of Hydrology*, *10*(3), 282–290, doi: http://dx.doi.org/10.1016/0022-1694(70)90255-6.
- Neff, J. C., and G. P. Asner (2001), Dissolved Organic Carbon in Terrestrial Ecosystems: Synthesis and a Model, *Ecosystems*, *4*(1), 29–48, doi:10.1007/s100210000058.
- Oni, S. K. (2015), Unpublished.
- Oni, S. K., M. N. Futter, K. Bishop, S. J. Köhler, M. Ottosson-Löfvenius, and H. Laudon (2013), Long-term patterns in dissolved organic carbon, major elements and trace metals in boreal headwater catchments: trends, mechanisms and heterogeneity, *Biogeosciences*, *10*(4), 2315–2330, doi:10.5194/bg-10-2315-2013.
- Oni, S. K., M. N. Futter, C. Teutschbein, and H. Laudon (2014), Cross-scale ensemble projections of dissolved organic carbon dynamics in boreal forest streams, *Climate Dynamics*, *42*(9–10), 2305–2321, doi:10.1007/s00382-014-2124-6.
- Öquist, M. G., et al. (2014), The Full Annual Carbon Balance of Boreal Forests Is Highly Sensitive to Precipitation, *Environmental Science & Technology Letters*, *1*(7), 315–319, doi:10.1021/ez500169j.
- Peralta-tapia, A., R. a. Sponseller, A. Ågren, D. Tetzlaff, C. Soulsby, and H. Laudon (2015), Scale-dependent groundwater contributions influence patterns of winter base-flow stream chemistry in boreal catchments, *Journal of Geophysical Research: Biogeosciences*, *120*, 847–858, doi:10.1002/2014JG002878.Received.
- Pers, C., L. Rahm, A. Jonsson, and M. Jansson (2001), Modelling dissolved organic carbon turnover in humic Lake, *Environmental monitoring and assessment*, *6*, 159–172.
- Pumpanen, J., et al. (2014), Precipitation and net ecosystem exchange are the most important drivers of DOC flux in upland boreal catchments, *Journal of Geophysical Research: Biogeosciences*, pp. n/a–n/a, doi:10.1002/2014JG002705.
- R Core Team (2014), *R: A Language and Environment for Statistical Computing*, R Foundation for Statistical Computing, Vienna, Austria.
- Rankinen, K., T. Karvonen, and D. Butterfield (2004), A simple model for predicting soil temperature in snow-covered and seasonally frozen soil: model description and testing, *Hydrology and Earth System Sciences*, *8*(4), 706–716, doi:10.5194/hess-8-706-2004.
- Seibert, J., S. Uhlenbrook, C. Leibundgut, and S. Halldin (2000), Multiscale Calibration and Validation of a Conceptual Rainfall-Runoff Model, *Physics and Chemistry of the Earth*, *25*(1), 59–64.
- Seibert, J., T. Grabs, S. Köhler, H. Laudon, M. Winterdahl, and K. Bishop (2009), Linking soil and stream-water chemistry based on a riparian flow-concentration integration model, *Hydrology and Earth System Sciences Discussions*, *6*(4), 5603–5629, doi:10.5194/hessd-6-5603-2009.
- Soetaert, K., T. Petzoldt, and W. R. Setzer (2014), deSolve: General Solvers for Initial Value Problems of Ordinary Differential Equations (ODE), Partial Differential Equations (PDE), Differential Algebraic Equations (DAE), and Delay Differential Equations (DDE).
- Thackeray, S. J. (2014), Freshwater Ecosystems and the Carbon Cycle. In: Excellence in Ecology Series J. J. Cole (2013). Volume 18. International Ecology Institute, Oldendorf, Germany. 125 pp., *Freshwater Biology*, *59*(8), 1781, doi:10.1111/fwb.12382.
- Tiwari, T., H. Laudon, K. Beven, and A. M. Ågren (2014), Downstream changes in DOC: Inferring contributions in the face of model uncertainties, *Water Resources Research*, *50*(1), 514–525, doi:10.1002/2013WR014275.
- Tranvik, L. J., et al. (2009), Lakes and reservoirs as regulators of carbon cycling and climate, *Limnology and Oceanography*, *54*(1), 2298–2314.
- Vähätalo, A., M. Salkinoja-salonen, P. Taalas, and K. Salonen (2000), Spectrum of the quantum yield for photochemical mineralization of dissolved organic carbon in a humic lake, *Limnology and Oceanography*, *45*(3), 664–676.
- Weyhenmeyer, G. A., and J. Karlsson (2009), Nonlinear response of dissolved organic carbon concentrations in boreal lakes to increasing temperatures, *Limnology and Oceanography*, *54*(6-part.2), 2513–2519, doi:10.4319/lo.2009.54.6-part.2.2513.
- Weyhenmeyer, G. A., M. Fröberg, E. Karlton, M. Khalili, D. Kothawala, J. Temmerud, and L. J. Tranvik (2012), Selective decay of terrestrial organic carbon during transport from land to sea, *Global Change Biology*, *18*(1), 349–355, doi:10.1111/j.1365-2486.2011.02544.x.
- Winterdahl, M., M. Futter, S. Köhler, H. Laudon, J. Seibert, and K. Bishop (2011a), Riparian soil temperature modification of the relationship between flow and dissolved organic carbon concentration in a boreal stream, *Water Resources Research*, *47*(8), W08,532, doi:10.1029/2010WR010235.
- Winterdahl, M., J. Temmerud, M. N. Futter, S. Löfgren, F. Moldan, and K. Bishop (2011b), Riparian zone influence on stream water dissolved organic carbon concentrations at the Swedish integrated monitoring sites., *Ambio*, *40*(8), 920–30, doi:10.1007/s13280-011-0199-4.
- Winterdahl, M., M. Erlandsson, M. N. Futter, G. A. Weyhenmeyer, and K. Bishop (2014), Intra-annual variability of organic carbon concentrations in running waters: Drivers along a climatic gradient, *Global Biogeochemical Cycles*, *28*(4), 451–464, doi:10.1002/2013GB004770.
- Worrall, F., T. P. Burt, and J. K. Adamson (2008), Linking pulses of atmospheric deposition to DOC release in an upland peat-covered catchment, *Global Biogeochemical Cycles*, *22*(4), GB4014, doi:10.1029/2008GB003177.
- Wrede, S., J. Seibert, and S. Uhlenbrook (2013), Distributed conceptual modelling in a Swedish lowland catchment: a multi-criteria model assessment, *Hydrology Research*, *44*(2), 318, doi:10.2166/nh.2012.056.
- Wu, H., C. Peng, T. R. Moore, D. Hua, C. Li, Q. Zhu, M. Peichl, M. a. Arain, and Z. Guo (2013), Modeling dissolved organic carbon in temperate forest soils: TRIPLEX-DOC model development and validation, *Geoscientific Model Development Discussions*, *6*(2), 3473–3508, doi:10.5194/gmdd-6-3473-2013.
- Xu, N., and J. E. Saiers (2010), Temperature and Hydrologic Controls on Dissolved Organic Matter Mobilization and Transport within a Forest Topsoil, *Environmental science & technology*, *44*(14), 5423–5429.
- Xu, N., J. E. Saiers, H. F. Wilson, and P. A. Raymond (2012), Simulating streamflow and dissolved organic matter export from a forested watershed, *Water Resources Research*, *48*(5), W05,519, doi:10.1029/2011WR011423.

- Yurova, A., A. Sirin, I. Buffam, K. Bishop, and H. Laudon (2008), Modeling the dissolved organic carbon output from a boreal mire using the convection-dispersion equation: Importance of representing sorption, *Water Resources Research*, *44*(7), W07411, doi:10.1029/2007WR006523.
- Zhang, C., R. C. Jamieson, F.-R. Meng, R. J. Gordon, and C. P.-A. Bourque (2013), Simulation of monthly dissolved organic carbon concentrations in small forested watersheds, *Ecological Modelling*, *250*, 205–213, doi:10.1016/j.ecolmodel.2012.11.007.
-





# Biologically labile photoproducts from riverine dissolved organic carbon in the coastal waters

Ville Kasurinen<sup>1,2</sup>, Hanna Aarnos<sup>3</sup>, Yufei Gu<sup>4</sup>, and Anssi V. Vähätalo<sup>4</sup>

<sup>1</sup>University of Helsinki, Department of Forest Sciences, P.O. Box 27, Helsinki, Finland

<sup>2</sup>Norwegian University of Science and Technology, 7491 Trondheim, Norway

<sup>3</sup>University of Helsinki, Department of Environmental Sciences, P.O. Box 65, 00014 Helsinki, Finland

<sup>4</sup>University of Jyväskylä, Department of Bio and Environmental Sciences, P.O. Box 35, 40014, Jyväskylä, Finland

Correspondence to: Ville Kasurinen (ville.kasurinen@helsinki.fi)

Published:

**Abstract.** In order to assess the production of biologically labile photoproducts (BLPs) from non-labile terrestrial dissolved organic carbon (tDOC) in the coastal ocean, we collected water samples from ten major rivers, removed labile tDOC and mixed the residual tDOC with artificial seawater for microbial and photochemical experiments. Bacteria grew on the residual non-labile tDOC with a growth efficiency of 11.5% (mean; range from 3.6% to 15.3%). Simulated solar radiation transformed a part of tDOC into BLPs, which stimulated bacterial respiration and production, but did not change bacterial growth efficiency compared to the non-irradiated dark controls. In the irradiated waters, the amount of BLPs stimulating bacterial production were linearly dependent on the photochemical bleaching of terrestrial chromophoric dissolved organic matter (tCDOM). The apparent quantum yields for BLPs supporting bacterial production ranged from 9.5 to 76 (median 36.1)  $\mu\text{mol C mol photons}^{-1}$  at 330 nm. The corresponding values for BLPs supporting bacterial respiration ranged from 57 to 1204 (median 186)  $\mu\text{mol C mol photons}^{-1}$ . According to the calculations based on spectral apparent quantum yields and local solar radiation, the annual production of BLPs ranged from 21 (St. Lawrence) to 584 (Yangtze)  $\text{mmol C m}^{-2} \text{yr}^{-1}$  in the plumes of the examined rivers. Complete photobleaching of tCDOM in the coastal ocean was estimated to produce 10 Tg C BLPs  $\text{yr}^{-1}$  from the rivers examined. In the entire global coastal ocean, the corresponding estimate is 38 Tg C BLPs  $\text{yr}^{-1}$  (15% of riverine tDOC), which support 4 Tg C  $\text{yr}^{-1}$  bacterial production and 34 Tg C  $\text{yr}^{-1}$  bacterial respiration.

## 1 Introduction

Rivers transport 246 Tg C  $\text{yr}^{-1}$  of terrestrial dissolved organic carbon (tDOC) to the ocean Cai (2011). A part of ( $19 \pm 16\%$ ; Søndergaard and Middelboe (1995)) tDOC is biologically labile and consumed by bacteria quickly after the entrance to marine recipient in the estuaries and continental shelves (Lønborg et al., 2009; Lønborg and Alvarez-Salgado, 2012). The remaining majority of tDOC ( $81 \pm 16\%$ ) Søndergaard and Middelboe (1995) is non-labile and transported offshore. In the coastal waters, the primary sinks for non-labile tDOC are slow microbial metabolism or photochemical transformations (Bauer et al., 2013). The importance photochemical transformation increases with the residence time of tDOC, because the biological lability of tDOC decreases faster than the photochemical reactivity of tDOC (Vähätalo and Wetzel, 2004; Vähätalo et al., 2010). Photochemical reactions can transform non-labile tDOC to dissolved inorganic carbon (DIC) or biologically labile photoproducts (BLPs), the latter being rapidly assimilated by microbes (Wetzel et al., 1995). The assimilation of non-labile tDOC (directly or after photochemical transformation into BLPs) contributes to the heterotrophy of coastal waters (Smith and Hollibaugh, 1993) and couples tDOC to marine food webs (Vähätalo and Järvinen, 2007; Vähätalo et al., 2011).

By operational definition, BLPs are photochemically produced compounds that are biologically more labile than the original pool of compounds in non-irradiated DOC. The amount of BLPs is typically quantified experimentally as bacterial respiration, bacterial production or associated loss of DOC (= bacterial carbon demand) in irradiated DOC in excess of that found in non-irradiated dark control DOC like

e.g. in 23 studies reviewed by Mopper and Kieber (2002). In order to relate the experimental findings to environmental processes, the amounts of BLPs have been related to the number of photons absorbed by chromophoric dissolved organic matter (CDOM) yielding an apparent quantum yield (AQY) for the production of BLPs (Miller et al., 2002; Vähätalo et al., 2011; Aarnos et al., 2012; Reader and Miller, 2014; Cory et al., 2014).

The production of individual BLP compounds depends on the photochemical loss of CDOM (photobleaching; Kieber et al. (1990); Miller and Moran (1997); Bertilsson and Tranvik (2000); Obernosterer and Herndl (2000)). The relationship between photobleaching and the photochemical production of BLPs is linear for formaldehyde, glyoxylate, carbon monoxide and carboxylic acids (Kieber et al., 1990; Miller and Moran, 1997; Bertilsson and Tranvik, 2000). Although, the relationship between the production of BLPs and photobleaching could be also used to estimate the photoproduction of BLPs in the surface waters, it has rarely been used for such a purpose (Obernosterer and Herndl, 2000).

The bacterial production on BLPs depends in part on bacterial growth efficiency (BGE) on BLPs. Irradiation of DOC can decrease (15 studies) or increase BGE (5 studies) compared to non-irradiated DOC (reviewed by Abboudi et al. (2008)). Despite these comparisons between irradiated and non-irradiated DOC, BGE on BLPs has not been previously determined.

This study estimates the production of BLPs from non-labile tDOC in the coastal waters and determines BGE on BLPs. We collected water samples from ten large rivers and stored them with indigenous microbes to remove biologically labile tDOC. The remaining non-labile tDOC was mixed (1:1) with artificial seawater to simulate the chemical matrix of coastal ocean. The sterile filtered mixtures were irradiated with simulated solar radiation. The irradiated waters received indigenous bacteria and the amount of BLPs was determined separately as bacterial production (BP on BLPs) and respiration (BR on BLPs) in excess of that found in the non-irradiated dark control waters. The BP or BR on BLPs was related to the photobleaching of tCDOM and also to the number of absorbed photons for the calculations of spectral AQYs. The annual production of BP and BR on BLPs ( $\text{mol C m}^{-2} \text{ yr}^{-1}$ ) in the river plumes was calculated from AQYs and the annual solar radiation in the coastal ocean in the front of each river. We estimated the production of BLPs by each river ( $\text{mol C yr}^{-1} \text{ river}^{-1}$ ) from the annual tCDOM flux using the relationship between BLPs and the photobleaching of tCDOM. As the rivers examined contribute 28% of tDOC flux to the ocean, we dared to extrapolate our finding to a global scale simply by assuming that the rivers examined here are representative for the remaining 72% of tDOC flux by other rivers.

## 2 Material and Methods

### 2.1 Material

The rivers selected for this study (Table 1) reside in five continents, drain 25% of the land area, and contribute 33% to the freshwater discharge to the ocean (Carlson, 2002; Cauwet, 2002; Coynel et al., 2005; Milliman and Farnsworth, 2011). For the collection of water samples, empty polyethylene containers (cleaned with detergent, rinsed with HCl and finally copiously rinsed with ion exchanged water; MQ) were shipped to the local collaborators at ten major rivers (see acknowledgments, Supplementary information). The containers were filled in the center of the stream by direct immersion below the surface, except for the Mississippi and St. Lawrence Rivers where water about 3 m below the surface was collected with Niskin bottles. The samples collected for this study has been used earlier for the determination of dissolved black carbon (Jaffé et al., 2013), molecular composition of DOM (Wagner et al., 2015), dissolved iron (Xiao et al., 2013) and the photochemical isotopic fractionation of tDOC (Lalonde et al., 2014).

Artificial seawater was prepared according to Kester et al. (1967) by dissolving pro analysis grade of inorganic salts (VWR International) to MQ water. Based on a separate experiment (Supplementary Information), artificial seawater did not contain labile DOC affecting the determinations of BLPs. Prior to use, glassware and quartzware were washed in a dishwasher, rinsed out with 7% HCl and MQ water, and combusted for several hours ( $450^\circ \text{C}$ ).

### 2.2 Experimental

#### 2.2.1 Sample preparation

Although solar radiation transforms photoreactive tDOC across its entire journey from estuaries towards open ocean, the dilution and advection of tDOC into transparent seawater increase its phototransformation in offshore waters, where the phototransformation of tDOC primarily takes place (Medeiros et al., 2015). This phototransformation concerns non-labile tDOC, since labile tDOC has been consumed earlier close to shore (Medeiros et al., 2015). In order to mimic the biological consumption of labile tDOC, the collected water samples were not filtered or preserved, but kept in darkness and sent to our laboratory in Helsinki, Finland by air cargo. The median transport time between the sampling and the arrival to Helsinki was 33 days (Table 1) and allowed the heterotrophic consumption of labile tDOC during the transportation, leaving behind the non-labile tDOC. In our St. Lawrence river sample, the proportion of labile tDOC was  $19 \pm 1\%$  ( $n = 3$ ; (Lalonde et al., 2014)), which is in agreement with the proportion of labile DOC being  $19 \pm 16\%$  in rivers and coastal waters (Søndergaard and Middelboe, 1995; Lønborg and Alvarez-Salgado, 2012). Upon arrival to

the laboratory, the water samples were filtered through 1- $\mu\text{m}$  filters (quick rinsed membrane cartridge, Nuclepore or double layer of track-etch polyester membrane filter cartridge, Graver Technologies) and stored in the dark at +4 °C.

In order to assess BGEs and the production of BLPs from non-labile tDOC under conditions representing coastal waters, the 1  $\mu\text{m}$ -filtered river water samples were mixed 1:1 with artificial seawater. In the mixtures, the ionic composition was similar to that of seawater but the salinity (16) was half of that found in the ocean. For abiotic photochemical experiments, the 1  $\mu\text{m}$  filtered river water samples mixed with artificial seawater were further aseptically filtered through 0.2  $\mu\text{m}$  membrane filters (Palls Supor 200) into 170 mL glass or quartz flasks to be closed with ground-glass stoppers without headspace. Our salinity adjustment followed by filtration mimicked the flocculation of riverine iron and related loss in the photochemical reactivity of tDOC in coastal waters (Minor et al., 2006; White et al., 2010).

### 2.2.2 Irradiations

Photochemical reactivity of riverine tDOC is highest upon entrance to estuary, but it will decrease with increasing residence time in sunlit water (e.g., Andrews et al. (2000); Vähätalo and Wetzel (2004)). Our aim was not to determine the photoreactivity of tDOC in river water, instead our experimental irradiations were designed to degrade approximately half of tCDOM to assess a typical (median) photochemical reactivity of tDOC along its transport from estuaries towards open ocean. The quartz flasks were irradiated for 44 h to 46 h with 765  $\text{W m}^{-2}$  simulated solar radiation (Atlas Suntest CPS+ solar simulator) in a MQ-water bath regulated to 20 °C with a Lauda RE-112 thermostat like in our earlier study (Aarnos et al., 2012) (Supplementary information). The glass flasks wrapped into aluminum foil were kept in the same water bath (dark controls) or at 4 °C (initials). During the irradiations, photochemical oxygen consumption was estimated to be less than 50% from the initial  $\text{O}_2$  concentration in the diluted samples (Xie et al., 2004). The dose of ultraviolet radiation received by the samples corresponded to 26-27 days of the mean ultraviolet radiation absorbed by the surface of Earth, when calculated from the Earth's annual global mean energy budget (Kiehl and Trenberth, 1997) accounting for the spectral irradiance of Suntest CPS+ and the ASTM G173-03 solar reference spectrum.

### 2.2.3 Bioassays

For the bioassays, the irradiated and the dark control samples from each river received a 10% (vol/vol) inoculum of bacterioplankton prepared from their corresponding river by passing the 1  $\mu\text{m}$ -filtered river water through GF/F filters (nominal pore size of 0.7  $\mu\text{m}$ , Whatman) for the removal of the grazers of bacterioplankton. The bioassay samples received  $\text{NH}_4\text{Cl}$  and  $\text{KH}_2\text{PO}_4$  to the final concentrations of 1.2  $\text{mg N L}^{-1}$

and 0.13  $\text{mg P L}^{-1}$ , respectively, and were divided into two aliquots for the determination of bacterial respiration (BR) or bacterial production (BP).

### 2.2.4 Bacterial respiration

BR was determined as a consumption of dissolved oxygen ( $\text{O}_2$ ) measured with needle-type oxygen microsensor optodes (PreSens GmbH, Regenburg, NTH-PSt1-L5-TF-NS40) (Warkentin et al., 2007, 2011) at 15 minutes intervals from aliquots closed in biological oxygen demand bottles incubated in darkness in a water bath at 20 °C (Lauda RE-112 thermostat). An optode was inserted into the sample via a hole drilled through the ground-glass stopper and sealed with parafilm. The drift of instrument defining the detection limit for BR was measured in three blank experiments, where MQ water was incubated for 300 hours under the conditions identical to respiration measurements. During the blank experiments, the apparent decline of  $\text{O}_2$  was  $1.5 \pm 0.5 \mu\text{mol L}^{-1} 300 \text{ h}^{-1}$  (mean  $\pm$  sd,  $n = 3$ ). The decline in the concentration of  $\text{O}_2$  was converted into an increase in the concentration of  $\text{CO}_2$  assuming 1:1 molar ratio between the consumed  $\text{O}_2$  and the produced  $\text{CO}_2$  in BR. The selected respiratory quotient makes our study comparable to earlier studies, which have used values ranging from 0.82 to 1.2 (Søndergaard and Middelboe, 1995; del Giorgio et al., 1997; del Giorgio and Cole, 1998; Cory et al., 2014). The temporal trend of accumulated  $\text{CO}_2$  was determined by a polynomial fitting to the measurements with the smooth spline function in R software (R Core Team, 2014).

### 2.2.5 Bacterial production

To determine bacterial production (BP), 10 mL samples were preserved with formaldehyde (final concentration 5%) daily from the aliquots incubated in the dark at room temperature (mean 22 °C, range from 20 °C to 24 °C) with an air-head space. The bacterial cells from the preserved samples were filtered on 0.2  $\mu\text{m}$  polycarbonate filters (GE water & Process Technologies) and stained with acridine orange (Hobbie et al., 1977). Bacterial densities were estimated from cell counts from  $\geq 20$  fields with an epifluorescence microscope (Aristoplan). The cell volumes were determined by digital image analysis (Image Analysis & LabMicrobe software; Massana et al. 1997). The volumes of cells were converted to carbon using a conversion factor of 0.12  $\text{pg C } (\mu\text{m}^3)^{0.7}$  and the total carbon-biomass of bacterioplankton assemblage was calculated by multiplying the organic carbon content of cells with the density of cells (Norland, 1993).

### 2.2.6 Defining BLPs and BGEs

For the bacteria growing in the irradiated sample, the response to BLPs was considered to be largest in the end of logarithmic growth phase defined as the first day with maximum biomass during the 12 day-long bioassay (Stepanuskas

et al., 2002). The first maximum biomass was determined separately for each irradiated tDOC among the bacterial samples preserved daily across the entire length of bioassay. On the day of maximum biomass (varying from 5 to 12 days) the difference in the accumulated BP or BR between the dark control and the irradiated tDOC represented the BP or BR on BLPs. To best of our knowledge, our study is the first one, which sought for the maximum response of bacteria to BLPs separately for each sample prior to calculating BGEs. Previously fixed times varying from 1.5 to 7.8 days have been used (Reche et al., 1998; Anesio et al., 2000; Farjalla et al., 2001; Anesio et al., 2005; Amado et al., 2006; Pullin et al., 2004; Vähätalo et al., 2003; McCallister and Bauer, 2005; Smith and Benner, 2005; Abboudi et al., 2008). The bacterial growth efficiency (BGE) was calculated as  $BP/(BP+BR)$ .

### 2.3 Analytical measurements

The absorbance by CDOM was measured with a spectrophotometer (Shimadzu UV 2550) in triplicates against MQ water reference using a 0.05 m quartz cuvette. The absorbance by CDOM was converted into an absorption coefficient ( $a_{CDOM,\lambda}$ ) accounting for the path length of the cuvette and transforming the 10-base logarithm to a Napierian-based logarithm ( $\ln(10)$ ).

### 2.4 The apparent quantum yields for the production of BLPs

Spectral apparent quantum yields (AQYs) for the production of BLPs supporting bacterial production (BP) or bacterial respiration (BR) ( $AQY_{BP,\lambda}$  or  $AQY_{BR,\lambda}$ ) were calculated as:

$$AQY_{BP,\lambda} \text{ or } AQY_{BR,\lambda} = \frac{BP \text{ or } BR \text{ on BLPs}}{\text{photons absorbed by } tCDOM(\lambda)} \quad (1)$$

where BP or BR on BLPs are the bacterial production or respiration based on BLPs (mol C) and photons absorbed represents the spectrally resolved absorption of photons by tCDOM during the irradiation experiment (mol photons at the spectral range from  $\lambda$  290 nm to  $\lambda$  750 nm). The latter was calculated by accounting for the spectral dose of photons, the optical path length, and the absorption characteristics of samples as explained in the supplementary material.  $AQY_{BP,\lambda}$  and  $AQY_{BR,\lambda}$  were assumed to depend on wavelength according to:

$$AQY_{\lambda} = c e^{-d\lambda} \quad (2)$$

where  $AQY_{\lambda}$  is  $AQY_{BP,\lambda}$  or  $AQY_{BR,\lambda}$ ,  $c$  (mol C mol photons<sup>-1</sup>) and  $d$  (nm<sup>-1</sup>) are positive constants, and  $\lambda$  is the wavelength (nm). The parameters  $c$  and  $d$  in Eq. 2 were iterated from Eq. 1 by unconstrained nonlinear

optimization (the 'fminsearch' function of the Matlab 7.9.0) as in our earlier publications (Vähätalo et al., 2011; Aarnos et al., 2012) (Supplementary information).

### 2.5 The production of BLPs based on AQYs

The measured  $AQY_{BP,\lambda}$  or  $AQY_{BR,\lambda}$  was used to calculate the production rate of BLPs in the river plumes according to:

$$pr = \int_{\lambda_{min}}^{\lambda_{max}} AQY_{\lambda} Q_{\lambda} (a_{CDOM,\lambda} a_{tot,\lambda}^{-1}) d\lambda \quad (3)$$

where  $pr$  is the production rate of BLPs supporting BP or BR over the entire water column (mol C m<sup>-2</sup> yr<sup>-1</sup>),  $AQY_{\lambda}$  is  $AQY_{BP,\lambda}$  or  $AQY_{BR,\lambda}$ ,  $Q_{\lambda}$  represents the spectrum of solar radiation absorbed by the entire water column (mol photons m<sup>-2</sup> yr<sup>-1</sup> nm<sup>-1</sup>), and the ratio  $a_{CDOM,\lambda} a_{tot,\lambda}^{-1}$  (dimensionless) is the contribution of tCDOM to the total absorption coefficient  $a_{tot,\lambda}$  (m<sup>-1</sup> nm<sup>-1</sup>) (Aarnos et al., 2012). The integration was done from  $\lambda_{min}$  of 290 nm to  $\lambda_{max}$  of 750 nm.  $Q_{\lambda}$  was calculated as the product of a standard solar radiation spectrum (ASTM G173-03; Chu and Liu (2009)) normalized with global radiation and the annual mean global radiation determined for the area of each river plume examined (Hatzianastassiou et al., 2005) (See supporting information). Terrestrial CDOM was assumed to absorb all photolytic photons ( $a_{CDOM,\lambda} a_{tot,\lambda}^{-1} = 1$ ; Eq. 3). Therefore the calculated rates apply for those coastal regions, where tCDOM from rivers dominates the absorption of photolytic solar radiation (e.g. river plumes).

### 2.6 The production of BLPs based on photobleaching

The annual production of BLPs from tCDOM of each river in coastal ocean was estimated from the relationship between BLPs and photobleaching. Photobleaching was assumed to be the only sink for tCDOM discharged by rivers to coastal ocean (Nelson and Siegel, 2013). In this case, the amount of photobleached tCDOM equals the tCDOM flux by the rivers. The annual tCDOM fluxes for Lena, Mississippi and St. Lawrence rivers were taken from the literature (Stedmon et al., 2011; Spencer et al., 2013) and converted to  $a_{CDOM,300}$  flux with spectral slope coefficients reported for Lena by Stedmon et al. (2011) and measured for Mississippi (17.6  $\mu\text{m}^{-1}$ ) and St. Lawrence (16.3  $\mu\text{m}^{-1}$ ) in the present study. In the absence of published fluxes for the remaining rivers, the annual tCDOM fluxes were estimated by multiplying the measured  $a_{CDOM,300}$  with the annual water discharge (Milliman and Farnsworth, 2011). The production of BLPs supporting BP by each river (mol C yr<sup>-1</sup>) was calculated by multiplying the tCDOM flux of each river (m<sup>2</sup> yr<sup>-1</sup>) with the relationship (mol C m<sup>-2</sup>) between the BP on BLPs and photobleaching of tCDOM at 300 nm. The BR on BLPs was calculated from the mean BGE on BLPs (BR= BP/BGE-BP).

**Table 1.** Locations and dates for sampling. City refers to a location close to the site of sampling given by coordinates. Transport time expresses the days elapsed between the sampling and the arrival of the sample to laboratory.

River	Location		Date			
	Country	City	Latitude	Longitude	Sampling	Transport time
Rio Negro*	Brazil	Manaus	03°07'59"S	59°54'09"W	3 June 2010	82
Rio Solimões*	Brazil	Manaus	03°07'58"S	59°54'04"W	3 June 2010	82
Congo	Congo	Kinshasa	04°18'18"S	15°28'32"E	1 May 2009	25
Danube	Romania	Tulcea	45°13'38"N	28°44'50"E	19 Apr. 2010	21
Ganges-Brah.**	Bangladesh	Dhaka	23°34'12"N	90°10'53"E	1 Oct. 2009	68
Lena	Russia	Tiksi	71°54'14"N	127°15'16"E	16 Aug. 2009	155
Mekong	Kambodza	Phnom Penh	11°33'28"N	104°56'53"E	21 Aug. 2009	34
Mississippi	USA	New Orleans	29°02'20"N	89°19'20"W	22 Apr. 2009	34
Paraná	Argentina	Buenos Aires	34°18'07"S	58°32'47"W	29 Mar. 2009	18
St. Lawrence	Canada	Quebec	46°54'45"N	70°52'32"W	12 Jun. 2009	33
Yangtze	China	Shanghai	31°45'49"N	121°2'22"E	7 Sep. 2009	17

\*Amazon river sample was prepared by mixing samples from Rio Negro (25%) and Rio Solimões (75%)

\*\*Ganges-Brahmaputra

**Table 2.** Absorption coefficients of chromophoric dissolved organic matter at wavelength 300 nm ( $a_{\text{CDOM},300}; \text{m}^{-1}$ ) in the initial, the dark and the irradiated samples (mean  $\pm$  sd of three determinations), the amount of photobleaching (Dark - Irradiated) given as absorption coefficient ( $\Delta a_{\text{CDOM},300}; \text{m}^{-1}$ ) as well as the relative difference (%) between the irradiated and to dark controls ((Dark-Irradiated)/Dark).

River	$a_{\text{CDOM},300}$			Photobleaching	
	Initial	Dark	Irradiated	$\Delta a_{\text{CDOM},300}$	(Dark-Irradiated)/Dark (%)
Amazon	13.06 $\pm$ 0.03	12.92 $\pm$ 0.02	5.97 $\pm$ 0.02	6.95 $\pm$ 0.04	54 $\pm$ 0.1
Congo	21.61 $\pm$ 0.03	21.54 $\pm$ 0.03	9.12 $\pm$ 0.03	12.42 $\pm$ 0.06	58 $\pm$ 0.1
Danube	4.08 $\pm$ 0.03	3.79 $\pm$ 0.01	1.73 $\pm$ 0.02	2.06 $\pm$ 0.03	54 $\pm$ 0.4
Ganges-Brah*	1.08 $\pm$ 0.03	1.12 $\pm$ 0.03	0.64 $\pm$ 0.03	0.48 $\pm$ 0.06	43 $\pm$ 1.1
Lena	10.92 $\pm$ 0.04	10.86 $\pm$ 0.02	5.22 $\pm$ 0.03	5.64 $\pm$ 0.05	52 $\pm$ 0.2
Mekong	2.41 $\pm$ 0.02	2.41 $\pm$ 0.01	1.21 $\pm$ 0.03	1.20 $\pm$ 0.04	50 $\pm$ 1.0
Mississippi	5.90 $\pm$ 0.05	6.01 $\pm$ 0.05	2.79 $\pm$ 0.04	3.22 $\pm$ 0.09	54 $\pm$ 0.3
Paraná	4.49 $\pm$ 0.08	4.48 $\pm$ 0.01	2.70 $\pm$ 0.01	1.78 $\pm$ 0.02	40 $\pm$ 0.1
St. Lawrence	6.39 $\pm$ 0.17	6.29 $\pm$ 0.07	3.12 $\pm$ 0.16	3.17 $\pm$ 0.23	50 $\pm$ 2.0
Yangtze	2.57 $\pm$ 0.05	2.63 $\pm$ 0.08	1.26 $\pm$ 0.03	1.37 $\pm$ 0.15	52 $\pm$ 0.3

\*Ganges-Brahmaputra

Finally, the total production of BLPs ( $\text{mol C yr}^{-1}$ ) was obtained as a sum of BR and BP on BLPs.

## 2.7 Statistical analysis

Statistical differences between the irradiated and the dark control samples were tested with two-tailed paired t-tests (heteroscedastic). We used linear regression to evaluate the relationship between photobleaching and BP based on BLPs. All statistical analyses were carried out using R-language (R Core Team, 2014).

## 3 Results

### 3.1 Photobleaching of tCDOM in a seawater matrix

When 0.2  $\mu\text{m}$  filtered river waters without labile tDOC (Table 1) were mixed with artificial seawater and irradiated, the simulated solar radiation photobleached tCDOM at 300 nm ( $a_{\text{CDOM},300}$ ) by  $50.4 \pm 2.6\%$  (mean  $\pm$  sd; Table 2). The amount of photobleaching expressed as absorption coefficient ranged from  $0.48 \pm 0.06 \text{ m}^{-1}$  (Ganges-Brahmaputra) to  $12.42 \pm 0.06 \text{ m}^{-1}$  (Congo) when calculated as the difference in  $a_{\text{CDOM},300}$  between the dark control and the irradiated samples ( $\Delta a_{\text{CDOM},300}$ , Table 2).

### 3.2 Bacterial production

In order to assess the bacterial production (BP) on the irradiated and the dark control non-labile tDOC, we introduced an

**Table 3.** Bacterial cell densities ( $10^9$  cells  $L^{-1}$ , mean  $\pm$  sd of two replicates) in the beginning of bioassay ( $t = 0$ ) and at the time of maximum cell density in the irradiated (Irradiated) samples and in the dark control samples (Dark), the time of maximal density (in days) and the relative increase in the density based on BLPs: ((Irradiated-Dark)/Dark (%))

River	Cell density			Time of max density	
	$t = 0$	Dark	Irradiated	(d)	(%)
Amazon	0.01	$0.67 \pm 0.02$	$1.54 \pm 0.04$	8	$130 \pm 01$
Congo	0.03	$1.89 \pm 0.04$	$4.01 \pm 0.12$	5	$112 \pm 02$
Danube	0.02	$0.50 \pm 0.02$	$1.04 \pm 0.02$	8	$108 \pm 04$
Ganges-Brah*	0.02	$0.48 \pm 0.03$	$0.73 \pm 0.07$	5	$52 \pm 05$
Lena	0.03	$0.36 \pm 0.07$	$0.48 \pm 0.04$	6	$33 \pm 15$
Mekong	0.02	$0.64 \pm 0.06$	$1.00 \pm 0.04$	12	$56 \pm 08$
Mississippi	0.02	$1.58 \pm 0.03$	$2.53 \pm 0.15$	10	$60 \pm 06$
Paraná	0.24	$0.80 \pm 0.03$	$1.09 \pm 0.03$	9	$36 \pm 01$
St. Lawrence	0.03	$0.59 \pm 0.01$	$0.87 \pm 0.00$	12	$47 \pm 01$
Yangtze	0.03	$0.64 \pm 0.06$	$1.08 \pm 0.02$	9	$69 \pm 13$

\*Ganges-Brahmaputra

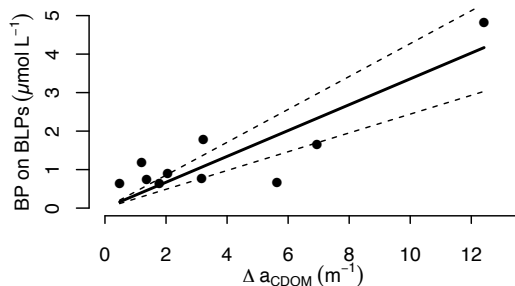


**Figure 1.** The relationship between the bacterial production based on biologically labile photoproducts (BP on BLPs) and the photobleached CDOM at 300 nm ( $\Delta a_{\text{CDOM},300}$ ). Dots show individual samples, the solid line is a linear fit and the dotted lines show the 95% confidence intervals of linear fit. The solid line shows a linear model without an intercept:  $\text{BP on BLPs} = b \Delta a_{\text{CDOM},300}$ . The model had  $R^2 = 0.87$  and a highly significant ( $F_{1,9} = 68.7$ ,  $p < 0.001$ ) regression coefficient  $b = 0.336 \pm 0.040 \text{ mmol C m}^{-2}$ , where the error represents 95% confidence interval. A model without an intercept was selected, because a linear model with an intercept had worse fit ( $R^2 = 0.72$ ) and the intercept was not statistically different from zero ( $t_{1,8} = 0.67$ ,  $p = 0.52$ ).

inoculum of riverine bacterioplankton to the irradiated and the dark control samples resulting in the bacterial cell densities from  $0.006$  to  $0.240 \times 10^9$  cells  $L^{-1}$  ( $t = 0$  in Table 3). The bacteria increased their densities by one to two orders of magnitude in five to 12 days (compared to initial densities) and grew (Table 3) from 33% to 130% more in the irradiated tDOC than in the dark controls (Table 3).

The bacterial cell densities were converted to biomasses by accounting for the bacterial cell volumes, which were not different between the dark control and the irradiated sam-

ples (paired t-test,  $df = 9$ ,  $p > 0.05$ ). In the dark controls, the accumulated BP ranged from  $0.5 \pm 0.1$  (Lena) to  $3.9 \pm 0.2$  (Congo)  $\mu\text{mol C L}^{-1}$  (Figure 2). BP was higher in the irradiated than in the dark control samples (paired t-test,  $df = 9$ ,  $p = 0.003$ ) and ranged from  $1.2 \pm 0.1$  (Lena) to  $8.7 \pm 0.6$  (Congo)  $\mu\text{mol C L}^{-1}$  (Figure 2). BP on BLPs, ranged from  $0.6 \pm 0.3$  (Ganges-Brahmaputra) to  $4.8 \pm 0.8$  (Congo)  $\mu\text{mol C L}^{-1}$ , calculated as the difference between the irradiated and the dark control samples (Figure 2). The BP on BLPs was significantly dependent on the photobleaching by a linear regression coefficient of  $0.336 \pm 0.040 \text{ mmol C m}^{-2}$ , where the error represents 95% confidence interval for the regression coefficient (details in Figure 1).

### 3.3 Bacterial respiration

In the dark controls, bacterial respiration (BR) accumulated usually linearly with time indicating relatively constant rates of respiration throughout the bioassays (Figure 3). In the irradiated samples, the kinetics of BR was different and the rates typically higher than in the dark control samples (Figure 3). The BR on BLPs (Figure 4) was calculated from the difference in respiration between the irradiated and the dark control samples (Figure 3). After a lag-phase, BR on BLPs typically accumulated rapidly, but leveled off at the late phase of bioassay (Figure 4). The BR on BLPs accumulated by the time of maximum biomass was undetectable ( $-1.4 \pm 1.39 \mu\text{mol C L}^{-1}$ ) with Ganges-Brahmaputra BLPs and highest ( $27.8 \pm 1.33 \mu\text{mol C L}^{-1}$ ) with Yangtze BLPs (Figure 4).

### 3.4 Bacterial growth efficiency

When BGE was calculated from the biomass (Figure 2) and the respiration gained by the time of maximum biomass (Figure 3, 4), it was lowest 3.0% and highest 27.7% in the irradiated DOC from Yangtze and Ganges-Brahmaputra, respec-

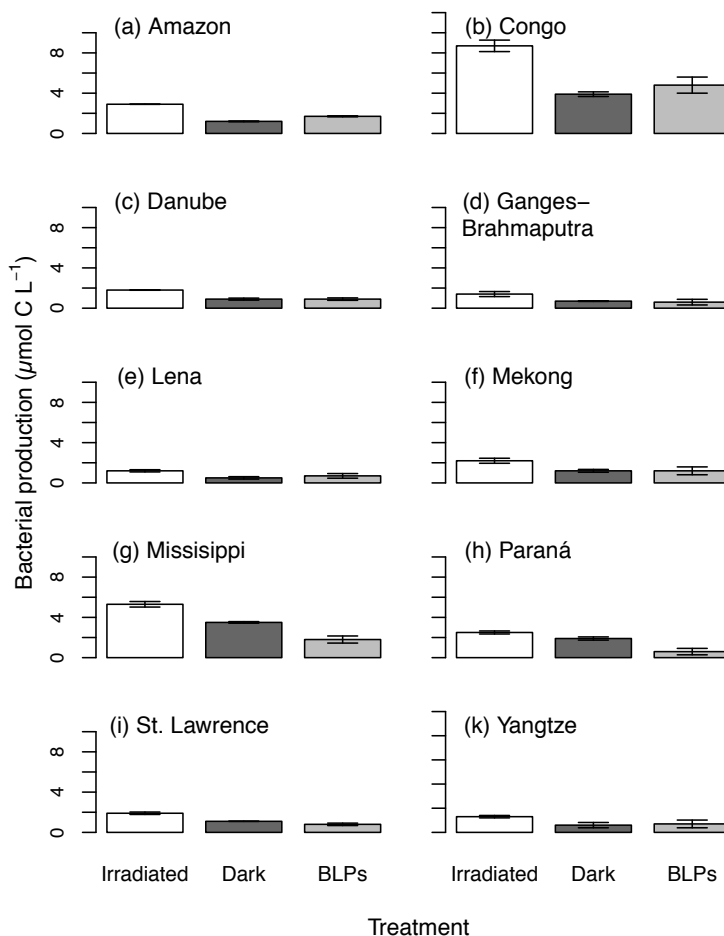


**Figure 2.** Bacterial production ( $\mu\text{mol C L}^{-1}$ ; mean  $\pm$  sd,  $n = 2$ ) on the irradiated DOC (Irradiated), on the dark control DOC (Dark) and on BLPs, the latter calculated as the difference between the treatments (BLPs = Irradiated-Dark) by the end of logarithmic growth phase specified in Table 3

tively, while in the dark controls BGE ranged from 3.6% (Yangtze) to 15.3% (Amazon) (Table 4). BGE on BLPs ranged from 2.8% (Yangtze) to 21.5% (Amazon) (Table 4). The BGEs were not different among the irradiated DOC, the 435 dark control DOC or BLPs (paired t-test,  $df = 7$ ,  $p > 0.05$ ) (Table 4).

### 3.5 Apparent quantum yields and production rates of BLPs

When the BP on BLPs (Figure 2) was divided by the 430 spectrum of photons absorbed during the irradiation, the spectral AQY for the production of BLPs supporting BP

( $\text{AQY}_{\text{BP},\lambda}$ ; Eq. 2) was defined by the parameters  $c$  and  $d$  shown in Table 5. Based on these parameters, the calculated  $\text{AQY}_{\text{BP}}$  ranged from 9.5 to 76 with median of 36.1  $\mu\text{mol C mol photons}^{-1}$  at 330 nm, a wavelength of solar radiation responsible for highest production of BLPs (Table 5) (Miller et al., 2002; Vähätalo et al., 2011; Aarnos et al., 2012). The corresponding values for the production of BLPs supporting BR ( $\text{AQY}_{\text{BR},330}$ ) ranged from 57 to 1203 with median of 186  $\mu\text{mol C mol photons}^{-1}$  (Table 5).

In the river plumes, the annual production of BLPs supporting BP ranged from 1.0 (Lena) to 33  $\text{mmol C m}^2 \text{ yr}^{-1}$  (Ganges-Brahmaputra) (Table 6) when calculated (Eq. 3) with  $\text{AQY}_{\text{BP},\lambda}$  (Table 5) and the local annual mean solar irra-

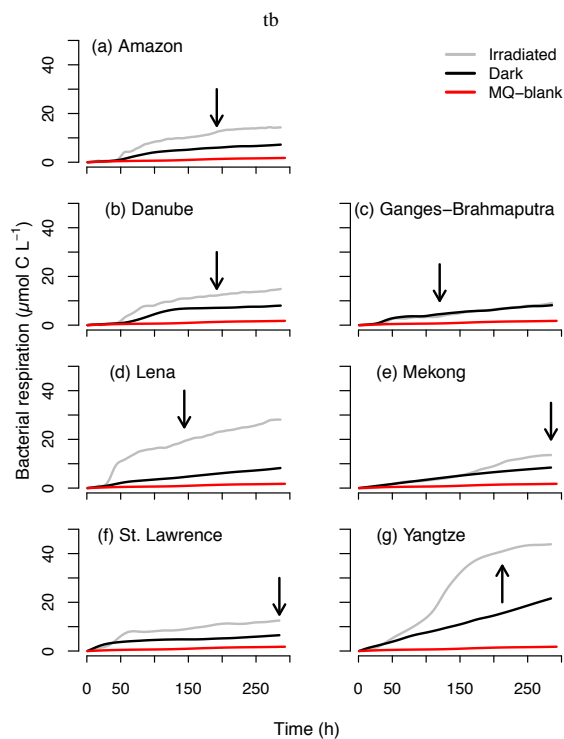


**Figure 3.** Cumulative bacterial respiration during the bioassay in the irradiated (gray line; Irradiated), and dark control samples (black line; Dark). Red line shows corresponds to an apparent decline of O<sub>2</sub> in the MQ-blank experiment (MQ-blank) and black arrows point out the end of log-phase in the irradiated samples (Table 3). In panel c) irradiated and dark lines are overlapping.

**Table 4.** Bacterial growth efficiency (%) (mean ± sd) on the irradiated DOC, the dark control DOC and on BLPs. BGE was calculated from BP (Figure 2) and BR (Figures 3,4). NA = not available.

River	BGE (%)		
	Irradiated	Dark	BLPs
Amazon	18.8 ± 0.7	15.3 ± 1.0	21.5 ± 2.0
Danube	12.8 ± 0.7	11.2 ± 0.1	15.5 ± 1.3
Ganges-Brah.*	27.7 ± 2.5	13.4 ± 1.7	NA
Lena	5.8 ± 0.1	9.9 ± 0.4	4.5 ± 0.9
Mekong	14.0 ± 0.2	12.5 ± 3.5	15.8 ± 4.5
St. Lawrence	13.2 ± 1.7	14.5 ± 2.1	12.0 ± 4.5
Yangtze	3.0 ± 0.2	3.6 ± 1.0	2.8 ± 1.1
Average	13.6 ± 8.1	11.5 ± 3.9	12.0 ± 7.2

\*Ganges-Brahmaputra

dianc in the coastal ocean at the front of each river. The corresponding production of BLPs supporting BR ranged from 19 (St Lawrence) to 574 mmol C m<sup>-2</sup> yr<sup>-1</sup> (Yangtze) (Ta-

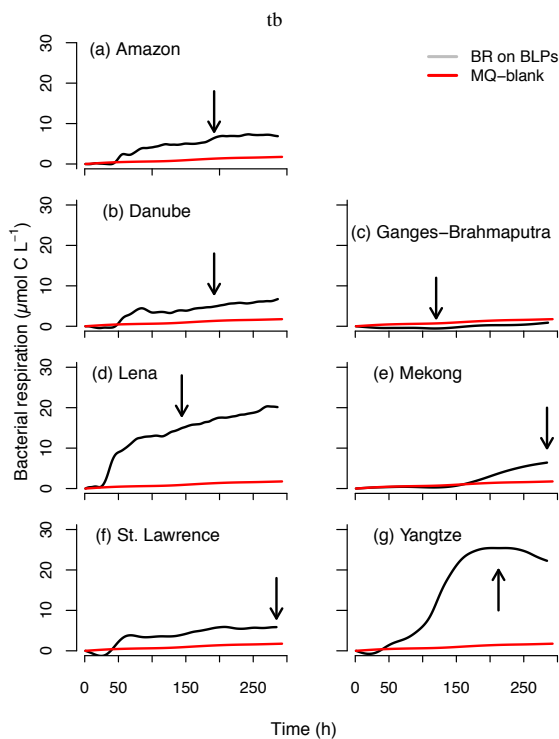


**Figure 4.** Cumulative bacterial respiration based on BLPs (BR on BLPs) calculated from Figure 3 as the difference between irradiated and dark. Further details found in Figure 3.

ble 6). The total production of BLPs ranged from 21 (St Lawrence) to 584 mmol C m<sup>-2</sup> yr<sup>-1</sup> (Yangtze) when calculated as the sum of BLPs supporting BP and BR (Table 6).

### 3.5.1 An estimate for the global production of BLPs

The relationship between BP on BLPs and  $\Delta a_{\text{CDOM},300}$  (Fig 1) was multiplied with the annual tCDOM fluxes (Table 7) to estimate the photobleaching of tCDOM and the related production of BLPs from non-labile tDOC of each river in the coastal ocean. The photobleaching of tCDOM fluxes was calculated to promote altogether  $1.14 \pm 0.3$  Tg C yr<sup>-1</sup> BP on BLPs (mean ± 95% confidence interval correspond that of linear regression, Fig. 1; Table 7). The corresponding amount of BR on BLPs was  $9.5 \pm 4.8$  Tg C yr<sup>-1</sup> when accounting for the 12.0% BGE on BLPs (Table 7). The sum of BP and BR on BLPs was  $10.6 \pm 4.5$  Tg C yr<sup>-1</sup> representing the total production of BLPs (Table 7). This total production of BLPs corresponds to  $15 \pm 6.8\%$  of the total DOC flux ( $69$  Tg C yr<sup>-1</sup>) of examined rivers (Table 7). Assuming that the rivers examined responsible for 28% of global tDOC flux (Cai, 2011) are representative for the remaining 72% tDOC

**Table 5.** The apparent quantum yields for the production of BLPs supporting bacterial production and respiration at 330 nm ( $\mu\text{mol C mol absorbed photons}^{-1}$ ), as well as the parameters  $c$  and  $d$  ( $\text{nm}^{-1}$ ) for the calculation of spectral AQYs (Eq. 2).

River	BP			BR		
	AQY <sub>BP,330</sub>	$c$	$d$	AQY <sub>BR,330</sub>	$c$	$d$
Amazon	18.6	0.44	0.0305	56.5	0.57	0.0279
Congo	42.0	0.52	0.0286	-	-	-
Danube	35.9	0.49	0.0289	147.8	0.66	0.0255
Ganges-Brah*	75.7	0.59	0.0271	-	-	-
Lena	9.9	0.37	0.0319	186.2	0.73	0.0251
Mekong	60.8	0.57	0.0277	269.6	0.78	0.0241
Mississippi	56.1	0.57	0.0280	-	-	-
Paraná	20.1	0.41	0.0301	-	-	-
St.Lawrence	9.5	0.37	0.0320	71.5	0.59	0.0273
Yangtze	36.2	0.49	0.0289	1203.6	1.03	0.0205

\*Ganges-Brahmaputra, "-" not determined

**Table 6.** Calculated annual production of biologically labile photoproducts ( $\text{mmol C m}^{-2} \text{yr}^{-1}$ ) supporting bacterial production (BP on BLPs) and respiration (BR on BLPs) separately as well as their sum (BLPs). For these calculations, Eq. 3 received AQY<sub>BP, $\lambda$</sub>  or AQY<sub>BR, $\lambda$</sub>  from Table 5 and the spectral annual global radiation in the front of rivers examined.

River	BP on BLPs	BR on BLPs	BLPs
Amazon	8.1	27.8	35.9
Congo	20.0	-	-
Danube	9.4	46.7	56.1
Ganges-Brahmaputra	32.6	-	-
Lena*	1.0	25.8	26.8
Mekong	24.2	132.1	156.3
Mississippi	22.1	-	-
Paraná	6.4	-	-
St.Lawrence	2.0	18.9	20.9
Yangtze	10.2	573.8	584.0

\* "-" = not determined

\*the attenuation of solar radiation by sea ice ignored.

flux to ocean, the estimate for the global coastal production<sup>485</sup> of BLPs from tDOC is  $38.0 \pm 15.9 \text{ Tg C yr}^{-1}$  supporting  $4.1 \pm 1.1 \text{ Tg C yr}^{-1}$  BP and  $33.9 \pm 16.9 \text{ Tg C yr}^{-1}$  BR.

## 4 Discussion

### 4.1 Global fluxes of BLPs from tDOC

Our study estimates the production of BLPs from tDOC in the coastal waters in the front of ten major rivers across five continents. Our extrapolation to the BLPs from tDOC<sup>495</sup> in global coastal ocean ( $38.0 \pm 15.9 \text{ Tg C yr}^{-1}$ ) contributes little to the production of BLPs in global coastal waters estimated earlier ( $206 \text{ Tg C yr}^{-1}$ ) (Miller et al., 2002). The earlier estimate is nearly as large as global riverine tDOC flux to the ocean ( $246 \text{ Tg C yr}^{-1}$ ) (Cai, 2011) and must include<sup>500</sup> BLPs from marine DOC. Similarly, BLPs were concluded to originate from both marine DOC and tDOC in the Baltic Sea (Aarnos et al., 2012). Although samples collected from coastal waters are most relevant for assessing the coastal pho-

tochemical transformation of DOC, it is difficult to separate the transformation of tDOC from that of marine DOC. The experimental design of present study allows to set the focus only on the photochemical transformation of tDOC in the coastal waters.

According to the present study, a typical BGE on BLPs is 12% and thus the majority of assimilated BLPs will be respired to dissolved inorganic carbon (DIC) totaling  $33.9 \pm 16.9 \text{ Tg C yr}^{-1}$  in the global coastal waters. This amount provides an indirect terrestrial source of DIC to coastal ocean in addition to the riverine flux of DIC ( $407 \text{ Tg C yr}^{-1}$ ) (Cai, 2011)). This study estimates that BLPs from tDOC support  $4.1 \pm 1.1 \text{ Tg C yr}^{-1}$  of BP in the global coastal waters. This BP is not alone a source of carbon to food webs, but is associated with nitrogen (N) and phosphorus (P) bound in bacterial biomass (Smith and Benner, 2005; Vähätalo et al., 2011). Assuming stoichiometric amounts of N and P associated to bacterial biomass (mass C:N:P ratio of 17:4:1) (Goldman et al., 1987), the assimilation of BLPs from terrestrial tDOC transfers  $4.1 \text{ Tg C yr}^{-1}$ ,

**Table 7.** The absorption coefficient of CDOM at 300 nm, water discharge, CDOM and tDOC fluxes, bacterial production (BP) and respiration (BR) based on BLPs, the total amount of BLPs and the fraction of BLPs from the tDOC flux.

River	$a_{\text{CDOM},300}$	discharge	CDOM flux	tDOC flux	BP based on BLPs	BR based on BLPs	BLPs (BP+BR)	$\frac{\text{BLPs}}{\text{DOC}}$
	( $\text{m}^{-1}$ )	( $\text{km}^3 \text{yr}^{-1}$ )	( $\text{Gm}^2 \text{yr}^{-1}$ )	( $\text{Tg C yr}^{-1}$ )	(fraction)			
Amazon	26.4	6300	166320	37.5	0.670	5.583	6.235	0.17
Congo	49.4	1300	64220	10.2	0.259	2.156	2.415	0.24
Danube	7.6	210	1596	0.6	0.006	0.054	0.060	0.10
Ganges-Brah*	2.1	1120	2352	3.6	0.009	0.079	0.088	0.02
Lena	21.2	520	27818	3.6	0.112	0.934	1.046	0.29
Mekong	5.1	550	2805	0.9	0.011	0.094	0.105	0.12
Mississippi	11.6	490	8800	3.5	0.035	0.295	0.331	0.09
Paraná	8.4	530	4452	5.9	0.018	0.149	0.167	0.03
St. Lawrence	12.0	340	612	1.6	0.002	0.021	0.023	0.01
Yangtze	5.0	900	4500	1.8	0.018	0.151	0.169	0.09
Total		12260	283475	69.06	1.142	9.516	10.658	
Average**	23.1							0.15

$a_{\text{CDOM},300}$  refers to the measured values from the water samples upon their arrival, water discharge from Milliman and Farnsworth (2011), CDOM fluxes are calculated as the product of  $a_{\text{CDOM},300}$  and water discharges, but for Mississippi, St. Lawrence and Lena published CDOM fluxes were used (Stedmon et al., 2011; Spencer et al., 2013). DOC flux is from Cauwet (2002) but updated for Amazon (Coynel et al., 2005) and calculated for Mekong as the product of water discharge and DOC measured ( $1.58 \text{ mg L}^{-1}$ ) upon arrival of the Mekong sample, BP on BLPs is calculated from CDOM flux using the slope  $0.336 \text{ mmol C m}^{-2}$  (Figure 1), BR is calculated using BGE of 12.0% on BLPs.

\*Ganges-Brahmaputra, \*\*discharge weighted average

505 1.06  $\text{Tg N yr}^{-1}$  and 0.26  $\text{Tg P yr}^{-1}$  to the coastal food webs 535  
through the grazers of bacterioplankton.

#### 4.2 Phototransformation of tDOC in inland vs. coastal waters

510 The annual production of BLPs from tDOC in the global  
coastal waters ( $38.0 \pm 15.9 \text{ Tg C yr}^{-1}$ ) estimated in this  
study is larger than the global photochemical production  
of DIC (from 13 to 35  $\text{Tg C yr}^{-1}$ ) in lakes and reservoirs  
(Koehler et al., 2014). This comparison indicates that al-  
545 though solar radiation transforms a remarkable amount of  
tDOC in lakes and reservoirs, a major part of tDOC is photo-  
515 transformed in the coastal waters.

Although the photoreactivity of DOC and thus the rates of  
phototransformation per area or volume are generally higher  
550 in fresh than in marine waters (Minor et al. (2006); White  
et al. (2010); Aarnos et al. (2012) and references therein)  
several factors limit phototransformation in inland waters.  
Freshwaters (streams in particular) can be shaded by ripar-  
555 ian vegetation and receive down to 1% of solar radiation  
incident to unshaded marine waters (Vähätalo et al., 2005).  
525 Photolytic solar ultraviolet radiation (UVR) attenuates often  
faster (even within a few centimeters) in fresh waters than  
in marine waters beyond turbid estuaries, where it can pen-  
560 etrate up to tens of meters (Cloern, 1987; Vähätalo et al.,  
2000; Kuivikko et al., 2007). The steep attenuation of UVR  
530 in freshwaters is primarily caused by tDOC itself or more  
precisely by tCDOM part of it (Morris et al., 1995). Addi-  
tionally, eroded particulate matter (e.g., clay) can attenuate  
UVR effectively in rivers in particular (Davies-Colley and  
565 Smith, 2001).

Accounting for the major role of CDOM for the attenua-  
tion of UVR, it is instructive to evaluate its content in fresh  
and marine waters. One representative value for freshwater  
 $a_{\text{CDOM},300}$  can be considered to be  $23.1 \text{ m}^{-1}$ , the mean for  
rivers examined in this study (Table 7). These rivers integrate  
the water quality from their catchments covering 25% of the  
land and have the mean DOC of  $5.6 \text{ mg CL}^{-1}$ , which is  
close to the mean of  $5.7 \text{ mg CL}^{-1}$  for 7500 lakes distributed  
over six continents (Sobek et al. (2007); Table 7). A repre-  
sentative oceanic  $a_{\text{CDOM}}$  at 325 nm can be considered to be  $0.12$   
 $\text{m}^{-1}$ , an approximate mean of 1276 measurements across the  
Atlantic and the Pacific Ocean (Nelson and Siegel, 2013).  
Accounting for the spectral slope of  $18 \mu\text{m}^{-1}$ , a representa-  
540 tive freshwater  $a_{\text{CDOM},325}$  can be calculated to be  $14.7 \text{ m}^{-1}$   
and 123-fold higher than the corresponding oceanic value  
(Nelson and Siegel, 2013). If attenuated by  $a_{\text{CDOM},325}$  alone,  
UVR at 325 nm from the zenith will be reduced to 1% of sur-  
face values at the depth of 0.31 m and 38 m in representative  
fresh and in oceanic water, respectively. UVR at 325 nm is a  
relevant wavelength for photochemistry, because it is close to  
e.g., a median wavelength of 330 nm responsible for the pro-  
duction of BLPs (Miller et al., 2002; Vähätalo et al., 2011;  
Aarnos et al., 2012). For representative freshwater, the pho-  
tochemical transformation of tDOC would be limited mostly  
( $> 99\%$ ) to the depths shallower than 0.31 m. Such a shal-  
low depth ( $< 0.3 \text{ m}$ ) of photolytic layer have been found in  
many lakes (Salonen and Vähätalo, 1994; Amon and Ben-  
545 ner, 1996; Granéli et al., 1996; Reitner et al., 1997; Vähätalo  
et al., 2000; Pers et al., 2001; Aarnos et al., 2012), in the  
Amazon River (Amon and Benner, 1996) and in a freshwater  
end of estuary (Pullin et al., 2004). In these previous studies,

the depth of photolytic layer has been  $\leq 15\%$  from the depth of mixing layer or the mean depth (Salonen and Vähätalo, 1994; Amon and Benner, 1996; Granéli et al., 1996; Reitner et al., 1997; Vähätalo et al., 2000; Pers et al., 2001; Pullin et al., 2004; Aarnos et al., 2012). These studies also demonstrate that the majority ( $\geq 85\%$  in the examples above) of tDOC in inland waters can reside below the photolytic layer, where phototransformation is negligible.

The photochemistry of tDOC in inland water can be also limited by high loadings of tDOC and relatively short residence times of tDOC. For example, photochemical reactions mineralize DOC in Swedish lakes from 1.2 to 6 g C m<sup>-2</sup> lake area yr<sup>-1</sup> (Koehler et al., 2014). In comparison, Swedish lakes receive 30 to 341 g tDOC m<sup>-2</sup> lake area yr<sup>-1</sup> when calculated from the export (2.3 to 26.2 g C m<sup>-2</sup> catchment area yr<sup>-1</sup>) Wallin et al. (2015) and the drainage ratio of 13, which relates the area of catchment (land + water) to the area of water (Algesten et al., 2004). The drainage ratio of lakes on non-glaciated land is 27 (Verpoorter et al., 2014) indicating that tDOC loading from catchments to inland waters is high also globally. Although the photochemical sink of tDOC is important in lakes with a deep photolytic layer relative to mean depth (Molot and Dillon, 1997) and with a long residence time of tDOC (Molot and Dillon, 1997; Müller et al., 2013), high loadings of tDOC can offset the photochemical sink of tDOC in lakes (Vähätalo et al., 2002; Müller et al., 2013). For example, photobleaching turns over the tCDOM content of epilimnion during a summer stratification period in a humic Lake Valkea-Kotinen but the input of tCDOM from the catchment more or less compensates these losses (Vähätalo et al., 2002). Similarly, in a chain of hydrologically connected lakes, the photochemical losses of tDOC in the upper lakes are offset by the tDOC input to the lakes lower in the chain (Müller et al., 2013). The residence time of tDOC is shortest in rivers, where the photochemical sink is considered nearly negligible relative to the input of tDOC from upstream, which is quickly transported downstream towards the ocean (Amon and Benner, 1996; Riggsbee et al., 2008). Thus, the coastal ocean receives roughly 10<sup>15</sup> m<sup>2</sup> yr<sup>-1</sup> photoreactive tDOC quantified as a<sub>CDOM,300</sub> when upscaling the estimated tCDOM flux of studied rivers (Table 7) to a global scale.

The coastal ocean beyond the turbid estuaries provides favorable conditions for the phototransformation of tDOC for several reasons. Because density is lower for river water than seawater, river water will mix with seawater at the sunlit surface layer of water column without shading by riparian vegetation (Vodacek et al., 1997; Del Vecchio and Subramaniam, 2004; Fichot and Benner, 2014). The drainage ratio for the ocean is 1.3 (calculated from Table 2.4 in Milliman and Farnsworth (2011)) and tDOC loading to the ocean is much lower than to the inland waters. The dilution of the freshwater end member (a<sub>CDOM,325</sub> = 14.7 m<sup>-1</sup>) with the oceanic end member (a<sub>CDOM,325</sub> = 0.12 m<sup>-1</sup>) will increase the exposure of tDOC to photolytic solar radiation in the deeper depths of

water column (Vodacek et al., 1997; Del Vecchio and Subramaniam, 2004). Mixing includes a lateral transport (i.e., advection) of tDOC offshore, spreads tDOC over an increasing area of sunlit waters and increases the phototransformation of tDOC (Vodacek et al., 1997; Medeiros et al., 2015). Global rivers discharge the majority of tDOC to mid and low latitude ocean (Milliman and Farnsworth, 2011), where tDOC can have a long residence time in sunlit offshore waters. In these waters, solar radiation can photobleach tCDOM completely and be the final sink for the photoreactive tDOC (Vähätalo and Wetzel, 2008; Spencer et al., 2009; Nelson and Siegel, 2013).

#### 4.2.1 BLPs, photobleaching and tCDOM fluxes

In this study, the production of BLPs is related to the photobleaching of tCDOM with a R<sup>2</sup> value of 0.87 (Figure 1). Similar relationships has been found earlier for individual or groups of BLP-compounds (Kieber et al., 1990; Bertilsson and Tranvik, 2000). For example,  $\Delta a_{\text{CDOM},300}$  explains extremely well (R<sup>2</sup> > 96%) of the photoproduction of three individual BLP-compounds: formaldehyde, acetaldehyde and glyoxylate (Kieber et al., 1990). R<sup>2</sup> was 0.67 for the relationship between a group of BLPs (carboxylic acids) and  $\Delta a_{\text{CDOM},365}$  determined for 38 Swedish lakes (Bertilsson and Tranvik, 2000). Our R<sup>2</sup>-value (Figure 1) is higher than the corresponding one for 38 lake water samples (Bertilsson and Tranvik, 2000). This is at first glance surprising since our tDOC samples were collected from ten global rivers covering many climates and types of land uses not limited to one region (Sweden) (Bertilsson and Tranvik, 2000). The relatively high R<sup>2</sup>-values in this study may be explained in part by the same chemical matrix (artificial coastal water) used in our experiments. Additionally, the rivers examined here integrate the variability of DOM across their large catchments. For example, one third of 7838 different chemical compounds assigned by ultrahigh-resolution mass spectral analysis to the water samples examined in this study were shared among all river samples ((Wagner et al., 2015)). A conclusion from this and other studies (Kieber et al., 1990; Miller and Moran, 1997; Bertilsson and Tranvik, 2000; Obernosterer and Herndl, 2000) is that the production of BLPs can be quantitatively linked the photobleaching of tCDOM, which makes it as a useful proxy for the production of BLPs.

Our estimate for the global production of BLPs from tDOC bases on an assumption that the riverine tCDOM flux will be photobleached completely in the coastal ocean. We used published tCDOM fluxes for Mississippi, St. Lawrence and Lena Rivers (Stedmon et al., 2011; Spencer et al., 2013), but for the remaining rivers the tCDOM flux was estimated simply by multiplying the measured tCDOM with the published water discharge (Table 7). This method provides only rough estimates for tCDOM fluxes and causes uncertainty also for our global estimates of BLPs. Therefore, additional data on riverine tCDOM fluxes in the future will improve our

estimate for CDOM fluxes and related production of BLPs.

675 The majority of global riverine tCDOM flux enters to the  
 mixing layer of coastal waters, where solar radiation pho-  
 tobleaches tCDOM efficiently and leaves not traces of tC-  
 DOM to be found in the surface of open ocean (review by  
 Nelson and Siegel (2013) and references therein). Our as-  
 680 sumption for complete photobleaching may not hold entirely  
 for the rivers (such as Lena in this study) discharging to the  
 Arctic Ocean, which transfer  $78\ 200\ \text{Gm}^2\ \text{yr}^{-1}$  of CDOM  
 735 to the North Atlantic (calculated for 300 nm from the slope  
 and the flux estimated by Granskog et al. (2012)). A part of  
 685 this CDOM flux is directed to the deep ocean without pho-  
 tobleaching as a part of deep water formation in the North  
 Atlantic (Nelson and Siegel, 2013). 740

#### 4.2.2 AQYs for BLPs

Our  $\text{AQY}_{\text{BP},330\text{S}}$  ( $9.5\text{--}76\ \mu\text{mol C mol photons}^{-1}$  Table 5)  
 690 overlap the range of  $\text{AQY}_{\text{BP},330}$  in the Baltic Sea (23 to 111  
 $\mu\text{mol C mol photons}^{-1}$ ) (Vähätalo et al., 2011; Aarnos et al.,  
 2012). Our  $\text{AQY}_{\text{BR},330\text{S}}$  (57 to 1204 ( $\mu\text{mol C mol photons}^{-1}$ )  
 are generally lower than the previously reported 1391  
 695 ( $\mu\text{mol C mol photons}^{-1}$ ) for Altamaha River and 1090  
 ( $\mu\text{mol C mol photons}^{-1}$ ) for water draining a salt marsh  
 (Miller et al., 2002), but similar to those for rivers and lakes  
 in Alaska (Cory et al., 2014). In the earlier studies, the  
 $\text{AQY}_{\text{BPS}}$  reported by Aarnos et al. (2012) are lower than  
 $\text{AQY}_{\text{BRS}}$  reported by Miller et al. (2002) and Cory et al.  
 700 (2014). The same can be concluded from our simultaneous  
 750 determinations of  $\text{AQY}_{\text{BP}}$  and  $\text{AQY}_{\text{BR}}$ .

In this study, BLPs were consumed by riverine bacteria,  
 which survived at the coastal salinities, increased their  
 biomass by one to two orders of magnitude and reached a  
 705 detectable peak in biomass within  $\leq 12$  days. These bacteria  
 can be considered to represent the fresh water members in  
 the whole community of coastal waters (Kisand et al.,  
 2005), which includes also marine bacteria that were absent  
 in our experiments (Pineiro et al., 2013). We assumed  
 710 that our bacterial communities consume BLPs similarly like  
 full coastal communities, because the bioavailability of DOC  
 rather than the community composition determines the con-  
 sumption of DOC by bacteria (Judd et al., 2006). Further re-  
 search is needed to assess potential differences in the con-  
 715 sumption of BLPs between full and freshwater members of  
 coastal bacterial communities. 765

Although our bioassays for the determination of BLPs  
 lasted up to 12 days, the initial cell densities of inoculum  
 were low and typical densities found in surface waters were  
 720 not found until the end of bioassay (Table 3). The  $\text{AQY}_{\text{BR},330}$   
 of Miller et al. (2002) are generally higher than found in the  
 present study (Table 5, 6). Possible explanations for the dif-  
 ference in  $\text{AQY}_{\text{BR},330}$  are long irradiation time in our study  
 and a thousand-times larger bacterial inoculum in an earlier  
 725 study Miller et al. (2002). Additionally the bioassay of Miller  
 et al. (2002) lasted 14 days and longer than  $\leq 12$  days in the

present study. The bacteria used by Miller et al. (2002) were  
 able to assimilate BLPs extensively resulting in higher AQYs  
 than in our study.

BLPs include numerous individual compounds (Moran  
 and Zepp, 1997; Vähätalo, 2009; Rossel et al., 2013). The  
 BLPs determined in this study likely represent the most  
 bioavailable fraction of BLPs (Kieber and Mopper, 1987).  
 We cannot exclude a possibility that some BLPs degraded  
 photochemically further to  $\text{CO}_2$  during our irradiations  
 (Bertilsson and Tranvik, 1998). The number of known chemi-  
 cally distinct BLP-compounds was 14 in an early review  
 (Moran and Zepp, 1997), but had increased to 44 in a later re-  
 view (Vähätalo, 2009). A recent study identified 1835 chemi-  
 cal compounds that were produced by photochemical reac-  
 tions (Rossel et al., 2013). From these formulae 44% were  
 not observed in a treatment with high microbial activity indi-  
 cating that the number of BLP-compounds was 807 (Rossel  
 et al., 2013). As the present study refers to the most bioavail-  
 able fraction of BLPs, the entire pool of BLPs is likely larger  
 than what was measured in this study. Therefore, our pro-  
 duction estimates for BLPs from tDOC in the coastal waters  
 (Table 5, 6, 7) should be treated as minimum estimates.

#### 4.2.3 BGEs on BLPs and non-labile tDOC

Our BGE on BLPs ( $12.0 \pm 7.2\%$ ; Table 4) provides the first  
 direct estimate for the BGE of microbial communities on a  
 group of compounds classified as BLPs. Our values can be  
 compared to BGEs reported for single BLP-compounds such  
 as acetic and formic acids (Bertilsson and Tranvik, 1998;  
 Remington et al., 2011). BGEs on formic and acetic acids  
 has been 2% and 41%, in one study (Bertilsson and Tran-  
 vik, 1998), but 20–27% and 73–80%, respectively, in another  
 study (Remington et al., 2011). The earlier studies demon-  
 strate that BGE on a single BLP compound can vary and thus  
 it is a challenge to determine BGE separately for each BLP  
 compound and compile them together for an overall BGE on  
 all BLPs. Such a simple overall BGE ( $12.0 \pm 7.2\%$ ) can now  
 be applied on BLPs based on the results of the present study.

Our BGE on tDOC in the dark controls ( $11.5 \pm 3.9\%$ , Ta-  
 ble 4) represents an estimate for BGE on non-labile tDOC in  
 coastal waters. This estimate falls to the lower range of hun-  
 dreds BGE determinations done with freshly collected wa-  
 ter representing BGEs primarily on labile DOC (del Giorgio  
 and Cole, 1998). Our BGE on non-labile tDOC is similar to  
 BGE (mean 11%) on tDOC aged for 100 to 450 days (As-  
 mala et al., 2014). An extensive aging of humic lake water by  
 6 years resulted in BGEs of 5–6% (Kragh et al., 2008). The  
 results of this (Fig 2, 3; Table 3, 4) and earlier studies (Kragh  
 et al., 2008; Vähätalo et al., 2010; Asmala et al., 2014) em-  
 phasize that bacteria can assimilate non-labile tDOC, but  
 with a relatively low BGE.

## 5 Conclusions

Our study was designed to assess the photochemical transformation and the microbial consumption of non-labile tDOC in coastal waters. The non-labile fraction represents the majority (typically >80%) of tDOC, which is expected to be photochemically transformed primarily in transparent offshore waters beyond turbid estuaries after the consumption of labile tDOC. Our study shows that bacteria will continue the assimilation of tDOC after the consumption of labile fraction but with a low BGE. Solar radiation-induced photochemical reactions transform non-labile tDOC into BLPs, which stimulate bacterial growth but at low BGEs. Thus much of non-labile tDOC assimilated by bacteria directly or after photo-transformation is primarily respired.

This study indicates that in the global coastal ocean, solar radiation transforms at least 15% of tDOC ( $> 38 \text{ Tg C yr}^{-1}$ ) into BLPs. As this amount is larger than the photomineralization of tDOC in lakes and reservoirs, solar radiation transfers tDOC more in the coastal than in the inland waters. In inland waters, the steep attenuation of photolytic solar radiation and a short residence time for tDOC limit its phototransformation and lead into a large scale export of photoreactive tDOC to coastal ocean. In the coastal ocean, the mixing of tDOC with transparent oceanic waters and the advection of tDOC over large areas promote the photochemical transformation of tDOC.

*Acknowledgements.* We thank the scientists and their teams responsible for sampling river waters: E. M. Paolucci (Paraná), D. E. Musibono (Congo), A. Shantz (Mekong), S. R. Khan (Ganges-Brahmaputra), Q. Huang (Yangtze), W. Schneider (Lena), A. Rivas and C. E. Rezende (Amazon), E. Petrescu (Danube), and H. E. Reader (Mississippi). We are grateful to Dr. Nicolas Hatzianastassiou for providing the annual doses of global radiation for the river plumes. This research was funded by the Finnish Academy and by the Nordic Center of Excellence CRAICC (Cryosphere-atmosphere interactions in a changing Arctic climate). We also thank the Academy of Finland Center of Excellence (project number 1118615) and Norwegian University of Science and Technology (NTNU) We highly appreciate the efforts of Frank Berninger regarding statistical testing and analyses.

## References

Aarnos, H., Ylöstalo, P., and Vähätalo, A. V.: Seasonal photo-transformation of dissolved organic matter to ammonium, dissolved inorganic carbon, and labile substrates supporting bacterial biomass across the Baltic Sea, *Journal of Geophysical Research*, 117, 1–14, doi:10.1029/2010JG001633, <http://www.agu.org/pubs/crossref/2012/2010JG001633.shtml>, 2012.

Abboudi, M., Jeffrey, W. H., Ghiglione, J.-F., Pujo-Pay, M., Oriol, L., Sempéré, R., Charrière, B., and Joux, F.: Effects of photochemical transformations of dissolved organic matter on bacterial metabolism and diversity in three contrasting coastal sites

in the Northwestern Mediterranean Sea during summer., *Microbial Ecology*, 55, 344–57, doi:10.1007/s00248-007-9280-8, <http://www.ncbi.nlm.nih.gov/pubmed/17674086>, 2008.

Algesten, G., Sobek, S., Bergström, A.-K., Ågren, A., Tranvik, L. J., and Jansson, M.: Role of lakes for organic carbon cycling in the boreal zone, *Global Change Biology*, 10, 141–147, doi:10.1046/j.1529-8817.2003.00721.x, <http://dx.doi.org/10.1111/j.1365-2486.2003.00721.x>, 2004.

Amado, A. M., Farjalla, V. F., Esteves, F. D. a., Bozelli, R. L., Roland, F., and Enrich-Prast, A.: Complementary pathways of dissolved organic carbon removal pathways in clear-water Amazonian ecosystems: photochemical degradation and bacterial uptake., *FEMS microbiology ecology*, 56, 8–17, doi:10.1111/j.1574-6941.2006.00028.x, <http://www.ncbi.nlm.nih.gov/pubmed/16542400>, 2006.

Amon, R. M. W. and Benner, R.: Bacterial utilization of different size classes of dissolved organic matter, *Limnology and Oceanography*, 41, 41–51, doi:10.4319/lo.1996.41.1.0041, 1996.

Andrews, S. S., Caron, S., Zafriou, O. C., and Zafriou, O. C.: Photochemical Oxygen Consumption in Marine Waters : A Major Sink for Colored Dissolved Organic Matter ?, *Limnology and Oceanography*, 45, 267–277, 2000.

Anesio, A., Theil-Nielsen, J., and Graneli, W.: Bacterial Growth on Photochemically Transformed Leachates from Aquatic and Terrestrial Primary Producers, *Microbial ecology*, 40, 200–208, doi:10.1007/s002480000045, <http://www.springerlink.com/index/q3bwgmfbbaq0avh.pdf>, 2000.

Anesio, A. M., Granéli, W., Aiken, G. R., Kieber, D. J., Mopper, K., and Grane, W.: Effect of Humic Substance Photodegradation on Bacterial Growth and Respiration in Lake Water, *Applied and environmental microbiology*, 71, 6267–6275, doi:10.1128/AEM.71.10.6267, 2005.

Asmla, E., Autio, R., Kaartokallio, H., Stedmon, C. a., and Thomas, D. N.: Processing of humic-rich riverine dissolved organic matter by estuarine bacteria: effects of predegradation and inorganic nutrients, *Aquatic Sciences*, 76, 451–463, doi:10.1007/s00027-014-0346-7, <http://link.springer.com/10.1007/s00027-014-0346-7>, 2014.

Bauer, J. E., Cai, W.-J., Raymond, P. A., Bianchi, T. S., Hopkinson, C. S., and Regnier, P. A. G.: The changing carbon cycle of the coastal ocean., *Nature*, 504, 61–70, doi:10.1038/nature12857, <http://www.ncbi.nlm.nih.gov/pubmed/24305149>, 2013.

Bertilsson, S. and Tranvik, L.: Photochemical transformation of dissolved organic matter in lakes, *Limnology and Oceanography*, 45, 753–762, doi:10.4319/lo.2000.45.4.0753, <http://www.aslo.org/lo/toc/vol{ }45/issue{ }4/0753.html>, 2000.

Bertilsson, S. and Tranvik, L. J.: Photochemically Produced Carboxylic Acids as Substrates for Freshwater Bacterioplankton, *Limnology and Oceanography*, 43, 885–895, 1998.

Cai, W.-J.: Estuarine and Coastal Ocean Carbon Paradox: CO<sub>2</sub> Sinks or Sites of Terrestrial Carbon Incineration?, *Annual Review of Marine Science*, 3, 123–145, doi:10.1146/annurev-marine-120709-142723, <http://www.annualreviews.org/doi/abs/10.1146/annurev-marine-120709-142723>, 2011.

Carlson, C. A.: Production and Removal Processes, in: *Biogeochemistry of Marine Dissolved Organic Matter*, edited by Hansell, D. A. and Carlson, C. A., chap. 4, pp. 91–151, Elsevier, doi:10.1016/B978-012323841-2/50006-3, <http://www>

- sciencedirect.com/science/article/pii/B9780123238412500063, 945  
2002.
- Cauwet, G.: DOM in the Coastal Zone., in: *Biogeochemistry of Marine Dissolved Organic Matter*, edited by Hansell, D. A. and Carlson, C. A., chap. 12, pp. 579–609, Academic Press, San Diego, doi:10.1016/B978-012323841-2/50014-2, <http://www.sciencedirect.com/science/article/pii/B9780123238412500142>, 2002.
- Chu, S. and Liu, L.: Analysis of terrestrial solar radiation exergy, *Solar Energy*, 83, 1390–1404, doi:10.1016/j.solener.2009.03.011, <http://linkinghub.elsevier.com/retrieve/pii/S0038092X09000607>, 2009.
- Cloern, J. E.: Turbidity as a control on phytoplankton biomass and productivity in estuaries, *Continental Shelf Research*, 7, 1367–1381, doi:10.1016/0278-4343(87)90042-2, 1987.
- Cory, R. M., Ward, C. P., Crump, B. C., and Kling, G. W.: Sunlight controls water column processing of carbon in arctic fresh waters, *Science*, 345, 925–928, doi:10.1126/science.1253119, <http://www.sciencemag.org/cgi/doi/10.1126/science.1253119>, 2014.
- Coyne, A., Seyler, P., Etcheber, H., Meybeck, M., and Orange, D.: Spatial and seasonal dynamics of total suspended sediment and organic carbon species in the Congo River, *Global Biogeochemical Cycles*, 19, 1–17, doi:10.1029/2004GB002335, <http://www.agu.org/pubs/crossref/2005/2004GB002335.shtml>, 2005.
- Davies-Colley, R. J. and Smith, D. G.: Turbidity (Suspen)Ed Sediment, and Water Clarity: a Review, *Journal of the American Water Resources Association*, 37, 1085–1101, doi:10.1111/j.1752-1688.2001.tb03624.x, 2001.
- del Giorgio, P. A. and Cole, J. J.: Bacterial growth efficiency in natural aquatic systems, *Annual Review of Ecology and Systematics*, 29, 503–541, doi:10.1146/annurev.ecolsys.29.1.503, <http://dx.doi.org/10.1146/annurev.ecolsys.29.1.503>, 1998.
- del Giorgio, P. A., Cole, J. J., and Cimleris, A.: Respiration rates in bacteria exceed phytoplankton production in unpolluted aquatic systems, *Nature*, 385, 148–151, doi:10.1038/385148a0, 1997.
- Del Vecchio, R. and Subramaniam, A.: Influence of the Amazon River on the surface optical properties of the western tropical North Atlantic Ocean, *Journal of Geophysical Research*, 109, doi:10.1029/2004JC002503, <http://doi.wiley.com/10.1029/2004JC002503>, 2004.
- Farjalla, V., Anesio, A., Bertilsson, S., and Granéli, W.: Photochemical reactivity of aquatic macrophyte leachates: abiotic transformations and bacterial response, *Aquatic Microbial Ecology*, 24, 187–195, doi:10.3354/ame024187, <http://www.int-res.com/abstracts/ame/v24/n2/p187-195/>, 2001.
- Fichot, C. G. and Benner, R.: The fate of terrigenous dissolved organic carbon in a river-influenced ocean margin, *Global Biogeochemical Cycles*, 28, 300–318, doi:10.1002/2013GB004670, 2014.
- Goldman, J. C., Caron, D. A., and Dennett, M. R.: Regulation of gross growth efficiency and ammonium regeneration in bacteria by substrate C:N ratio, *Limnology and Oceanography*, 32, 1239–1252, doi:10.4319/lo.1987.32.6.1239, 1987.
- Granéli, W., Lindell, M., and Tranvik, L.: Photo-oxidative production of dissolved inorganic carbon in lakes of different humic content and Lars Tranvik, *Limnology and Oceanography*, 41, 698–706, doi:10.4319/lo.1996.41.4.0698, 1996.
- Granskog, M. A., Stedmon, C. A., Dodd, P. A., Amon, R. M. W., Pavlov, A. K., De Steur, L., and Hansen, E.: Characteristics of colored dissolved organic matter (CDOM) in the Arctic outflow in the Fram Strait: Assessing the changes and fate of terrigenous CDOM in the Arctic Ocean, *Journal of Geophysical Research: Oceans*, 117, 1–13, doi:10.1029/2012JC008075, 2012.
- Hatzianastassiou, N., Matsoukas, C., Fotiadi, A., Pavlakis, K. G., Drakakis, E., Hatzidimitriou, D., and Vardavas, I.: Global distribution of Earth's surface shortwave radiation budget, *Atmospheric Chemistry and Physics Discussions*, 5, 4545–4597, doi:10.5194/acpd-5-4545-2005, <http://www.atmos-chem-phys-discuss.net/5/4545/2005/>, 2005.
- Hobbie, J. E., Daley, R. J., and Jasper, S.: Use of nuclepore filters for counting bacteria by fluorescence microscopy . Use of Nuclepore Filters for Counting Bacteria by Fluorescence Microscopy, *Applied and Environmental Microbiology*, 33, 1225–1228, 1977.
- Jaffé, R., Ding, Y., Niggemann, J., Vahatalo, A. V., Stubbins, A., Spencer, R. G. M., Campbell, J., and Dittmar, T.: Global charcoal mobilization from soils via dissolution and riverine transport to the oceans, *Science*, 340, 345–347, doi:10.1126/science.1231476, <http://www.sciencemag.org/cgi/doi/10.1126/science.1231476>, 2013.
- Judd, K. E., Crump, B. C., and Kling, G. W.: Variation in dissolved organic matter controls bacterial production and community composition., *Ecology*, 87, 2068–79, <http://www.ncbi.nlm.nih.gov/pubmed/16937646>, 2006.
- Kester, D. R., Duedall, I. W., Connors, D. N., and Pytkowic, R.: Preparation of artificial seawater, *Limnology and Oceanography*, 12, 176–179, doi:10.4319/lo.1967.12.1.0176, 1967.
- Kieber, D. J. and Mopper, K.: Photochemical formation of glyoxylic and pyruvic acids in seawater, *Marine Chemistry*, 21, 135–149, doi:10.1016/0304-4203(87)90034-X, <http://www.sciencedirect.com/science/article/pii/030442038790034X>, 1987.
- Kieber, R. J., Zhou, X., and Mopper, K.: Formation of carbonyl compounds from UV-induced photodegradation of humic substances in natural waters: Fate of riverine carbon in the sea, *Limnology and Oceanography*, 35, 1503–1515, doi:10.4319/lo.1990.35.7.1503, 1990.
- Kiehl, J. T. and Trenberth, K. E.: Earth's Annual Global Mean Energy Budget, *Bulletin of the American Meteorological Society*, 78, 197–208, doi:10.1175/1520-0477(1997)078<0197:EAGMEB>2.0.CO;2, 1997.
- Kisand, V., Andersson, N., and Wikner, J.: Bacterial freshwater species successfully immigrate to the brackish water environment in the northern Baltic, *Limnology and Oceanography*, 50, 945–956, doi:10.4319/lo.2005.50.3.0945, 2005.
- Koehler, B., Landelius, T., Weyhenmeyer, G. A., Machida, N., and Tranvik, L. J.: Sunlight-induced carbon dioxide emissions from inland waters, *Global Biogeochemical Cycles*, 28, 696–711, doi:10.1002/2014GB004850, <http://dx.doi.org/10.1002/2014GB004850>, 2014.
- Kragh, T., Søndergaard, M., and Tranvik, L.: Effect of exposure to sunlight and phosphorus-limitation on bacterial degradation of coloured dissolved organic matter (CDOM) in freshwater., *FEMS Microbiology Ecology*, 64, 230–9, doi:10.1111/j.1574-6941.2008.00449.x, <http://www.ncbi.nlm.nih.gov/pubmed/18312374><http://onlinelibrary.wiley.com/doi/10.1111/j.1574-6941.2008.00449.x/full>, 2008.
- Kuivikko, M., Kotiaho, T., Hartonen, K., Tanskanen, A., and Vähätalo, A. V.: Modeled direct photolytic decomposition of poly-

- brominated diphenyl ethers in the Baltic Sea and the Atlantic Ocean., *Environmental Science & Technology*, 41, 7016–21, <http://www.ncbi.nlm.nih.gov/pubmed/17993142>, 2007.
- Lalonde, K., Vähätalo, A. V., and Gélinas, Y.: Revisiting the disappearance of terrestrial dissolved organic matter in the ocean: a  $\delta^{13}\text{C}$  study, *Biogeosciences*, 11, 3707–3719, doi:10.5194/bg-11-3707-2014, <http://www.biogeosciences.net/11/3707/2014/>, 2014.
- Lönborg, C. and Alvarez-Salgado, X. A.: Recycling versus export of bioavailable dissolved organic matter in the coastal ocean and efficiency of the continental shelf pump, *Global Biogeochemical Cycles*, 26, 1–12, doi:10.1029/2012GB004353, <http://doi.wiley.com/10.1029/2012GB004353>, 2012.
- Lönborg, C., Álvarez-Salgado, X. A., Davidson, K., and Miller, A. E.: Production of bioavailable and refractory dissolved organic matter by coastal heterotrophic microbial populations, *Estuarine, Coastal and Shelf Science*, 82, 682–688, doi:10.1016/j.ecss.2009.02.026, <http://linkinghub.elsevier.com/retrieve/pii/S0272771409000985>, 2009.
- Massana, R., Gasol, J. M., Björnsen, P. K., Black-Burn, N., Hagström, Å., Hietanen, S., Hygum, B. H., Kuparinen, J., and Peders-Álio, C.: Measurement of bacterial size via image analysis of epifluorescence preparations: description of an inexpensive system and solutions to some of the most common problems, *Scientia Marina*, 61, 397–407, 1997.
- McCallister, S. and Bauer, J.: Effects of sunlight on decomposition of estuarine dissolved organic C, N and P and bacterial metabolism, *Aquatic Microbial Ecology*, 40, 25–35, [https://aquaticbiogeochem.osu.edu/files/aquaticbiogeochem/2005McCallisterBaueretal\( \)AME.pdf](https://aquaticbiogeochem.osu.edu/files/aquaticbiogeochem/2005McCallisterBaueretal( )AME.pdf), 2005.
- Medeiros, P. M., Seidel, M., Ward, N. D., Carpenter, E. J., Gomes, H. R., Niggemann, J., Krusche, A. V., Richey, J. E., Yager, P. L., and Dittmar, T.: Fate of the Amazon River dissolved organic matter in the tropical Atlantic Ocean, *Global Biogeochemical Cycles*, pp. n/a–n/a, doi:10.1002/2015GB005115, <http://doi.wiley.com/10.1002/2015GB005115>, 2015.
- Miller, W. L. and Moran, M. A.: Interaction of photochemical and microbial processes in the degradation of refractory dissolved organic matter from a coastal marine environment, *Limnology and Oceanography*, 42, 1317–1324, doi:10.4319/lo.1997.42.6.1317, <http://www.jstor.org/stable/10.2307/2839130>, 1997.
- Miller, W. L., Moran, M. A., and Sheldon, W. M.: Determination of apparent quantum yield spectra for the formation of biologically labile photoproducts, *Limnology and Oceanography*, 47, 343–352, doi:10.4319/lo.2002.47.2.0343, <http://www.jstor.org/stable/10.2307/3068981>, 2002.
- Milliman, J. D. and Farnsworth, K. L.: *River Discharge to the Coastal Ocean: A Global Synthesis*, vol. 24, Cambridge University Press, Cambridge, doi:<http://dx.doi.org/10.5670/oceanog.2011.108>, 2011.
- Minor, E. C., Pothen, J., Dalzell, B. J., Abdulla, H., and Mopper, K.: Effects of salinity changes on the photodegradation and ultraviolet-visible absorbance of terrestrial dissolved organic matter, *Limnology and Oceanography*, 51, 2181–2186, doi:10.4319/lo.2006.51.5.2181, <http://www.aslo.org/lo/toc/vol{ }51/issue{ }5/2181.html>, 2006.
- Molot, L. and Dillon, P.: Photolytic regulation of dissolved organic carbon in northern lakes, *Global Biogeochemical Cycles*, 11, 357–365, <http://onlinelibrary.wiley.com/doi/10.1029/97GB01198/full>, 1997.
- Mopper, K. and Kieber, D. J.: Photochemistry and the Cycling of Carbon, Sulfur, Nitrogen and Phosphorus, in: *Biogeochemistry of Marine Dissolved Organic Matter*, edited by Hansell, D. A. and Carlson, C. A., chap. Chapter 9, pp. 455–507, Elsevier, doi:10.1016/B978-012323841-2/50011-7, <http://www.sciencedirect.com/science/article/pii/B9780123238412500117>, 2002.
- Moran, M. and Zepp, R.: Role of photoreactions in the formation of biologically labile compounds from dissolved organic matter, *Limnology and Oceanography*, 42, 1307–1316, <http://www.aslo.org/lo/toc/vol{ }42/issue{ }6/1307.pdf>, <http://www.jstor.org/stable/10.2307/2839129>, 1997.
- Morris, D. P., Zagarese, H., Williamson, C. E., Balseiro, E. G., Hargreaves, B. R., Modenutti, B., Moeller, R., and Queimalinos, C.: The attenuation of solar UV radiation in lakes and the role of dissolved organic carbon, *Limnology and Oceanography*, 40, 1381–1391, doi:10.4319/lo.1995.40.8.1381, 1995.
- Müller, R. A., Futter, M. N., Sobek, S., Nisell, J., Bishop, K., and Weyhenmeyer, G. A.: Water renewal along the aquatic continuum offsets cumulative retention by lakes: implications for the character of organic carbon in boreal lakes, *Aquatic Sciences*, 75, 535–545, doi:10.1007/s00027-013-0298-3, <http://link.springer.com/10.1007/s00027-013-0298-3>, 2013.
- Nelson, N. B. and Siegel, D. A.: The global distribution and dynamics of chromophoric dissolved organic matter, *Annual Review of Marine Science*, 5, 447–76, doi:10.1146/annurev-marine-120710-100751, <http://www.ncbi.nlm.nih.gov/pubmed/22809178>, 2013.
- Norland, S.: The relationship between biomass and volume of bacteria, in: *Handbook of Methods in Aquatic Microbial Ecology*, edited by Kemp, P., Sherr, B., Sherr, E., and Cole, J., pp. 303–307, Lewis Publishers, BocaRaton, 1993.
- Obernosterer, I. and Herndl, G.: Differences in the optical and biological reactivity of the humic and nonhumic dissolved organic carbon component in two contrasting coastal marine environments, *Limnology and Oceanography*, 45, 1120–1129, doi:10.4319/lo.2000.45.5.1120, <http://www.jstor.org/stable/10.2307/2670702>, 2000.
- Pers, C., Rahm, L., Jonsson, A., and Jansson, M.: Modelling dissolved organic carbon turnover in humic Lake, *Environmental monitoring and assessment*, 6, 159–172, doi:10.1023/A:1011953730983, 2001.
- Pineiro, S., Chauhan, A., Berhane, T. K., Athar, R., Zheng, G., Wang, C., Dickerson, T., Liang, X., Lymperopoulou, D. S., Chen, H., Christman, M., Louime, C., Babiker, W., Stine, O. C., and Williams, H. N.: Niche Partition of Bacterioplankton Operational Taxonomic Units Along Salinity and Temporal Gradients in the Chesapeake Bay Reveals Distinct Estuarine Strains, *Microbial Ecology*, 65, 652–660, doi:10.1007/s00248-013-0186-3, 2013.
- Pullin, M. J., Bertilsson, S., Goldstone, J. V., and Voelker, B. M.: Effects of sunlight and hydroxyl radical on dissolved organic matter: Bacterial growth efficiency and production of carboxylic acids and other substrates, *Limnology and Oceanography*, 49, 2011–2022, doi:10.4319/lo.2004.49.6.2011, <http://www.aslo.org/lo/toc/vol{ }49/issue{ }6/2011.html>, 2004.

- R Core Team: R: A Language and Environment for Statistical Computing, R Foundation for Statistical Computing, Vienna, Austria, <http://www.r-project.org/>, 2014. 1180
- Reader, H. E. and Miller, W. L.: The efficiency and spectral photon dose dependence of photochemically induced changes to the bioavailability of dissolved organic carbon, *Limnology and Oceanography*, 59, 182–194, doi:10.4319/lo.2014.59.1.0182, [http://www.aslo.org/lo/toc/vol\[\\_\]59/issue\[\\_\]1/0182.html](http://www.aslo.org/lo/toc/vol[_]59/issue[_]1/0182.html), 2014. 1185
- Reche, I., Pace, M., and Cole, J.: Interactions of Photobleaching and Inorganic Nutrients in Determining Bacterial Growth on Colored Dissolved Organic Carbon., *Microbial ecology*, 36, 270–280, <http://www.ncbi.nlm.nih.gov/pubmed/9852507>, 1998. 1130
- Reitner, B., Herndl, G. J., and Herzig, A.: Role of ultraviolet-B radiation on photochemical and microbial oxygen consumption in a humic-rich shallow lake, *Limnology and Oceanography*, 42, 950–960, doi:10.4319/lo.1997.42.5.0950, 1997. 1190
- Remington, S., Krusche, A., and Richey, J.: Effects of DOM photochemistry on bacterial metabolism and CO<sub>2</sub> evasion during falling water in a humic and a white-water river in the Brazilian Amazon, *Biogeochemistry*, 105, 185–200, doi:10.1007/s10533-010-9565-8, <http://www.springerlink.com/index/OR500624243181W7.pdf><http://www.springerlink.com/index/10.1007/s10533-010-9565-8>, 2011. 1195
- Riggsbee, J. A., Orr, C. H., Leech, D. M., Doyle, M. W., and Wetzel, R. G.: Suspended sediments in river ecosystems: Photochemical sources of dissolved organic carbon, dissolved organic nitrogen, and adsorptive removal of dissolved iron, *Journal of Geophysical Research: Biogeosciences*, 113, 1–12, doi:10.1029/2007JG000654, 2008. 1200
- Rossel, P. E., Vähätalo, A. V., Witt, M., and Dittmar, T.: Molecular composition of dissolved organic matter from a wetland plant (*Juncus effusus*) after photochemical and microbial decomposition (1.25 yr): Common features with deep sea dissolved organic matter, *Organic Geochemistry*, 60, 62–71, doi:10.1016/j.orggeochem.2013.04.013, <http://linkinghub.elsevier.com/retrieve/pii/S0146638013000971>, 2013. 1205
- Salonen, K. and Vähätalo, A.: Photochemical mineralisation of dissolved organic matter in lake Skjervatjern, *Environmental International*, 20, 307–312, doi:10.1016/0160-4120(94)90114-7, 1994. 1210
- Smith, E. and Benner, R.: Photochemical transformations of riverine dissolved organic matter: effects on estuarine bacterial metabolism and nutrient demand, *Aquatic Microbial Ecology*, 40, 37–50, doi:10.3354/ame040037, <http://www.int-res.com/abstracts/ame/v40/n1/p37-50/>, 2005. 1220
- Smith, S. V. and Hollibaugh, J. T.: Coastal Metabolism and the Oceanic Organic Carbon Balance, *Reviews of Geophysics*, 31, 75–89, 1993. 1225
- Sobek, S., Tranvik, L. J., Prairie, Y. T., and Cole, J. J.: Patterns and regulation of dissolved organic carbon: An analysis of 7, 500 widely distributed lakes, *Limnology and Oceanography*, 52, 1208–1219, 2007. 1230
- Søndergaard, M. and Middelboe, M.: A cross-system analysis of labile dissolved organic carbon, *Marine Ecology Progress Series*, 118, 283–294, doi:10.3354/meps118283, <http://www.int-res.com/abstracts/meps/v118/p283-294/>, 1995. 1235
- Spencer, R. G. M., Stubbins, A., Hernes, P. J., Baker, A., Mopper, K., Aufdenkampe, A. K., Dyda, R. Y., Mwamba, V. L., Mangangu, A. M., Wabakanghanzi, J. N., and Six, J.: Photochemical degradation of dissolved organic matter and dissolved lignin phenols from the Congo River, *Journal of Geophysical Research*, 114, G03 010, doi:10.1029/2009JG000968, <http://doi.wiley.com/10.1029/2009JG000968><http://www.agu.org/pubs/crossref/2009/2009JG000968.shtml>, 2009. 1240
- Spencer, R. G. M., Aiken, G. R., Dornblaser, M. M., Butler, K. D., Holmes, R. M., Fiske, G., Mann, P. J., and Stubbins, A.: Chromophoric dissolved organic matter export from U.S. rivers, *Geophysical Research Letters*, 40, 1575–1579, doi:10.1002/grl.50357, <http://doi.wiley.com/10.1002/grl.50357>, 2013. 1245
- Stedmon, C., Amon, R., Rinehart, A., and Walker, S.: The supply and characteristics of colored dissolved organic matter (CDOM) in the Arctic Ocean: Pan Arctic trends and differences, *Marine Chemistry*, 124, 108–118, doi:10.1016/j.marchem.2010.12.007, <http://linkinghub.elsevier.com/retrieve/pii/S0304420311000065>, 2011. 1250
- Stepanuskas, R., Jørgensen, N. O. G., Eigaard, O. R., Zvikas, A., Tranvik, L. J., and Leonardson, L.: Summer inputs of riverine nutrients to the Baltic Sea: bioavailability and eutrophication relevance, *Ecological Monographs*, 72, 579–597, 2002. 1255
- Vähätalo, A. and Järvinen, M.: Photochemically produced bioavailable nitrogen from biologically recalcitrant dissolved organic matter stimulates production of a nitrogen-limited microbial food web in the Baltic Sea, *Limnology and oceanography*, 52, 132–143, 2007. 1260
- Vähätalo, A., Salkinoja-salonen, M., Taalas, P., and Salonen, K.: Spectrum of the quantum yield for photochemical mineralization of dissolved organic carbon in a humic lake, *Limnology and Oceanography*, 45, 664–676, doi:10.4319/lo.2000.45.3.0664, 2000. 1265
- Vähätalo, A. V.: Light, Photolytic Reactivity and Chemical Products, vol. 2, *Likens*, Oxford, volume 2 edn., 2009. 1270
- Vähätalo, A. V. and Wetzel, R. G.: Photochemical and microbial decomposition of chromophoric dissolved organic matter during long (months - years) exposures, *Marine Chemistry*, 89, 313–326, doi:10.1016/j.marchem.2004.03.010, <http://linkinghub.elsevier.com/retrieve/pii/S0304420304000957>, 2004. 1275
- Vähätalo, A. V., Salonen, K., Sasaki, E., and Salkinoja-Salonen, M. S.: Bleaching of color of kraft pulp mill effluents and natural organic matter in lakes, *Canadian Journal of Fisheries and Aquatic Sciences*, 59, 808–818, doi:10.1139/F02-047, 2002. 1280
- Vähätalo, A. V., Salonen, K., Münster, U., Järvinen, M., and Wetzel, R. G.: Photochemical transformation of allochthonous organic matter provides bioavailable nutrients in a humic lake, *Archiv für Hydrobiologie*, 156, 287–314, doi:10.1127/0003-9136/2003/0156-0287, [http://www.ingentaeselect.com/rpsv/cgi-bin/cgi?ini=xref\[&\]body=linker\[&\]reqdoi=10.1127/0003-9136/2003/0156-0287](http://www.ingentaeselect.com/rpsv/cgi-bin/cgi?ini=xref[&]body=linker[&]reqdoi=10.1127/0003-9136/2003/0156-0287), 2003. 1285
- Vähätalo, A. V., Wetzel, R. G., and Paerl, H. W.: Light absorption by phytoplankton and chromophoric dissolved organic matter in the drainage basin and estuary of the Neuse River, North Carolina (U.S.A.), *Freshwater Biology*, 50, 477–493, doi:10.1111/j.1365-2427.2004.01335.x, <http://doi.wiley.com/10.1111/j.1365-2427.2004.01335.x>, 2005. 1290
- Vähätalo, A. V., Aarnos, H., and Mäntyniemi, S.: Biodegradability continuum and biodegradation kinetics of natural organic matter described by the beta distribution, *Biogeochemistry*, 100, 227–

- 240, doi:10.1007/s10533-010-9419-4, <http://link.springer.com/1295>  
10.1007/s10533-010-9419-4, 2010.
- Vähätalo, A. V., Aarnos, H., Hoikkala, L., and Lignell, R.: Photochemical transformation of terrestrial dissolved organic matter supports hetero- and autotrophic production in coastal waters, *Marine Ecology Progress Series*, 423, 1–1300  
14, doi:10.3354/meps09010, <http://www.int-res.com/abstracts/meps/v423/p1-14/>, 2011.
- Vähätalo, A. V. A. and Wetzel, R. R. G.: Long-Term Photochemical and Microbial Decomposition of Wetland-Derived Dissolved Organic Matter with Alteration of 13C:12C Mass Ratio, *Limnology and Oceanography*, 53, 1387–1392, doi:10.4319/lo.2008.53.4.1387, <http://www.jstor.org/stable/10.2307/40058260>, 2008.
- Verpoorter, C., Kutser, T., Seekell, D. A., and Tranvik, L. J.: A global inventory of lakes based on high-resolution satellite imagery, *Geophysical Research Letters*, 41, 2014GL060641, doi:10.1002/2014GL060641, 2014.
- Vodacek, A., Blough, N. V., Degrandpre, M. D., Peltzer, E. T., and Nelson, R. K.: Seasonal variation of CDOM and DOC in the Middle Atlantic Bight: Terrestrial inputs and photooxidation, *Limnology and Oceanography*, 42, 674–686, doi:10.4319/lo.1997.42.4.0674, 1997.
- Wagner, S., Riedel, T., Niggemann, J., Vähätalo, A. V., Dittmar, T., and Jaffe, R.: Linking the Molecular Signature of Heteroatomic Dissolved Organic Matter To Watershed Characteristics in World Rivers, *Environmental Science & Technology*, Article AS, doi:10.1021/acs.est.5b00525, <http://pubs.acs.org/doi/abs/10.1021/acs.est.5b00525>, 2015.
- Wallin, M. B., Weyhenmeyer, G. A., Bastviken, D., Chmiel, H. E., Peter, S., Sobek, S., and Klemetsson, L.: Temporal control on concentration, character, and export of dissolved organic carbon in two hemiboreal headwater streams draining contrasting catchments, *Journal of Geophysical Research: Biogeosciences*, 3, 1–15, doi:10.1002/2014JG002814, 2015.
- Warkentin, M., Freese, H. M., Karsten, U., and Schumann, R.: New and fast method to quantify respiration rates of bacterial and plankton communities in freshwater ecosystems by using optical oxygen sensor spots., *Applied and Environmental Microbiology*, 73, 6722–6729, doi:10.1128/AEM.00405-07, <http://www.pubmedcentral.nih.gov/articlerender.fcgi?artid=2074954> & tool=pmcentrez & rendertype=abstract, 2007.
- Warkentin, M., Freese, H. M., and Schumann, R.: Bacterial activity and bacterioplankton diversity in the eutrophic River Warnow—direct measurement of bacterial growth efficiency and its effect on carbon utilization., *Microbial Ecology*, 61, 190–200, doi:10.1007/s00248-010-9729-z, <http://www.ncbi.nlm.nih.gov/pubmed/20676625>, 2011.
- Wetzel, R. G., Hatcher, P. G., and Bianchi, T. S.: Natural photolysis by ultraviolet irradiance of recalcitrant dissolved organic matter to simple substrates for rapid bacterial metabolism, *Limnology and Oceanography*, 40, 1369–1380, 1995.
- White, E. M., Kieber, D. J., Sherrard, J., Miller, W. L., and Mopper, K.: Carbon dioxide and carbon monoxide photoproduction quantum yields in the Delaware Estuary, *Marine Chemistry*, 118, 11–21, doi:10.1016/j.marchem.2009.10.001, <http://linkinghub.elsevier.com/retrieve/pii/S0304420309001455>, 2010.
- Xiao, Y.-H., Sara-Aho, T., Hartikainen, H., and Vähätalo, A. V.: Contribution of ferric iron to light absorption by chromophoric dissolved organic matter, *Limnology and Oceanography*, 58, 653–662, doi:10.4319/lo.2013.58.2.0653, [http://www.aslo.org/lo/toc/vol\[\\_\]58/issue\[\\_\]2/0653.html](http://www.aslo.org/lo/toc/vol[_]58/issue[_]2/0653.html), 2013.
- Xie, H., Zafriou, O. C., Cai, W.-J., Zepp, R. G., and Wang, Y.: Photooxidation and Its Effects on the Carboxyl Content of Dissolved Organic Matter in Two Coastal Rivers in the Southeastern United States, *Environmental Science & Technology*, 38, 4113–4119, doi:10.1021/es035407t, <http://pubs.acs.org/doi/abs/10.1021/es035407t>, 2004.

## References

- Aarnos, H., Ylöstalo, P., and Vähätalo, A. V.: Seasonal photo-transformation of dissolved organic matter to ammonium, dissolved inorganic carbon, and labile substrates supporting bacterial biomass across the Baltic Sea, *Journal of Geophysical Research*, 117, 1–14, doi:10.1029/2010JG001633, <http://www.agu.org/pubs/crossref/2012/2010JG001633.shtml>, 2012.
- Abboudi, M., Jeffrey, W. H., Ghiglione, J.-F., Pujo-Pay, M., Oriol, L., Sempéré, R., Charrière, B., and Joux, F.: Effects of photochemical transformations of dissolved organic matter on bacterial metabolism and diversity in three contrasting coastal sites in the Northwestern Mediterranean Sea during summer., *Microbial Ecology*, 55, 344–57, doi:10.1007/s00248-007-9280-8, <http://www.ncbi.nlm.nih.gov/pubmed/17674086>, 2008.
- Algesten, G., Sobek, S., Bergström, A.-K., Ågren, A., Tranvik, L. J., and Jansson, M.: Role of lakes for organic carbon cycling in the boreal zone, *Global Change Biology*, 10, 141–147, doi:10.1046/j.1529-8817.2003.00721.x, <http://dx.doi.org/10.1111/j.1365-2486.2003.00721.x>, 2004.
- Amado, A. M., Farjalla, V. F., Esteves, F. D. a., Bozelli, R. L., Roland, F., and Enrich-Prast, A.: Complementary pathways of dissolved organic carbon removal pathways in clear-water Amazonian ecosystems: photochemical degradation and bacterial uptake., *FEMS microbiology ecology*, 56, 8–17, doi:10.1111/j.1574-6941.2006.00028.x, <http://www.ncbi.nlm.nih.gov/pubmed/16542400>, 2006.
- Amon, R. M. W. and Benner, R.: Bacterial utilization of different size classes of dissolved organic matter, *Limnology and Oceanography*, 41, 41–51, doi:10.4319/lo.1996.41.1.0041, 1996.
- Andrews, S. S., Caron, S., Zafriou, O. C., and Zafriou, O. C.: Photochemical Oxygen Consumption in Marine Waters : A Major Sink for Colored Dissolved Organic Matter ?, *Limnology and Oceanography*, 45, 267–277, 2000.
- Anesio, A., Theil-Nielsen, J., and Graneli, W.: Bacterial Growth on Photochemically Transformed Leachates from Aquatic and Terrestrial Primary Producers, *Microbial ecology*, 40, 200–208, doi:10.1007/s002480000045, <http://www.springerlink.com/index/q3bwgmfbbaq0avh.pdf>, 2000.
- Anesio, A. M., Graneli, W., Aiken, G. R., Kieber, D. J., Mopper, K., and Grane, W.: Effect of Humic Substance Photodegradation on Bacterial Growth and Respiration in Lake Water, *Applied and environmental microbiology*, 71, 6267–6275, doi:10.1128/AEM.71.10.6267, 2005.
- Asmala, E., Autio, R., Kaartokallio, H., Stedmon, C. a., and Thomas, D. N.: Processing of humic-rich riverine dissolved organic matter by estuarine bacteria: effects of predegradation and inorganic nutrients, *Aquatic Sciences*, 76, 451–

- 463, doi:10.1007/s00027-014-0346-7, <http://link.springer.com/1410>  
10.1007/s00027-014-0346-7, 2014.
- Bauer, J. E., Cai, W.-J., Raymond, P. A., Bianchi, T. S., Hopkinson, C. S., and Regnier, P. A. G.: The changing carbon cycle of the coastal ocean., *Nature*, 504, 61–70, doi:10.1038/nature12857, <http://www.ncbi.nlm.nih.gov/pubmed/24305149>, 2013.
- Bertilsson, S. and Tranvik, L.: Photochemical transformation of dissolved organic matter in lakes, *Limnology and Oceanography*, 45, 753–762, doi:10.4319/lo.2000.45.4.0753, [http://www.aslo.org/lo/toc/vol\[\\_\]45/issue\[\\_\]4/0753.html](http://www.aslo.org/lo/toc/vol[_]45/issue[_]4/0753.html), 2000.
- Bertilsson, S. and Tranvik, L. J.: Photochemically Produced Carboxylic Acids as Substrates for Freshwater Bacterioplankton, *Limnology and Oceanography*, 43, 885–895, 1998.
- Cai, W.-J.: Estuarine and Coastal Ocean Carbon Paradox: CO<sub>2</sub> Sinks or Sites of Terrestrial Carbon Incineration?, *Annual Review of Marine Science*, 3, 123–145, doi:10.1146/annurev-marine-120709-142723, <http://www.annualreviews.org/doi/abs/10.1146/annurev-marine-120709-142723>, 2011.
- Carlson, C. A.: Production and Removal Processes, in: *Biogeochemistry of Marine Dissolved Organic Matter*, edited by Hansell, D. A. and Carlson, C. A., chap. 4, pp. 91–151, Elsevier, doi:10.1016/B978-012323841-2/50006-3, <http://www.sciencedirect.com/science/article/pii/B9780123238412500063>, 2002.
- Cauwet, G.: DOM in the Coastal Zone., in: *Biogeochemistry of Marine Dissolved Organic Matter*, edited by Hansell, D. A. and Carlson, C. A., chap. 12, pp. 579–609, Academic Press, San Diego, doi:10.1016/B978-012323841-2/50014-2, <http://www.sciencedirect.com/science/article/pii/B9780123238412500142>, 2002.
- Chu, S. and Liu, L.: Analysis of terrestrial solar radiation energy, *Solar Energy*, 83, 1390–1404, doi:10.1016/j.solener.2009.03.011, <http://linkinghub.elsevier.com/retrieve/pii/S0038092X09000607>, 2009.
- Cloern, J. E.: Turbidity as a control on phytoplankton biomass and productivity in estuaries, *Continental Shelf Research*, 7, 1367–1381, doi:10.1016/0278-4343(87)90042-2, 1987.
- Cory, R. M., Ward, C. P., Crump, B. C., and Kling, G. W.: Sunlight controls water column processing of carbon in arctic fresh waters, *Science*, 345, 925–928, doi:10.1126/science.1253119, <http://www.sciencemag.org/cgi/doi/10.1126/science.1253119>, 2014.
- Coyne, A., Seyler, P., Etcheber, H., Meybeck, M., and Orange, D.: Spatial and seasonal dynamics of total suspended sediment and organic carbon species in the Congo River, *Global Biogeochemical Cycles*, 19, 1–17, doi:10.1029/2004GB002335, <http://www.agu.org/pubs/crossref/2005/2004GB002335.shtml>, 2005.
- Davies-Colley, R. J. and Smith, D. G.: Turbidity (Suspended Sediment, and Water Clarity: a Review, *Journal of the American Water Resources Association*, 37, 1085–1101, doi:10.1111/j.1752-1688.2001.tb03624.x, 2001.
- del Giorgio, P. A. and Cole, J. J.: Bacterial growth efficiency in natural aquatic systems, *Annual Review of Ecology and Systematics*, 29, 503–541, doi:10.1146/annurev.ecolsys.29.1.503, <http://dx.doi.org/10.1146/annurev.ecolsys.29.1.503>, 1998.
- del Giorgio, P. A., Cole, J. J., and Cimleris, A.: Respiration rates in bacteria exceed phytoplankton production in unproductive aquatic systems, *Nature*, 385, 148–151, doi:10.1038/385148a0, 1997.
- Del Vecchio, R. and Subramaniam, A.: Influence of the Amazon River on the surface optical properties of the western tropical North Atlantic Ocean, *Journal of Geophysical Research*, 109, doi:10.1029/2004JC002503, <http://doi.wiley.com/10.1029/2004JC002503>, 2004.
- Farjalla, V., Anesio, A., Bertilsson, S., and Granéli, W.: Photochemical reactivity of aquatic macrophyte leachates: abiotic transformations and bacterial response, *Aquatic Microbial Ecology*, 24, 187–195, doi:10.3354/ame024187, <http://www.int-res.com/abstracts/ame/v24/n2/p187-195/>, 2001.
- Fichot, C. G. and Benner, R.: The fate of terrigenous dissolved organic carbon in a river-influenced ocean margin, *Global Biogeochemical Cycles*, 28, 300–318, doi:10.1002/2013GB004670, 2014.
- Goldman, J. C., Caron, D. A., and Dennett, M. R.: Regulation of gross growth efficiency and ammonium regeneration in bacteria by substrate C:N ratio, *Limnology and Oceanography*, 32, 1239–1252, doi:10.4319/lo.1987.32.6.1239, 1987.
- Granéli, W., Lindell, M., and Tranvik, L.: Photo-oxidative production of dissolved inorganic carbon in lakes of different humic content and Lars Tranvik, *Limnology and Oceanography*, 41, 698–706, doi:10.4319/lo.1996.41.4.0698, 1996.
- Granskog, M. A., Stedmon, C. A., Dodd, P. A., Amon, R. M. W., Pavlov, A. K., De Steur, L., and Hansen, E.: Characteristics of colored dissolved organic matter (CDOM) in the Arctic outflow in the Fram Strait: Assessing the changes and fate of terrigenous CDOM in the Arctic Ocean, *Journal of Geophysical Research: Oceans*, 117, 1–13, doi:10.1029/2012JC008075, 2012.
- Hatzianastassiou, N., Matsoukas, C., Fotiadi, A., Pavlakis, K. G., Drakakis, E., Hatzidimitriou, D., and Vardavas, I.: Global distribution of Earth's surface shortwave radiation budget, *Atmospheric Chemistry and Physics Discussions*, 5, 4545–4597, doi:10.5194/acpd-5-4545-2005, <http://www.atmos-chem-phys-discuss.net/5/4545/2005/>, 2005.
- Hobbie, J. E., Daley, R. J., and Jasper, S.: Use of nuclepore filters for counting bacteria by fluorescence microscopy. Use of Nuclepore Filters for Counting Bacteria by Fluorescence Microscopy, *Applied and Environmental Microbiology*, 33, 1225–1228, 1977.
- Jaffé, R., Ding, Y., Niggemann, J., Vahatalo, A. V., Stubbins, A., Spencer, R. G. M., Campbell, J., and Dittmar, T.: Global charcoal mobilization from soils via dissolution and riverine transport to the oceans, *Science*, 340, 345–347, doi:10.1126/science.1231476, <http://www.sciencemag.org/cgi/doi/10.1126/science.1231476>, 2013.
- Judd, K. E., Crump, B. C., and Kling, G. W.: Variation in dissolved organic matter controls bacterial production and community composition., *Ecology*, 87, 2068–79, <http://www.ncbi.nlm.nih.gov/pubmed/16937646>, 2006.
- Kester, D. R., Duedall, I. W., Connors, D. N., and Pytkowic, R.: Preparation of artificial seawater, *Limnology and Oceanography*, 12, 176–179, doi:10.4319/lo.1967.12.1.0176, 1967.
- Kieber, D. J. and Mopper, K.: Photochemical formation of glyoxylic and pyruvic acids in seawater, *Marine Chemistry*, 21, 135–149, doi:10.1016/0304-4203(87)90034-X, <http://www.sciencedirect.com/science/article/pii/030442038790034X>, 1987.
- Kieber, R. J., Zhou, X., and Mopper, K.: Formation of carbonyl compounds from UV-induced photodegradation of humic substances in natural waters: Fate of riverine carbon in the sea, *Limnology and Oceanography*, 35, 1503–1515, doi:10.4319/lo.1990.35.7.1503, 1990.

- Kiehl, J. T. and Trenberth, K. E.: Earth's Annual Global Mean Energy Budget, *Bulletin of the American Meteorological Society*, 78, 197–208, doi:10.1175/1520-0477(1997)078<0197:EAGMEB>2.0.CO;2, 1997. <sup>1530</sup>
- Kisand, V., Andersson, N., and Wikner, J.: Bacterial freshwater species successfully immigrate to the brackish water environment in the northern Baltic, *Limnology and Oceanography*, 50, 945–956, doi:10.4319/lo.2005.50.3.0945, 2005. <sup>1475</sup>
- Koehler, B., Landelius, T., Weyhenmeyer, G. A., Machida, N., and Tranvik, L. J.: Sunlight-induced carbon dioxide emissions from inland waters, *Global Biogeochemical Cycles*, 28, 696–711, doi:10.1002/2014GB004850, <http://dx.doi.org/10.1002/2014GB004850>, 2014. <sup>1480</sup>
- Kragh, T., Søndergaard, M., and Tranvik, L.: Effect of exposure to sunlight and phosphorus-limitation on bacterial degradation of coloured dissolved organic matter (CDOM) in freshwater., *FEMS Microbiology Ecology*, 64, 230–9, doi:10.1111/j.1574-6941.2008.00449.x, <http://www.ncbi.nlm.nih.gov/pubmed/18312374><http://onlinelibrary.wiley.com/doi/10.1111/j.1574-6941.2008.00449.x/full>, 2008. <sup>1485</sup>
- Kuivikko, M., Kotiaho, T., Hartonen, K., Tanskanen, A., and Vähätalo, A. V.: Modeled direct photolytic decomposition of polybrominated diphenyl ethers in the Baltic Sea and the Atlantic Ocean., *Environmental Science & Technology*, 41, 7016–21, <http://www.ncbi.nlm.nih.gov/pubmed/17993142>, 2007. <sup>1490</sup>
- Lalonde, K., Vähätalo, A. V., and Gélinas, Y.: Revisiting the disappearance of terrestrial dissolved organic matter in the ocean: a  $\delta^{13}\text{C}$  study, *Biogeosciences*, 11, 3707–3719, doi:10.5194/bg-11-3707-2014, <http://www.biogeosciences.net/11/3707/2014/>, 2014. <sup>1495</sup>
- Lønborg, C. and Alvarez-Salgado, X. A.: Recycling versus export of bioavailable dissolved organic matter in the coastal ocean and efficiency of the continental shelf pump, *Global Biogeochemical Cycles*, 26, 1–12, doi:10.1029/2012GB004353, <http://doi.wiley.com/10.1029/2012GB004353>, 2012. <sup>1500</sup>
- Lønborg, C., Álvarez-Salgado, X. A., Davidson, K., and Miller, A. E.: Production of bioavailable and refractory dissolved organic matter by coastal heterotrophic microbial populations, *Estuarine, Coastal and Shelf Science*, 82, 682–688, doi:10.1016/j.ecss.2009.02.026, <http://linkinghub.elsevier.com/retrieve/pii/S0272771409000985>, 2009. <sup>1505</sup>
- Massana, R., Gasol, J. M., Bjørnsen, P. K., Black-Burn, N., Hagström, Å., Hietanen, S., Hygum, B. H., Kuparinen, J., and Peders-Alio, C.: Measurement of bacterial size via image analysis of epifluorescence preparations: description of an inexpensive system and solutions to some of the most common problems, *Scientia Marina*, 61, 397–407, 1997. <sup>1510</sup>
- McCallister, S. and Bauer, J.: Effects of sunlight on decomposition of estuarine dissolved organic C, N and P and bacterial metabolism, *Aquatic microbial ...*, 40, 25–35, <https://aquaticbiogeochem.osu.edu/files/aquaticbiogeochem/2005McCallisterBaueretal{}.AME.pdf>, 2005. <sup>1520</sup>
- Medeiros, P. M., Seidel, M., Ward, N. D., Carpenter, E. J., Gomes, H. R., Niggemann, J., Krusche, A. V., Richey, J. E., Yager, P. L., and Dittmar, T.: Fate of the Amazon River dissolved organic matter in the tropical Atlantic Ocean, *Global Biogeochemical Cycles*, pp. n/a–n/a, doi:10.1002/2015GB005115, <http://doi.wiley.com/10.1002/2015GB005115>, 2015. <sup>1525</sup>
- Miller, W. L. and Moran, M. A.: Interaction of photochemical and microbial processes in the degradation of refractory dissolved organic matter from a coastal marine environment, *Limnology and Oceanography*, 42, 1317–1324, doi:10.4319/lo.1997.42.6.1317, <http://www.jstor.org/stable/10.2307/2839130>, 1997.
- Miller, W. L., Moran, M. A., and Sheldon, W. M.: Determination of apparent quantum yield spectra for the formation of biologically labile photoproducts, *Limnology and Oceanography*, 47, 343–352, doi:10.4319/lo.2002.47.2.0343, <http://www.jstor.org/stable/10.2307/3068981>, 2002.
- Milliman, J. D. and Farnsworth, K. L.: *River Discharge to the Coastal Ocean: A Global Synthesis*, vol. 24, Cambridge University Press, Cambridge, doi:<http://dx.doi.org/10.5670/oceanog.2011.108>, 2011.
- Minor, E. C., Pothen, J., Dalzell, B. J., Abdulla, H., and Mopper, K.: Effects of salinity changes on the photodegradation and ultraviolet-visible absorbance of terrestrial dissolved organic matter, *Limnology and Oceanography*, 51, 2181–2186, doi:10.4319/lo.2006.51.5.2181, <http://www.aslo.org/toc/vol{ }51/issue{ }5/2181.html>, 2006.
- Molot, L. and Dillon, P.: Photolytic regulation of dissolved organic carbon in northern lakes, *Global Biogeochemical Cycles*, 11, 357–365, <http://onlinelibrary.wiley.com/doi/10.1029/97GB01198/full>, 1997.
- Mopper, K. and Kieber, D. J.: Photochemistry and the Cycling of Carbon, Sulfur, Nitrogen and Phosphorus, in: *Biogeochemistry of Marine Dissolved Organic Matter*, edited by Hansell, D. A. and Carlson, C. A., chap. Chapter 9, pp. 455–507, Elsevier, doi:10.1016/B978-012323841-2/50011-7, <http://www.sciencedirect.com/science/article/pii/B9780123238412500117>, 2002.
- Moran, M. and Zepp, R.: Role of photoreactions in the formation of biologically labile compounds from dissolved organic matter, *Limnology and Oceanography*, 42, 1307–1316, <http://www.aslo.org/lo/toc/vol{ }42/issue{ }6/1307.pdf><http://www.jstor.org/stable/10.2307/2839129>, 1997.
- Morris, D. P., Zagarese, H., Williamson, C. E., Balseiro, E. G., Hargreaves, B. R., Modenutti, B., Moeller, R., and Queimalinos, C.: The attenuation of solar UV radiation in lakes and the role of dissolved organic carbon, *Limnology and Oceanography*, 40, 1381–1391, doi:10.4319/lo.1995.40.8.1381, 1995.
- Müller, R. A., Futter, M. N., Sobek, S., Nisell, J., Bishop, K., and Weyhenmeyer, G. A.: Water renewal along the aquatic continuum offsets cumulative retention by lakes: implications for the character of organic carbon in boreal lakes, *Aquatic Sciences*, 75, 535–545, doi:10.1007/s00027-013-0298-3, <http://link.springer.com/10.1007/s00027-013-0298-3>, 2013.
- Nelson, N. B. and Siegel, D. A.: The global distribution and dynamics of chromophoric dissolved organic matter., *Annual Review of Marine Science*, 5, 447–76, doi:10.1146/annurev-marine-120710-100751, <http://www.ncbi.nlm.nih.gov/pubmed/22809178>, 2013.
- Norland, S.: The relationship between biomass and volume of bacteria, in: *Handbook of Methods in Aquatic Microbial Ecology*, edited by Kemp, P., Sherr, B., Sherr, E., and Cole, J., pp. 303–307, Lewis Publishers, BocaRaton, 1993.
- Obernosterer, I. and Herndl, G.: Differences in the optical and biological reactivity of the humic and nonhumic dissolved organic carbon component in two contrast-

- ing coastal marine environments, *Limnology and Oceanography*, 45, 1120–1129, doi:10.4319/lo.2000.45.5.1120, <http://www.jstor.org/stable/10.2307/2670702>, 2000. <sup>1645</sup>
- Pers, C., Rahm, L., Jonsson, A., and Jansson, M.: Modelling dissolved organic carbon turnover in humic Lake, *Environmental monitoring and assessment*, 6, 159–172, doi:10.1023/A:1011953730983, 2001. <sup>1590</sup>
- Pineiro, S., Chauhan, A., Berhane, T. K., Athar, R., Zheng, G., Wang, C., Dickerson, T., Liang, X., Lymperopoulou, D. S., Chen, H., Christman, M., Louime, C., Babiker, W., Stine, O. C., and Williams, H. N.: Niche Partition of Bacteriovorax Operational Taxonomic Units Along Salinity and Temporal Gradients in the Chesapeake Bay Reveals Distinct Estuarine Strains, *Microbial Ecology*, 65, 652–660, doi:10.1007/s00248-013-0186-3, 2013. <sup>1595</sup>
- Pullin, M. J., Bertilsson, S., Goldstone, J. V., and Voelker, B. M.: Effects of sunlight and hydroxyl radical on dissolved organic matter: Bacterial growth efficiency and production of carboxylic acids and other substrates, *Limnology and Oceanography*, 49, 2011–2022, doi:10.4319/lo.2004.49.6.2011, <http://www.aslo.org/lo/toc/vol{ }49/issue{ }6/2011.html>, 2004. <sup>1600</sup>
- R Core Team: R: A Language and Environment for Statistical Computing, R Foundation for Statistical Computing, Vienna, Austria, <http://www.r-project.org/>, 2014. <sup>1605</sup>
- Reader, H. E. and Miller, W. L.: The efficiency and spectral photon dose dependence of photochemically induced changes to the bioavailability of dissolved organic carbon, *Limnology and Oceanography*, 59, 182–194, doi:10.4319/lo.2014.59.1.0182, <http://www.aslo.org/lo/toc/vol{ }59/issue{ }1/0182.html>, 2014. <sup>1610</sup>
- Reche, I., Pace, M., and Cole, J.: Interactions of Photobleaching and Inorganic Nutrients in Determining Bacterial Growth on Colored Dissolved Organic Carbon., *Microbial ecology*, 36, 270–280, <http://www.ncbi.nlm.nih.gov/pubmed/9852507>, 1998. <sup>1615</sup>
- Reitner, B., Herndl, G. J., and Herzig, A.: Role of ultraviolet-B radiation on photochemical and microbial oxygen consumption in a humic-rich shallow lake, *Limnology and Oceanography*, 42, 950–960, doi:10.4319/lo.1997.42.5.0950, 1997. <sup>1620</sup>
- Remington, S., Krusche, A., and Richey, J.: Effects of DOM photochemistry on bacterial metabolism and CO<sub>2</sub> evasion during falling water in a humic and a white-water river in the Brazilian Amazon, *Biogeochemistry*, 105, 185–200, doi:10.1007/s10533-010-9565-8, <http://www.springerlink.com/index/0R500624243181W7.pdf><http://www.springerlink.com/index/10.1007/s10533-010-9565-8>, 2011. <sup>1625</sup>
- Riggsbee, J. A., Orr, C. H., Leech, D. M., Doyle, M. W., and Wetzel, R. G.: Suspended sediments in river ecosystems: Photochemical sources of dissolved organic carbon, dissolved organic nitrogen, and adsorptive removal of dissolved iron, *Journal of Geophysical Research: Biogeosciences*, 113, 1–12, doi:10.1029/2007JG000654, 2008. <sup>1630</sup>
- Rossel, P. E., Vähätalo, A. V., Witt, M., and Dittmar, T.: Molecular composition of dissolved organic matter from a wetland plant (*Juncus effusus*) after photochemical and microbial decomposition (1.25 yr): Common features with deep sea dissolved organic matter, *Organic Geochemistry*, 60, 62–71, doi:10.1016/j.orggeochem.2013.04.013, <http://linkinghub.elsevier.com/retrieve/pii/S0146638013000971>, 2013. <sup>1640</sup>
- Salonen, K. and Vähätalo, A.: Photochemical mineralisation of dissolved organic matter in lake Skjervatjern, *Environment international*, 20, 307–312, doi:10.1016/0160-4120(94)90114-7, 1994.
- Smith, E. and Benner, R.: Photochemical transformations of riverine dissolved organic matter: effects on estuarine bacterial metabolism and nutrient demand, *Aquatic Microbial Ecology*, 40, 37–50, doi:10.3354/ame040037, <http://www.int-res.com/abstracts/ame/v40/n1/p37-50/>, 2005.
- Smith, S. V. and Hollibaugh, J. T.: Coastal Metabolism and the Oceanic Organic Carbon Balance, *Reviews of Geophysics*, 31, 75–89, 1993.
- Sobek, S., Tranvik, L. J., Prairie, Y. T., and Cole, J. J.: Patterns and regulation of dissolved organic carbon : An analysis of 7, 500 widely distributed lakes, *Limnology and Oceanography*, 52, 1208–1219, 2007.
- Søndergaard, M. and Middelboe, M.: A cross-system analysis of labile dissolved organic carbon, *Marine Ecology Progress Series*, 118, 283–294, doi:10.3354/meps118283, <http://www.int-res.com/abstracts/meps/v118/p283-294/>, 1995.
- Spencer, R. G. M., Stubbins, A., Hernes, P. J., Baker, A., Mopper, K., Aufdenkampe, A. K., Dyda, R. Y., Mwamba, V. L., Mangangu, A. M., Wabakanghanzi, J. N., and Six, J.: Photochemical degradation of dissolved organic matter and dissolved lignin phenols from the Congo River, *Journal of Geophysical Research*, 114, G03010, doi:10.1029/2009JG000968, <http://doi.wiley.com/10.1029/2009JG000968><http://www.agu.org/pubs/crossref/2009/2009JG000968.shtml>, 2009. <sup>1665</sup>
- Spencer, R. G. M., Aiken, G. R., Dornblaser, M. M., Butler, K. D., Holmes, R. M., Fiske, G., Mann, P. J., and Stubbins, A.: Chromophoric dissolved organic matter export from U.S. rivers, *Geophysical Research Letters*, 40, 1575–1579, doi:10.1002/grl.50357, <http://doi.wiley.com/10.1002/grl.50357>, 2013.
- Stedmon, C., Amon, R., Rinehart, A., and Walker, S.: The supply and characteristics of colored dissolved organic matter (CDOM) in the Arctic Ocean: Pan Arctic trends and differences, *Marine Chemistry*, 124, 108–118, doi:10.1016/j.marchem.2010.12.007, <http://linkinghub.elsevier.com/retrieve/pii/S0304420311000065>, 2011.
- Stepanuskas, R., Jørgensen, N. O. G., Eigaard, O. R., Zvikas, A., Tranvik, L. J., and Leonardson, L.: Summer inputs of riverine nutrients to the Baltic Sea : bioavailability and eutrophication relevance, *Ecological Monographs*, 72, 579–597, 2002.
- Vähätalo, A. and Järvinen, M.: Photochemically produced bioavailable nitrogen from biologically recalcitrant dissolved organic matter stimulates production of a nitrogen-limited microbial food web in the Baltic Sea, *Limnology and oceanography*, 52, 132–143, 2007.
- Vähätalo, A., Salkinoja-salonen, M., Taalas, P., and Salonen, K.: Spectrum of the quantum yield for photochemical mineralization of dissolved organic carbon in a humic lake, *Limnology and Oceanography*, 45, 664–676, doi:10.4319/lo.2000.45.3.0664, 2000.
- Vähätalo, A. V.: Light, Photolytic Reactivity and Chemical Products, vol. 2, *Likens*, Oxford, volume 2 edn., 2009.
- Vähätalo, A. V. and Wetzel, R. G.: Photochemical and microbial decomposition of chromophoric dissolved organic matter during long (months - years) exposures, *Marine Chem-*

- istry, 89, 313–326, doi:10.1016/j.marchem.2004.03.010, <http://www.sciencedirect.com/science/article/pii/S0304420304000957>, 2004.
- Vähätalo, A. V., Salonen, K., Sasaki, E., and Salkinoja-Salonen, M. S.: Bleaching of color of kraft pulp mill effluents and natural organic matter in lakes, *Canadian Journal of Fisheries and Aquatic Sciences*, 59, 808–818, doi:10.1139/F02-047, 2002.
- Vähätalo, A. V., Salonen, K., Münster, U., Järvinen, M., and Wetzel, R. G.: Photochemical transformation of allochthonous organic matter provides bioavailable nutrients in a humic lake, *Archiv für Hydrobiologie*, 156, 287–314, doi:10.1127/0003-9136/2003/0156-0287, <http://www.ingenta.com/rpsv/cgi-bin/cgi?ini=xref&body=linker&reqdoi=10.1127/0003-9136/2003/0156-0287>, 2003.
- Vähätalo, A. V., Wetzel, R. G., and Paerl, H. W.: Light absorption by phytoplankton and chromophoric dissolved organic matter in the drainage basin and estuary of the Neuse River, *North Carolina (U.S.A.)*, *Freshwater Biology*, 50, 477–493, doi:10.1111/j.1365-2427.2004.01335.x, <http://doi.wiley.com/10.1111/j.1365-2427.2004.01335.x>, 2005.
- Vähätalo, A. V., Aarnos, H., and Mäntyniemi, S.: Biodegradability continuum and biodegradation kinetics of natural organic matter described by the beta distribution, *Biogeochemistry*, 100, 227–240, doi:10.1007/s10533-010-9419-4, <http://link.springer.com/10.1007/s10533-010-9419-4>, 2010.
- Vähätalo, A. V., Aarnos, H., Hoikkala, L., and Lignell, R.: Photochemical transformation of terrestrial dissolved organic matter supports hetero- and autotrophic production in coastal waters, *Marine Ecology Progress Series*, 423, 1–14, doi:10.3354/meps09010, <http://www.int-res.com/abstracts/meps/v423/p1-14/>, 2011.
- Vähätalo, A. V. A. and Wetzel, R. R. G.: Long-Term Photochemical and Microbial Decomposition of Wetland-Derived Dissolved Organic Matter with Alteration of 13C:12C Mass Ratio, *Limnology and Oceanography*, 53, 1387–1392, doi:10.4319/lo.2008.53.4.1387, <http://www.jstor.org/stable/10.2307/40058260>, 2008.
- Verpoorter, C., Kutser, T., Seekell, D. A., and Tranvik, L. J.: A global inventory of lakes based on high-resolution satellite imagery, *Geophysical Research Letters*, 41, 2014GL060641, doi:10.1002/2014GL060641, 2014.
- Vodacek, A., Blough, N. V., Degrandpre, M. D., Peltzer, E. T., and Nelson, R. K.: Seasonal variation of CDOM and DOC in the Middle Atlantic Bight: Terrestrial inputs and photooxidation, *Limnology and Oceanography*, 42, 674–686, doi:10.4319/lo.1997.42.4.0674, 1997.
- Wagner, S., Riedel, T., Niggemann, J., Vähätalo, A. V., Dittmar, T., and Jaffe, R.: Linking the Molecular Signature of Heteroatomic Dissolved Organic Matter To Watershed Characteristics in World Rivers, *Environmental Science & Technology*, Article AS, doi:10.1021/acs.est.5b00525, <http://pubs.acs.org/doi/abs/10.1021/acs.est.5b00525>, 2015.
- Wallin, M. B., Weyhenmeyer, G. A., Bastviken, D., Chmiel, H. E., Peter, S., Sobek, S., and Klemetsson, L.: Temporal control on concentration, character, and export of dissolved organic carbon in two hemiboreal headwater streams draining contrasting catchments, *Journal of Geophysical Research: Biogeosciences*, 3, 1–15, doi:10.1002/2014JG002814, 2015.
- Warkentin, M., Freese, H. M., Karsten, U., and Schumann, R.: New and fast method to quantify respiration rates of bacterial and plankton communities in freshwater ecosystems by using optical oxygen sensor spots., *Applied and Environmental Microbiology*, 73, 6722–6729, doi:10.1128/AEM.00405-07, <http://www.pubmedcentral.nih.gov/articlerender.fcgi?artid=2074954&tool=pmcentrez&rendertype=abstract>, 2007.
- Warkentin, M., Freese, H. M., and Schumann, R.: Bacterial activity and bacterioplankton diversity in the eutrophic River Warnow—direct measurement of bacterial growth efficiency and its effect on carbon utilization., *Microbial Ecology*, 61, 190–200, doi:10.1007/s00248-010-9729-z, <http://www.ncbi.nlm.nih.gov/pubmed/20676625>, 2011.
- Wetzel, R. G., Hatcher, P. G., and Bianchi, T. S.: Natural photolysis by ultraviolet irradiance of recalcitrant dissolved organic matter to simple substrates for rapid bacterial metabolism, *Limnology and Oceanography*, 40, 1369–1380, 1995.
- White, E. M., Kieber, D. J., Sherrard, J., Miller, W. L., and Mopper, K.: Carbon dioxide and carbon monoxide photoproduction quantum yields in the Delaware Estuary, *Marine Chemistry*, 118, 11–21, doi:10.1016/j.marchem.2009.10.001, <http://www.sciencedirect.com/science/article/pii/S0304420309001455>, 2010.
- Xiao, Y.-H., Sara-Aho, T., Hartikainen, H., and Vähätalo, A. V.: Contribution of ferric iron to light absorption by chromophoric dissolved organic matter, *Limnology and Oceanography*, 58, 653–662, doi:10.4319/lo.2013.58.2.0653, [http://www.aslo.org/lo/toc/vol\[\\_\]58/issue\[\\_\]2/0653.html](http://www.aslo.org/lo/toc/vol[_]58/issue[_]2/0653.html), 2013.
- Xie, H., Zafiriou, O. C., Cai, W.-J., Zepp, R. G., and Wang, Y.: Photooxidation and Its Effects on the Carboxyl Content of Dissolved Organic Matter in Two Coastal Rivers in the Southeastern United States, *Environmental Science & Technology*, 38, 4113–4119, doi:10.1021/es035407t, <http://pubs.acs.org/doi/abs/10.1021/es035407t>, 2004.